

UNCLASSIFIED

AD NUMBER
AD914705
NEW LIMITATION CHANGE
TO Approved for public release, distribution unlimited
FROM Distribution authorized to U.S. Gov't. agencies only; Test and Evaluation; Jun 1972. Other requests shall be referred to Air Force Flight Dynamics Lab., Wright-Patterson AFB, OH 45433.
AUTHORITY
AFWAL ltr, 11 Feb 1980

THIS PAGE IS UNCLASSIFIED

L
AFFDL-TR-73-77

AD 914705

ADVANCED METALLIC AIR VEHICLE STRUCTURE PROGRAM

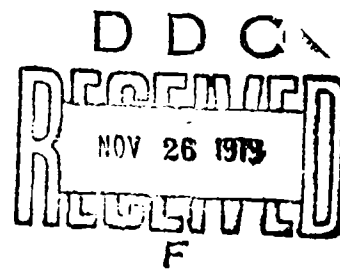
SECOND INTERIM REPORT

*GENERAL DYNAMICS
CONVAIR AEROSPACE DIVISION
FORT WORTH OPERATION*

C. E. HART, et al

TECHNICAL REPORT AFFDL-TR-73-77

JULY 1973



"TEST + EVALUATION"

Distribution limited to U.S. Government Agencies only: Statement applied June 1972. Other requests for this document must be referred to Air Force Flight Dynamics Laboratory (FB-A), Wright Patterson Air Force Base, Ohio 45433.

**AIR FORCE FLIGHT DYNAMICS LABORATORY
AIR FORCE SYSTEMS COMMAND
WRIGHT-PATTERSON AIR FORCE BASE, OHIO 45433**

THIS REPORT HAS BEEN DELIMITED
AND CLEARED FOR PUBLIC RELEASE
UNDER DOD DIRECTIVE 5200.20 AND
NO RESTRICTIONS ARE IMPOSED UPON
ITS USE AND DISCLOSURE.

DISTRIBUTION STATEMENT A

APPROVED FOR PUBLIC RELEASE;
DISTRIBUTION UNLIMITED.

Best Available Copy

NOTICES

When Government drawings, specifications, or other data are used for any purpose other than in connection with a definitely related Government procurement operation, the United States Government thereby incurs no responsibility nor any obligation whatsoever; and the fact that the government may have formulated, furnished, or in any way supplied the said drawings, specifications, or other data, is not to be regarded by implication or otherwise as in any manner licensing the holder or any other person or corporation, or conveying any rights or permission to manufacture, use, or sell any patented invention that may in any way be related thereto.

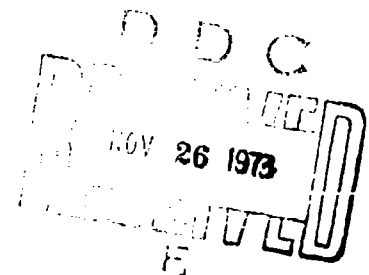
Copies of this report should not be returned unless return is required by security considerations, contractual obligations, or notice on a specific document.

ADVANCED METALLIC AIR VEHICLE STRUCTURE PROGRAM

*GENERAL DYNAMICS
CONVAIR AEROSPACE DIVISION
FORT WORTH OPERATION*

"TEST + EVALUATION"

Distribution limited to U.S. Government Agencies only: Statement applied June 1972. Other requests for this document must be referred to Air Force Flight Dynamics Laboratory (FB-A), Wright Patterson Air Force Base, Ohio 45433.



FOREWORD

This report presents the results of the second six months of the carry on program for an Advanced Metallic Air Vehicle Structure. The report period overlaps two phases in the program; two months of Phase Ib, Preliminary Design and four months of Phase II, Detail Design and Analysis. The efforts reported herein were sponsored by the Air Force Flight Dynamics Laboratory (AFFDL) under joint management and technical direction of AFFDL and Air Force Material Laboratory (AFML), Wright Patterson Air Force Base, Ohio.

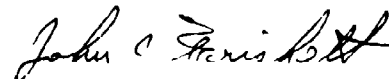
This work was performed under contract F33615-73-C-3001 "Advanced Metallic Air Vehicle Structures" (AMAVS) as part of the Advanced Metallic Structures Advanced Development Program (AMS ADP), Program Element Number 63211F, Project Number 486U. John C. Frishett, Major, USAF, is the ADP Manager while Mr. Frank D. Boensch FB-A is the Project Engineer for the AMAVS Program.

Principal Convair contributors to this report were:

R. C. Bissell	Dr. H. I. McHenry
D. L. Duncan	R. E. Miller
C. E. Hart	J. M. Shults
E. K. Hensley	A. F. Stern
J. W. Jennings	W. O. Sunafrank
C. D. Lantz	W. M. Walker
J. L. McDaniel	

This work was performed during the period 16 December 1972 to 15 June 1973. It was submitted by the authors on 20 June 1973.

This technical report has been reviewed and is approved.



John C. Frishett, Major, USAF
Program Manager, AMS Program Office
Structures Division

A B S T R A C T

Refinement of the three designs for a wing carrythrough structure was continued to the end of Phase Ib. On the basis of trade studies, materials and component testing and the results of NDI and manufacturing development work, two of the configurations were chosen for the detail design phase.

Materials testing was substantially completed for the beta annealed 6Al-4V titanium and testing is underway for the Beta C titanium and 10 Ni steel. Group I component tests (those performed to verify design concepts) are virtually complete. Tests to evaluate the welding, brazing and bonding processes are also well underway.

Design of the test fixture is proceeding with some manufacturing effort already started. Detail design and analysis of the simulated fuselage structure for the test article is also in work.

Additional trade studies were conducted early in Phase II and several design changes were incorporated into the two wing carrythrough structure configurations as a result of these studies. A ZfO panel was added to the "No Box" Box design. The Fail Safe Removable Lug Configuration was redesignated the Fail Safe Integral Lug Configuration after an integral lower plate-lug arrangement was selected for detail design.

TABLE OF CONTENTS

<u>Section</u>		<u>Page</u>
I	INTRODUCTION	1
II	TECHNOLOGY ADVANCEMENT	5
	2.1 Brazed Damage Tolerant Structures	6
	2.1.1 Brazing Process	6
	2.1.2 Brazed Joint Strength	7
	2.1.3 Crack Retardation at Brazed Joints	7
	2.1.4 Conclusions	8
	2.2 Bonded Laminated Structure	8
	2.2.1 Bonding Process	8
	2.2.2 Strength of Bonded Joints	9
	2.2.3 Inspection of Bonded Joints	9
	2.2.4 Conclusions	9
	2.3 Materials	10
	2.3.1 Beta Annealed 6Al-4V Titanium	10
	2.3.2 10 Ni Steel	11
	2.3.3 Beta C Titanium	11
III	TECHNICAL DISCIPLINES PROGRESS	13
	3.1 Engineering	13
	3.1.1 Structural Design	13
	3.1.2 Structural Analysis	45
	3.1.3 Fatigue and Fracture Analysis	98
	3.1.4 Materials Engineering	133
	3.2 Testing	190
	3.2.1 Materials Testing	190
	3.2.2 Component Testing	190
	3.2.3 Full Scale Testing	195

TABLE OF CONTENTS (Continued)

<u>Section</u>	<u>Page</u>
3.3 Quality Assurance and NDI	202
3.3.1 Brazed Joint Evaluations	202
3.3.2 Bonding Evaluations	218
3.3.3 EB and GTA Welding Evaluations	222
3.4 Manufacturing Development	230
3.4.1 Adhesive Bonded Metal Laminated Structure Process Development	230
3.4.2 Laminated Brazing Process Development	245
3.4.3 Weld Development	250
3.4.4 Machining	265
3.4.5 Manufacturing Engineering Design Support	266
 APPENDIX A - PHYSICAL CHARACTERISTICS OF RAW MATERIAL AND DESIGN VERIFICATION TEST SPECIMENS	 A-1
 REFERENCES	 275

LIST OF ILLUSTRATIONS

<u>Figure</u>		<u>Page</u>
1	Lower Plate - Brazed Ti, FSRL Alternate No. III, Study of	15
2	Longeron Splice - Lwr, Aft, Outbd, FSIL Config	17
3	Beam Instl - X _F 99.00 Lower Plate, FSIL Configuration	21
4	Lower Plate - Brazed Ti, FSRL Alternate No. IV, Study of	23
5	Y _F 947.0 Bhd, Arched - AMAVS, FSIL Config., Study of	27
6	Y _F 977.0 Bhd, Arched - AMAVS, FSIL Config., Study of	29
7	Lower Lug & Panel at Z _f 0.0 Wing Carry Thru, No-Box Box, Study of	31
8	Bulkhead Y _f 992 - No-Box Box, Proposal of	41
9	Bulkhead Y _f 932	43
10	FSRL-4-1 Math Model	49
11	Y _F 947 Arched-Beam Bulkhead Bar Elements	50
12	Y _F 947 Arched-Beam Bulkhead Plate Elements	51
13	Y _F 977 Arched-Beam Bulkhead Bar Elements	52
14	Y _F 977 Arched-Beam Bulkhead Plate Elements	53
15	B004 3/8 Scale Lug Test Specimen Stress at 200,000 # Load	55
16	B004 3/8 Scale Lug Test Specimen	56
17	603FTB004 TLO-IV and TLO-V Setups with Finer Grid Simulation Around Lug I.D.	58

LIST OF ILLUSTRATIONS (Continued)

<u>Figure</u>		<u>Page</u>
18	FSRL Lower Lug Fine Grid Model	59
19	FSRL Configuration TLO Simulation of Lower Lug	61
20	FSRL Upper Plate Nastran Buckling Model	62
21	FSRL Upper Plate - Nastran Model Plate Thicknesses	63
22	FSRL Upper Cover Buckling Mode Shape ASKA 2	64
23	Element Arrangement for Nastran Models of Simply Supported Plate with One Longitudinal Stiffener	65
24	Geometry of Simply Supported Plate with One Longitudinal Stiffener	67
25	Comparison of Critical Compressive Stresses for Simply Supported Plate with One Longitudinal Stiffener Results From NACA TN No. 1825 Vs Nastran Models	68
26	Mode Shape for Case 2 Nastran Model - 4x8 Grid	69
27	NBB Math Model of Lower Plate at $Z_F = 0.0$	72
28	Math Model of Lower Plate at $Z_F = 0.0$, NBB	73
29	Element Max Principal Stresses (KSI)	75
30	Element Max Principal Stresses (KSI) in 0.3 Steel Between $X_F=84$ and $X_F=119$	77
31	NBB-3 TR4 ITERATION $Z_F=0$ Lower Plate	79
32	Model Structural Weights Vs. Stress Cycle Iterative Solution	80
33	NBB-4 TR4 Iteration, Input Gages and Areas $Z_F=0$ Lower Plate	81
34	NBB-4 TR4 Iteration, 4 Cycles $Z_F=0$ Lower Plate Thicknesses and Areas	82

LIST OF ILLUSTRATIONS (Continued)

<u>Figure</u>		<u>Page</u>
35	Lower Surface Deflections - ASKA 2	83
36	Lower Surface Deflections - ASKA 10	84
37	NBB-6 Bar and Plate Arrangement	86
38	NBB-7 Bar and Plate Arrangement	87
39	'No Box' Box Optimization Studies for Lower Plate Configuration at Z_F0	89
40	"No Box" Box Upper Lug and Cover - A3S Buckling Model	90
41	"No Box" Box Upper Lug and Cover - Buckled Mode Shape for Condition ASKA 10	91
42	Section Forward of Station YF 992	95
43	Section Aft of Station YF 992	96
44	FSRL Lower Plate Lug Ti 6Al-4V (β , MA) All Negative Stresses Set = 0 $K_T = 5$	99
45	Fatigue Crack Growth 10 Nickel Steel Dry Air RW Grain Direction	103
46	Fatigue Crack Growth 10 NI Steel Sump Water Tank Water RW Grain Direction	105
47	Fatigue Crack Growth Beta Annealed 6Al-4V Titanium Dry Air - RW Grain Direction	107
48	Fatigue Crack Growth Beta Annealed 6Al-4V Titanium Sump Tank Water	109
49	Crack Growth Test 10 Nickel Steel FTJ10940-185 Specimen No. 3	112
50	Crack Growth Test 10 Nickel Steel FTJ10940-185 Specimen No. 5	113

LIST OF ILLUSTRATIONS (Continued)

<u>Figure</u>		<u>Page</u>
51	Crack Growth Test 10 Nickel Steel FTJ10940-185 Specimen No. 4	114
52	Crack Growth Test 10 Nickel Steel FTJ10940-185 Specimen No. 2	115
53	Crack Growth Test 10 Nickel Steel FTJ10940-185 Specimen No. 2	116
54	Crack Growth Test Beta Annealed 6Al-4V Titanium FTJ10940-153 Specimen No. 1	117
55	Crack Growth Test Beta Annealed 6Al-4V Titanium FTJ10940-153 Specimen No. 2	118
56	Crack Growth Test Beta Annealed 6Al-4V Titanium FTJ10940-153 Specimen No. 4	119
57	Crack Growth Test Beta Annealed 6Al-4V-Titanium FTJ10940-152 Specimen No. 2	120
58	Crack Growth Test Beta Annealed 6Al-4V Titanium FTJ10940-152 Specimen No. 1	121
59	Test Problem 1	123
60	A Square Plate With a Center Crack Under Anti- symmetric Corner Loads	124
61	A Rectangular Plate With Two Parallel Cracks Under Tension	125
62	Damage Tolerance Test Specimen	126
63	K_I vs a For The Damage Tolerance Test Specimen Under Tension	128
64	Idealized Fail-Safe Integral Lower Plate	129

LIST OF ILLUSTRATIONS (Continued)

<u>Figure</u>		<u>Page</u>
65	K_I vs a For The Idealized Fail-Safe Brazed Lower Plate	130
66	Triangular Plate Element	131
67	10 NI Steel - Welding Properties - Development Test Program	135
68	6AL-4V TI Brazed Lamina Mechanical Properties Test Development Test Program	137
69	10 NI Steel - Material Properties, Development Test Program	139
70	603FTB005 Number 2 Braze Assembly 200X (1% HF, 2% HNO_3 ETCH)	154
71	Braze Joint Environmental Sensitivity Test Results	160
72	Electron Beam Welded 6Al-4V Titanium Fatigue Data	164
73	Test Panel Geometry	157
74	Overlap Shear Results Bonded 6Al-6V-2Sn Titanium Alloy/AF66 Adhesive (-65°F)	170
75	Overlap Shear Results Bonded 6Al-6V-2Sn Titanium Alloy/AF 66 Adhesive (80°F)	171
76	Overlap Shear Results Bonded 6Al-6V-2Sn Titanium Alloy/AF 66 Adhesive (180°F)	172
77	Overlap Shear Results Bonded 6Al-6V-2Sn Titanium Alloy/PL-717 Adhesive (-65°F)	173
78	Overlap Shear Results Bonded 6Al-6V-2Sn Titanium Alloy/PL-717 Adhesive (80°F)	174
79	Overlap Shear Results Bonded 6Al-6V-2Sn Titanium Alloy/PL-717 Adhesive (180°F)	175

LIST OF ILLUSTRATIONS (Continued)

<u>Figure</u>		<u>Page</u>
80	B-Allowables Bonded 6Al-6V-2Sn Titanium Alloy/PL-717 Adhesive	178
81	B-Allowables Bonded 6Al-6V-2Sn Titanium Alloy/AF 66 Adhesive	179
82	PL 717 Adhesive and Beta C Titanium Alloy Test at -65F	183
83	PL 717 Adhesive and Beta C Titanium Alloy Test at 80F	184
84	PL 717 Adhesive and Beta C Titanium Alloy Test at 180F	185
85	B-Allowables Bonded "Beta C" (3Al-8V-6Cr-4Mo-4Zr) Titanium Alloy/PL 717 Adhesive	186
86	Comparison of B-Allowables for Two Titanium Alloys Bonded with PL 717 Adhesive	187
87	AMAVS Full Scale Test (Overall View)	196
88	Initial Shipment of Hardware	197
89	Final Shipment of Hardware	199
90	EB and GTA Welding NDI Specimens	205
91	Bonded Sandwich NDI Specimens	207
92	Bonded Laminate NDI Specimens	209
93	Raw Material and Brazed NDI Specimens	211
94	Rough Sketch of NDI Specimen MD3189-1	213
95	Rough Sketch of NDI Specimen MD3189-2	214
96	Rough Sketch of NDI Specimen MD3208	215
97	Rough Sketch of NDI Specimen MD3209	216

LIST OF ILLUSTRATIONS (Continued)

<u>Figure</u>		<u>Page</u>
98	Ultrasonic C-Scan of NDI Specimen MD3208	217
99	Ultrasonic C-Scan of 603FTB005#2 Before Fatigue Testing	219
100	Ultrasonic C-Scan of 603FTB005#2 After Fatigue Testing	219
101	Through Transmission C-Scan Recording of 603FTB012-1-1	220
102	Disassembly of 603FTB012-1-1 Second Bond Line	220
103	Disassembly of 603FTB012-1-1 Third Bond Line	221
104	Sandwich Panel MD3195, Through Transmission Recording with Disassembly of Half "A"	223
105	Sandwich Panel MD3196, Through Transmission Recording with Disassembly of Half "A"	223
106	Specimen MD3197, Through Transmission Recording with Disassembly of First Bond Line	224
107	Specimen MD3197 Through Transmission Recording with Disassembly of Second Bond Line	224
108	Specimen MD3198, Through Transmission Recording with Disassembly of First Bond Line	225
109	Specimen MD3198, Through Transmission Recording with Disassembly of Second Bond Line	225
110	Specimen MD3198, Through Transmission Recording and Disassembly of Bond Line #3	226
111	603FTB014 Adhesive Bonded Panel	237
112	603FTB014 Sheet Lamina Flatness	238
113	603FTB014 Sheet Lamina Flatness	239
114	603FTB014 Sheet Lamina Flatness	240

LIST OF ILLUSTRATIONS (Continued)

<u>Figure</u>		<u>Page</u>
115	603FTB012-7 Detail	243
116	603FTB012-7 Detail	244
117	603FTB012-1 Assembly	246
118	Brazing Test Panel with Built-in Voids	251
119	Brazing (Mismatch) Test Panel	251
120	Brazing (Gap) Test Panel	251
121	Cycle for Braze Time (Slow Cool) Evaluation	252
122	Typical Braze Cycle for Manufacturing Development Parts	253
123	Automatic 400-Amp. GTA Fusion Welder	255
124	GTA Plate Weld Fixture	256
125	Section of GTA Weld Fixture	258
126	Pulsed GTA Current Trace	259
127	GTA Welding Schedule for 10 Nickel Steel	260
128	10 Nickel Steel Welded Plate Filler Wire Reinforcement	261
129	Setup for Using Weld Tabs	262
130	Preliminary Cost Estimate Form	273

LIST OF TABLES

<u>Table</u>		<u>Page</u>
1	"No-Box" Cost Summary	35
2	Lwr Pivot Lug Cost Summary	36
3	Y _F 992 Bulkhead Cost Summary	37
4	Y _F 932 Bulkhead Cost Summary	38
5	Load Conditions	46
6	Summary of AMAVS Computer Analysis of Overall WCTS	47
7	Nastran Buckling Analysis Results for Various Grid Sizes	66
8	NBB Z _F = 0.0 Math Model Lower Plate Study	74
9	"No-Box" Box Lower Plate Resizing Runs	78
10	Panel Shear Flows Lbs/In	93
11	Longeron - Fore Aft Component Kips	94
12	Fatigue Crack Growth Tests	101
13	Spectrum-Environmental Crack Growth Tests	111
14	Design Allowables for TI 6Al-4V Beta Annealed Condition (Ref. FMS-1109A)	134
15	10 Nickel Steel Test Data	141
16	Acceptance Data 6Al-4V Titanium Beta Annealed	143
17	Beta C Titanium Received	147
18	Brazed Specimens	150
19	Brazed Panel (603R100-3) VQ/I Shear Data	152

LIST OF TABLES (Continued)

<u>Table</u>		<u>Page</u>
20	Sustained Load S.C.C. Tests - Braze Lap Shear Specimens	156
21	Tensile Test Results (Flat Type, 2.0" G.L.)	161
22	Fatigue Test Results of Beta Annealed 6Al-4V Titanium Welded on 3 Plate Thickness, Tested at R = 0.1, _{max} = 80 KSI	162
23	10 Nickel Steel Weldments - Mechanical Properties	165
24	AF66 Adhesive Bonded Titanium Alloy 6Al-6V-2Sn	168
25	PL 717 Adhesive Bonded Titanium Alloy 6Al-6V-2Sn	169
26	Adhesive Allowables Calculations	180
27	Overlap Shear Results Beta C Titanium Alloy and PL-717 Adhesive	182
28	Materials Test Program	191
29	Full Scale Test Fixture Status	201
30	Beta C Titanium Alloy 1/8-Inch Sheet Thickness Ground Vs Rolled & Pickled	233
31	Beta C Titanium Alloy 1/8-Inch Sheet Flatness Ground Vs. Rolled & Pickled	235
32	603FTB012 Adhesive Bonded Panels	241
33	Summary of Braze Parts with Pertinent Parameters	248

SECTION I

INTRODUCTION

This interim report summarizes the technical accomplishments from 16 December 1972 to 15 June 1973 for the Advanced Metallic Air Vehicle Structure Program. This work is a part of the Air Force's Advanced Metallic Structures, Advanced Development Program. It was performed under contract to the AFFDL by the Convair Aerospace Division of General Dynamics at Fort Worth, Texas.

The six months covered by this report include the last portion of Phase Ib, Preliminary Design and the first portion of Phase II, Detail Design. All tasks accomplished in Phase Ib were reported in AFTR-73-40 dated March 1973.

The three designs selected for further design and analysis in Phase Ib were evaluated at the conclusion of Phase Ib and two were selected for continuation in Phase II which started 1 April 1973. These two designs were designated:

Fail Safe Removable Lug (FSRL)

"No-Box" Box (NBB)

Detail design iterations and trade studies in Phase II accomplished significant changes to both of these designs resulting in many improvements particularly in producibility and cost.

The brazed lower plate of the FSRL was redesigned to a three element symmetrical configuration with the lug integral with the lower plate. This configuration was renamed Fail Safe Integral Lug (FSIL). This configuration offers many advantages including: lower weight, lower cost, improved producibility, and increased predictability as a result of the elimination of the lower lug to plate splice. New internal bulkheads featuring arched design at Stations 947 and 977 were added.

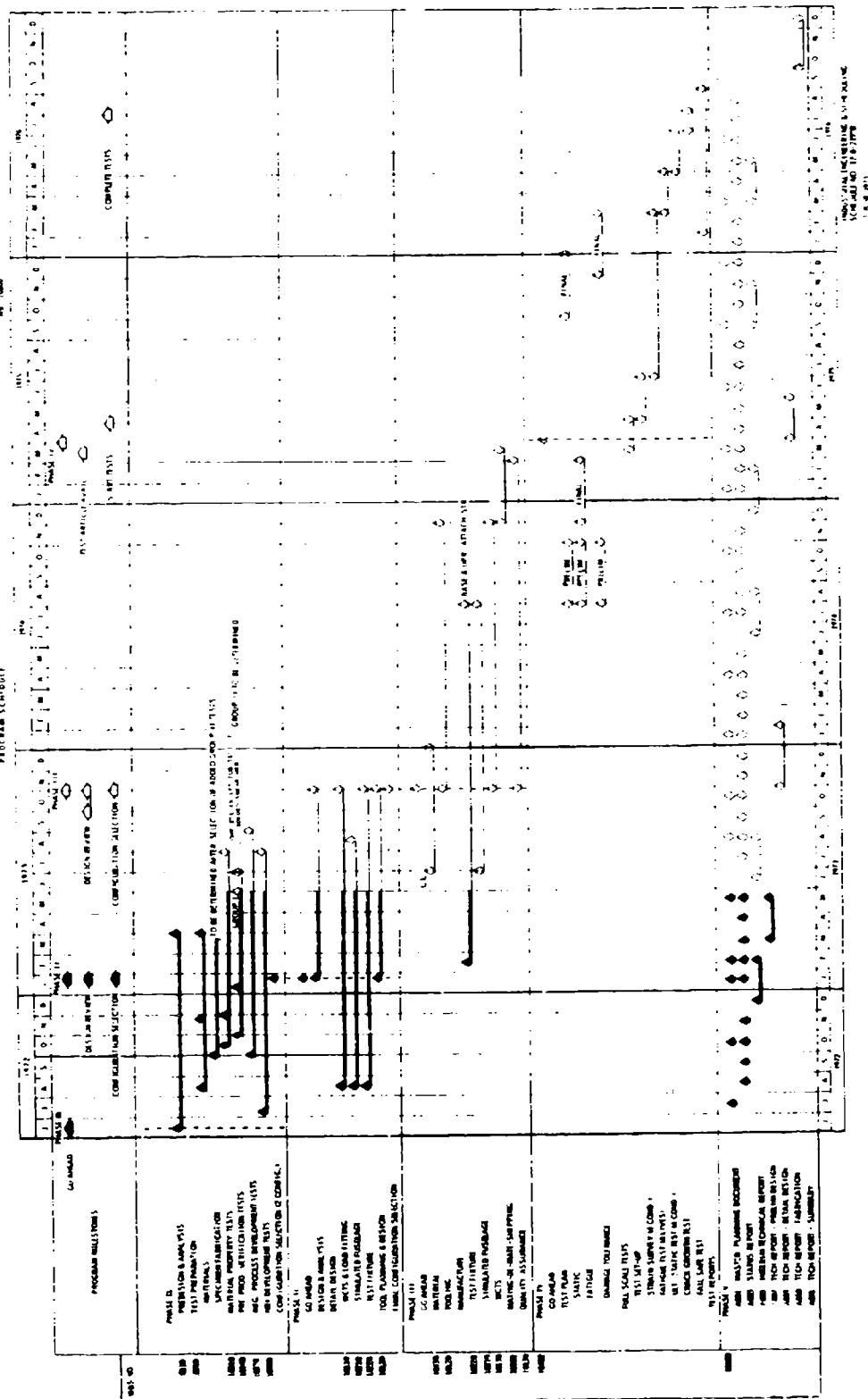
The NBB lower lug was redesigned by extending the lug to the centerline of the WCTS thus serving the functions of lug, lower plate (partial) and bulkhead rail. The fuel boundary was moved from the WCTS lower contour to $Z_F = 0$ and a titanium sandwich lower plate was added. The area from $Z_F = 0$ to lower contour was then designed as a fairing. Improved predictability, improved producibility and reduced cost resulted from these revisions.

The Development Test Program consisting of Material Testing, Component Testing, NDI Development and Manufacturing Development started in the first six months of the program was continued with most of the material testing and component testing completed.

The design and manufacture of the full scale test fixture were continued. The design of the various elements of the test fixture including base, dummy wings, simulated fuselage and upper forward and aft fuselage extensions is nearing completion. Manufacturing of the test fixture base is progressing satisfactorily.

An Open Design Review of the AMAVS Program was held at Fort Worth on 1-2 May 1973. One hundred and forty representatives from industry, Air Force, Navy and NASA were in attendance.

ADVANCED METALLIC AIR VEHICLE STRUCTURE PROGRAM SCHEDULE



SECTION II

TECHNOLOGY ADVANCEMENT

Recent developments in the fields of structures, materials and manufacturing are being applied to the WCTS design to demonstrate that advanced technology can increase the efficiency and the damage tolerance of aircraft structures. The results to date are encouraging. Projected efficiency improvements are ahead of the program goals:

Configuration	Cost Savings		Weight Savings	
	Goal	Projected	Goal	Projected
No-Box Box*	30%	38%	5%	10%
FSI	27%	37%	16%	19%

* - NBB projected costs are shown on page 35.

These highly efficient structures are designed in accordance with Air Force damage tolerance requirements which virtually preclude the possibility of structural failure. Specifically, these designs are either fail safe or safe crack growth as defined by MIL-8866A. Fail safe designs have limit load capacity with one element failed plus a residual fatigue life of 1/4 service life. Safe crack growth structure is designed such that a pre-existing flaw (0.15 inch in the critical dimension) is stable for one complete service life even if this flaw is located in the worst possible place with respect to the applied stresses and material properties. The achievement of efficient damage-tolerant designs is attributed to technology advancements in the fields of structures, materials and manufacturing.

The principal means of meeting the efficiency and damage tolerance goals of the AMAVS program has been through the development of innovative design concepts. The principal efficiency improvements over the baseline are attributed to:

- | | |
|---------------|------------------------------------------------------------|
| Weight | 1. Multiple layer damage tolerant lugs. |
| Cost & Weight | 2. Elimination of the lower lug-plate splice. |
| " " " | 3. Internal structural arrangement. |
| " " " | 4. Fewer fasteners. |
| Cost | 5. Fewer pieces. |
| " | 6. Use of aluminum in place of titanium in selected parts. |

Design ideas rarely qualify as technology advancements because the idea is limited to a particular application. However, the design strategy - based on technology integration - is worthy of consideration for the development of future Air Force systems. The key elements of the strategy are design iteration and developmental risk - both of which are normally minimized in Air Force production programs. In the AMAVS program, increased span time has been provided for design iteration; and design constraints normally applied to production programs to minimize developmental risk have been removed. Thus, implementation of this strategy into future Air Force programs requires special planning. High payoff design concepts need to be developed in parallel with the production system and implemented into the system upon demonstration of the payoff.

Specific technology advancements under development in the AMAVS program are discussed in the following subsections. Status of the developmental efforts and our current assessment of the merits and shortcomings of the technologies are reported.

2.1 BRAZED DAMAGE TOLERANT STRUCTURES

Brazing was selected as a joining method for the AMAVS Program with the idea that it would provide a joint of moderate strength which would also serve to retard crack growth from one side of the joint to the other. A materials and component test program has been conducted to test this thesis. The results of this test program with respect to brazed joint strength and crack retardation are summarized briefly in the following paragraphs.

2.1.1 Brazing Process

The important parameters affecting the quality of brazed joints have been identified and are being evaluated. The vacuum retort method of brazing using Dynabraz B brazing alloy and beta annealed 6Al-4V titanium plates has proven to be a feasible method for producing structural components using wide area brazing as a joining method.

Retort design and atmospheric control in the retort were two of the more important items which influenced the quality of the brazed components. Mismatch in adjacent cutter passes in machining the surfaces to be brazed was found to be very important. Complexity of the brazed joints and tolerances of mating pieces were also found to be important factors.

2.1.2 Brazed Joint Strength

High quality brazed joints have demonstrated excellent static strength for both lap-shear and VQ/I loadings. Good fatigue strength has also been demonstrated. The lap-shear static strength is reduced sharply if the joint is loaded eccentrically and peel forces are present.

The stress corrosion resistance of brazed lap shear specimens appears to be satisfactory. However, several failures have occurred prior to completion of 1000 hours of sustained loading. Most of these failures have occurred at 12 ksi sustained shear stress in specimens taken from one panel that is currently under metallurgical investigation. The other failures have occurred in specimens with high percentages of void leading to high net section shear stresses. Work is in progress to define the stress corrosion threshold and to find the significant metallurgical variables contributing to the stress corrosion process.

Static and fatigue tests have also been conducted on sub-standard joints to determine the effect of braze defects on joint strength. This data will aid decisions concerning acceptability of defects in structural joints.

2.1.3 Crack Retardation at Brazed Joints

Crack growth tests have been conducted on small test coupons and on relatively large components. There is considerable evidence that slow crack growth is retarded at the brazed joints and that a crack will not progress directly across the braze line. Delamination has generally occurred in the vicinity of cracks in laminated plate structure, further enhancing the crack retardation.

Attempts to achieve a rapidly running crack in the brazed components proved to be unsuccessful, primarily because of the excellent fracture toughness of the beta annealed 6Al-4V titanium. Therefore, no additional information has been obtained concerning the ability of a brazed joint to arrest a rapidly growing crack. Initial tests on a brittle material indicated that the brazed joint will arrest a rapid failure, again accompanied by delamination of the brazed joint.

In a multiple layer component such as the brazed pivot lug, cracks in regions of large stress gradients appear to be confined to one layer of material until a fatigue failure is initiated in adjacent layers. Because of this, the multiple layers do not act

independently and a crack cannot be confined to one layer of material until complete failure of that layer occurs. However, this same condition will exist if the layers are bolted together.

2.1.4 Conclusions

Results of development and testing already completed indicate that it is feasible to produce brazed structural components of sound quality. Experience has shown that simple symmetrical joints are easier to produce and have greater structural reliability. Belt sanding of large surfaces to eliminate machined steps improves the quality of the brazed joints. Successful completion of the larger component test specimens now in work will give confidence in the ability to scale-up the brazing techniques to production-size articles.

Crack growth testing has given confidence in the ability of brazed bars to serve as crack arrest members for the beta annealed 6Al-4V titanium lower plate. Additional testing will expand the range of initial flaws considered and provide residual strength data for full-scale sections of the lower plate.

2.2 BONDED LAMINATED STRUCTURE

The use of adhesive bonded laminated titanium structure to provide damage tolerance was proposed for several structural components of the WCTS. It has generally been conceded that the adhesive joint will serve as a crack arrest medium. Therefore, most of the emphasis of the development program has been placed on the bonding process, inspection characteristics and strength characteristics.

2.2.1 Bonding Process

Adhesive bonding of multi-ply titanium laminated structure has been very successful. Both mill annealed 6Al-4V and Beta C titanium sheets of .125 inch thickness have been bonded. A vacuum deaeration process has proven to be successful in preventing air entrapment between laminates. Two adhesives, PL717 and AF66, have produced good quality joints. The PL717 adhesive was judged to be slightly superior.

Large variations in bond line thicknesses were found to exist in the bonded laminated structure as a result of waviness in the sheets. These thickness variations did not affect the

strength adversely. It was discovered, however, that in the .125 inch thick material, large gaps between adjacent sheets can cause voids if the bonding pressure does not close the gap to the extent that the volume of available adhesive will fill the gap. This will occur even if all air has been evacuated from the cavity.

2.2.2 Strength of Bonded Joints

Strength tests were performed on specimens taken from ten-ply panels as well as the conventional bonded test specimens. All of the test data to date has proven to be entirely satisfactory. Test data is contained in section 3.1.4 of this report.

Static and fatigue tests were performed on bolted joint specimens using both straight shank fasteners and Taper-lok fasteners. These tests indicate load introduction into the bonded laminated structure will not present any problems which do not exist in monolithic structure. Tests also indicate that machining, drilling and reaming operations do not cause any unusual problems in laminated structure.

One of the proposed applications of bonded laminated structure was in shear webs for bulkheads and ribs. Tests were conducted to determine the buckling characteristics for two and three-ply laminations. The webs of Beta C titanium withstood shear stresses as high as 96000 psi before buckling. The buckling stress was in agreement with predicted values for monolithic webs of the same total thickness.

2.2.3 Inspection of Bonded Joints

Existing inspection techniques have been judged to be adequate for bonded laminates up to five plies. Some success was achieved in inspecting the ten-ply panels but it was not felt that these panels could be reliably inspected without further development work.

2.2.4 Conclusions

The bonding process employed is capable of producing high quality laminated panels. Reliable inspection techniques are available to inspect panels up to five plies in thickness.

The PL717 adhesive will provide good joint strength for the titanium alloys. The joints are highly reliable for both static

and fatigue loads. The adhesive has good peel strength and has adequate tensile strength to withstand any forces applied by highly loaded shear panels. In summary, this concept produces sound structural components and fulfilled all expectations. The properties of the structure are limited by the properties of the sheets being bonded together.

2.3 MATERIALS

A comprehensive materials testing program is being conducted to provide detail characterization of the "new" material/heat-treatments being used in the WCTS designs:

Beta annealed 6Al-4V titanium plate

10 Ni steel plate

Beta C titanium sheet

Design allowables, fatigue S/N curves and fracture mechanics properties are being determined for each material.

2.3.1 Beta Annealed 6Al-4V Titanium

The material tests planned for beta annealed 6Al-4V titanium are essentially complete. Results to date indicate that the alloy has excellent fracture resistance and satisfactory mechanical properties and fatigue strength. The fracture toughness tests indicate that the material has a typical plane strain fracture toughness (K_{IC}) in excess of 100 ksi $\sqrt{\text{in}}$ at room temperature and -65°F and in both the RW and WR grain directions. Therefore, the minimum guaranteed K_{IC} of 80 ksi $\sqrt{\text{in}}$ required by the procurement specification should be readily met. The fatigue crack growth behavior in both dry air and sump tank water is superior to that of other titanium alloys. There should be no problem in qualifying the lower plate and other critical structure to the safe crack growth requirements of the AMAVS program. Beta annealed 6Al-4V titanium is virtually immune to stress corrosion cracking. No crack extension occurred in test specimens that were loaded to initial stress intensities in excess of 70 ksi $\sqrt{\text{in}}$ and held for 1600 hours. The design allowables are about 5% lower than the MIL HDBK V values for conventional mill annealed 6Al-4V titanium, however, this was anticipated on the basis of Boeing SST studies and is of no consequence to the designs. The fatigue allowables are slightly lower than anticipated. Part of this reduction is attributed to the use of notched flat plate specimens to generate fatigue S/N curves.

2.3.2 10 Ni Steel

The material tests planned for 10 Ni steel are nearing completion. Results to date indicate that the alloy has excellent fracture resistance and satisfactory mechanical properties and fatigue strength. Charpy impact tests and the fracture behavior of the spectrum fatigue crack growth specimens indicate that 10 Ni steel has the excellent toughness reported by the developers, the Navy and U.S. Steel. The fatigue crack growth behavior is comparable to other high strength steels in dry air and the sensitivity to sump tank water is slight. The design allowables are essentially the same as those reported for other steels at the 195 ksi strength level. Fatigue testing is still in the initial stages. Initial results indicate that fatigue strength at $K_T = 1$ and 2.4 is approximately equal to that assumed for design - about 10% lower than D6ac steel (220-240 ksi strength level), and the fatigue strength at $K_T = 5$ is significantly lower than that assumed for design. The reduced fatigue strength at $K_T = 5$ will require a stress reduction in the lower lugs.

2.3.3 Beta C Titanium

Material testing on Beta C is approximately half finished. Results to date indicate that the alloy has excellent design allowables; but, relative to beta annealed 6Al-4V titanium, it has poor fracture resistance and fatigue strength. Of particular concern is the environmental enhanced crack growth observed in sump tank water. Further tests and metallurgical studies are in work to characterize the extent and nature of the environmental sensitivity. The fatigue strength is significantly lower than beta annealed 6Al-4V titanium - a factor of 2.5 on life in spectrum tests with $K_T = 2.4$. The environmental sensitivity and reduced fatigue strength, coupled with the relatively low modulus and high density of Beta C, have led to the replacement of Beta C with beta annealed 6Al-4V titanium in the WCTS designs.

SECTION III
TECHNICAL DISCIPLINES
PROGRESS

3.1 ENGINEERING

3.1.1 Structural Design

The two wing carrythrough structural configurations selected for detail design during Phase II have been modified since the end of Phase Ib to incorporate various trade study results. The two configurations, as modified, are described in this section and are identified as follows:

Fail-Safe Integral Lug (FSIL)

This configuration is distinguished by a brazed three-element lower plate with integral pivot lugs.

"No-Box" Box (NBB)

This configuration utilizes 10 Ni steel concentrated in area of the bulkheads as the primary load carrying material.

These configurations as described in the following paragraphs, reflect the results of trade studies and component tests conducted during the end of Phase Ib and the early part of Phase II.

3.1.1.1 Fail Safe Integral Lug Configuration

The fail-safe removable lug configuration has been renamed to reflect the integral lug concept now employed for the lower plate. An integral upper lug was incorporated during Phase Ib. Trade studies indicate that an integral lug is advantageous from both weight and cost considerations. This configuration will be identified in the future as the "Fail-Safe Integral Lug Configuration." The distinguishing feature of this configuration is still the brazed titanium lower plate and pivot lug.

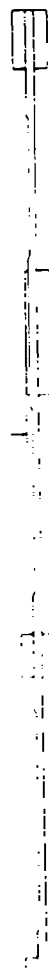
Additional trade studies, component test and material testing has resulted in redesign of the brazed lower plate assembly and the internal bulkheads at YF947 and YF977. A description of these redesigned components is discussed in the following pages. The remaining structural components are described in detail in the Phase Ib Preliminary Design Summary Report (AFFDL-TR-73-40), dated March 1973.

Lower Plate Assembly - Major revisions to the lower plate include an integral pivot lug and a symmetrically brazed assembly. The integral lug concept improves fabrication by eliminating the separate brazed assembly for the pivot lug and eliminating the critical fit between the lug and plate. The integral lug is also a more weight efficient configuration and improves structural reliability by deleting the dependence on mechanical fasteners for transferring the critical lug loads into the box structure. The symmetrically brazed concept permits the assembly to be used as either a left or right hand part, but requires separate bolt-on bulkhead attachment angles. Eccentric loading of the brazed joints is also minimized by the symmetrical design.

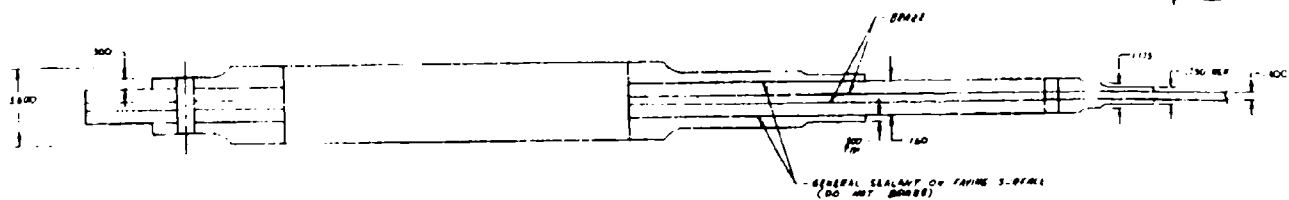
The brazed plate assembly shown in Figure 1 (Drawing 603R214) is constant thickness consisting of three laminae of beta annealed 6Al-4V titanium which extend to include the pivot lug. The one-piece center lamina is a solid thin plate whereas the one-piece upper and lower elements are profiled into five crack stopper bars, inboard of the lug region. The plate assembly, as brazed, is symmetrical about its horizontal centerline. Local machining will be required after brazing to obtain identity as either a left or right hand part.

The aft longeron splice fitting shown in Figure 2 (Drawing 603R228) consists of two elements of beta annealed 6Al-4V titanium, double-shear spliced to the brazed assembly. The upper element extends the full width of the plate and incorporates the vertical flange for attaching the closure rib. The lower element terminates after transferring the longeron load into the lower plate. This splice provides extra thickness to accommodate the baseline longeron interface requirement, and it reduces the material width required in the lower plate from 82 to 73 inches. Seventy-two inch width material has been developed as part of the SST contract.

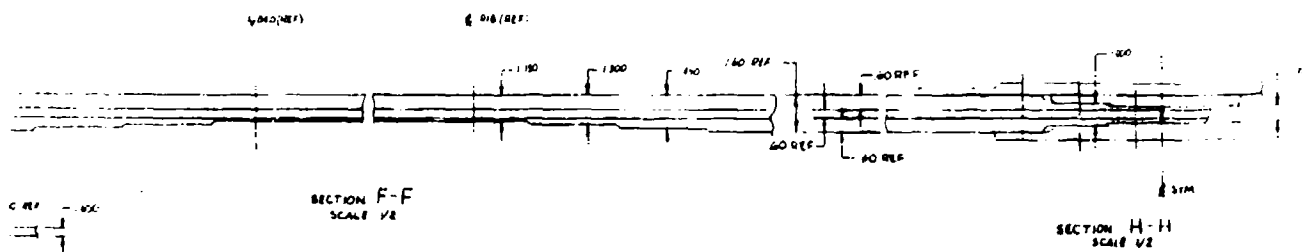
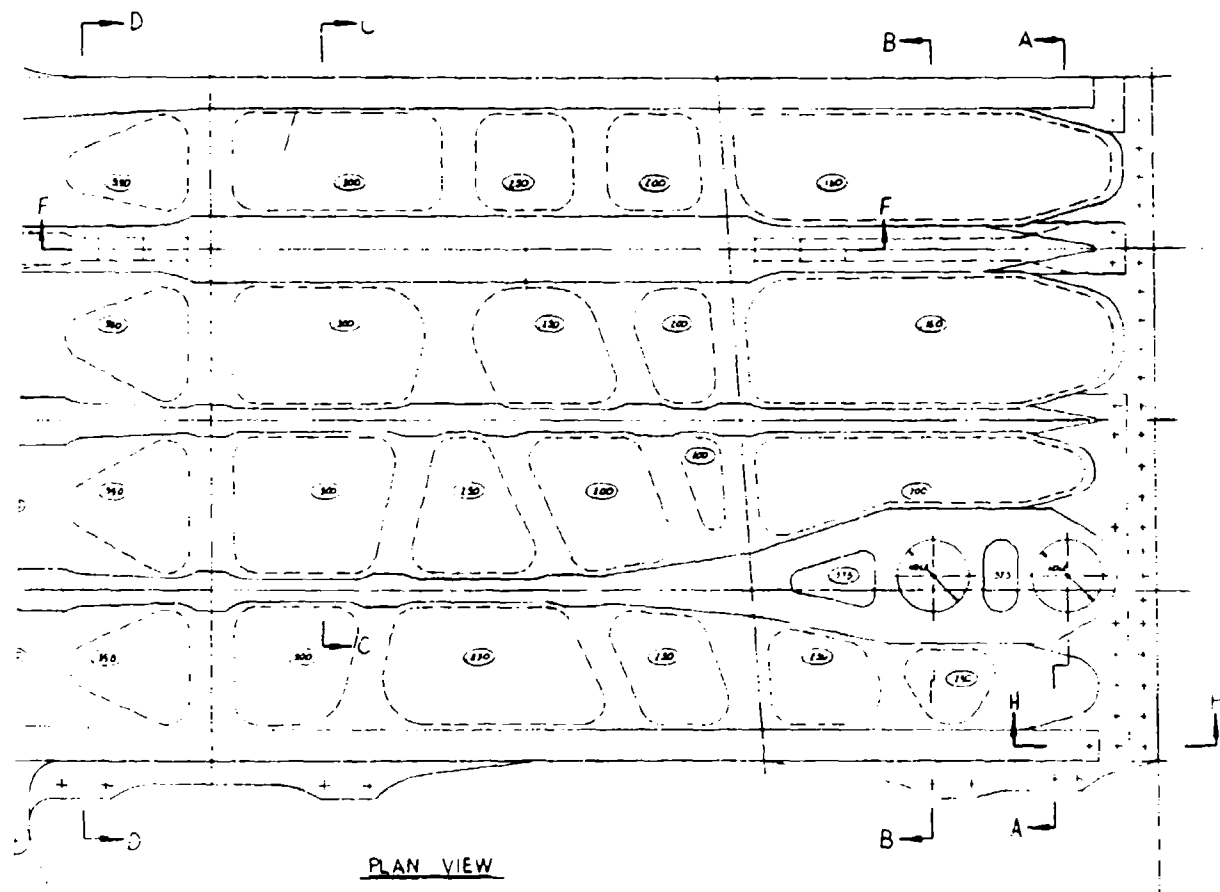
The forward longeron splice fitting, also shown in Figure 2 (Drawing 603R228), is integrally machined from 7050 aluminum plate and single-shear spliced to the lower surface of the brazed lower plate. The fitting extends the full width of the lower plate and includes a vertical flange for attaching the support structure for the lower contoured fairing.



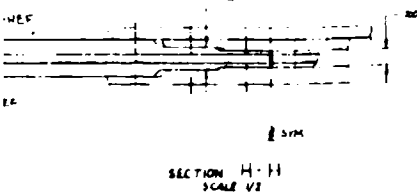
SECTION
PAGE 18



SECTION E-E
SCALE 1/8"



١٠٧٩
١٠٨٠

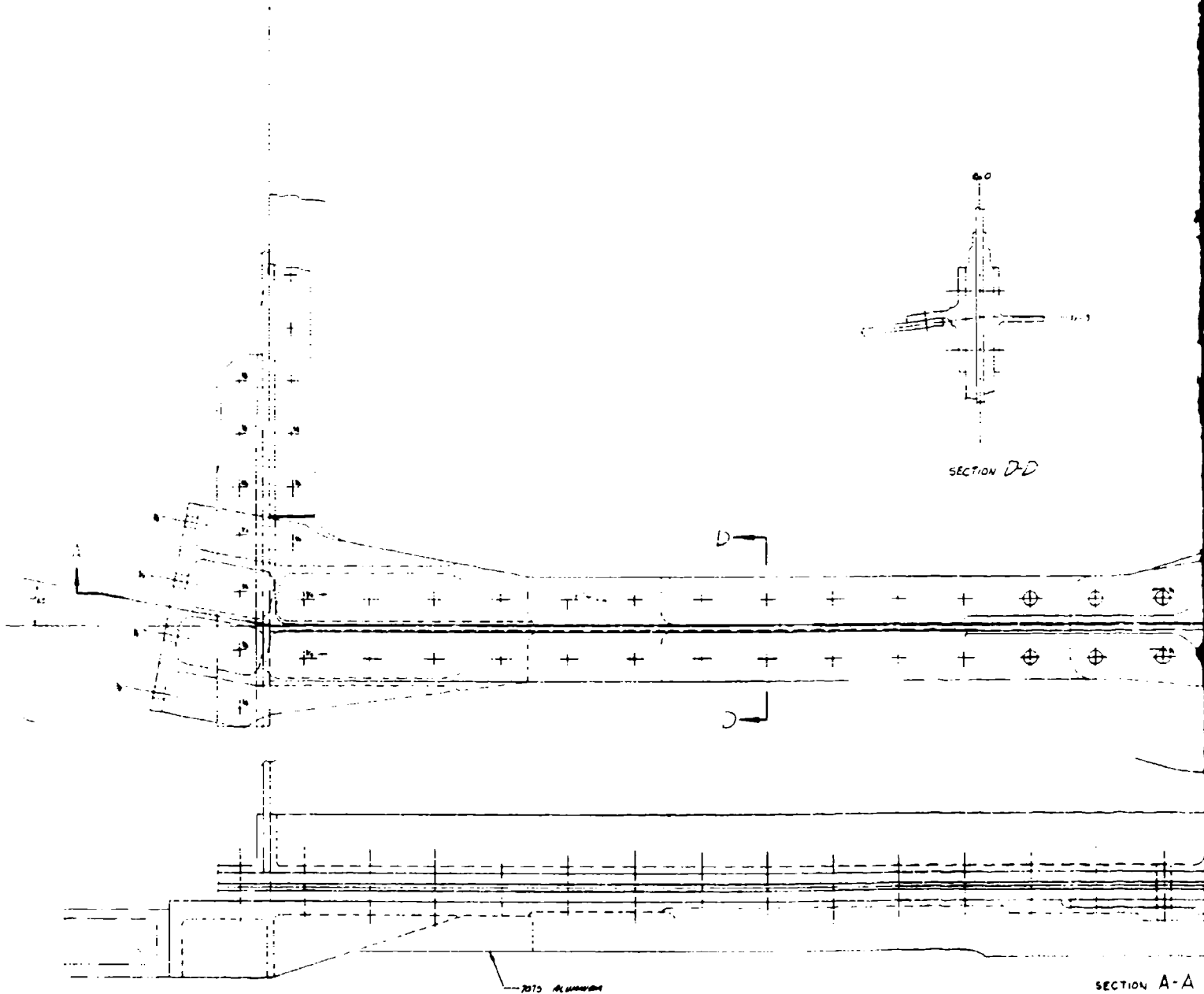


PRELIMINARY DESIGN DRAWING

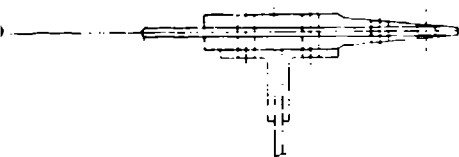
LOWER PLATE - BRAZED Tc.
FSRL ALTERNATE NO III
STUDY OF

GENERAL DYNAMICS
Convair Aerospace Division
For Study Approval

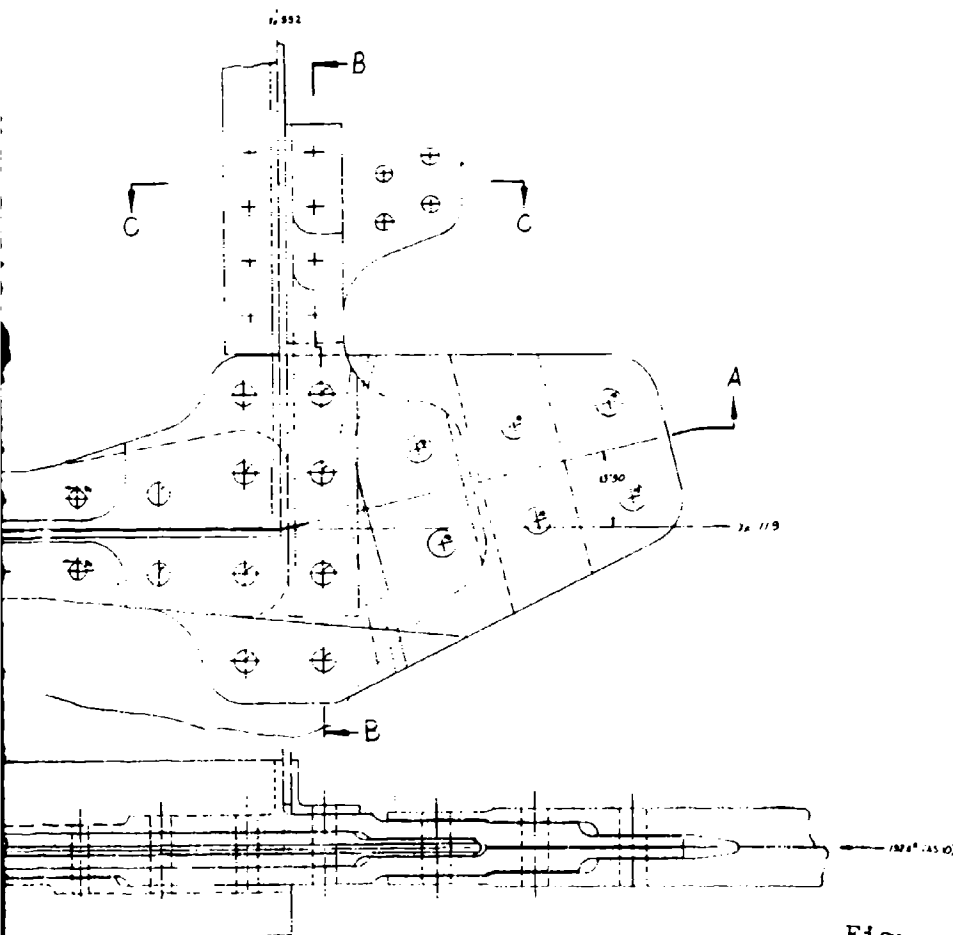
60SR214 B



SECTION A-A

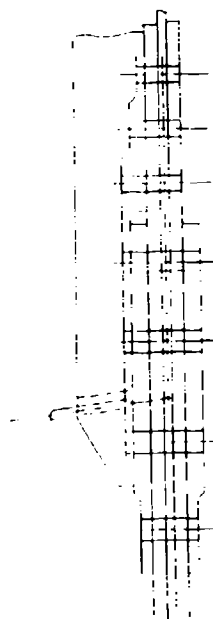


SECTION C-C



SECTION A-A

Figure 2



SECTION B-B

NOTES - (1) SEE PL. 10000
(2) MATERIAL TO BE 6061-T6 ALUMINUM

PRELIMINARY DESIGN DRAWING	
LONGERON SPlice LWR AFT OUTBD, FSIL CONFIG	
DESIGNED BY DYNAMICS	DATE JUL 19 1971
CHECKED BY DYNAMICS	603R228

Separate bolt-on lug reinforcements are required to supplement the strength capability of the brazed assembly, and to maintain baseline bearing thickness at the pivot hole. The attaching Taper-lok bolts are located in relatively low stressed areas and provide a positive control against element delamination.

Reinforcement beams shown in Figure 3 (Drawing 603R240) are made from 2024 aluminum and located at Xf99 to provide compression stability during negative loading conditions. The beams are attached to the lower surface of the plate assembly and extend to contour to provide support to the lower fairing.

Brazed Lower Plate Trade Study - This trade study evaluates the two additional brazed lower plate designs and compares the results with the Phase Ib design. The two additional designs were generated in Phase II to alleviate the brazing problems encountered with the two Phase Ib 3/8 Scale Lower Plate Component Test Specimens (603FTB005). The brazed surfaces of the first specimen were unsatisfactory to the extent that it was not suitable for testing. More rigid controls were employed during the fabrication of the second specimen to obtain an improved braze. This specimen was fatigue tested to only 2 ½ service lives before failure. This premature failure was attributed to a combination of eccentric shear loading on the brazed joints and substandard braze quality.

A new design concept employing three full width, symmetrically brazed, laminates was simulated in two full scale crack stopper demonstration test specimens (603FTB051). The test results indicated promise of achieving the necessary damage tolerance and improved fabrication reliability. As a result, the Phase Ib design was eliminated from contention and two configurations were generated utilizing this new design concept. One configuration consists of a removable lug, the other an integral lug. The integral lug configuration is shown on drawings 603R214 and 603R228 and was described in the previous paragraph. The bolt-on lug configuration is depicted in Figure 4 (Drawing 603R215). The Phase Ib design is described in the summary report (AFFDL-TR-73-40) dated March 1973 and is identified by the following drawings: 603R174, 603R147, and 603R140.

The results of the weight and cost trade studies conducted on the two additional configurations are summarized in the following table. The costs presented are average unit cost based on a production quantity of 200 ship sets.

STUDY	ITEM	CONFIGURATION	
		Phase II FSRL	Phase II FSIL
WEIGHT	Plate	1763#	1757#
	Attach Angles	134	140
	Lug	1206	837
	Long. Ftg.	*	155
	TOTAL	3103#	2889#
COST	Material	\$107,340	\$110,800
	Fabrication	65,004	42,336
	Tooling	10,476	7,036
	TOTAL	\$182,820	\$160,172

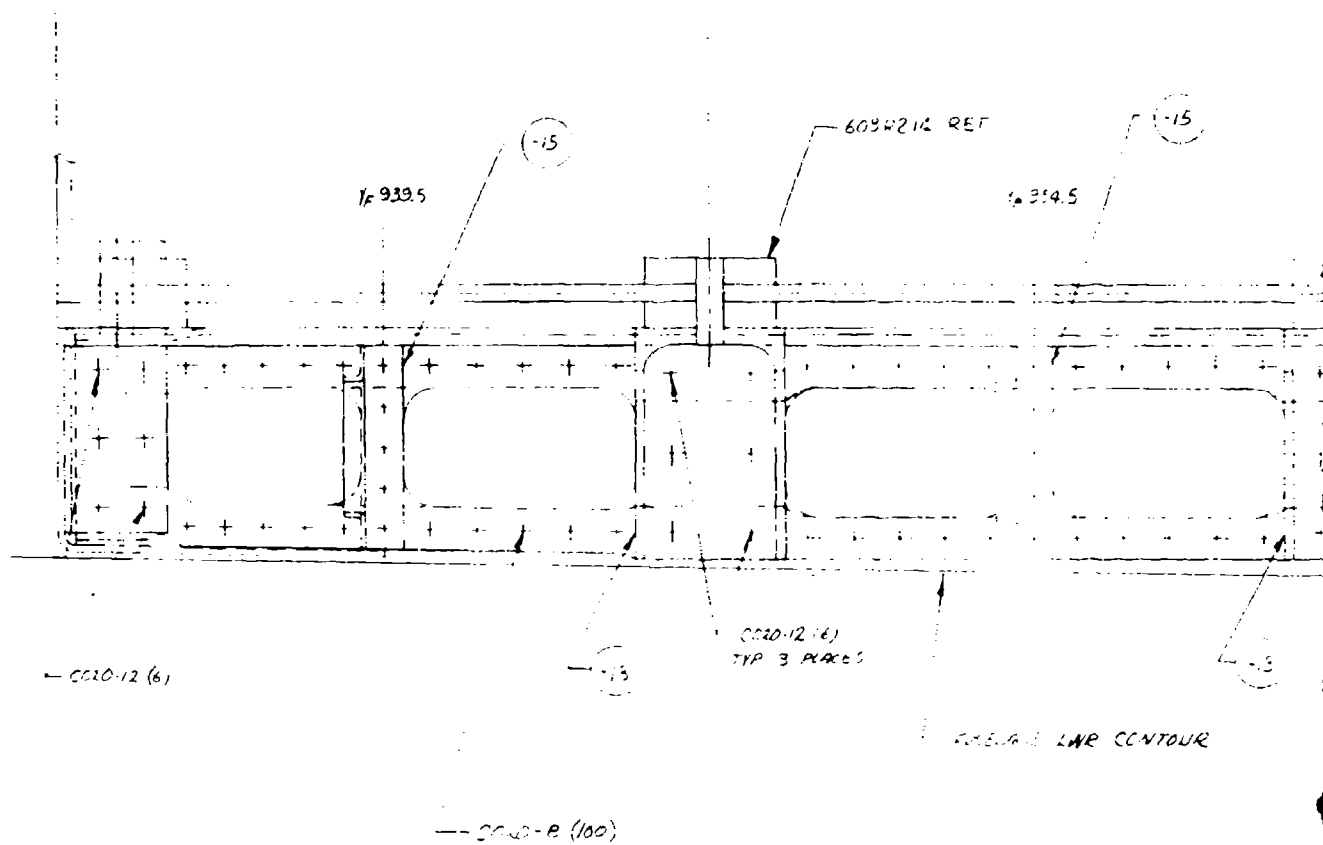
* Not applicable - Integral with lug.

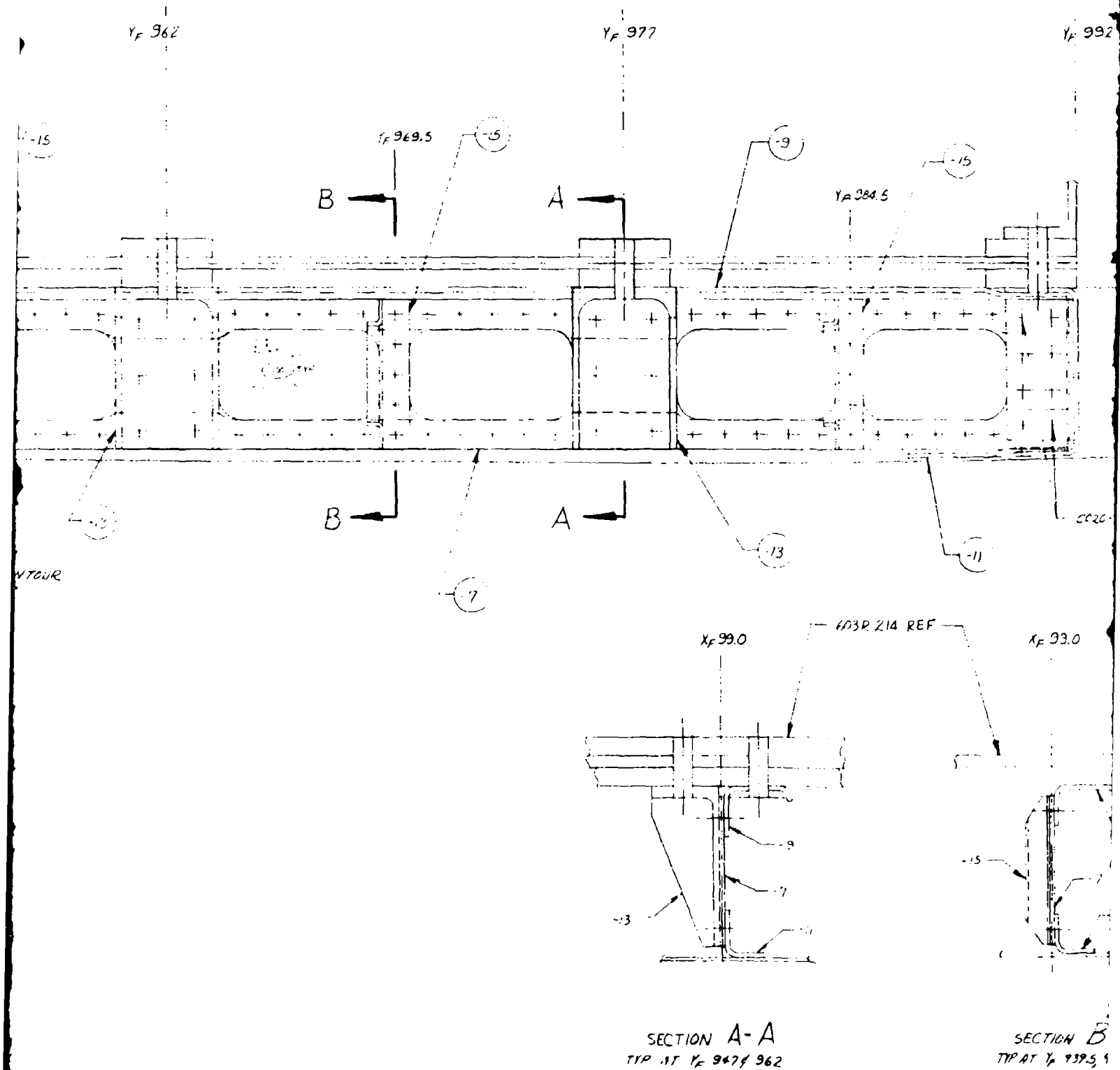
The detailed weight changes for the Phase II, lower plate designs and their attributing factors are summarized below.

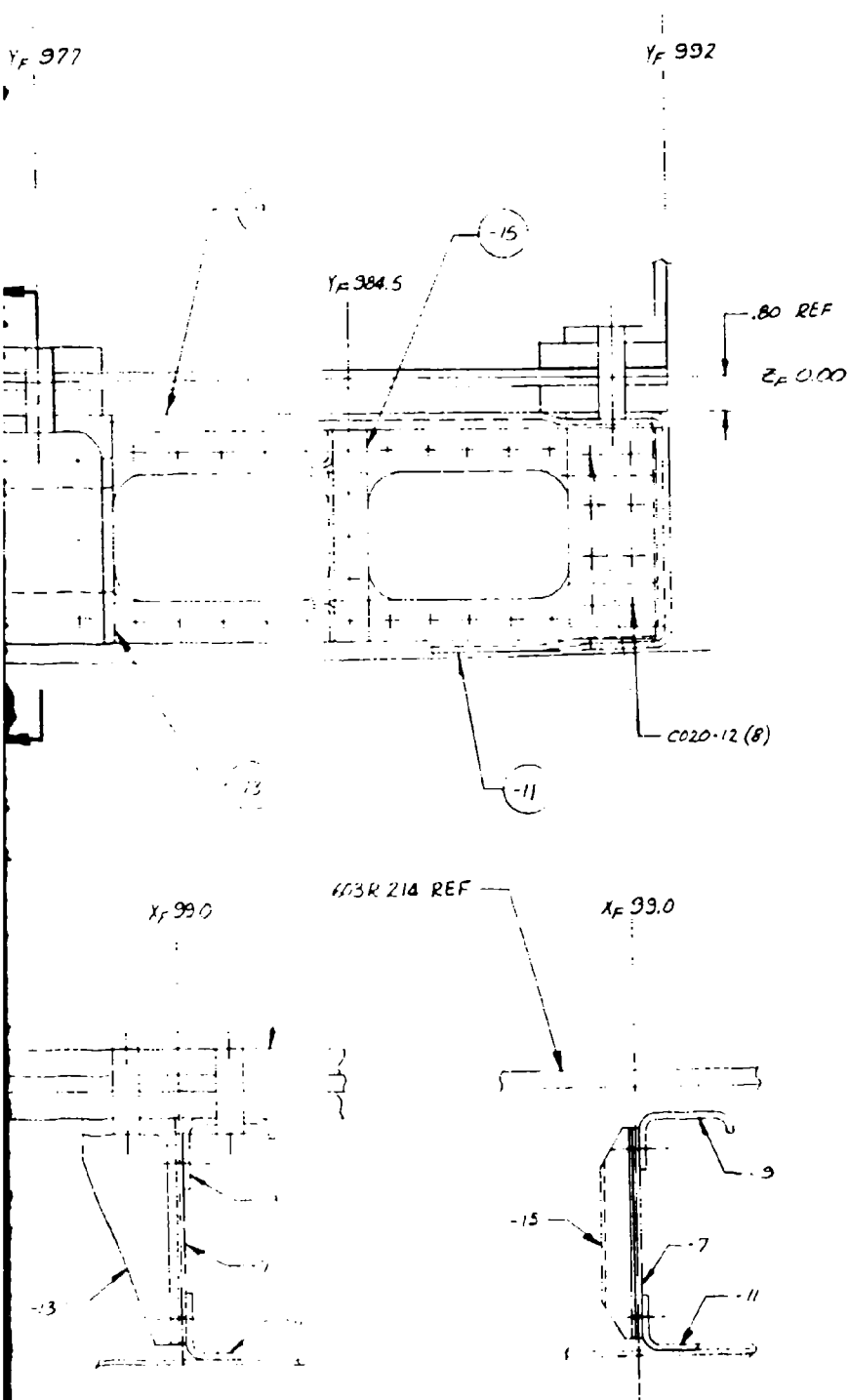
ITEM	CONFIGURATION	
	Phase II FSRL	Phase II FSIL
Net Section Loss in Plate	+76#	+76#
Titanium vs. Steel Long. Ftg.	-58	-58
Stress Reduction in Lug	+48	+48
Stress Reduction in Plate	+96	+96
Integral Lug	0	-214
NET TOTAL	+162#	-52#

The Phase II designs are based on equal stress levels which were reduced up to approximately 20% below the Phase Ib design in

Y.



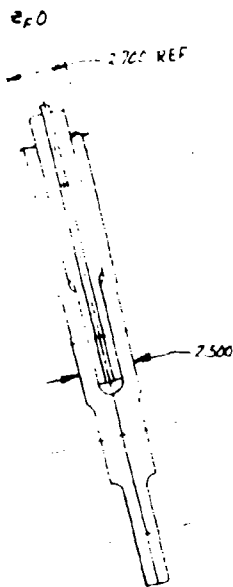




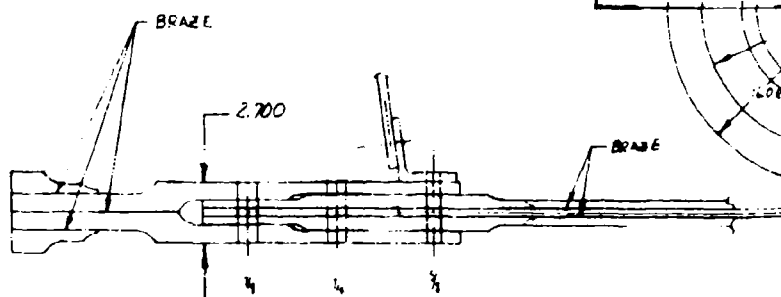
1. ALL MATERIAL TO BE 2024 ALUMINUM
NOTES~

Figure 3

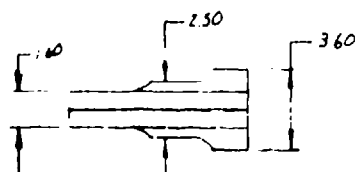
GENERAL DYNAMICS	
Fort Worth Division	FORT WORTH TEXAS
BEAM INSTR - X _F 9200 LOWER PLATE, FSIL CONFIGURATION	
CODE IDENT NO. 81755	SIZE 603R240
SCALE 1/2"	SHEET 1 of 1



SECTION F-F

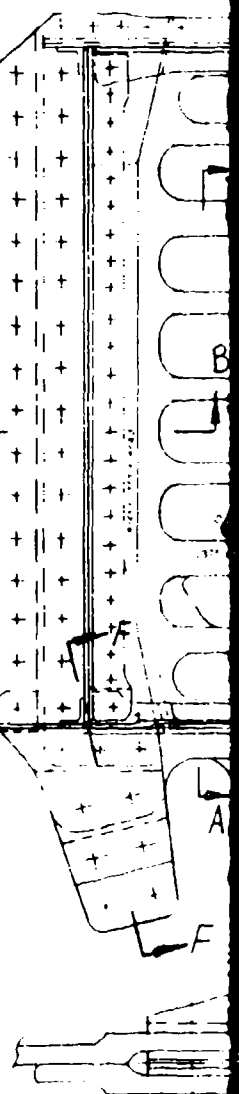


SECTION B-B
SCALE 1/4

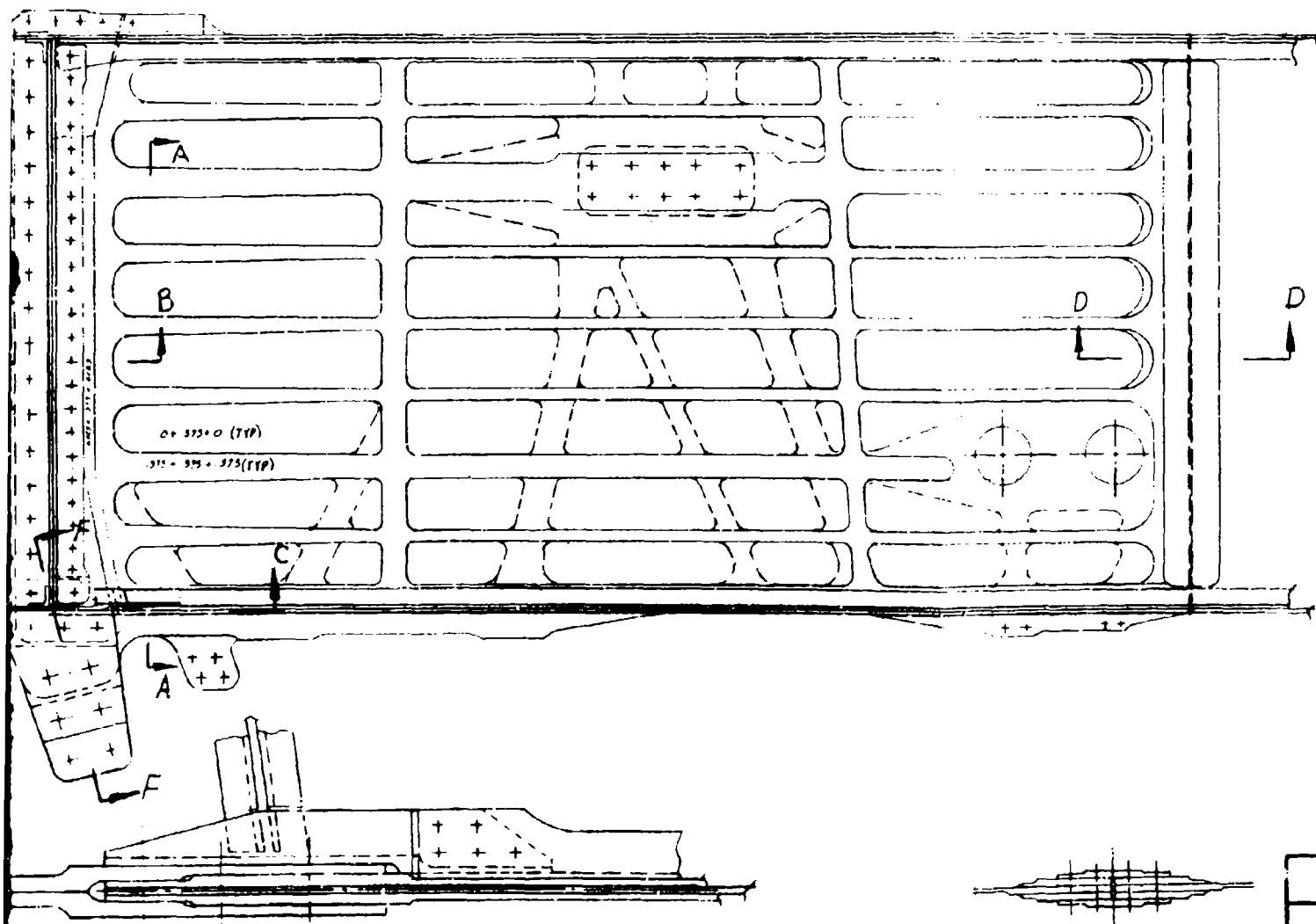


SECTION E-E
SCALE 1/4

SECTION A-A
SCALE 1/4



A/CWG-EXTENDED
THREE ROW OF
LONGERON TAB
EXTERNAL ATTACH
1/2 932 4 1/2 992 8
ADDED SECTION



SECTION C-C
SCALE 1/4

SECTION D-D
SCALE 1/4

GENERAL
Part W
LOWER
FSRL
CODE IDENT NO.
81755
DATE

A' CHG - EXTENDED LUG SPACE INBD TO INCLUDE
THREE ROW OF BOLTS. INCORPORATED AFT 5-80-99
LONGERON TAB INTO PIOT LUGS. DELETED ~~THREE~~
EXTERNAL ATTACHMENT ANGLES FOR THE
1-932 1/2 992 BHD'S, AND THE CLOSURE RIB.
ADDED SECTION E-K

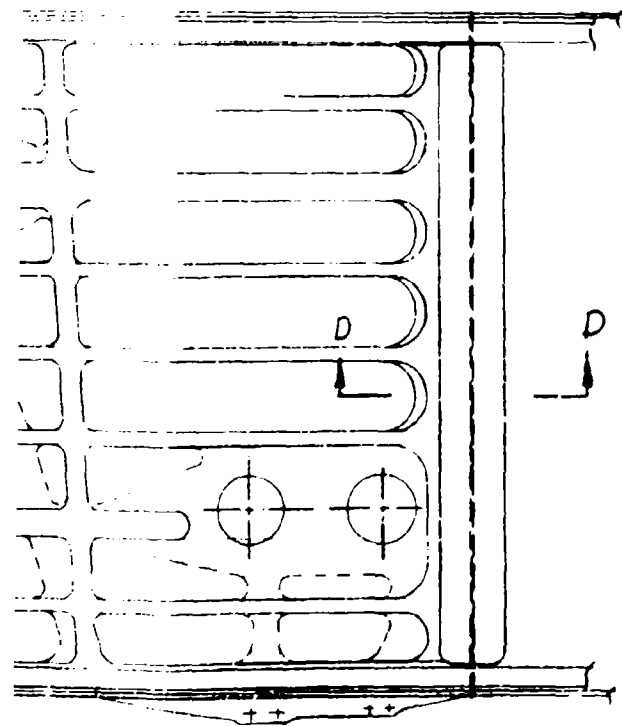


Figure 4



SECTION D-D
SCALE 1/4

GENERAL DYNAMICS	
Fort Worth Division	FORT WORTH, TEXAS
LOWER PLATE - BRAZED T ₆ , FSRL ALTERNATE NO. II, STUDY OF	
COOP. IDENT. NO. 81755	SIZE D 603R215 A
DATE 1-1-61	1-1-61

the more critical areas. The weight advantage of the integral lug configuration offset the penalty incurred by the stress reduction and net section loss.

Fabrication is the major cost factor between the integral and removable lug configurations. The integral lug concept eliminates the fabrication complexity of mating the pivot lug to the plate assembly and the added operations required for two brazed assemblies. The requirement for one set of brazed tools is also deleted. Additional fasteners are also required to accomplish the pivot lug splice.

The overall results of this study indicate adequate justification for the selection of the integral lug configuration.

Internal Bulkheads - The internal bulkheads located at Yf947 and Yf977 were redesigned into "arched" configurations as shown in Figures 5 and 6 (Drawings 603R238 and 603R239) respectively. The arched concept permits the use of lower cost aluminum construction by deleting the strain compatibility requirement with the titanium lower plate. Fastener reduction is also accomplished in the fatigue critical lower plate by eliminating the attachment of these bulkheads. The internal beam and its necessary attachments through the lower plate are still required, however, at Yf947 to support the MLG drag brace fitting.

Each bulkhead is partial-width, extending between the Xf39 rib and the outboard closure rib, with a mechanical splice at the Xf84 rib. All panels are adhesive bonded sandwich using 7050 aluminum and zee type edge members. The arched cutouts are reinforced with 7050 aluminum zee members formed to shape.

Internal Bulkhead Trade Study - This trade study was conducted to verify the feasibility of replacing the Phase Ib internal bulkheads with the arched bulkheads described in the preceding paragraph. The primary consideration was the structural integrity of the bulkheads themselves and their impact on adjacent structural components. Computer stress analysis verified the structural feasibility of aluminum arched bulkheads at Yf947 and Yf977 as described in Section 3.1.2.

The Phase Ib bulkhead designs utilized titanium construction at Yf947 and aluminum at Yf977. Computer stress analysis for the Yf977 bulkhead, however, indicated a need for titanium to satisfy the strain requirements of the titanium lower plate. The replacement of titanium with aluminum is an obvious cost reduction and the reduced surface area of the new design concept indicates an additional reduction.

3.1.1.2 "No-Box" Box Configuration

The basic design of the majority of "No-Box" structural components remains unchanged from the Phase Ib design. As a result of trade studies conducted during Phase Ib, changes were incorporated into several of these components. The most significant changes were made to the forward and aft bulkheads which reduced the material and machining requirements for these items. The lower cover was also changed from titanium to aluminum with a resulting material, tooling, and fabrication cost reduction. These studies and the basic design configuration are contained in the Phase Ib Preliminary Design Summary Report, AFFDL-TR-73-40, dated March 1973.

The "No-Box" design concept was changed early in Phase II to the extent that the structural lower contour panels were eliminated and replaced with a structural panel at Z_F0.0. This configuration change and additional design developments and studies are described in the following paragraphs. For those components that remain unchanged, refer to the AFFDL-TR-73-40 report.

Lower Pivot Lug and Z_F0.0 Panel - As a result of a trade study started late during Phase Ib which continued into Phase II, it was decided to incorporate a panel at approximately Z_F0.0 into the No-Box configuration. See drawing No. 603R237, Figure 7. This panel reacts shear and fuel pressure loads and a portion of the axial load. The major portion of the axial load is now carried by members integral with the pivot lug that extend inboard to the centerline of the box adjacent to the fore and aft bulkhead lower flanges. The lug loads were previously introduced directly into the bulkhead lower flanges. A single shear splice at the centerline provides lower plate continuity for the new design. It would be feasible to eliminate the centerline splice for a production run by using twenty seven (27) foot long plate material for the lower lug.

The basic lug material is finished to 1.50 inches thickness with doublers added with mechanical fasteners at the pivot pin hole and at the aft longeron interface to meet the baseline requirements.

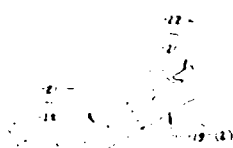
The Z_F0.0 panel is integral with the pivot lug inboard to X_F84. This segment consists of an integrally stiffened relatively thin machined plate. A beta annealed 6Al-4V titanium machined plate is utilized for the panel segment between the X_F39 rib and X_F84 rib. Beta annealed 6Al-4V titanium sandwich construction is used for the inboard panel from + X_F39 to - X_F39. The titanium

1,941'00 REF

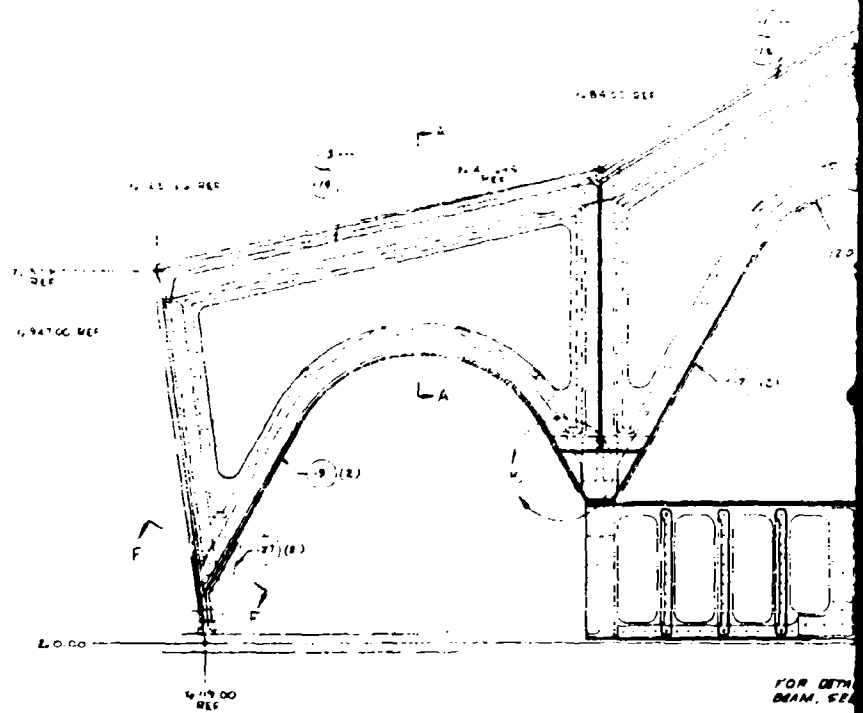
SECT. H-F
SCALE 1/4



SECT. A-A
SCALE 1/2

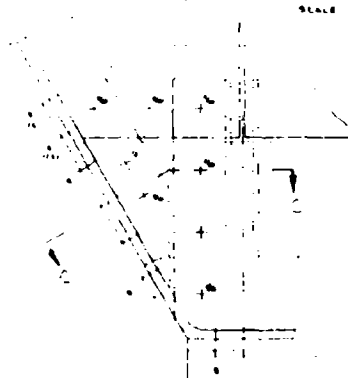


SECT. C-C
SCALE 1/2



FOR DETAIL
DIAM. SEE

1,941'00 BWT
VIEW LEG FWD - LH SIDE / RH SIDE
SCALE 1/4

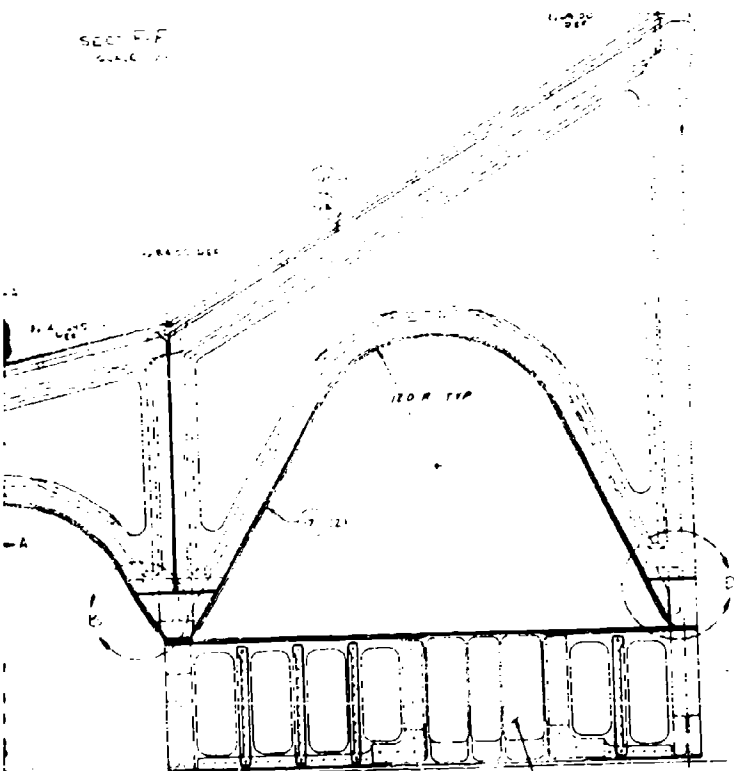


DETAIL B
SCALE 1/2

100 REF

100 REF

SEC. F-F
SCALE 1/4"

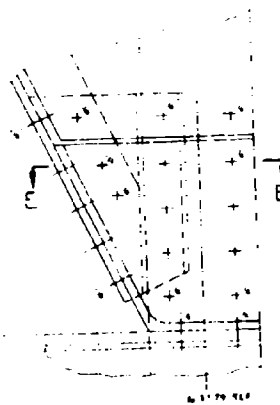


FOR DETAILS OF THIS
DEAM, SEE 603R131

Y. 3470 BHD
VIEW LEG FWD - LH SIDE (RM COP)
SCALE 1/4"

AND 10136-2403 REF

SEC. E-E
SCALE 1/4"



DETAIL D
SCALE 1/4"

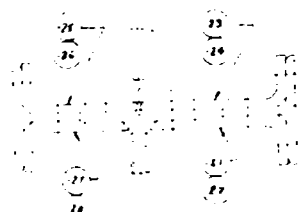
Figure 5

BONDED ASSEMBLIES CONSIST
OF 7000 ALUMINUM STRIPS,
BONDED AL NON-FERROUS COPING
AND 2000 AL END RIBBONS
7. OTHER PARTS ARE 7000
ALUMINUM

NOTES:	
Y. 3470 BHD, ARCHED-AWAYS, FSL CONFIG., STUDY OF	
603R238	

2

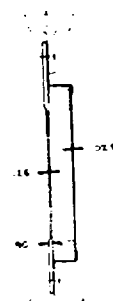
1,814.00 REF



SECTION D
SCALE 1/4"

1,417.00 REF

VERTICAL REF



SECTION E
SCALE 1/2"

VERTICAL REF



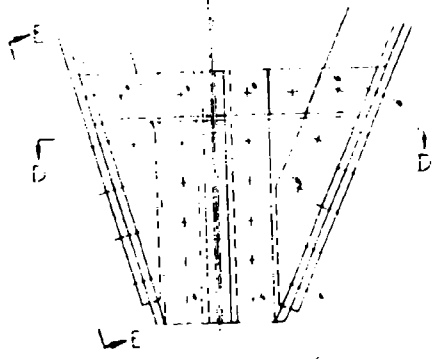
SECTION G
SCALE 1/4"

VERTICAL REF



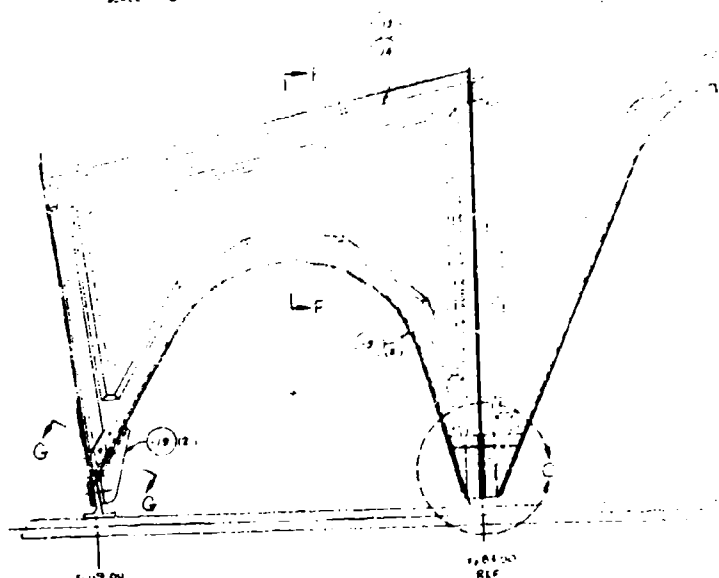
SECTION F
SCALE 1/4"

1,814.00 REF



SECTION H
SCALE 1/4"

1,000 REF



SECTION I
SCALE 1/4"

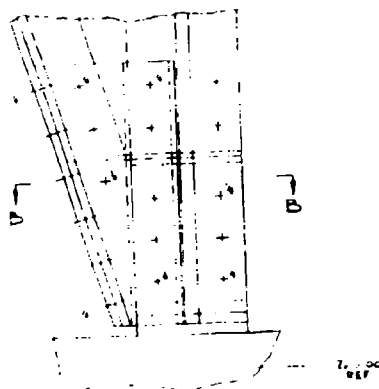
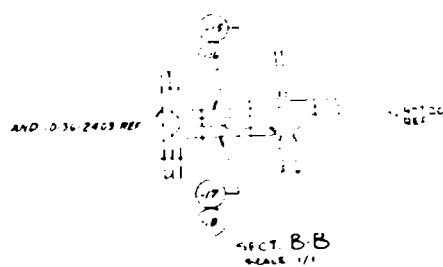
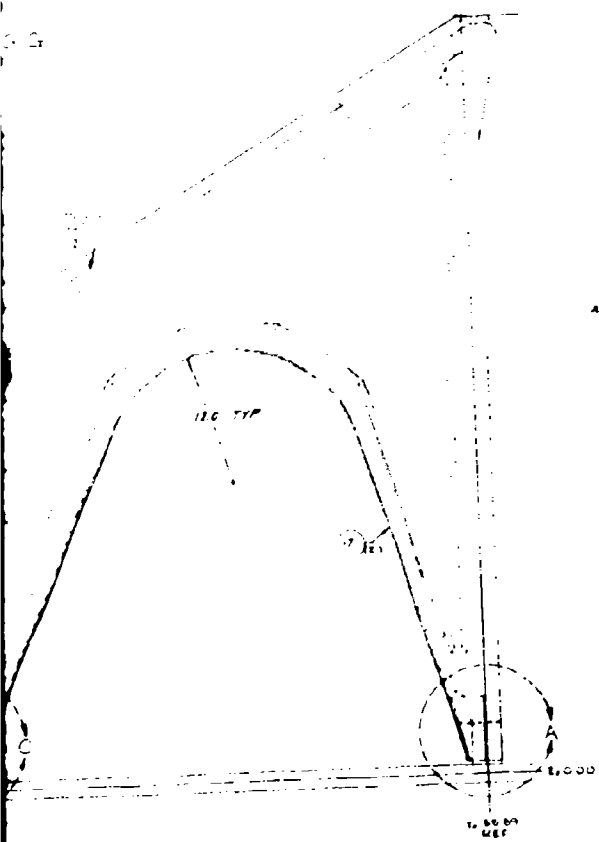
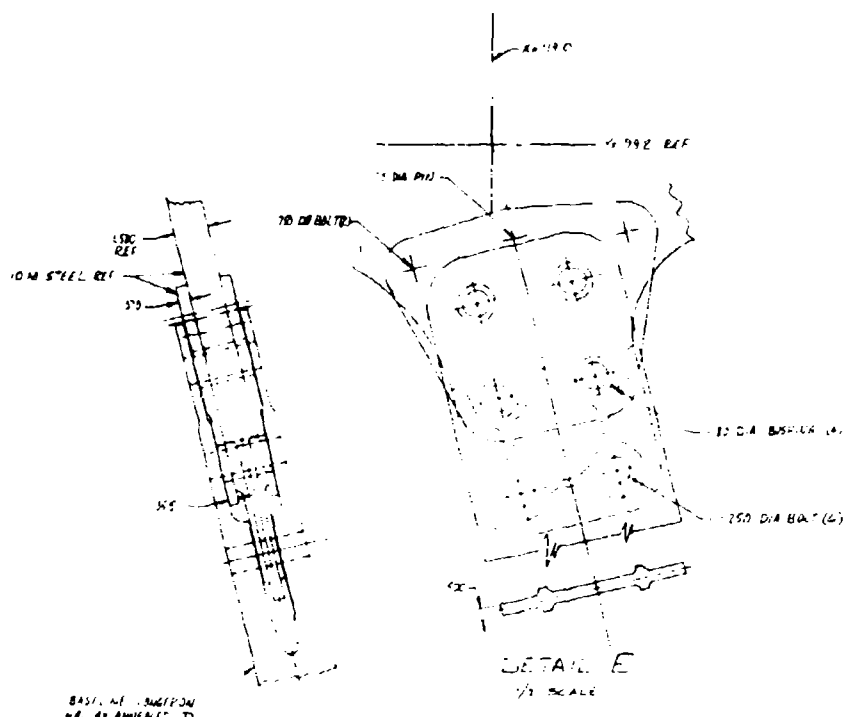


Figure 6

1. BONDED ASSEMBLIES CONSIST OF TWO ALUMINUM SPITS, EDGED AL NONSTICK COAT, AND 100% AL EDGE ADHESIVE. 2. OTHER PARTS ARE TEST ALUMINUM

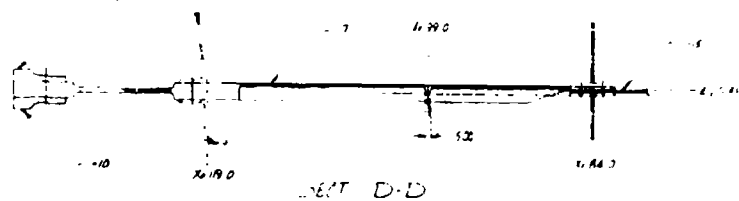
NOTES:	
Y. 911.0 BMD, ARCHED-MANNS, FAIL CONFIG., STUDY OF	
603	603R259

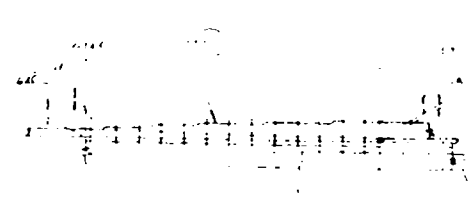


BASIC REF. SECTION
W. 40 ANGLE (C. T.)

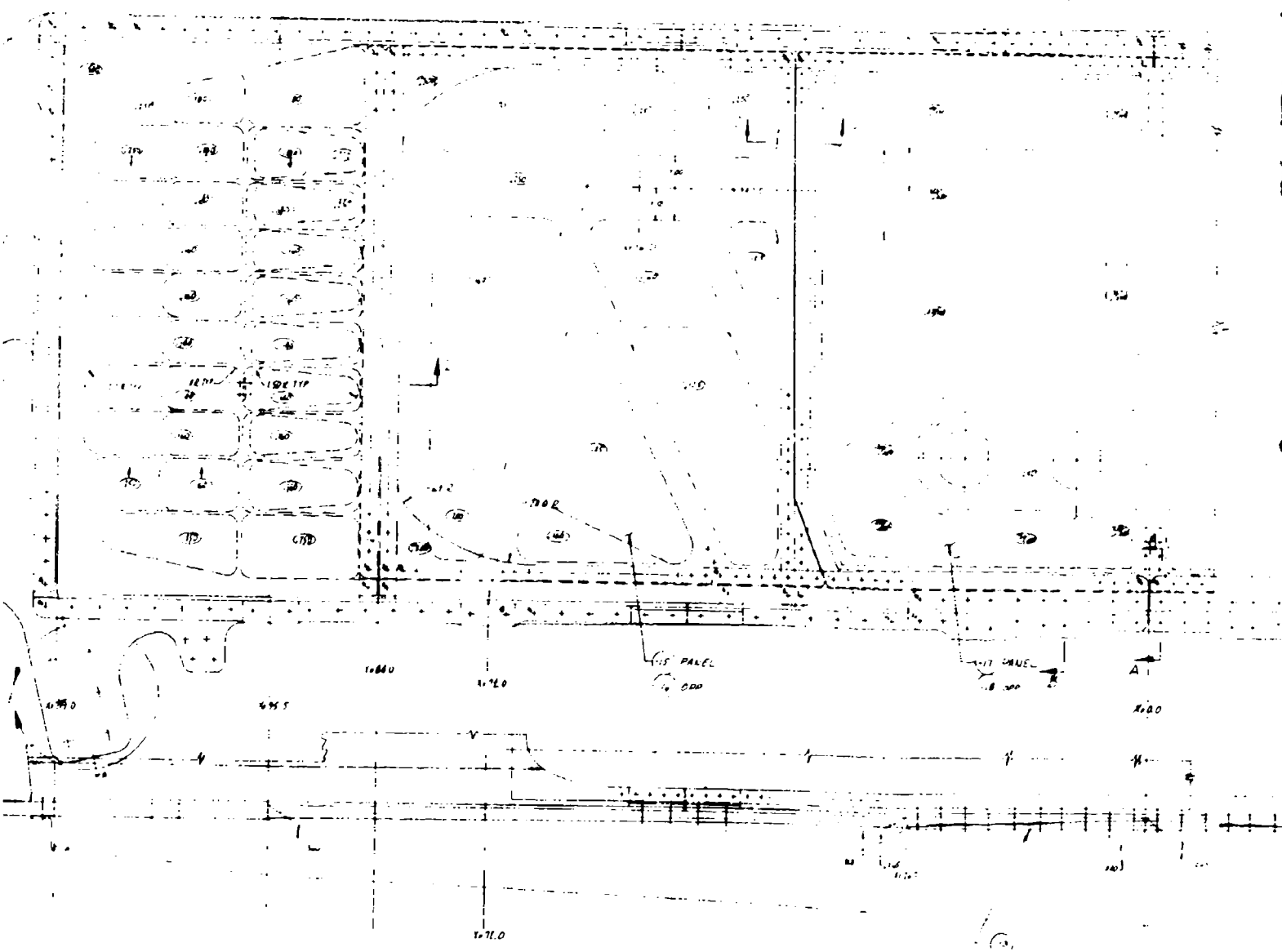
D
X-119.0

2 SLOTTED
150C REB
3120 REB





B



2

segments of the Z_F0.0 panel are attached to the pivot lug extensions with Taper-lok fasteners.

Additional trade study results involving these items are documented in the following paragraph.

"No-Box" Box Trade Study - The decision was made during Phase II trade studies to incorporate the Z_F0.0 panel for the following reasons:

1. Better structural continuity is provided by this arrangement. Relative deflections between the lower lug and the lower contour panel are eliminated.
2. The need for additional MLG support structure is eliminated.
3. The baseline fuel system can be retained.
4. Fuel tank purging should be simplified.
5. Load distribution in the lug - bulkhead splices may be improved.

The following table presents the weight and material requirement comparison for the two configurations.

	ORIGINAL CONFIGURATION		Z _F 0.0 PANEL CONFIGURATION	
	MATL WT	FINISH WT	MATL WT	FINISH WT
Y _F 932 BHD				
Lower OB Flg	1546#	260#	480#	90#
Lower IB Flg	823	178	389	75
Y _F 992 Bhd				
Lower OB Flg	3137	424	850	149
Lower IB Flg	1053	190	352	72
Lug	8741	1767	14360	2526
Lug Reinf	-	-		286
Longn Doubler	-	-		54
Splice Plate	392	103		41
Splice Plate	406	130		47
Y _F 95.5 Trunnion				
Back Up	716	47	-	-
TOTAL 10 NI PARTS	15814#	3099#	16431#	3340#

	ORIGINAL CONFIGURATION		ZF0.0 PANEL CONFIGURATION	
	MATL WT	FINISH WT	MATL WT	FINISH WT
Additional Parts Affected				
Lower Cover or Fairing		345#		*212#
MLG Side Load Ftg Backup		41		-
ZF0 Panel 0-39.5		-		110
TOTAL		3505#		3662#

*Baseline Weight Used

The weight increase of 157 lbs for the ZF0.0 panel configuration is judged to be acceptable in view of the previously mentioned advantages. This weight can be reduced approximately 40 lbs if a welded centerline splice is used or if the splice is eliminated.

The ZF0.0 panel configuration indicates a slightly higher 10 Nickel steel material requirement (617 lbs). However, this arrangement provides 2420 lbs of usable cut off stock.

Beta annealed 6Al-4V titanium was selected for the two in-board panels at ZF0.0 on the basis of optimized math model analyses which indicated a fifty pound weight reduction over an equivalent design using 7050 aluminum. The titanium panel design also resulted in the 10-Nickel steel lug extension operating at a more efficient stress level. See Table 1 for cost comparisons.

Preliminary cost estimates for incorporating the ZF0.0 panel into the "No-Box" configuration indicates a nominal cost reduction will be realized over the Phase Ib configuration. The Phase Ib "No-Box" configuration unit cost as reported in the AFFDL-TR-73, Phase Ib Preliminary Design Summary Report - Trade Studies is \$654,832 as compared to the current estimate of \$647,204 represents a cost reduction of \$7,627.

A summary of the cost comparisons is contained in Table 1. Tables 2, 3, and 4 contain a more detailed cost summary of the principal components affected by this configuration change.

Table 1

"NO-BOX" COST SUMMARY

Phase Ib "No-Box" Unit Cost

\$654,832

● Deletions

603R196 Y _F 932 BHD	\$ 79,672
603R195 Y _F 992 BHD	81,583
603R192 LWR PIV LUG	49,510
603R207 BACK-UP FTG	4,508
603R209 BACK-UP FTG	1,025
603R184 LWR PANELS	6,573

Deletion Cost \$222,871

● Replacements

603R236 Y _F 932 BHD	\$ 71,167
603R235 Y _F 992 BHD	70,679
603R237 LWR PIV LUG	65,027
603R237 X _F O PANEL	4,550
603R148 LWR FAIRING	3,820

Replacement Cost \$215,243

● COST DELTA

-\$ 7,628

-\$ 7,628

Phase II "No-Box" Unit Cost

\$647,204

Table 2 LWR PIVOT LUG COST SUMMARY

	MAT'L WT	COSTS				TOTAL	UNIT COST
		MAT'L	FACTORY	TOOLING			
<u>PARTS DELETED</u> 603R192 LWR PIV LUG 603R207 BACK-UP FTG DELETION COST	8741# 716#	\$ 40,012 3,280	\$ 9,236 1,181	\$ 262 47		\$ 49,510 <u>4,508</u>	\$ 54,018
<u>REPLACEMENT PARTS</u> 603R237 LWR LUG -7/-8 LWR PIV LUG -9/-10 LUG REINF -11 YF932 SPLICE -13 YF992 SPLICE -19/-20 LONGN DBLR -21/-22 LONGN DBLR REPLACEMENT COST COST DELTA 603R237 LWR LUG COST	7040# 2320# 108# 169# 128#	\$ 54,700	\$ 7,087 2,205 197 197 158 <u>158</u> \$ 10,002	\$ 155 46 42 42 20 <u>20</u> 325		\$ 65,027 <u>+ \$ 11,009</u>	\$ 65,027

Table 3 YF992 BULKHEAD COST SUMMARY

	MAT'L WT	COSTS			TOTAL	UNIT COST
		MAT'L	FACTORY	TOOLING		
PARTS DELETED 603R195 YF992 BHD -9/-10 LWR OB FLG -37 LWR IB FLG -11/-12 SPLICE DELETION COST	2137# 1053#	\$ 9,800 4,830	\$ 673* 363* 1,164**	*Incl Tool **Incl Tool & Mat'l	\$10,473 5,193 1,164 <u>\$16,830</u>	\$81,583
REPLACEMENT PARTS 603R235 YF992 BHD -9/-10 LWR OB FLG -7 LWR IB FLG REPLACEMENT COST COST DELTA 603R235 BHD COST	850# 352#	\$ 3,890 1,630	\$ 262* 144*		\$ 4,152 1,774 <u>\$ 5,926</u> <u>-\$10,904</u>	<u>\$70,679</u>

Table 4 YF932 BULKHEAD COST SUMMARY

	MAT'L WT	COSTS				UNIT COST
		MAT'L	FACTORY	TOOLING	TOTAL	
PARTS DELETED 603R196 YF932 BHD -17/-16 LWR OB FLG -19 LWR IB FLG -43 SPLICE DELETION COST	1546# 823#	\$ 7,100 3,770	\$ 524* 295* 1,129**	*Incl Tool **Incl Tool & Mat'l	\$7,624 4,065 1,129 <u>\$12,818</u>	\$79,672
REPLACEMENT PARTS 603R236 YF932 BHD -15/-16 LWR OB FLG -51 LWR IB FLG REPLACEMENT COST COST DELTA 603R236 BHD COST	480# 389#	\$ 2,200 1,780	\$ 181* 152*		\$ 2,381 <u>1,932</u> \$ 4,313 <u>-\$ 8,505</u>	 -\$ 8,505 \$71,167

Cost estimates for the 603R237 - X_F39 to + X_F39 panel, the 603R148 lower fairing and the 603R209 back-up fitting are based upon a ratio of the costs from similar existing parts. It should be noted that an expected additional cost reduction on the MLG drag brace fitting has not been estimated at this time.

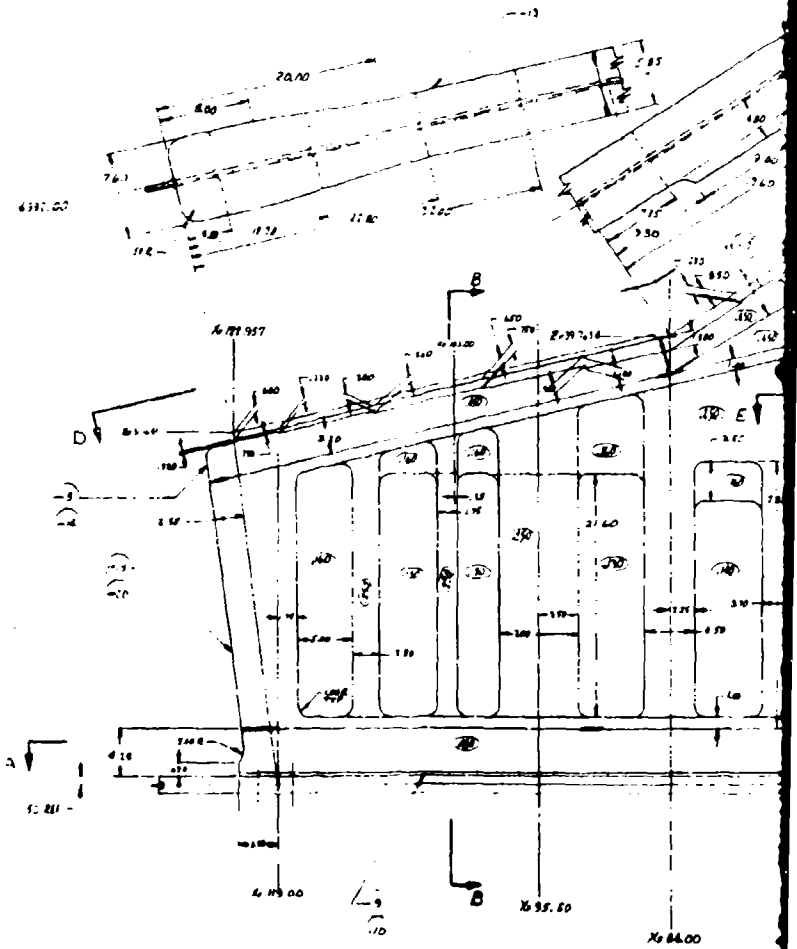
Lower Fairings - Since the Z_F0.0 panel reacts the shear and fuel pressure loads, the lower contour panels shown on drawing 603R184 in the Phase Ib report can revert to aerodynamic fairings reacting only air pressure loads. A design study is currently in work to revise the 603R148 "A" FSIL fairing design (also shown in the Phase Ib Report) to adapt these fairings to the No-Box fairing attach structure.

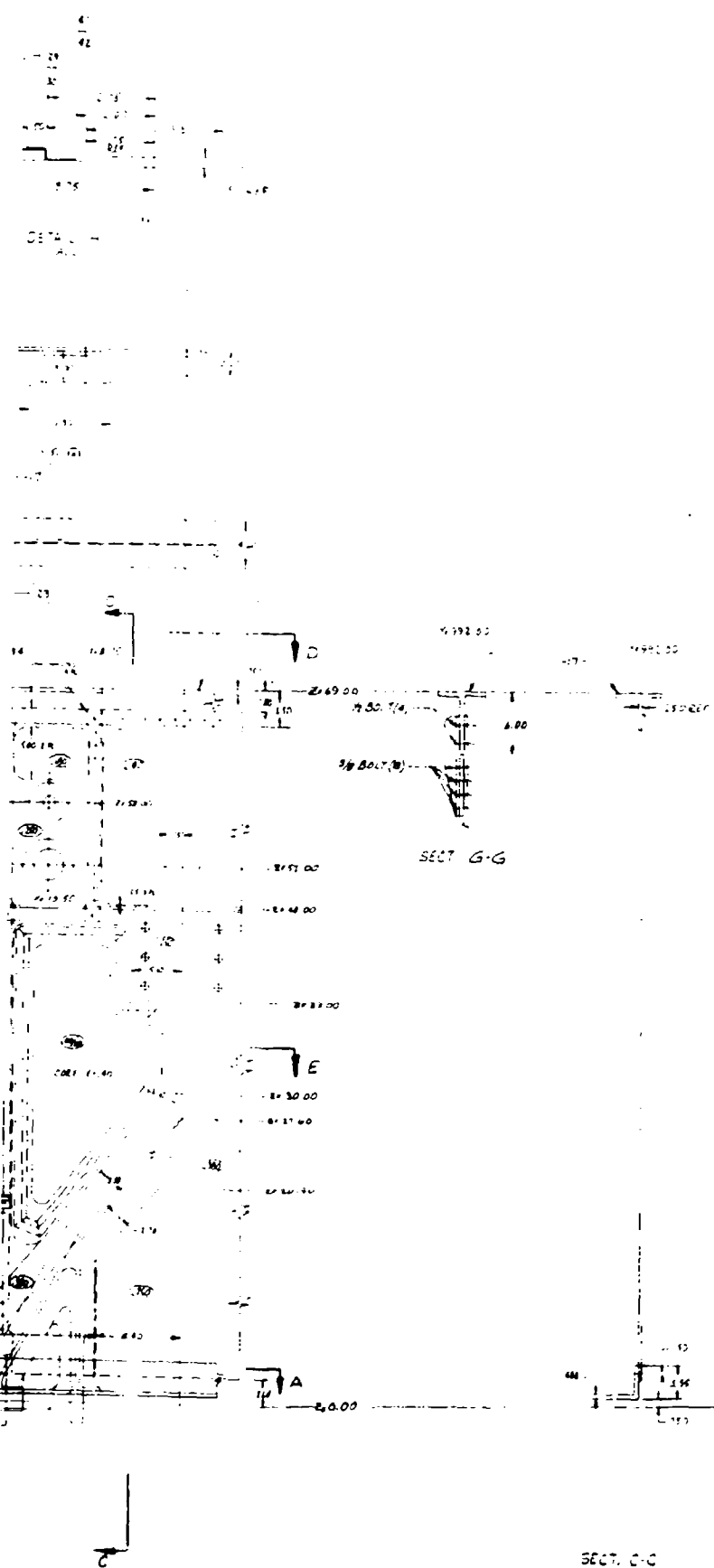
Forward and Aft Bulkheads - The Y_F932 and Y_F992 bulkheads were redesigned in the area of the lower flange to accommodate the Z_F0.0 panel design concept. Since the axial load is contained in the pivot leg extensions, the thicknesses of the lower flanges of both bulkheads were reduced to transfer only the shear load into the bulkhead webs. The redesigned bulkheads are shown on Drawing No. 603R235, Figure 8, and Drawing No. 603R236, Figure 9.

Internal Ribs - A design study of the modifications required to interface the Centerline Rib with the Z_F0.0 panel is shown on drawing No. 603R227, Figure 10.

The 603R175 X_F39 Rib design and 603R203 X_F84 Rib design shown in the Phase Ib report will be revised by "A" change to interface these ribs with the "No-Box" Z_F0.0 panel.

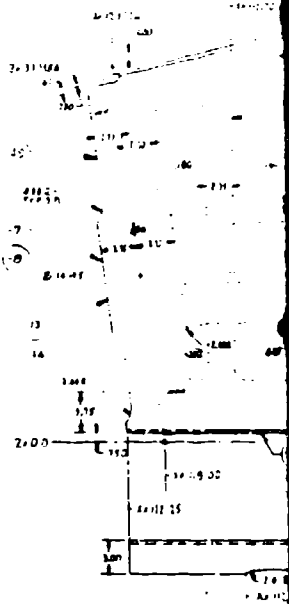
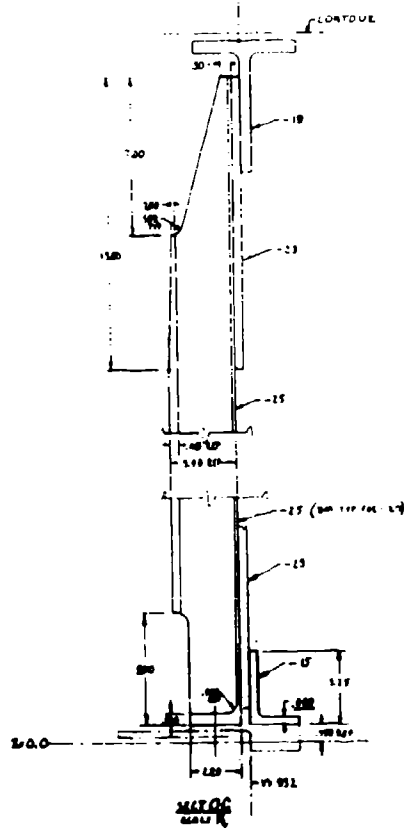
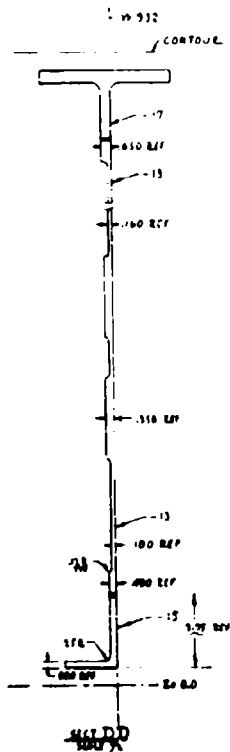
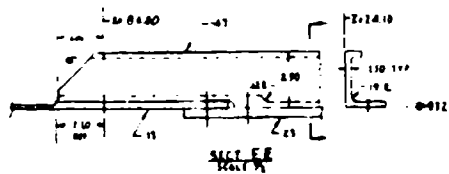
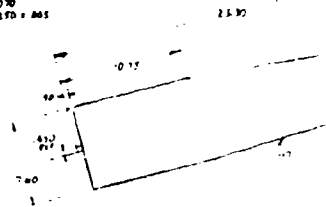
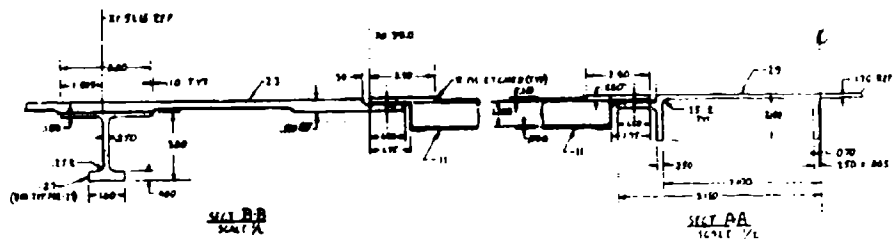
MLG Drag Brace Fitting - The "No-Box" configuration with the Z_F0.0 panel results in a different load distribution from the MLG drag brace fitting as compared to the previous design concept. As a result, a redesign of the 603R171 fitting shown in the Phase Ib Report is currently being studied. The previous fitting design required two beams at Y_F947 and a single beam at Y_F962 to react loads from the fitting and redistribute them to the internal ribs. The redesign study indicates that only one beam will be required at Y_F947 and the beam at Y_F962 can be eliminated since the fitting loads are reacted by the Z_F0.0 panel. The study also indicates that the drag brace fitting can be reduced in size which will result in an overall reduction in weight and material requirements. The design layout describing this revision will be published upon its completion.





1	2	3	4	5	6	7	8	9	10	11	12	13	14	15	16	17	18	19	20	21	22	23	24	25	26	27	28	29	30	31	32	33	34	35	36	37	38	39	40	41	42	43	44	45	46	47	48	49	50	51	52	53	54	55	56	57	58	59	60	61	62	63	64	65	66	67	68	69	70	71	72	73	74	75	76	77	78	79	80	81	82	83	84	85	86	87	88	89	90	91	92	93	94	95	96	97	98	99	100
---	---	---	---	---	---	---	---	---	----	----	----	----	----	----	----	----	----	----	----	----	----	----	----	----	----	----	----	----	----	----	----	----	----	----	----	----	----	----	----	----	----	----	----	----	----	----	----	----	----	----	----	----	----	----	----	----	----	----	----	----	----	----	----	----	----	----	----	----	----	----	----	----	----	----	----	----	----	----	----	----	----	----	----	----	----	----	----	----	----	----	----	----	----	----	----	----	----	----	-----

1	STEEL PLATE 1/2" THICK	100	SQ. FT.	1.50	150.00	
2	STEEL PLATE 1/4" THICK	200	SQ. FT.	0.75	150.00	
3	STEEL PLATE 1/8" THICK	300	SQ. FT.	0.375	112.50	
4	STEEL PLATE 1/16" THICK	400	SQ. FT.	0.1875	75.00	
5	STEEL PLATE 1/32" THICK	500	SQ. FT.	0.09375	46.875	
6	STEEL PLATE 1/64" THICK	600	SQ. FT.	0.046875	28.125	
7	STEEL PLATE 1/128" THICK	700	SQ. FT.	0.0234375	16.40625	
8	STEEL PLATE 1/256" THICK	800	SQ. FT.	0.01171875	9.375	
9	STEEL PLATE 1/512" THICK	900	SQ. FT.	0.005859375	5.2734375	
10	STEEL PLATE 1/1024" THICK	1000	SQ. FT.	0.0029296875	2.9296875	
11	STEEL PLATE 1/2048" THICK	1100	SQ. FT.	0.00146484375	1.611328125	
12	STEEL PLATE 1/4096" THICK	1200	SQ. FT.	0.000732421875	0.87890625	
13	STEEL PLATE 1/8192" THICK	1300	SQ. FT.	0.0003662109375	0.47607421875	
14	STEEL PLATE 1/16384" THICK	1400	SQ. FT.	0.00018310546875	0.25634765625	
15	STEEL PLATE 1/32768" THICK	1500	SQ. FT.	0.000091552734375	0.137329296875	
16	STEEL PLATE 1/65536" THICK	1600	SQ. FT.	0.0000457763671875	0.07325830078125	
17	STEEL PLATE 1/131072" THICK	1700	SQ. FT.	0.00002288818359375	0.038910000000000004	
18	STEEL PLATE 1/262144" THICK	1800	SQ. FT.	0.000011444091796875	0.020599200000000002	
19	STEEL PLATE 1/524288" THICK	1900	SQ. FT.	0.0000057220458984375	0.010912200000000001	
20	STEEL PLATE 1/1048576" THICK	2000	SQ. FT.	0.00000286102294921875	0.0057220000000000004	
21	STEEL PLATE 1/2097152" THICK	2100	SQ. FT.	0.000001430511474609375	0.0029841250000000004	
22	STEEL PLATE 1/4194304" THICK	2200	SQ. FT.	0.0000007152557373046875	0.0015725625000000002	
23	STEEL PLATE 1/8388608" THICK	2300	SQ. FT.	0.00000035762786865234375	0.0008225500000000001	
24	STEEL PLATE 1/16777216" THICK	2400	SQ. FT.	0.000000178813934326171875	0.00042816000000000004	
25	STEEL PLATE 1/33554432" THICK	2500	SQ. FT.	0.0000000894069671630859375	0.00021408000000000002	
26	STEEL PLATE 1/67108864" THICK	2600	SQ. FT.	0.00000004470348358154296875	0.00010704000000000001	
27	STEEL PLATE 1/134217728" THICK	2700	SQ. FT.	0.000000022351741790771484375	0.00005352000000000001	
28	STEEL PLATE 1/268435456" THICK	2800	SQ. FT.	0.0000000111758708953857421875	0.000026760000000000004	
29	STEEL PLATE 1/536870912" THICK	2900	SQ. FT.	0.00000000558793544769287109375	0.000013380000000000002	
30	STEEL PLATE 1/1073741824" THICK	3000	SQ. FT.	0.00000000279396772384643546875	0.000006690000000000001	
31	STEEL PLATE 1/2147483648" THICK	3100	SQ. FT.	0.000000001396983861923217734375	0.0000033450000000000004	
32	STEEL PLATE 1/4294967296" THICK	3200	SQ. FT.	0.0000000006984919309616088671875	0.0000016725000000000002	
33	STEEL PLATE 1/8589934592" THICK	3300	SQ. FT.	0.00000000034924596548080443359375	0.0000008362500000000001	
34	STEEL PLATE 1/17179869184" THICK	3400	SQ. FT.	0.000000000174622982740402216796875	0.00000041812500000000004	
35	STEEL PLATE 1/34359738368" THICK	3500	SQ. FT.	0.0000000000873114913702011083984375	0.00000020906250000000002	
36	STEEL PLATE 1/68719476736" THICK	3600	SQ. FT.	0.00000000004365574568510055419921875	0.00000010453125000000001	
37	STEEL PLATE 1/137438953472" THICK	3700	SQ. FT.	0.000000000021827872842550277099609375	0.000000052265625000000004	
38	STEEL PLATE 1/274877906944" THICK	3800	SQ. FT.	0.0000000000109139364212751385498046875	0.000000026132812500000002	
39	STEEL PLATE 1/549755813888" THICK	3900	SQ. FT.	0.00000000000545696821063756927490234375	0.000000013066406250000001	
40	STEEL PLATE 1/1099511627776" THICK	4000	SQ. FT.	0.000000000002728484105318784637451171875	0.0000000065332031250000004	
41	STEEL PLATE 1/2199023255552" THICK	4100	SQ. FT.	0.0000000000013642420526593923187255859375	0.0000000032666015625000002	
42	STEEL PLATE 1/4398046511104" THICK	4200	SQ. FT.	0.00000000000068212102632969615936279296875	0.00000000163330078125000004	
43	STEEL PLATE 1/8796093022208" THICK	4300	SQ. FT.	0.000000000000341060513164848079681396484375	0.00000000081665039062500002	
44	STEEL PLATE 1/17592186044416" THICK	4400	SQ. FT.	0.0000000000001705302565824240398406982421875	0.00000000040832519531250001	
45	STEEL PLATE 1/35184372088832" THICK	4500	SQ. FT.	0.00000000000008526512829121201992034912109375	0.000000000204162597656250004	
46	STEEL PLATE 1/70368744177664" THICK	4600	SQ. FT.	0.000000000000042632564145606009960174560546875	0.000000000102081298828125002	
47	STEEL PLATE 1/140737488355328" THICK	4700	SQ. FT.	0.0000000000000213162820728030049800872802734375	0.000000000051040649414062501	
48	STEEL PLATE 1/281474976710656" THICK	4800	SQ. FT.	0.00000000000001065814103640150249004364013671875	0.0000000000255203247070312504	
49	STEEL PLATE 1/562949953421312" THICK	4900	SQ. FT.	0.000000000000005329070518200751245021820068359375	0.0000000000127601623535156252	
50	STEEL PLATE 1/1125899906842624" THICK	5000	SQ. FT.	0.0000000000000026645352591003756225109100341796875	0.0000000000063800811767578126	
51	STEEL PLATE 1/2251799813685248" THICK	5100	SQ. FT.	0.00000000000000133226762955018781125545501708984375	0.0000000000031900405883789063	
52	STEEL PLATE 1/4503599627370496" THICK	5200	SQ. FT.	0.000000000000000666133814775093905627727508544921875	0.00000000000159502029418945315	
53	STEEL PLATE 1/9007199254740992" THICK	5300	SQ. FT.	0.0000000000000003330669073875469528138637504272109375	0.00000000000079751014709472657	
54	STEEL PLATE 1/18014398509481984" THICK	5400	SQ. FT.	0.000000000000000166533453693773476406931875021359375	0.00000000000039875507354736328	
55	STEEL PLATE 1/36028797018963968" THICK	5500	SQ. FT.	0.0000000000000000832667268468867382034659375106796875	0.00000000000019937753677368164	
56	STEEL PLATE 1/72057594037927936" THICK	5600	SQ. FT.	0.00000000000000004163336342344336910173296875533984375	0.00000000000009968876838684082	
57	STEEL PLATE 1/144115188075855872" THICK	5700	SQ. FT.	0.0000000000000000208166817117216845508664843752669921875	0.00000000000004984438419342041	
58	STEEL PLATE 1/288230376151711744" THICK	5800	SQ. FT.	0.000000000000000010408340855860842275433242187513349609375	0.000000000000024922192096710205	
59	STEEL PLATE 1/576460752303423488" THICK	5900	SQ. FT.	0.0000000000000000052041704279304211377166210937566748046875	0.0000000000000124610960483551025	
60	STEEL PLATE 1/1152921504606846976" THICK	6000	SQ. FT.	0.000000000000000002602085213965210568858310546875333740234375	0.00000000000000623054802417755125	
61	STEEL PLATE 1/2305843009213693952" THICK	6100	SQ. FT.	0.00000000000000000130104260698260528442915527343751668701171875	0.000000000000003115274012088775625	
62	STEEL PLATE 1/4611686018427387904" THICK	6200	SQ. FT.	0.00000000000000000065052130349130264221457763671875815924433984375	0.0000000000000015576370060443878125	
63	STEEL PLATE 1/9223372036854775808" THICK	6300	SQ. FT.	0.00000000000000000032526065174565132110728881835937541717529296875	0.00000000000000077881850302219390625	
64	STEEL PLATE 1/18446744073709551616" THICK	6400	SQ. FT.	0.0000000000000000001626303258728256605536444091796875208876461459375	0.000000000000000389409251511096953125	
65	STEEL PLATE 1/36893488147419103232" THICK	6500	SQ. FT.	0.000000000000000000081315162936412830276822204589843751044382307296875	0.0000000000000001947046257555484765625	
66	STEEL PLATE 1/73786976294838206464" THICK	6600	SQ. FT.	0.0000000000000000000406575814682064151384111022949218755221911536484375	0.00000000000000009735231287777423828125	
67	STEEL PLATE 1/147573952589676412928" THICK	6700	SQ. FT.	0.00000000000000000002032879073410320756920555114745093752610957682421875	0.000000000000000048676156438887119140625	
68	STEEL PLATE 1/295147905179352825856" THICK	6800	SQ. FT.	0.000000000000000000010164395367051603784602775573725468751305478941171875	0.0000000000000000243380782194435595703125	
69	STEEL PLATE 1/590295810358705651712" THICK	6900	SQ. FT.	0.0000000000000000000050821976835258018923013877868627343756527394705859375	0.00000000000000001216903910972177978515625	
70	STEEL PLATE 1/1180591620717411303424" THICK	7000	SQ. FT.	0.00000000000000000000254109884176290094615069389343136718753263697354296875	0.000000000000000006084519554860889892578125	
71	STEEL PLATE 1/2361183241434822606848" THICK	7100	SQ. FT.	0.00000000000000000000127054942088145047307534694671568359375163184886796875	0.0000000000000000030422597774304449462890625	
72	STEEL PLATE 1/4722366482869645213696" THICK	7200	SQ. FT.	0.000000000000000000000635274710440725236537673473357841796875815924433984375	0.00000000000000000152112988871522247314453125	
73	STEEL PLATE 1/9444732965739290427392" THICK	7300	SQ. FT.	0.000000000000000000000317637355220362618268836736678920898437540796222169921875	0.000000000000000000760564944357611236572265625	
74	STEEL PLATE 1/18889465931478580854784" THICK	7400	SQ. FT.	0.000000000000000000000158818677610181309134418368339460449218752039811108484375	0.0000000000000000003802824721788056182861328125	
75	STEEL PLATE 1/37778931862957161709568" THICK	7500	SQ. FT.	0.0000000000000000000000794093388050906545672091841697302246093751019905542421875	0.00000000000000000019014123608940280914306640625	
76	STEEL PLATE 1/75557863725914323419136" THICK	7600	SQ. FT.	0.00000000000000000000003970466940254532728360459208488651125468755099527712109375	0.000000000000000000095070618044701404571533203125	
77	STEEL PLATE 1/151115727451828646838272" THICK	7700	SQ. FT.	0.000000000000000000000019852334701272663641802296042443255627343752549638560546875	0.0000000000000000000475353090223507022857666015625	
78	STEEL PLATE 1/302231454	7800	SQ. FT.			



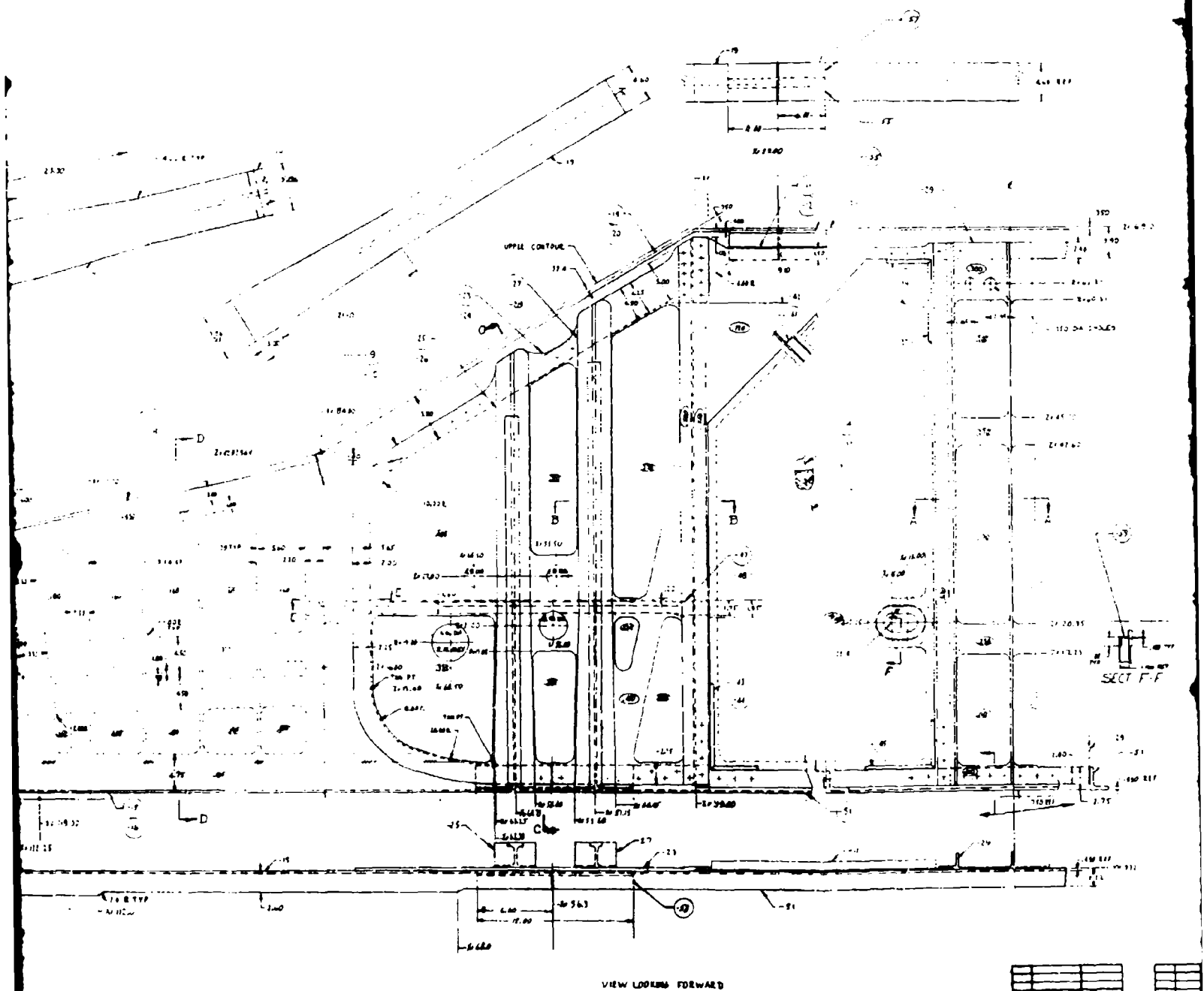
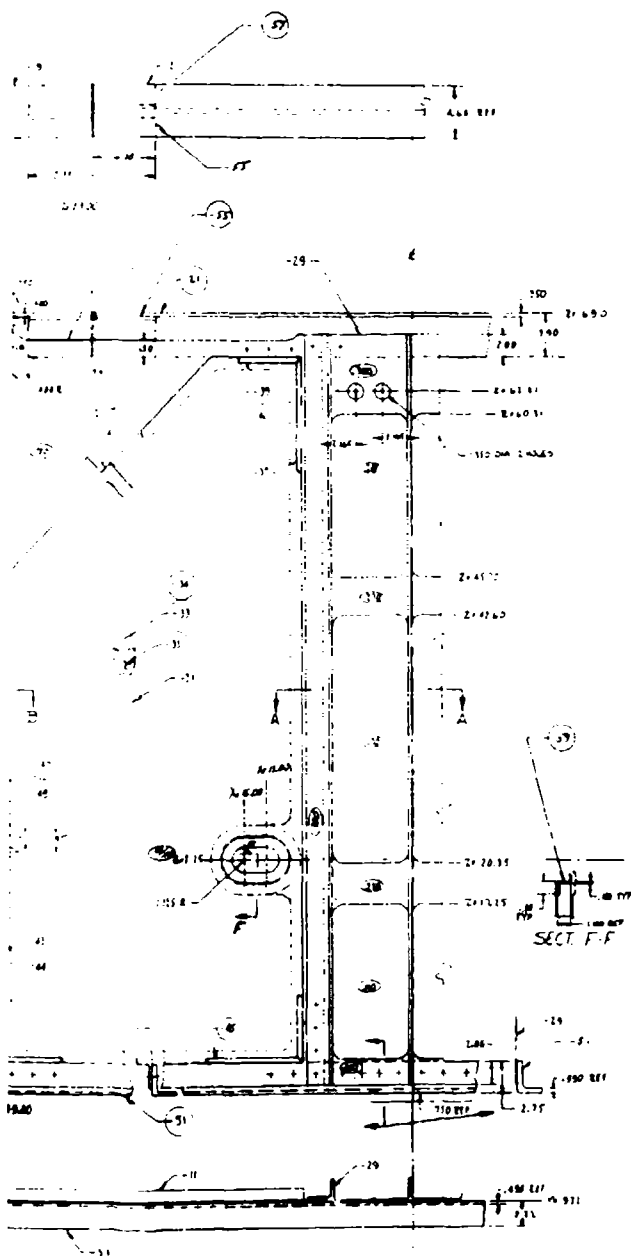


Figure 9

2



- 2 - 94-10 BOWDED AIRY
- PERFORM AND DRYING TAILORING
 - CLEAN WEB AND STIFFENING RIBS
 - APPLY ADHESIVE TO WEB AND STIFFENING RIBS
 - INSTALL FASTENERS
 - CURE ADHESIVE ONE WEEK AT 250°F (121°C)
- 1 - 104-12 BOWDED PANEL - 104-12 MEMBER FAB (104-12 FAB AND 104-12 FAB RIBS)

NOTE

BULHAFAD VI-932		J (G) R 23	
1	2	3	4
5	6	7	8
9	10	11	12
13	14	15	16
17	18	19	20
21	22	23	24
25	26	27	28
29	30	31	32
33	34	35	36
37	38	39	40
41	42	43	44
45	46	47	48
49	50	51	52
53	54	55	56
57	58	59	60
61	62	63	64
65	66	67	68
69	70	71	72
73	74	75	76
77	78	79	80
81	82	83	84
85	86	87	88
89	90	91	92
93	94	95	96
97	98	99	100

Figure 9

3

3.1.2 Structural Analysis

During the past six months, stress analysis efforts were directed toward completion of the Phase Ib preliminary design and the beginning of the detailed design, Phase II. Since the major portion of the work accomplished through the end of Phase Ib is discussed in detail in Sections 2.2, 6.1 and 6.2 of AFFDL-TR-73-40, this report covers primarily the period beginning in mid March 1973 and ending in June 1973. Because the Damage Tolerant Integral Lug configuration was eliminated from consideration, only the Fail Safe Integral Lug and No-Box Box configurations are discussed. No baseline loads changes were made. Loads work consisted essentially of revisions to Convair panel point loads to reflect current geometry. For reference, the load conditions are summarized in Table 5. Table 6 presents a summary of the usable overall math model runs made to date.

3.1.2.1 Fail Safe Integral Lug Stress Analysis

The stress analysis of the Fail Safe Integral Lug configuration during the latter part of the reporting period consisted of the following primary tasks:

1. Trade study support for the brazed lower plate and lug with particular emphasis on the stability of the lower plate under negative bending conditions.
2. Trade study support for the arched internal bulkheads at Y_F 947 and 977.
3. Finite element analysis of lugs and lug test specimens.
4. Finite element buckling analysis for upper lug and plate.
5. Development of an updated overall math model incorporating current design features and geometry, i.e. through layer lower plate, revised sweep actuator attachment, and other thickness, material, and area changes made during the design period.
6. Manual and computer aided analyses of miscellaneous local areas.

Table 5 LOAD CONDITIONS

<u>CONDITION IDENTIFICATION</u>			<u>CONDITION DESCRIPTION</u>	<u>SWEEP ANGLE</u>
<u>ASKA</u>	<u>CLASP NARSAP</u>	<u>CONVAIR</u>		
1	6603315	AS1	SYMMETRIC PART - ABRUPT ROLL	67.5°
1A	660331A	AS1A	ANTISYM. PART - ABRUPT ROLL	67.5°
2	110021	AS2	FLAPS DOWN, 2G LIMIT	15°
3	161432	AS3	11000 FT. 3G LIMIT	67.5°
4	110301	AS4	SPOILERS OPEN 70°, OG	15°
5	112120	AS5	SLATS OPEN 20°, 2G LIMIT	15°
6	810011	AS6	2PT BRAKED ROLL	15°
7	810025	AS7	GROUND TAXI, 2G LIMIT	15°
8	880012S	AS8	SYMMETRIC PART - GROUND TURN	15°
8A	880012A	AS8A	ANTISYM PART - GROUND TURN	15°
9	122221	AS9	20,000 FT, 2G LIMIT	25°
10	1600332	AS10	S.L., 3G LIMIT	67.5°
11	160316	AS11	S.L., 1G LIMIT	67.5°
	30341	AS300	STIFFNESS CONDITION - 10 ⁶ LBS. VERTICAL @ STA 1600	67.5°
	50541	AS500	STIFFNESS CONDITION - 10 ⁸ IN LBS. PITCHING MOMENT	67.5°

Table 6

SUMMARY OF AMA'S COMPUTER ANALYSIS OF OVERALL* WCTS

MODEL-RUN	LOAD CONDITIONS	COMPUTER PROCEDURE	REMARKS
FSRL-2-1	AS 2, 10, 9, 6	TN1	Loads Prior to Oct. 1972 Update from NAR. Wing Sweep Actuator Load Resolution to WCTS in Error.
FSRL-2-2	AS 5C, 7C, 11C, 500	TN1	Current Loads Incorporating NAR Oct. '72 Revision. Actuator Loads in Error (See Above)
FSRL-2-3	AS 2, 10, 9, 6	ASOP	Trial Run on AFFDL Computer Facility During Reporting Period 16 Feb. - 15 Mar. 1973. Loads Identical to FSRL-2-1.
FSRL-3-5	AS 2C, 6C, 10C, 500	TN1	Model Incorporates Aluminum Upper Cover and Revised Structural Gages Based on Results of Previous Runs. Load Conditions Rearranged to Incorporate AS 500 Stiffness Condition With Critical Static Design Conditions.
FSRL-4-1	AS 2C, 6C, 10C, 500	TN1	Model Identical to FSRL-3-5 But Incorporates The Arched Internal Bulkhead Concept at Y_{F947} and Y_{F977} .
FSRL-4-2	AS 3C, 4C, 1 L/H, 1 R/H C	TN1	Run Evaluates Critical Compression Loads in Lower Plate (AS 4C) and Includes Unsymmetrical Load Condition AS 1. Model Identical to FSRL-4-1
NBB-1-1	AS 2, 6, 9, 10	TN1	Same Load Conditions As FSRL-2-1
NBB-1-2	AS 5C, 7C, 11C, 500	TN1	Current Loads. Actuator Loads Corrected
* Does Not Include Analysis of Local Areas.			

Lower Plate - As a result of brazed joint failures in the 603FTB005 lower plate specimen, several alternate lower plate designs were studied. The main emphasis was on the three layer brazed design with symmetrical stiffeners. In order to obtain additional preliminary internal loads, TN1 run FSRL-4-2 was made as noted in Table 6.

Stability checks for ASKA conditions 4 and 7 were made for various arrangements. Both of these conditions cause shear and compressive loads in the lower plate with ASKA 4 giving the largest spanwise compressive loads. For the assumption of simple supports at the closure rib, $Y_F = 932$, $Y_F = 992$, and $X_F = 84$, it was found that a reasonable stiffener width within the desired plate thickness range could be achieved for ASKA 7. For AS4, however, it appeared more efficient to provide a fore and aft member at $X_F = 99$ supported at $Y_F = 932$ and $Y_F = 992$. Stiffener widths for this arrangement were determined for inclusion in the math model. In addition, the required dimensions of the fore and aft beam were determined.

The plate between $X_F = 84$ and $X_F = 39$ is stabilized by the drag brace support structure so no requirement for an additional stabilizing member was found necessary there.

From $X_F = 39$ to $X_F = 0$, the loads are less than in the outboard bay and because of partial restraint from the bay which is stiffened by the drag brace support structure, reasonable stiffener widths result with no intermediate support.

Preliminary work on a NASTRAN stability model for further checking was begun.

Arched Beam Bulkhead Study - The FSRL TN1 math model was modified to allow a trade study of arched beam internal bulkhead incorporation. The model was designated FSRL-4-1. The modification was made in a manner such that two trade studies could be performed:

1. Beams supporting the upper plate at $Y_F 947$ and $Y_F 977$ with deep gussets or arches at each end.
2. Beams as in 1. with no arches. This arrangement was not used in an actual run, however.

An isometric view of the revised model is shown in Figure 10. Figures 11 through 14 depict the revised bulkhead structure in the FSRL-4-1 model. It should be noted that this model was constructed from the FSRL-3-5 model (aluminum upper cover) and no

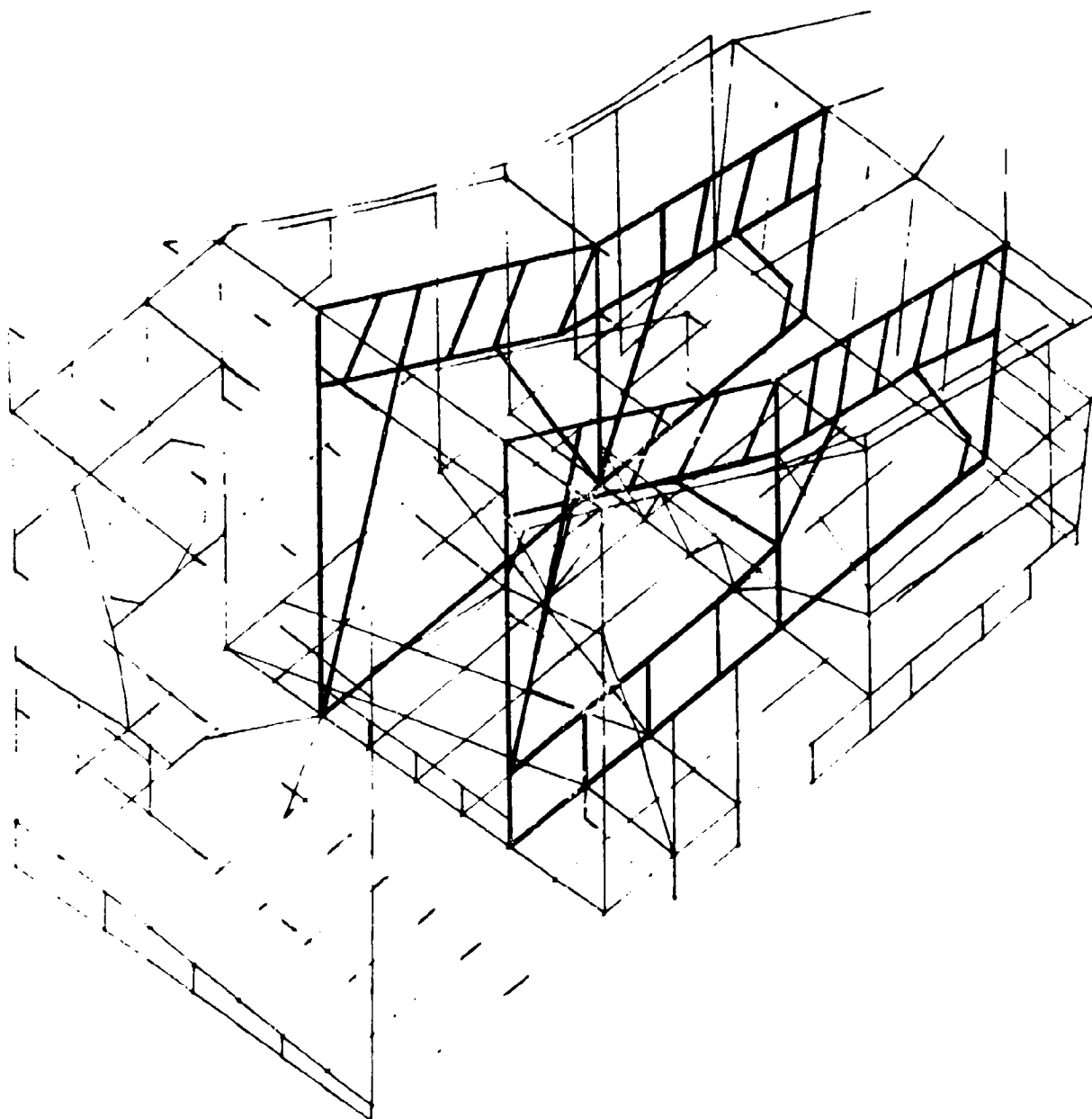


Figure 10 FSRL-4-1 MATH MODEL

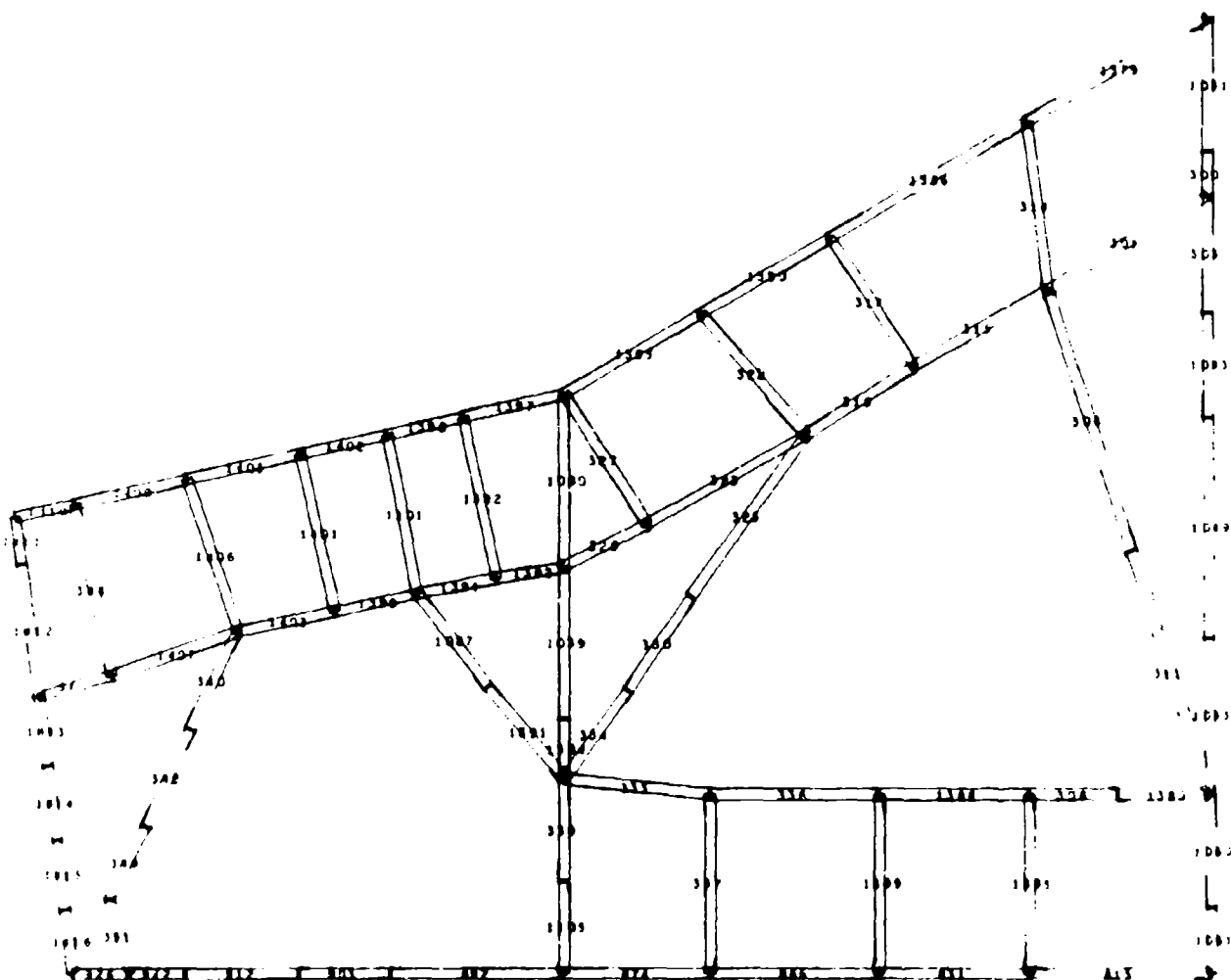


Figure 11 Y_F 947 ARCHED-BEAM BULKHEAD BAR ELEMENTS

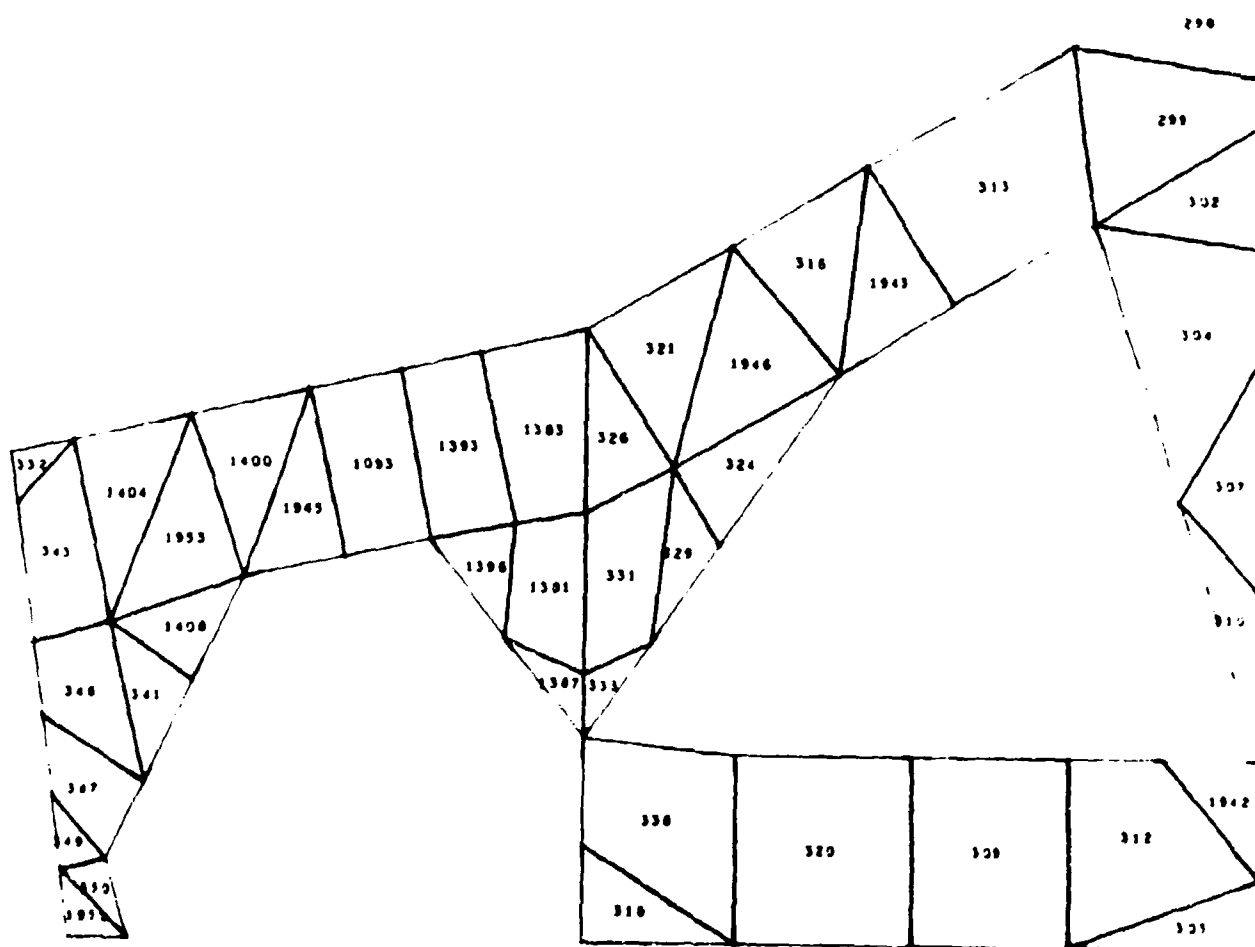


Figure 12 Y_F 947 ARCHED-BEAM BULKHEAD PLATE ELEMENTS

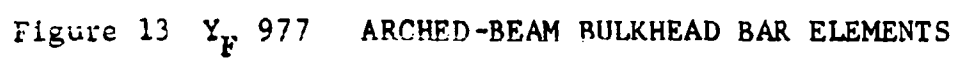


FIGURE 14 YF 977 BULKHEAD PLATE ELEMENTS

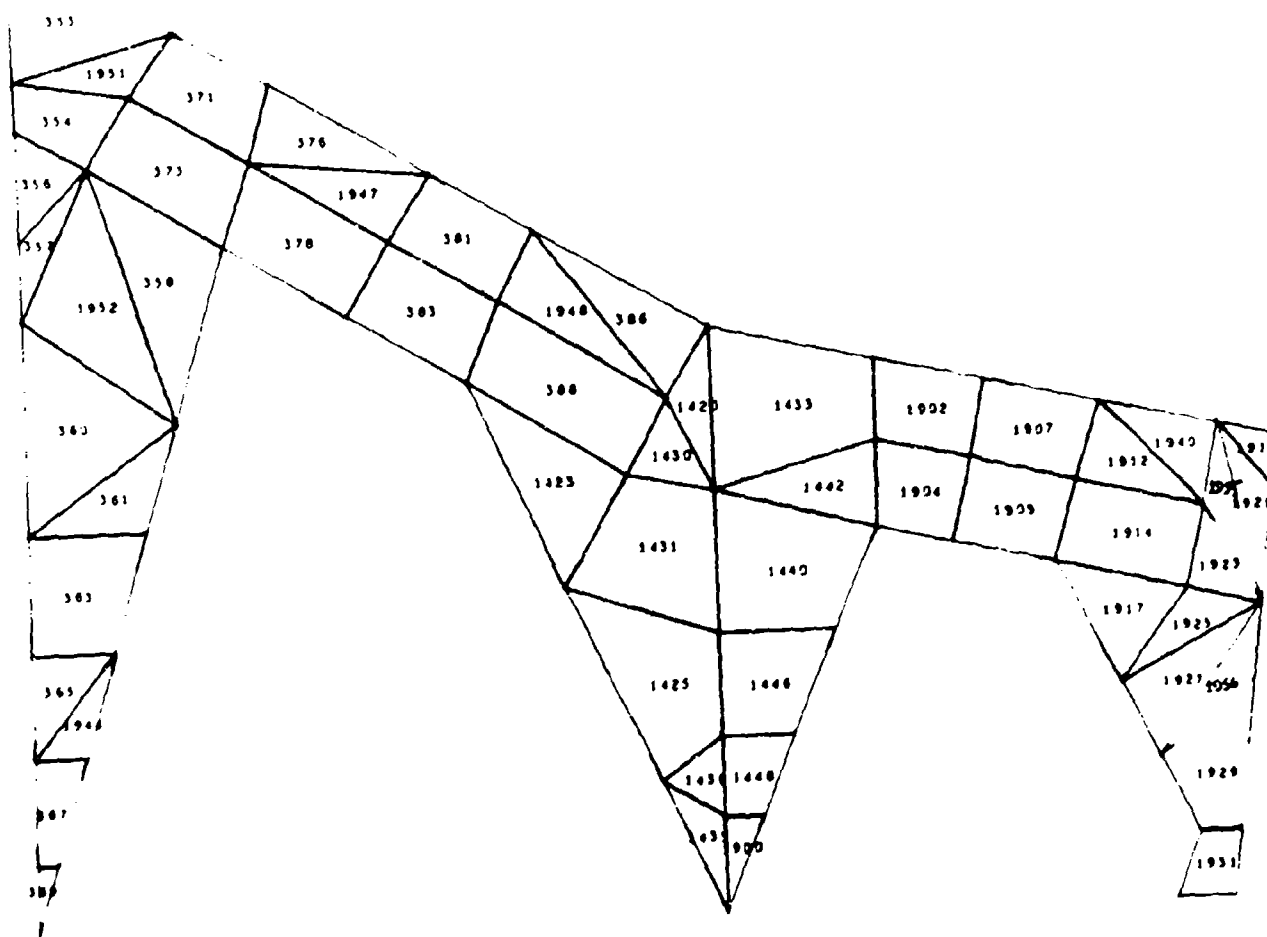


Figure 14 YF 977 ARCHED-BEAM BULKHEAD PLATE ELEMENTS

other changes were made so that a direct evaluation of the effects of the arched-beam concept could be made with respect to the FSRL-3-5 baseline. The revised bulkhead structure for this model was constructed from 7050 bent-up sheet stock and was sized to FSRL-3-5 loads.

The first TN1 stress analysis run made for the arched beam concept utilized load conditions AS2, AS6, AS10, and AS500. AS500 allowed a stiffness evaluation of the concept. A review of the results indicated that the arched bulkhead arrangement was feasible. In general, stress levels were up to 10% higher than those found in FSRL-3-5 which contained bulkheads at Y_{F947} and Y_{F977} with cutouts. There are at least two factors that would account for the stress increases:

1. Less axial material is available to act with the lower plate.
2. There is a stronger tendency for single cell torque box action to occur.

The bulkheads are being redesigned and resized based on loads data obtained from the analysis for incorporation in the updated math model.

The energy sum for AS500 deflections combined with AS300 virtual loads was found to be only 0.8% larger for FSRL-4-1 than for FSRL-3-5 so use of arched bulkheads appears to have an insignificant effect on stiffness. ($\frac{1}{2}$ box energy of $.0916 \times 10^8$ in. lbs. compared to $.0909 \times 10^8$ in. lbs.)

603FTB004 3/8 Scale Lug Specimen - In a continuing effort to obtain more accurate lug stress values with finite element analysis, a study effort was conducted utilizing linear strain computer procedure TLO and the results from strain surveys of the 603FTB004 3/8" scale lug test specimen. The objective of this effort was to develop a simulated pin mechanism to load lug math models and to obtain predicted stresses consistent with known test results. Strain survey results from the 603FTB004 specimen were obtained for a load of 200,000# and are shown in Figure 15 (solid line curve). A math model was then constructed representing the 603FTB004 specimen as shown in Figure 16. In place of the thick wall bushing, a mechanism of bars and triangles was constructed. The purpose of this arrangement was to load the pin at its centroid and let the bars transfer the load radially to the triangles. The triangles in turn load the lug I.D. in a manner consistent with the actual specimen. The bars were allowed to work only in compression. Those

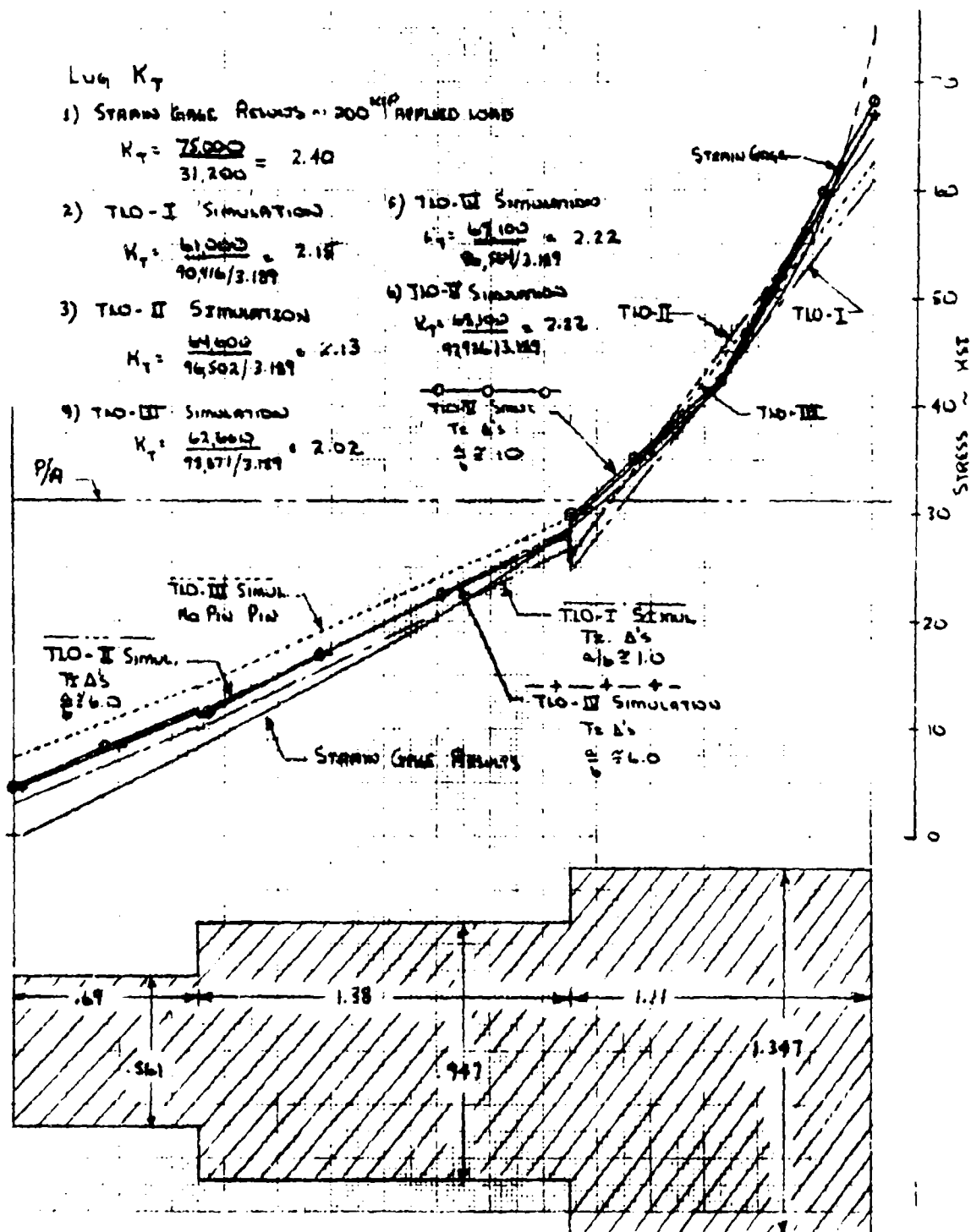


Figure 15 BOO4 3/8 SCALE LUG TEST SPECIMEN STRESS AT 200,000 # LOAD

SECTION A-A (REF. FIG. 8)

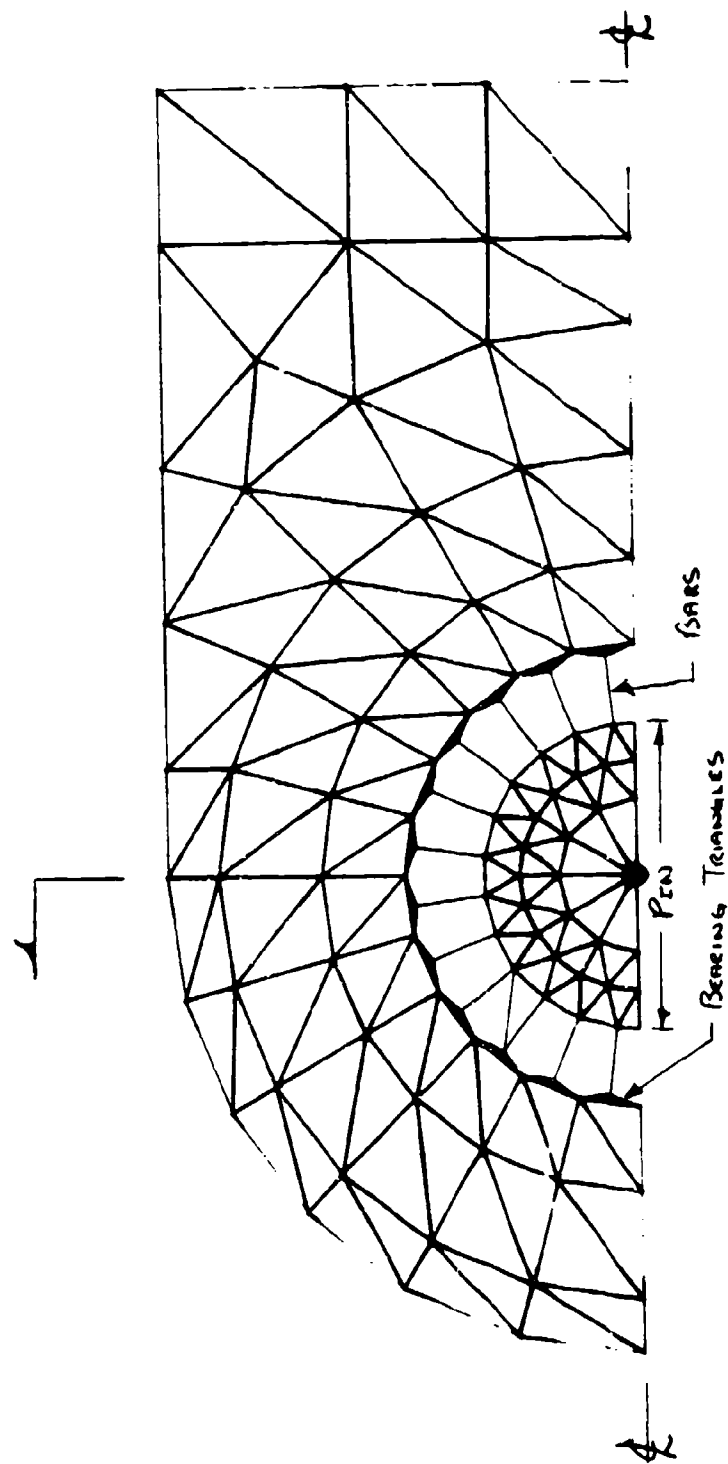


Figure 16 B004 3/8 SCALE LUG TEST SPECIMEN

expected to work in tension were given the elastic properties of rubber; those in compression, were made rigid. The bearing triangles were assigned a Young's Modulus of 16×10^6 psi to be strain compatible with the beta annealed 6Al-4V titanium lug.

The first attempt (TLO-I) utilized a bearing triangle aspect ratio (AR) = 1.0. As can be seen from Figure 15, the predicted stress at the lug I.D. was 61,000 psi versus an extrapolated value of 75,000 psi from the strain gage results. It was also learned that the AR = 1.0 permitted the bearing triangle to pick up and transfer 9.6% of the applied load at the critical section A-A, of Figure 16.

A second run (TLO-II) was made by increasing the bearing triangle AR to approximately 6.0. This increased the predicted stress level at the lug I.D. to 64,600 psi and dropped the triangle load transfer to 3.5%.

As a check, using conventional procedures, the lug was loaded with a uniform bearing distribution and the transfer mechanism was rendered ineffective by setting its elastic properties equal to rubber. This run (TLO-III) resulted in a predicted peak stress of 62,600 psi, midway between the first two runs, but resulted in relatively higher stresses around the lug outside diameter.

Since all three runs (TLO-I through III) produced relatively similar results, it was decided that better agreement could be obtained only through use of a finer grid in the large stress gradient region. Therefore, as shown in Figure 17, additional nodes and elements were added to double the coverage in the 1.347 in. thick boss. This run (TLO-IV) gave an increased peak stress at the lug I.D. of 67,100 psi and produced a stress distribution more closely approximating the results from the strain survey. See Figure 15.

As a final attempt to improve the model results the IV model was modified by increasing the bearing triangle aspect ratio (AR) from AR = 6 to AR = 10. This run was designated TLO-V. The stress variation across the lug was nearly identical to the IV run but the peak stress at the I.D. increased to 68,000 psi -- reference Figure 15. At this time, work on the 603FTB004 model was terminated to allow work to begin on the actual lug model.

Lower Lug Fine Grid Analysis - In order to get a more realistic stress distribution for the FSRL lower lug, a fine grid TLO model was set up. An overall view of the simulation is shown in Figure 18. This model incorporates a simulated wing pivot pin modeled to duplicate the bending stiffness of the actual pin and a load

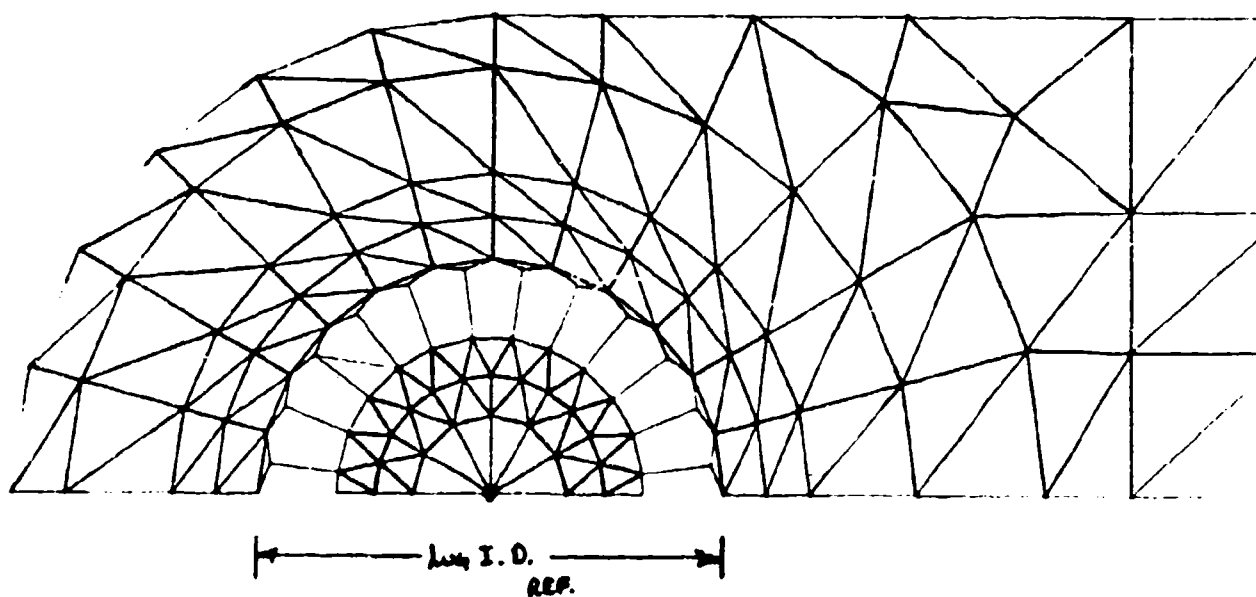


Figure 17 603FTB004 TLO-IV AND TLO-V SETUPS WITH FINER GRID
SIMULATION AROUND LUG I. D.

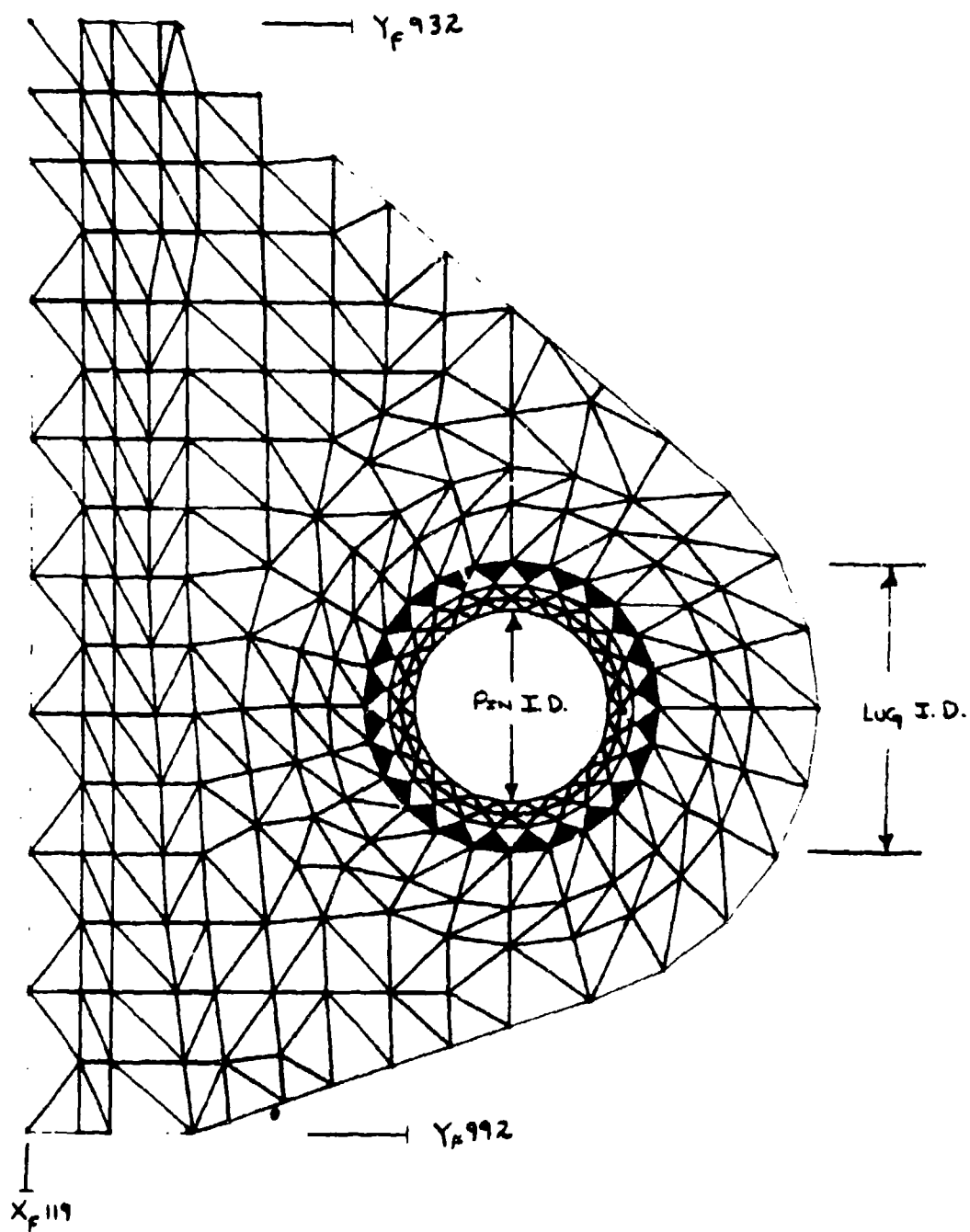


Figure 18 FSRL LOWER LUG FINE GRID MODEL

transfer mechanism as previously described. In addition, an attempt was made to simulate the actual load paths through the lug-lower plate splice joint. Figure 19 illustrates the simulated load paths used in the model in the splice region. This model was put on standby status pending final results of the 603FTB004 study and final lug-lower plate arrangement selection.

Finite Element Buckling Analysis - Work in this area consisted of a NASTRAN analysis of a portion of the upper plate and of a study on the effects of grid size reduction.

Upper Plate - A NASTRAN finite element model of a portion of the machined titanium upper plate was developed. As shown in Figure 20 the region selected is bounded by the closure rib, the X_{F84} rib, and the bulkheads at Y_{F992} and 977. Although use of Convair procedure AS3 would have been more economical, the stiffeners could not be simulated with A3S. Thicknesses are shown in Figure 21 .

The results of this analysis showed an eigenvalue of 5.52 for ASKA Cond. 2 with the point of maximum deflection at the center of the center panel. Figure 22 shows a plot of the buckling mode shape.

Grid Fineness Study - In order to gain additional insight into the effects of grid size on solution accuracy, example problems were set up for two ratios of stiffener area to plate thickness for several grid arrangements (Figure 23, Table 7). The basic example structure is shown in Figure 24 and consists of a simply supported plate with a central stiffener parallel to the load direction. The two plate thicknesses considered were selected so that in one case (1) the stiffener broke the plate up into two panels and in the other (case 2) overall buckling including the stiffener was predicted. The predicted buckling stresses based on NACA TN 1825 are shown as the solid curve in Figure 25 . Results for the NASTRAN solution for the stiffener critical (case 2) are also indicated in Figure 25 . A typical case 2 buckled mode shape is shown in Figure 26 . Work on the stable stiffener case (1) is in progress. It has been concluded thus far that the plate simulation can be rather crude without grossly affecting the eigenvalue when the stiffener is critical. The values for the two extreme grid sizes are within 10 percent.

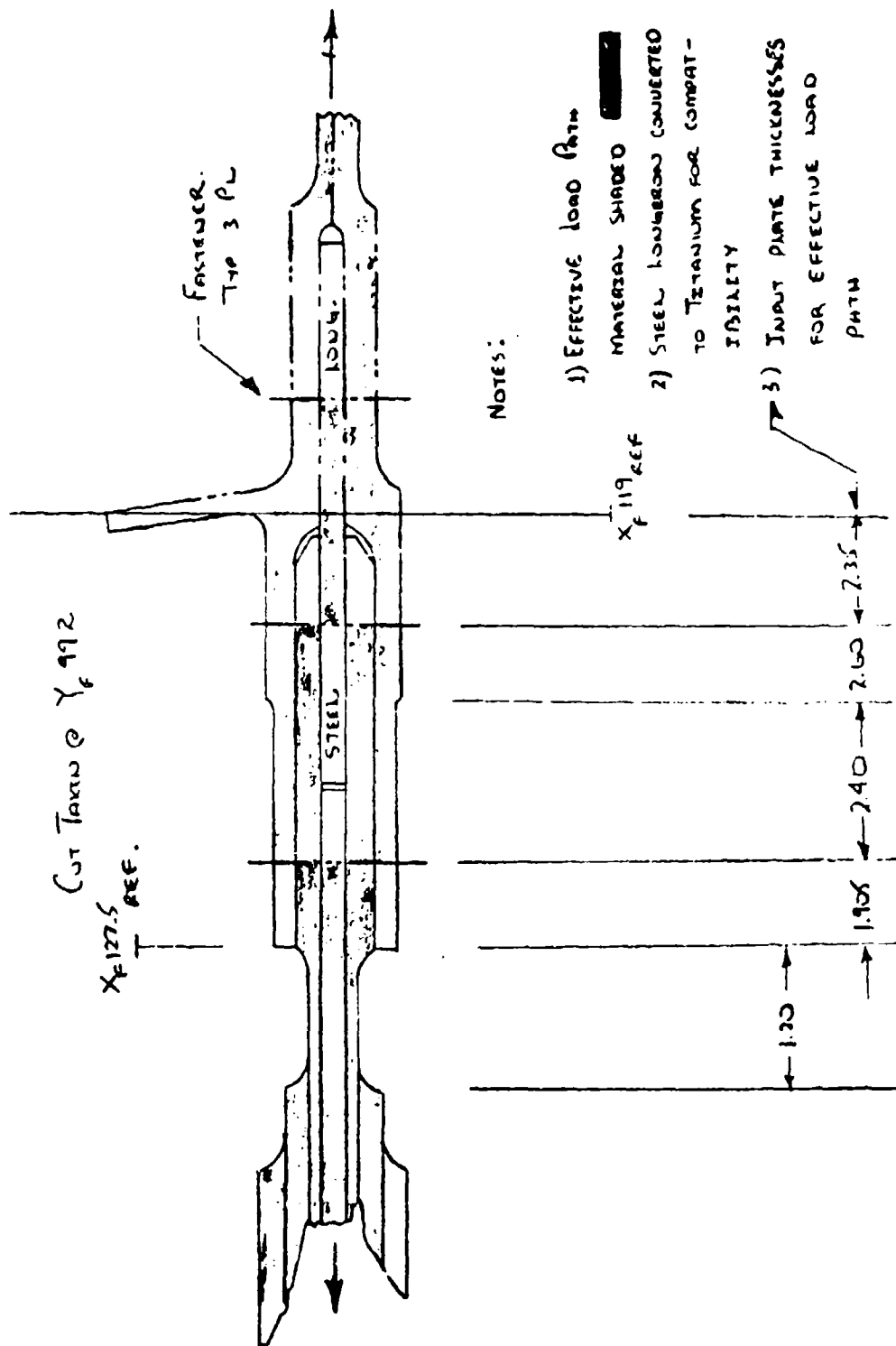


Figure 19 FSRL CONFIGURATION T20 SIMULATION OF LOWER LUG

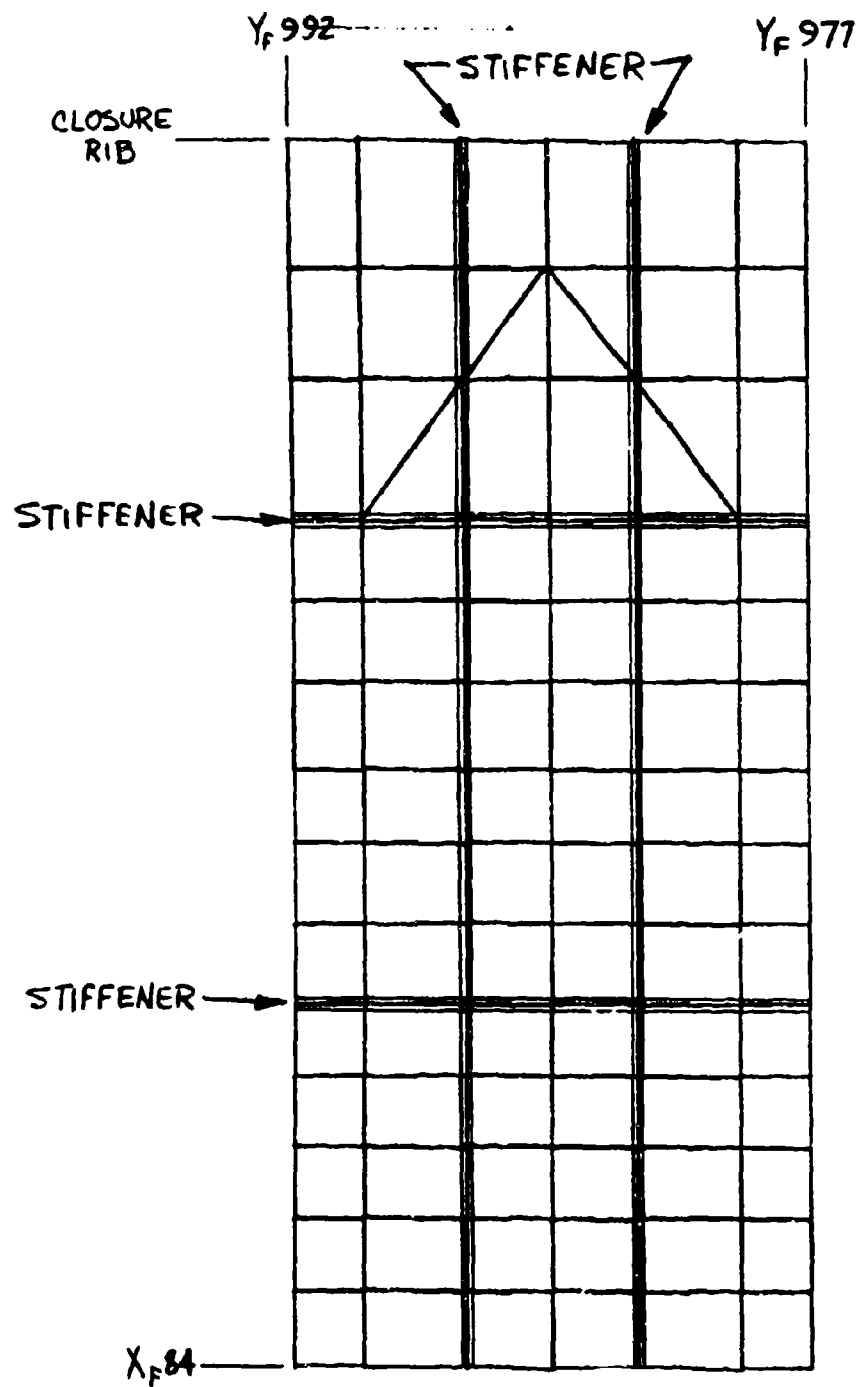
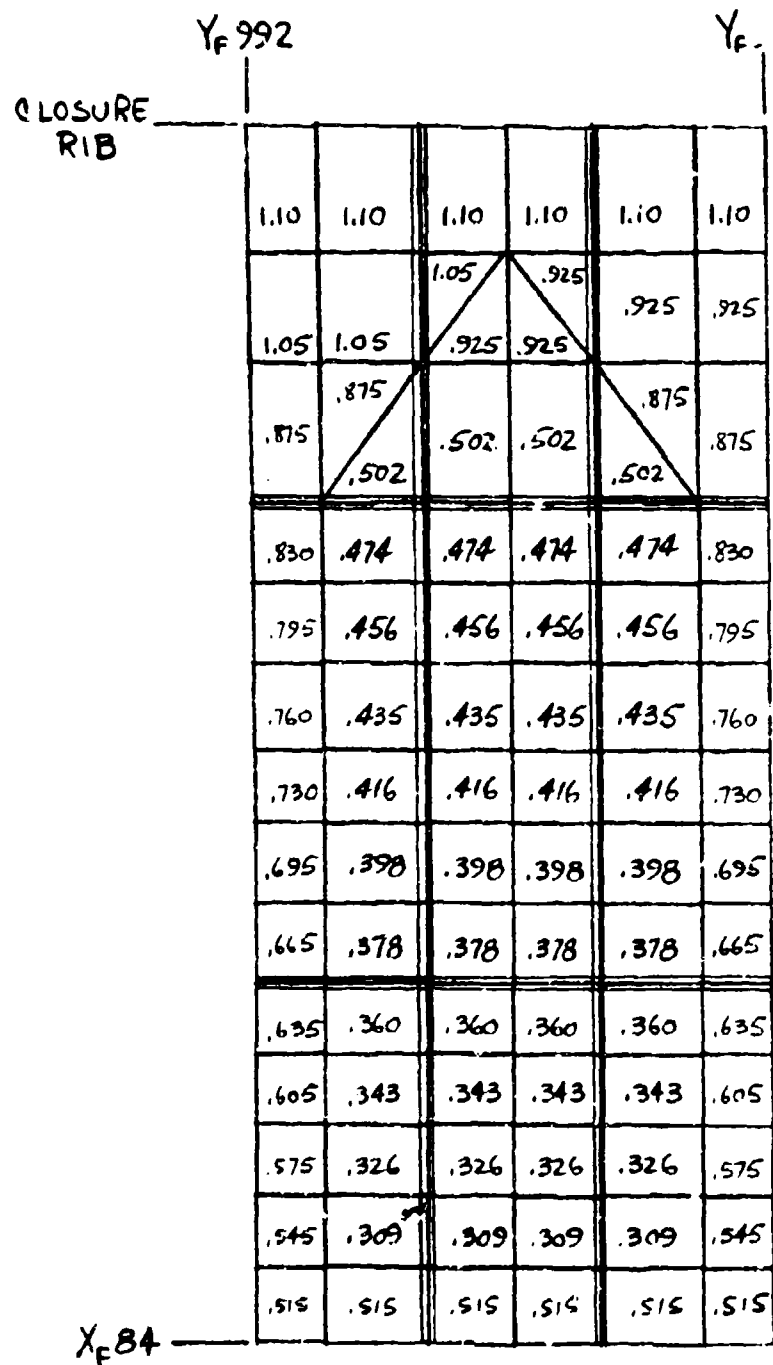


Figure 20 FSRL UPPER PLATE NASTRAN BUCKLING MODEL



UNREFINED MESH

Figure 21 FSRL UPPER PLATE - NASTRAN MODEL PLATE THICKNESSES

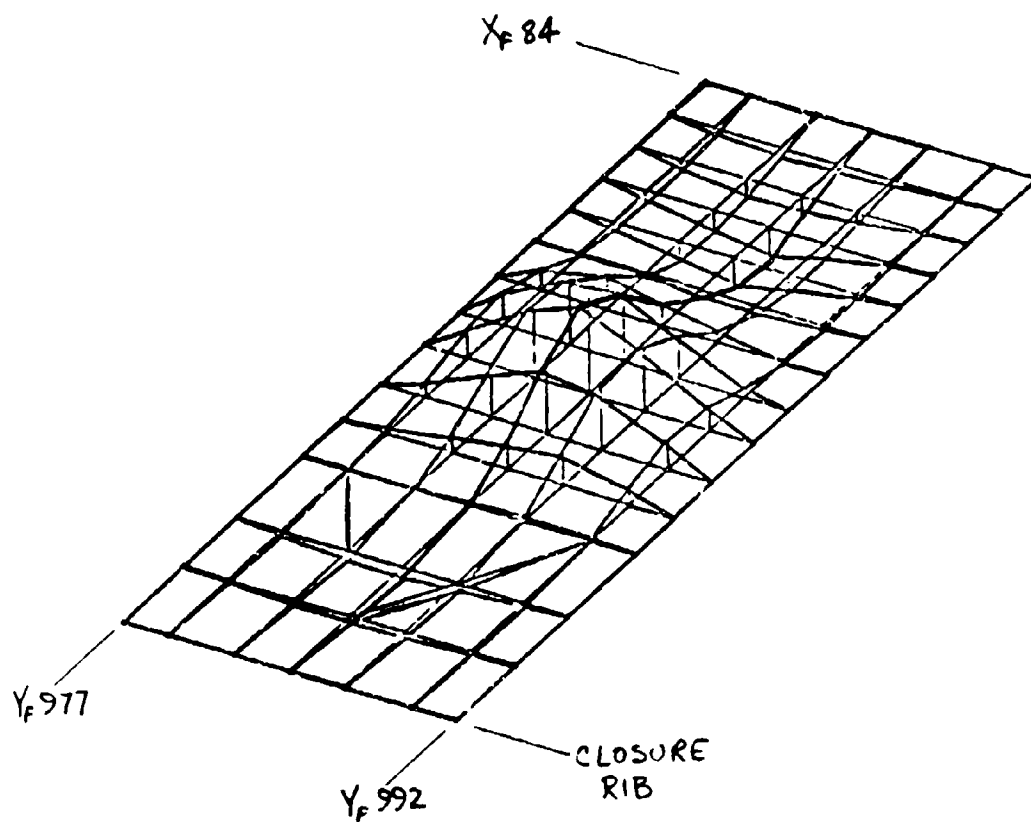


Figure 22 FSRL UPPER COVER BUCKLING MODE SHAPE ASKA 2

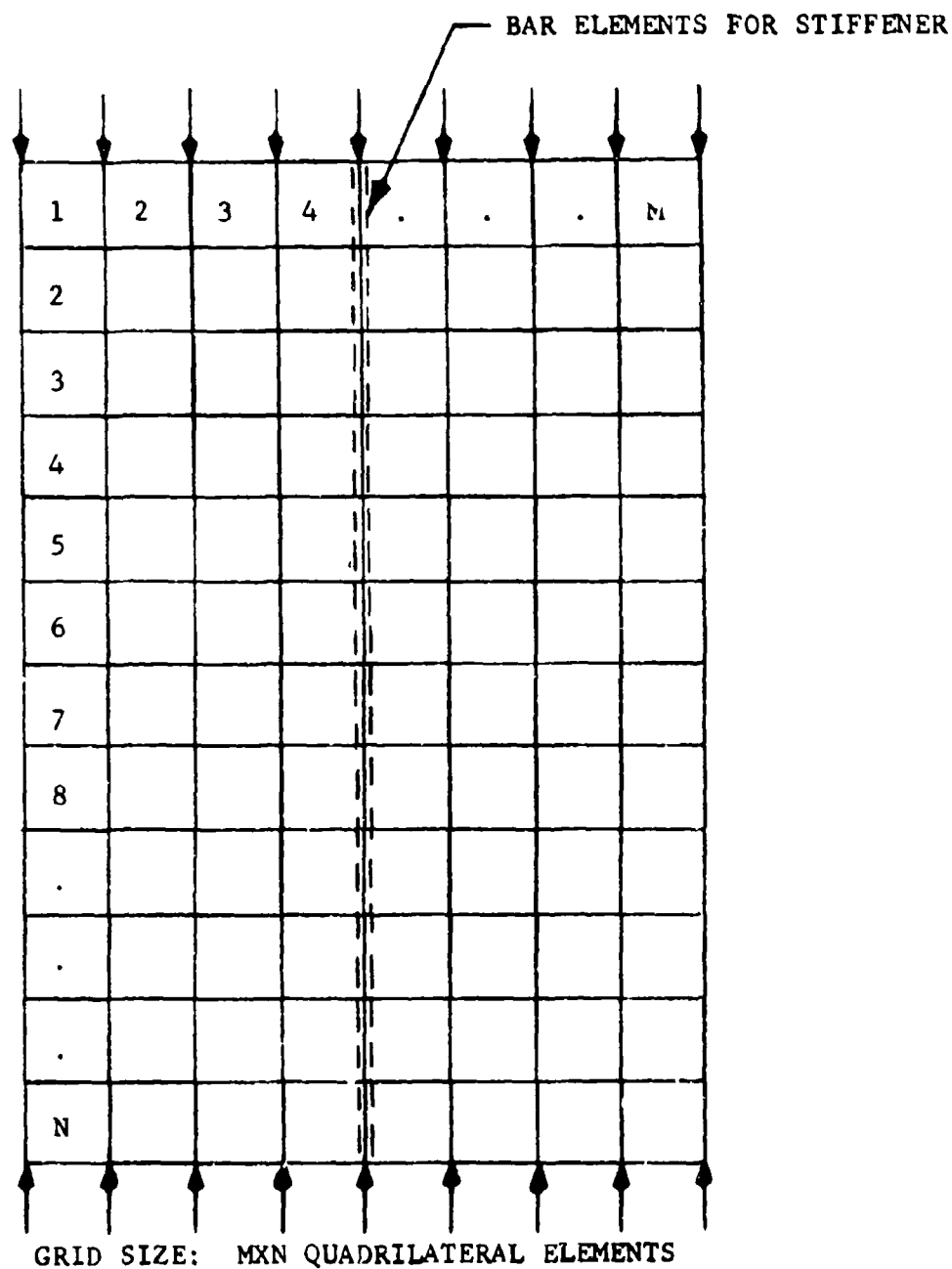


Figure 23 ELEMENT ARRANGEMENT FOR NASTRAN MODELS OF SIMPLY SUPPORTED PLATE WITH ONE LONGITUDINAL STIFFENER

Table 7

NASTRAN BUCKLING ANALYSIS RESULTS
FOR VARIOUS GRID SIZES

CASE*	h IN.	t _s IN.	t _p IN.	GRID SIZE MXN ELEMENTS	σ _r KSI
1	1.172	0.1365	0.1	4 X 6	
1	1.172	0.1365	0.1	8 X 6	
1	1.172	0.1365	0.1	4 X 12	
1	1.172	0.1365	0.1	8 X 12	
2	1.172	0.1365	0.1357	2 X 4	87.8
2	1.172	0.1365	0.1357	4 X 4	73.2
2	1.172	0.1365	0.1357	2 X 8	87.3
2	1.172	0.1365	0.1357	4 X 8	80.1

* Case 1 represents a plate critical design. Analysis not complete

* Case 2 represents a stiffener critical design.

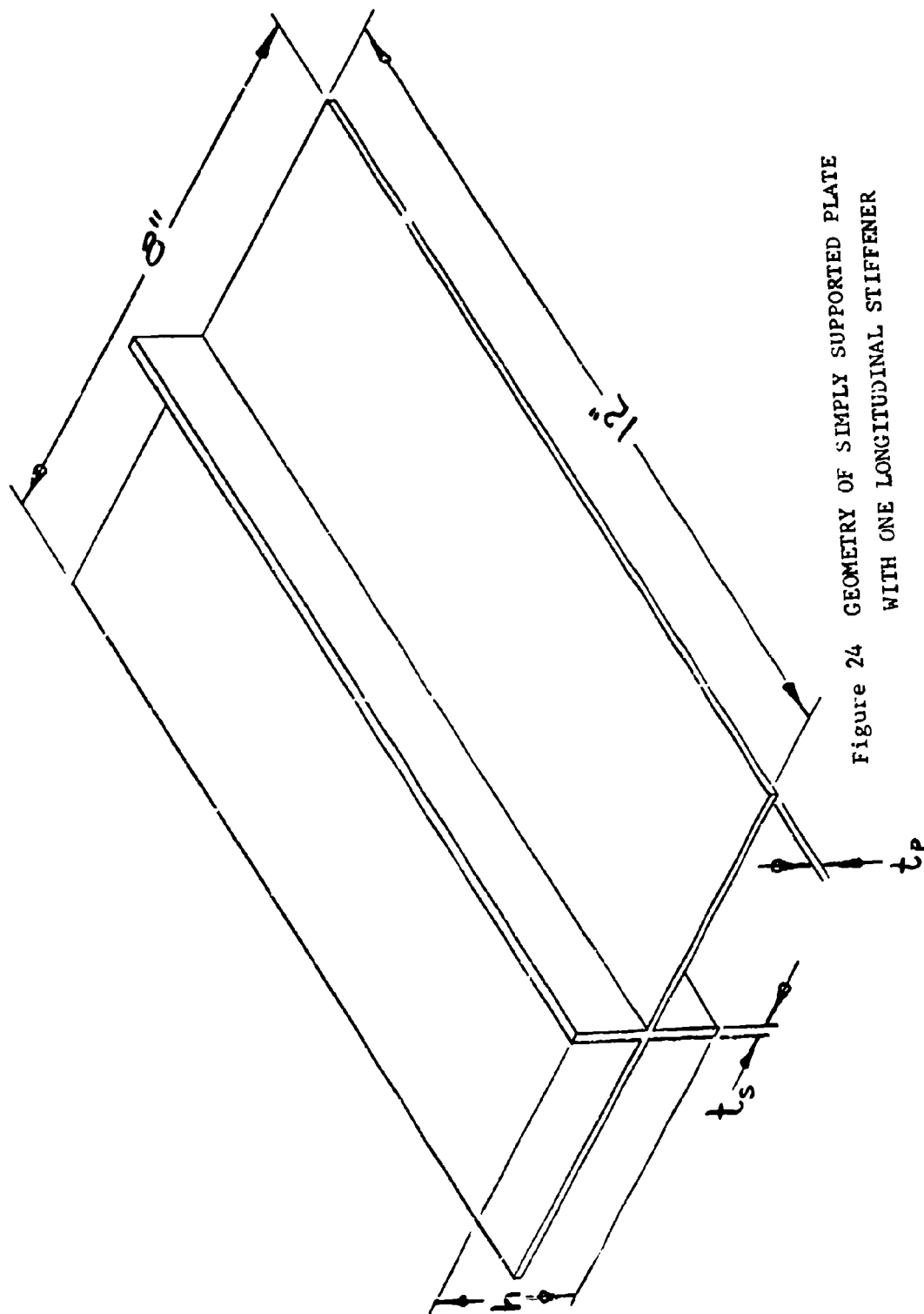


Figure 24 GEOMETRY OF SIMPLY SUPPORTED PLATE
WITH ONE LONGITUDINAL STIFFENER

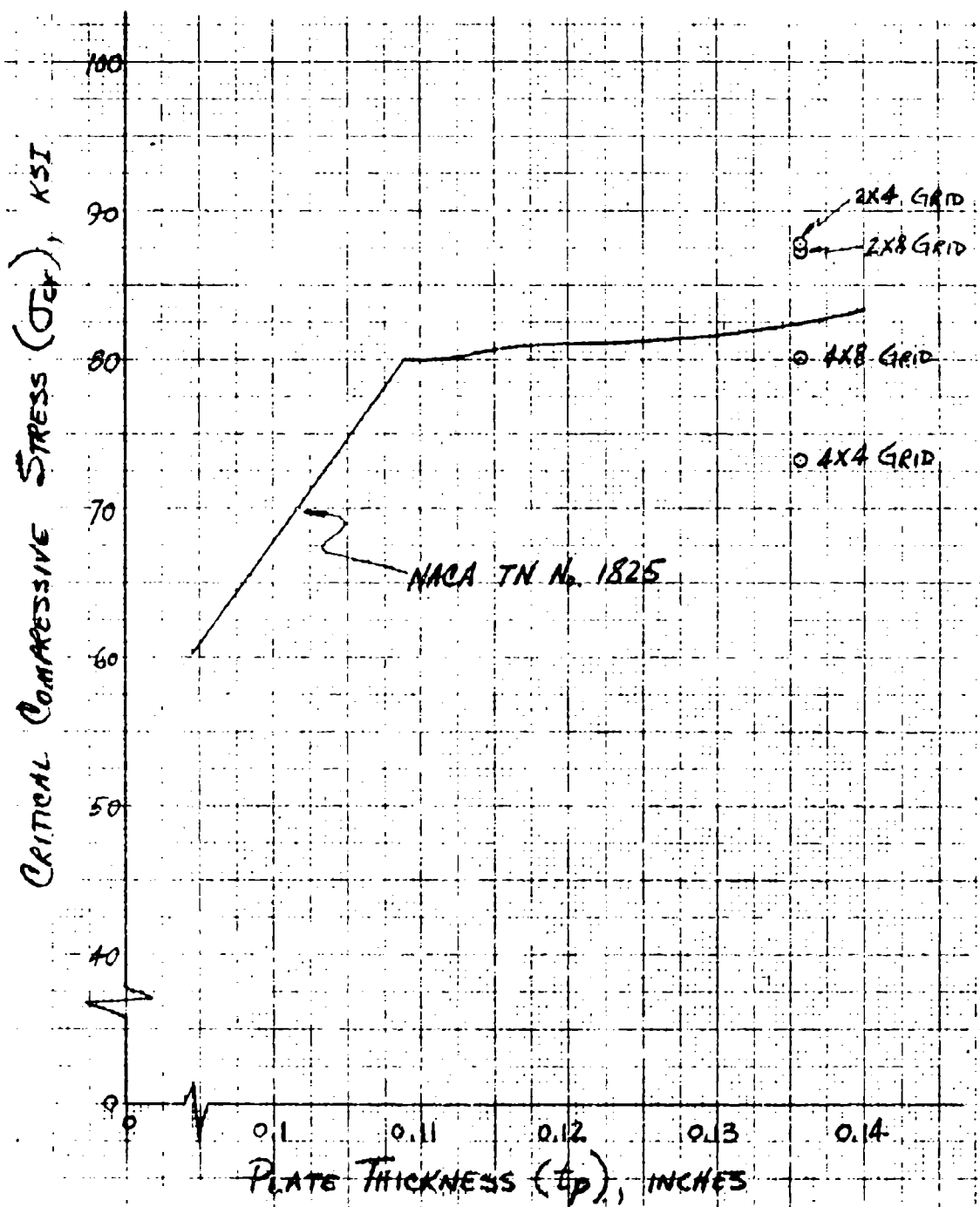


Figure 25 COMPARISON OF CRITICAL COMPRESSIVE STRESSES FOR SIMPLY SUPPORTED PLATE WITH ONE LONGITUDINAL STIFFENER RESULTS FROM NACA TN NO. 1825 VS NASTRAN MODELS

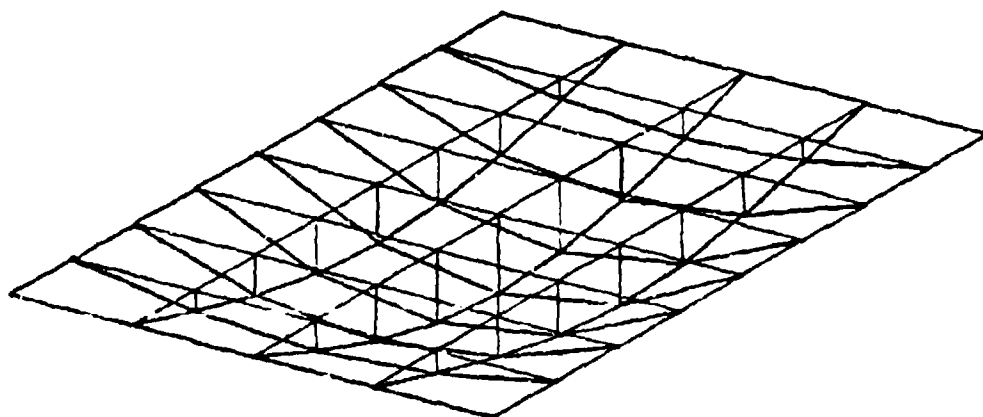


Figure 26 MODE SHAPE FOR CASE 2 NASTRAN
MODEL - 4X8 GRID

Updated Overall Finite Element Model - In order to provide a model which more accurately reflected the design as detail design began, a major revision to the overall model was begun and substantially completed during the reporting period. The new model includes the three-layer lower plate with integral lugs (FSIL), the arched bulkheads at $Y_F 947$ and $X_F 977$, the ti./al. upper plate, revised sweep actuator fitting attachment points, and other miscellaneous changes required by the updating. The applied panel point loads were revised for all loading node relocations involved.

Wing Sweep Actuator Fitting - Analysis of the redesigned wing sweep actuator fitting was begun.

Test Items - Stress data for component test planning and execution was provided as required.

Lower Aft Longerons Joint - The currently proposed longeron joint was reviewed for feasibility and positive results were obtained.

3.1.2.2 NBB Stress Analysis

The primary stress analysis tasks accomplished for the No-Box Box configuration were as follows:

1. Study of effects of relative deflections on the lower plate at $X_F = 119$ and on the upper plate at $X_F = 84$.
2. Trade study support for the lower plate configuration selection. ($Z_F = 0$ versus lower contour)
3. Development of an updated overall math model incorporating current design concepts and geometry.
4. Upper lug stability analysis.
5. Manual analysis of local areas.

Relative Deflection Studies - The NBB-1-1 overall math model results showed that for condition ASKA 2, the lug deflected outboard 0.67 inch at $Y_F 962$, $X_F 120.37$ while the lower panel deflected outboard 0.37 inches at the same X_F and Y_F location at $Z_F 5.646$. Since the relative deflection would have required flexing of the closure rib causing possible fatigue life reduction, additional studies were undertaken to assess the effects.

The lower plate model shown in Figure 27 and further described later, was modified by using orthotropic elements adjacent to the lug, fore and aft bulkheads, and the X_{F84} rib. The stiffnesses of the plate elements were such that they simulated the load path down to and through a lower contour panel so that an estimate could be made as to whether this path would carry enough load to significantly reduce the relative deflection. It was found that no significant reduction occurred which led to the conclusion that closure rib flexing would be required for the contour plate design. Two runs were made, NBB-1 & NBB-2.

A review of the upper plate step at X_{F84} indicated that significant relative deflections were also present at that location. Further review of this area will take place when the structural arrangement is firm. The capability of using orthotropic elements to simulate the local stiffness is being built into the overall math model.

Lower Plate Material Distribution Studies - Because of relative deflection problems and other design considerations an extensive study of the effects of material distribution on a $Z_F = 0$ lower plate was conducted so that an efficient and feasible arrangement could be obtained. A two dimensional TR4 model of the plate was constructed (Figure 27)

The TR4 model includes node locations which match existing nodes in the NBB-1 overall model at $Z_F = 0$. Loads were determined for the structure adjacent to and above $Z_F = 0.0$ from the overall math model run NBB-1 and used as applied loads on the $Z_F = 0.0$ math model. This method loaded the $Z_F = 0.0$ math model substantially the same as if it were integral with the overall model. Four load conditions, ASKA 2, 6, 9, and 10 were used in each run.

For the initial study of the effect of material distribution on the maximum stresses in the lower plate and lug, seven problems were run using combinations of 10 Nickel steel and aluminum of various thicknesses in zones A, B, and C (Figure 28) as shown in Table 8. The results of problem 179170A showed that acceptable stresses were achieved with a relatively even thickness over the plate between $X_F = 84$ and $X_F = 115.9$. The maximum principal stresses for P179170A induced by condition ASKA 2 are shown in Figure 29 for an aluminum plate 0.60 inch thick in zones A, B, and C of Figure 28.

Next, a 0.3 inch thick steel plate was tried in zones A, B, and C. The plate stress levels for ASKA 2 were acceptable

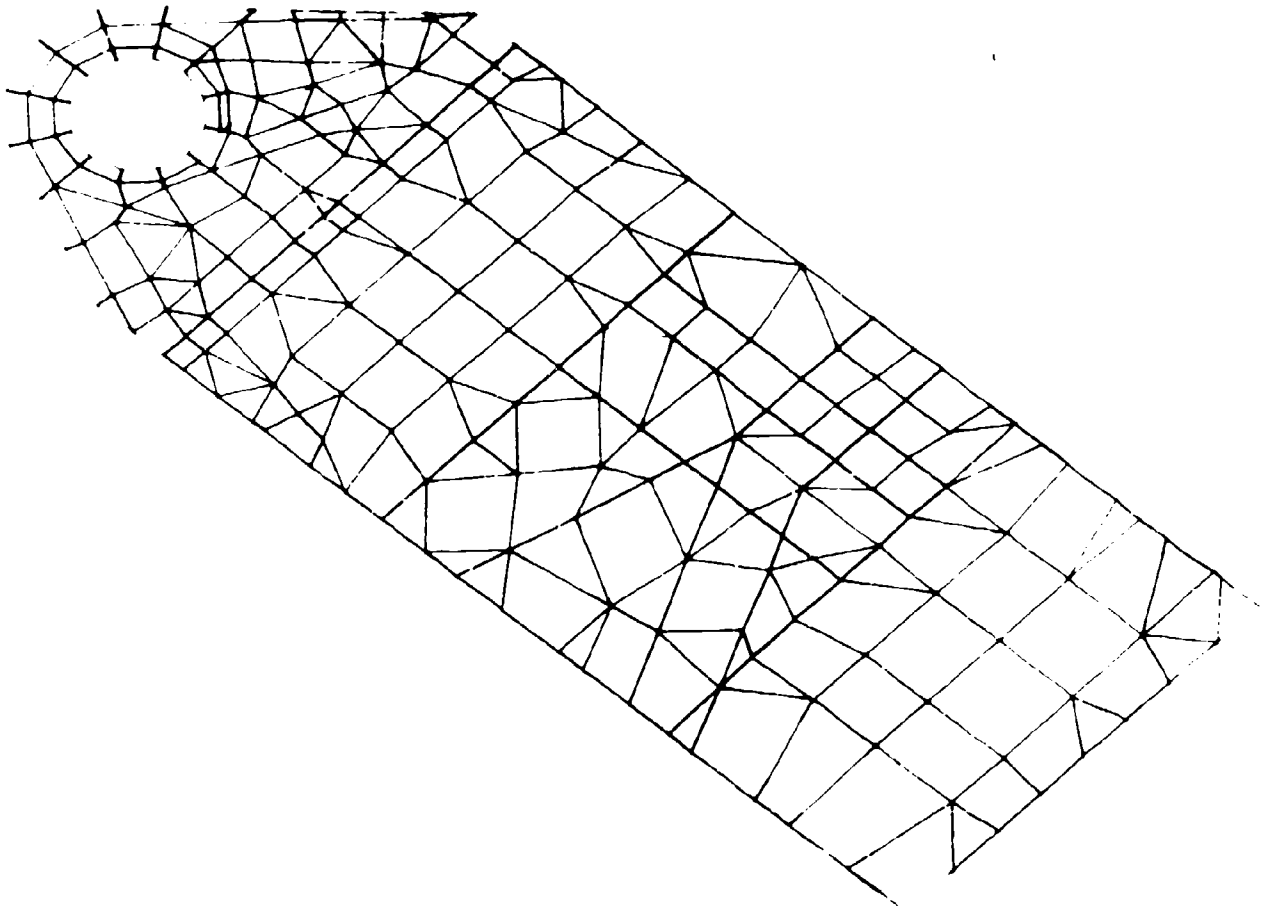


Figure 27 NBB MATH MODEL OF LOWER PLATE AT $Z_F = 0.0$

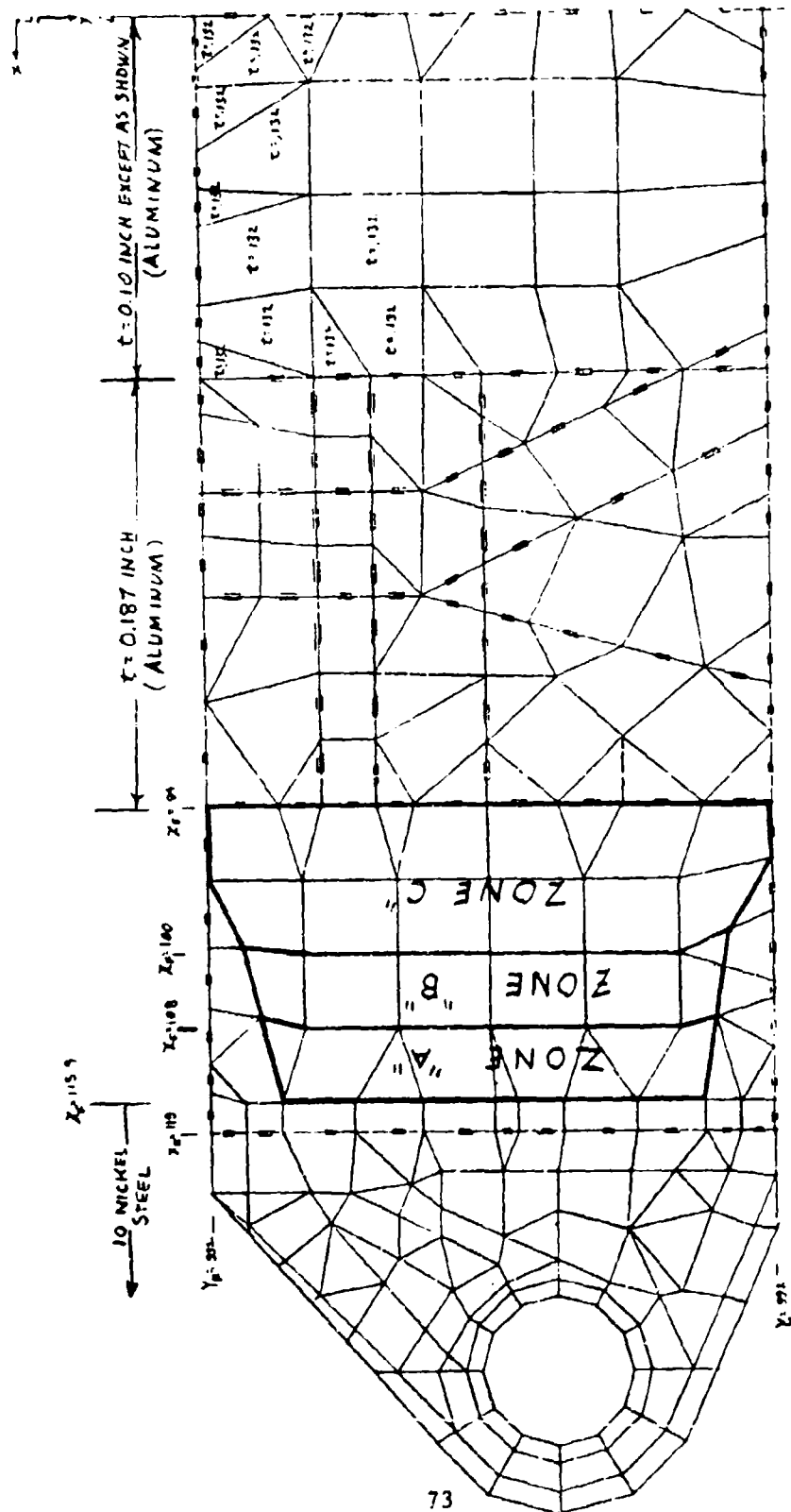


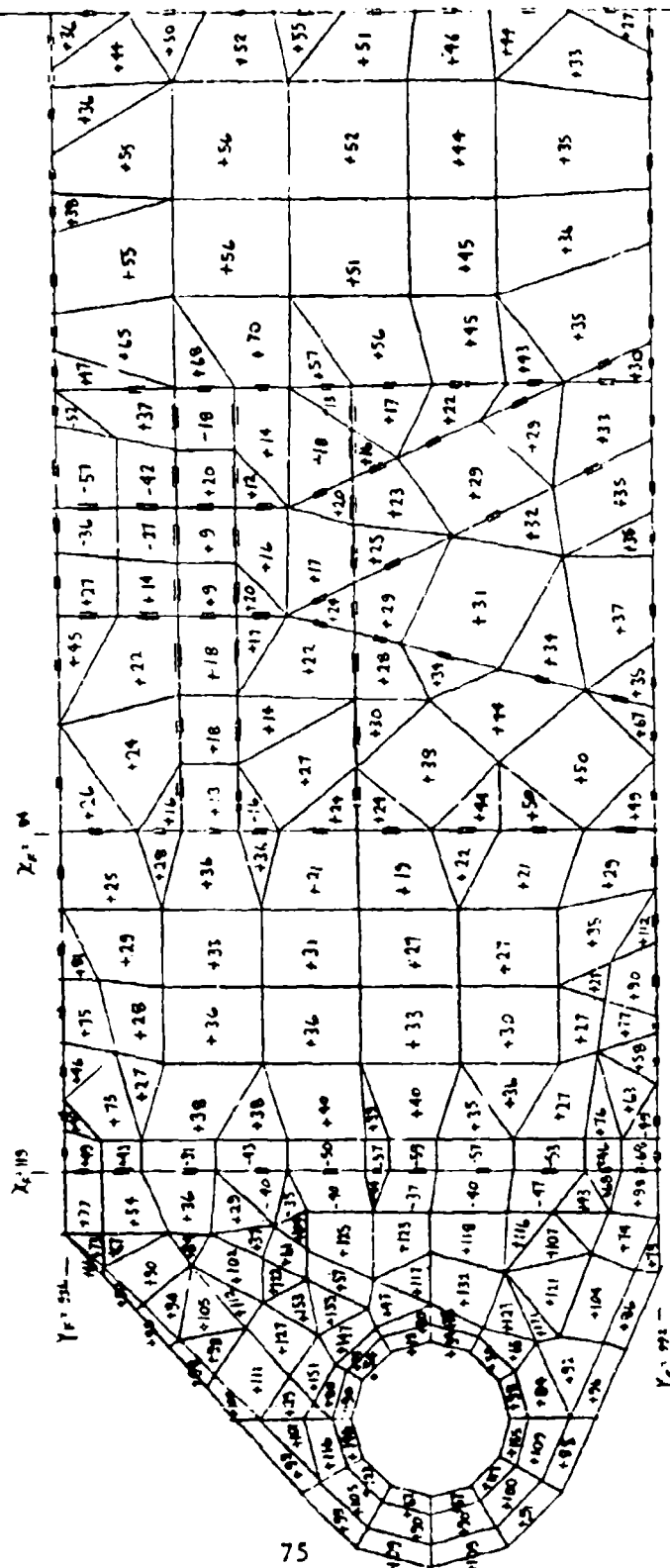
Table 8 NBB $Z_F = 0.0$ MATH MODEL LOWER PLATE STUDY

PROBLEM NUMBER	ZONE A (1)		ZONE B (1)		ZONE C (1)	
	MATERIAL (2)	THICKNESS (INCH)	MATERIAL (2)	THICKNESS (INCH)	MATERIAL (2)	THICKNESS (INCH)
P178249 B	AL	0.10	AL	0.10	AL	0.10
P178311A	STL	0.10	STL	0.10	AL	0.10
P178310A	STL	1.00	AL	0.10	AL	0.10
P179171B	STL	1.00	STL	1.00	AL	0.10
P179172A	STL	1.00	STL	1.00	AL	0.30
P178309A	AL	0.30	AL	0.30	AL	0.30
P179170A	AL	0.60	AL	0.60	AL	0.60

(1) FOR ZONE LOCATIONS SEE FIGURE Y

(2) MATERIAL CODE - AL = 7050 ALUMINUM, STL = 10 NICKEL STEEL,

PROJECT P-7311A
CONDITION A-KA 2



MATH MODEL OF LOWER PLATE AT $E_F = 0.0$, NBB

Figure 29 ELEMENT MAX PRINCIPAL STRESSES (KSI)

from a material property standpoint as shown in Figure 30 . Review of the ASKA 4 condition which causes compressive stresses on the lower surface that are approximately -37 percent of the ASKA 2 stresses (based on wing bending moment ratio), indicated that stiffeners were required to prevent buckling.

As a means of gaining further insight into the action of the ZF0 plate, the resizing option of TR4 (essentially the same as TN1) was exercised for several material arrangements. This resizing option uses a fully stressed approach for the members allowed to vary. No direct weight optimization is included. The runs made are summarized in Table 9 and discussed in the paragraphs that follow.

1. NBB-3

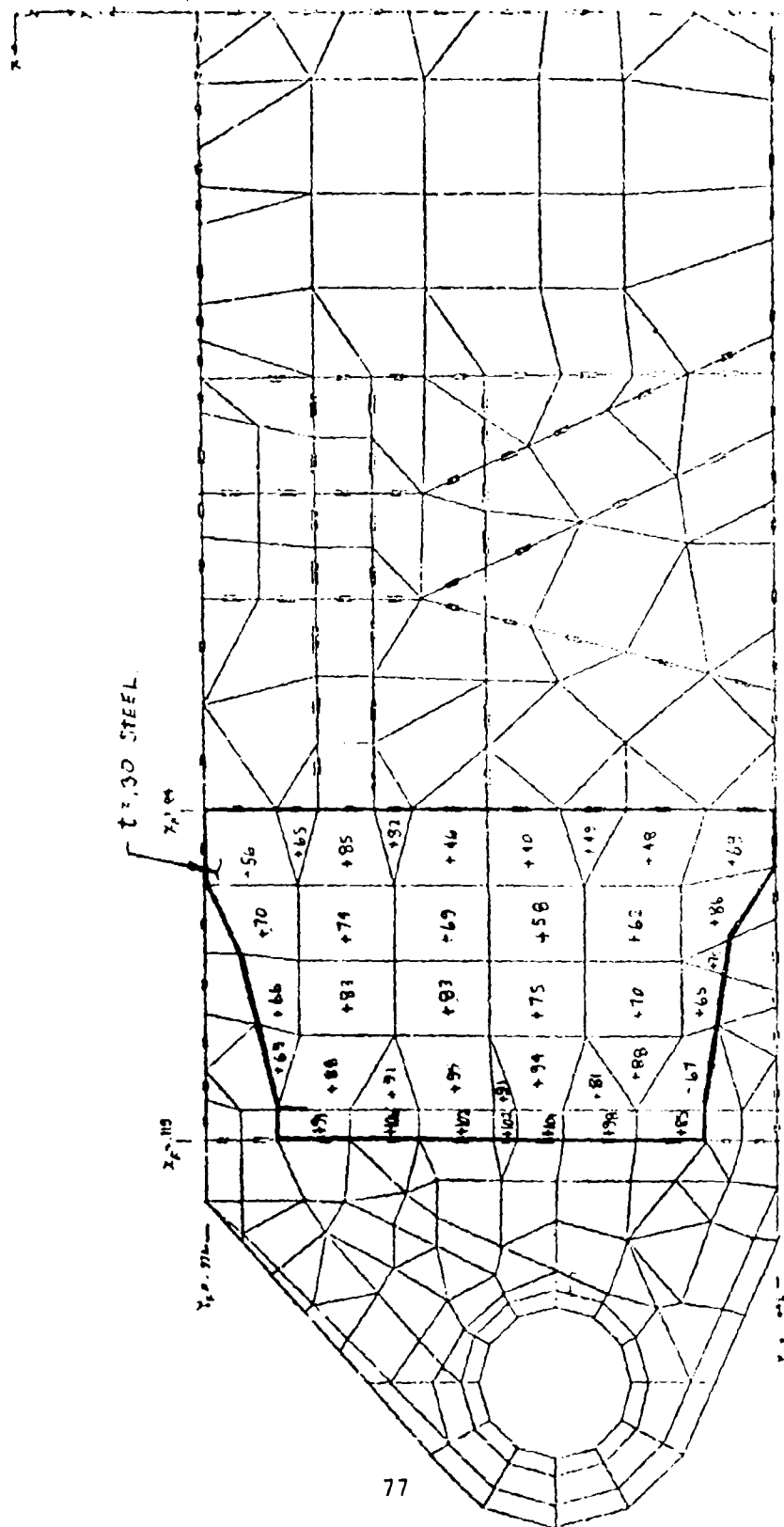
For NBB-3, the 10 Ni. steel portion was held constant at the values determined for the lower plate at contour. (Shaded area, Figure 31) An input gage of 0.10 was used for the 7050 al. The program was allowed to analyze and resize the structure six times. (Five iterations).

The final 7050 aluminum gages obtained are shown in Figure 31. The solution was close to convergence for the number of cycles noted since as shown by Figure 32 , the structural weight had reached a substantially constant value. On the average, this result was similar to the .60 aluminum requirement previously found satisfactory although the aluminum element stresses in the latter case were not as uniform since the gage was constant.

2. NBB-4

In order to determine a more efficient arrangement of material in the lower plate, both the 10 Nickel steel and the 7050 aluminum were allowed to vary. The initial input gages and area outboard of X_{F84} are shown in Figure 33 . As may be seen in Figure 32 the major portion of the resizing occurred in three iterations. The final gages and areas obtained outboard of X_{F84} are shown in Figure 34 . A typical inplane deflection plot is shown in Figure 35 for ASKA 2 and in Figure 36 for ASKA 10. It should be noted that all physical constraints such as minimum practical size for some members were not applied since only qualitative results were being sought. For this problem, the allowable effective stresses used were 45,000 psi for aluminum and 145,000 psi for steel. These are less than actual material ultimate strength because of fatigue considerations. The result

PROBLEM P179174A
CONDITION ASKA 2



MATH MODEL OF LOWER FLATE AT $Z_F = 0.0$, NBB
Figure 30 ELEMENT MAX PRINCIPAL STRESSES (KSI) IN 0.3 STEEL BETWEEN
 $X_F = 84$ AND $X_F = 119$

Table 9 "NO-BOX" BOX LOWER PLATE RESIZING RUNS

NO. OF
ITERATIONS ③

LOWER PLATE NOTES ②

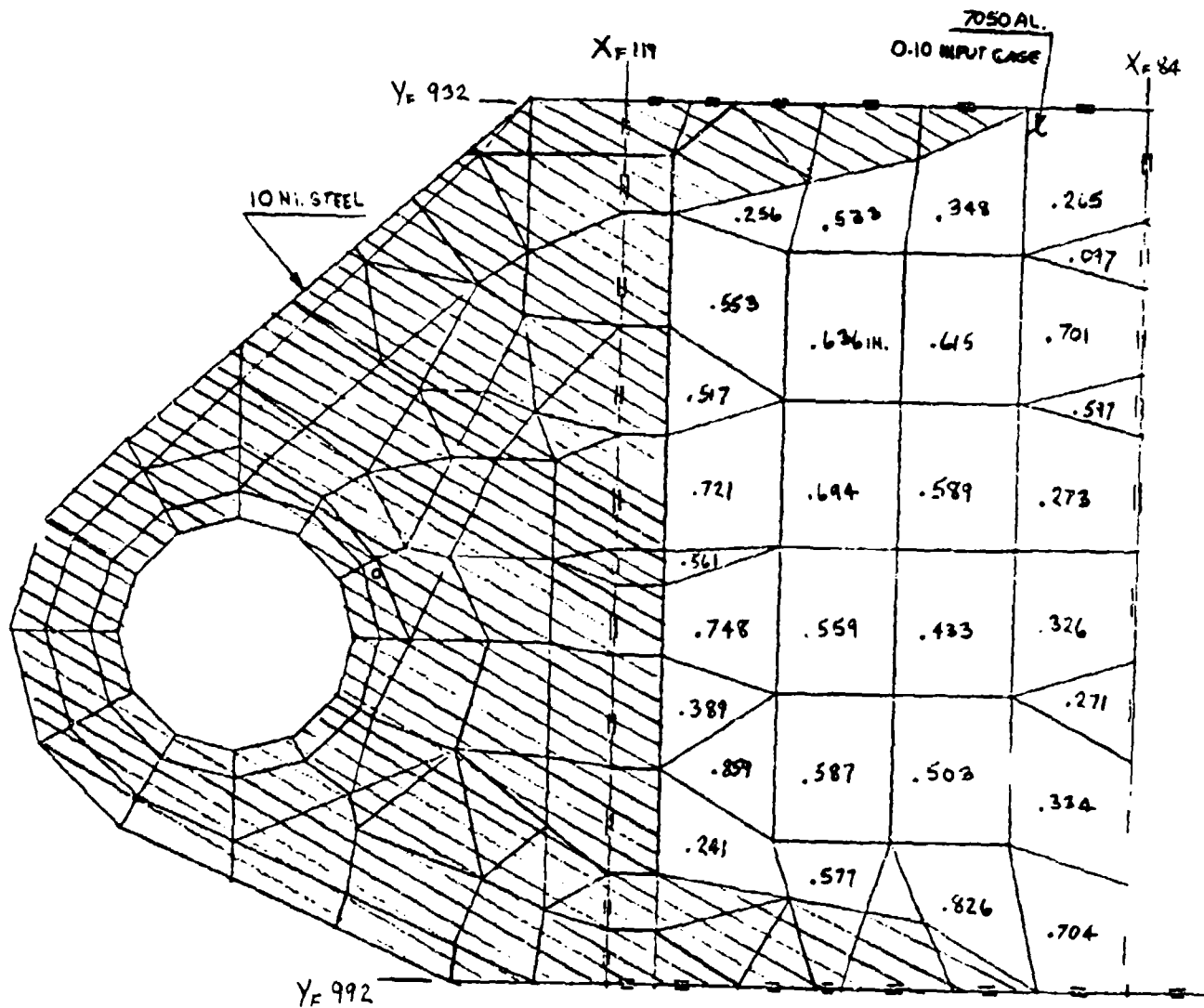
LUG AND BULKHEAD RAIL NOTES ①

RUN

NBB-3	Held Constant at Values Used for Lower Plate at Contour. See Figure 31	Initial Gage = 0.10. No Variation Allowed Inboard of X_{F84} .	5
NBB-4	Variable. See Figure 33 and 34 for Values Outboard of X_{F84} .	Variable. See Figure 33 and 34 for Values Outboard of X_{F84} .	3
NBB-5	Variable	Constant at Figure 33 Values.	2
NBB-6	Lug Pockets and Bulkhead Rails Variable.	Plates Variable. 10 Ni. Steel X_{F119} to X_{F84} . 7050 Al. X_{F84} to X_{F0} . Added four 10 Ni. Stiffeners X_{F119} to X_{F84} with Area Held Constant.	5
NBB-7	Lug Pockets and Bulkhead Rails Variable	Five 10 Ni. Stiffeners with Constant Areas. Steel Plates X_{F119} to X_{F84} .	3
NBB-8	Lug Pockets and Bulkhead Rails Variable	Five 10 Ni. Stiffeners with Constant Areas. Steel Plates X_{F119} to X_{F84} . T1. Plates X_{F84} to X_{F0} . All.Eff. Stress = 90,000 psi for T1.	3

① 10 Ni. Steel, Allowable Effective Stress = 145,000 psi.

② 7050 Al. Except as Noted. Allowable Effective Stress = 45,000 psi.



.XXX= FINAL GAGES, 7050 AL., 6 CYCLES

Figure 31 NBB-3 TR4 ITERATION Z_F0 LOWER PLATE

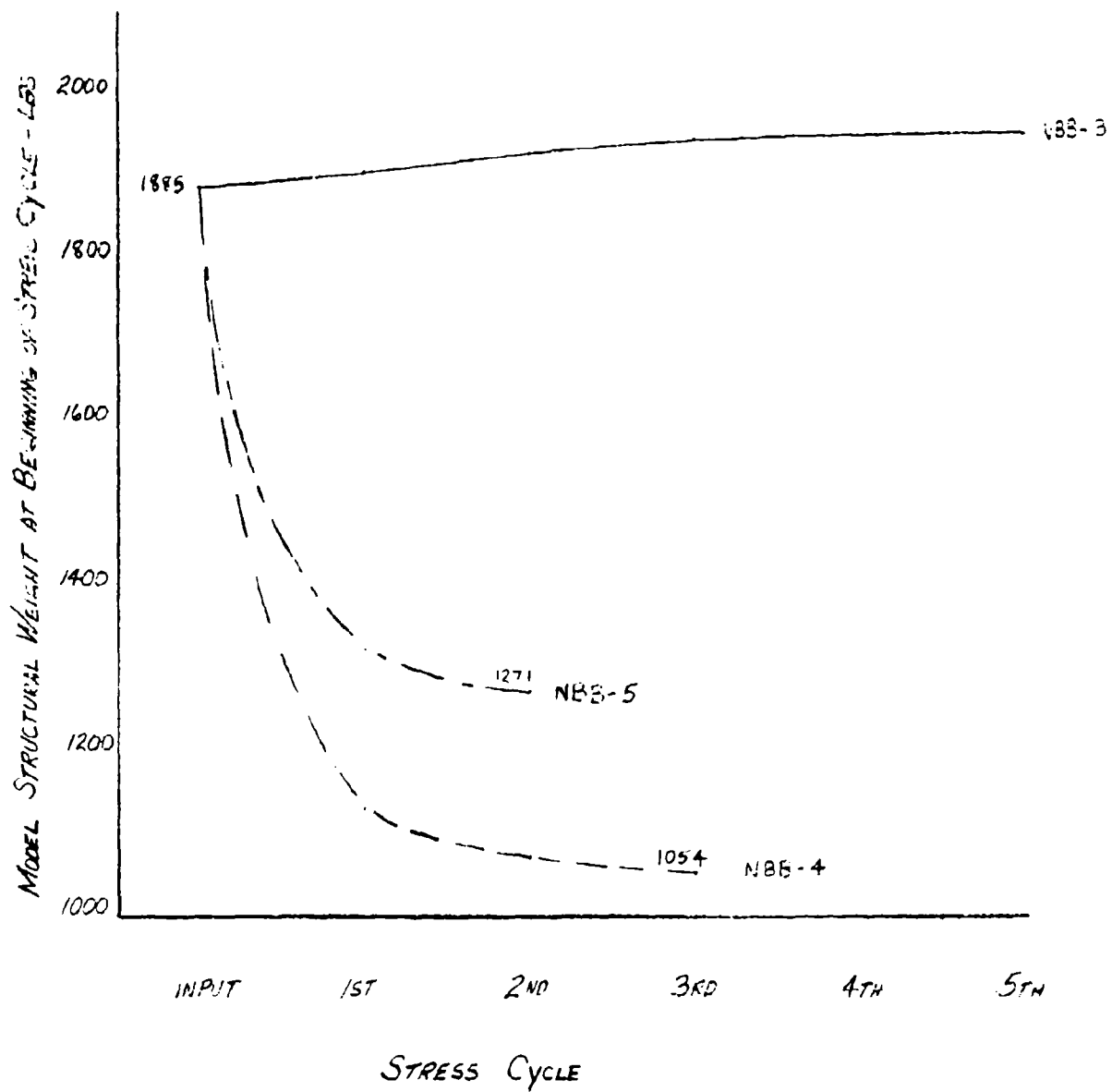


Figure 32 MODEL STRUCTURAL WEIGHT VS. STRESS CYCLE ITERATIVE SOLUTION

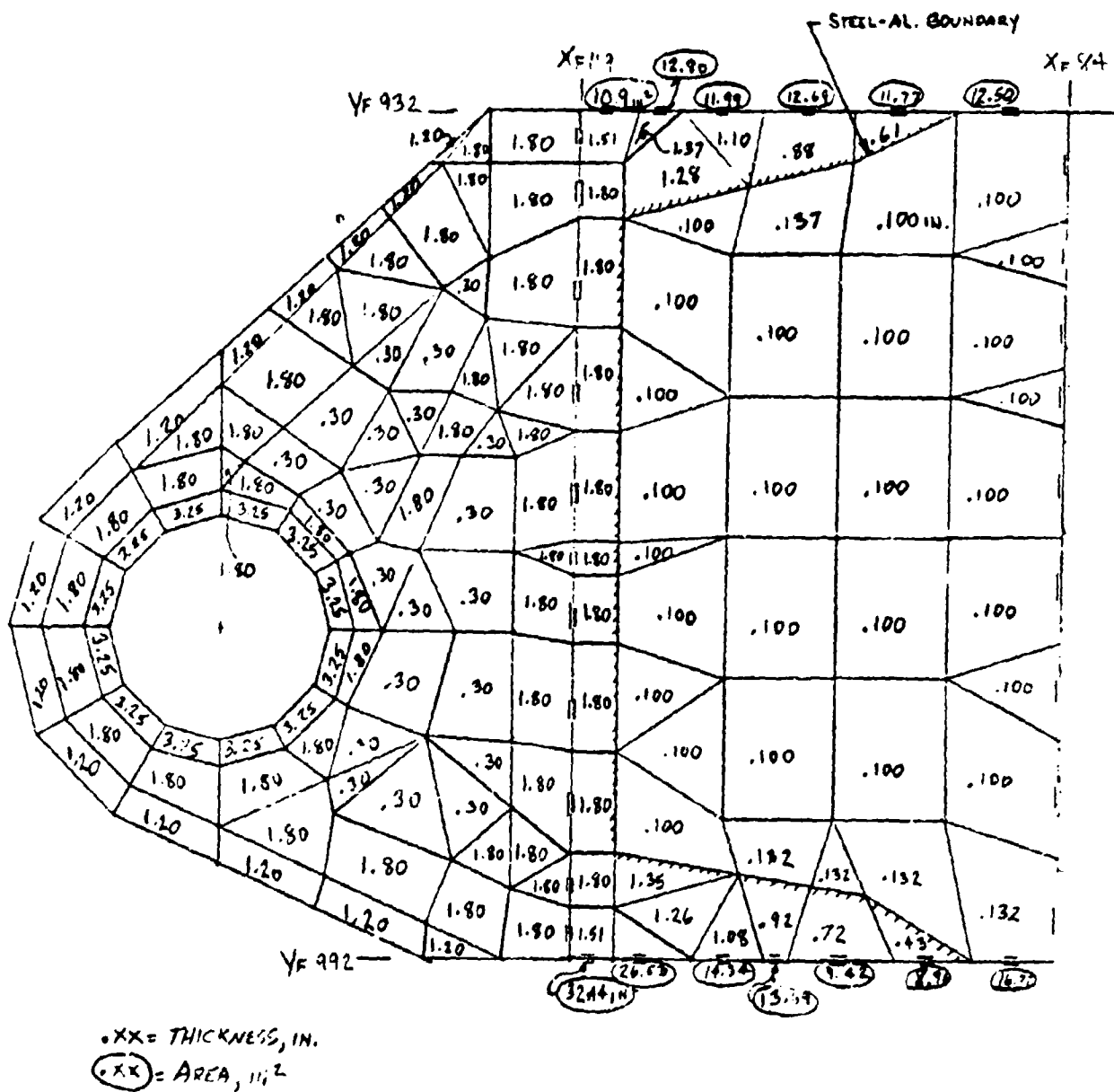
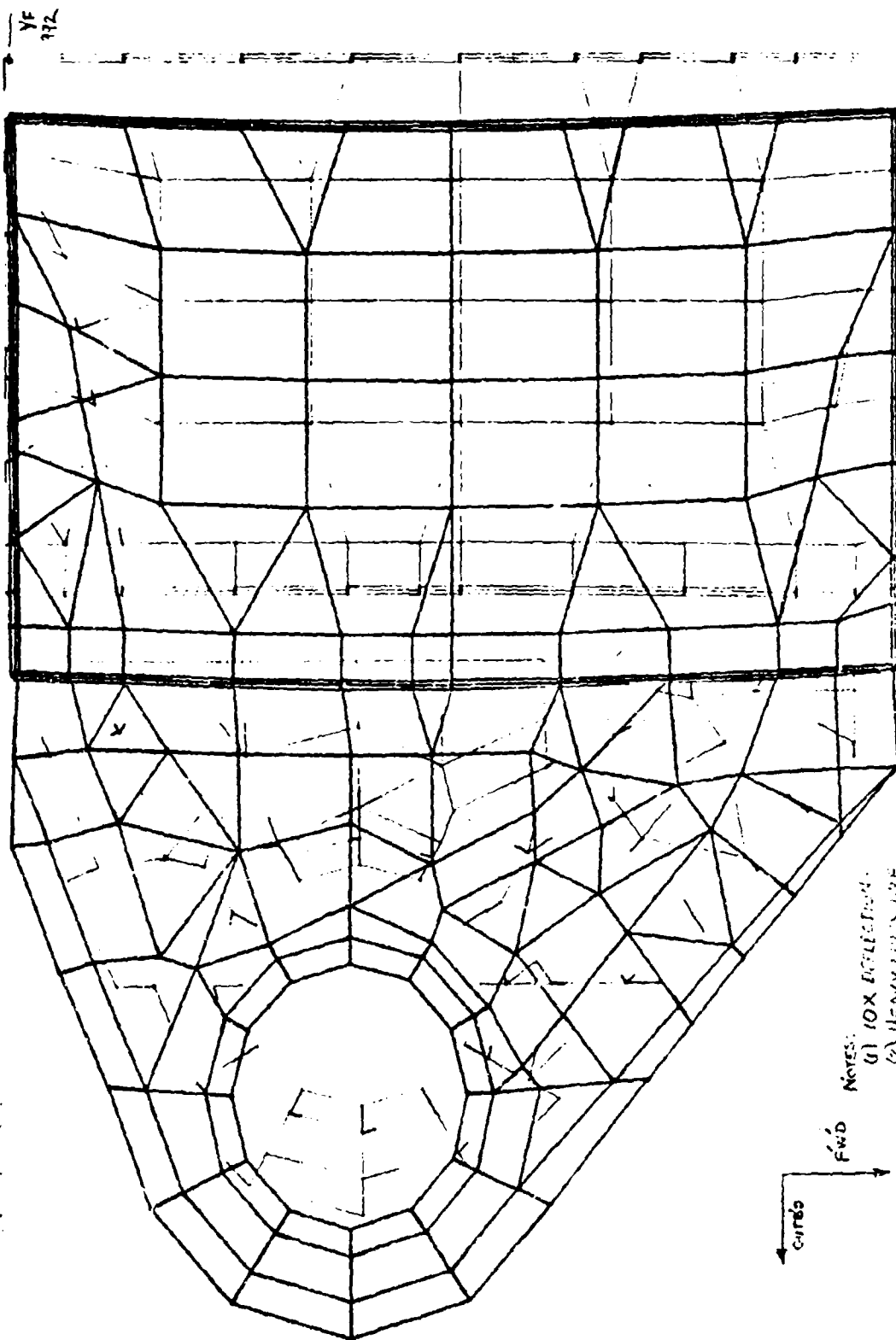


Figure 33 NBB-4 TR4 ITERATION, INPUT GAGES AND AREAS Z_{F0} LOWER PLATE

U.S. AIR FORCE
 AIR FORCE RESEARCH
 AND DEVELOPMENT
 DIVISION
 WRIGHT-PATTERSON
 AIR FORCE BASE
 OHIO 45433-6100



Notes:
 (1) 10X DEFLECTION
 (2) HEAVY LINES ARE
 DEFLECTION CURVE

Figure 35 LOWER SURFACE DEFLECTIONS - ASKA 2

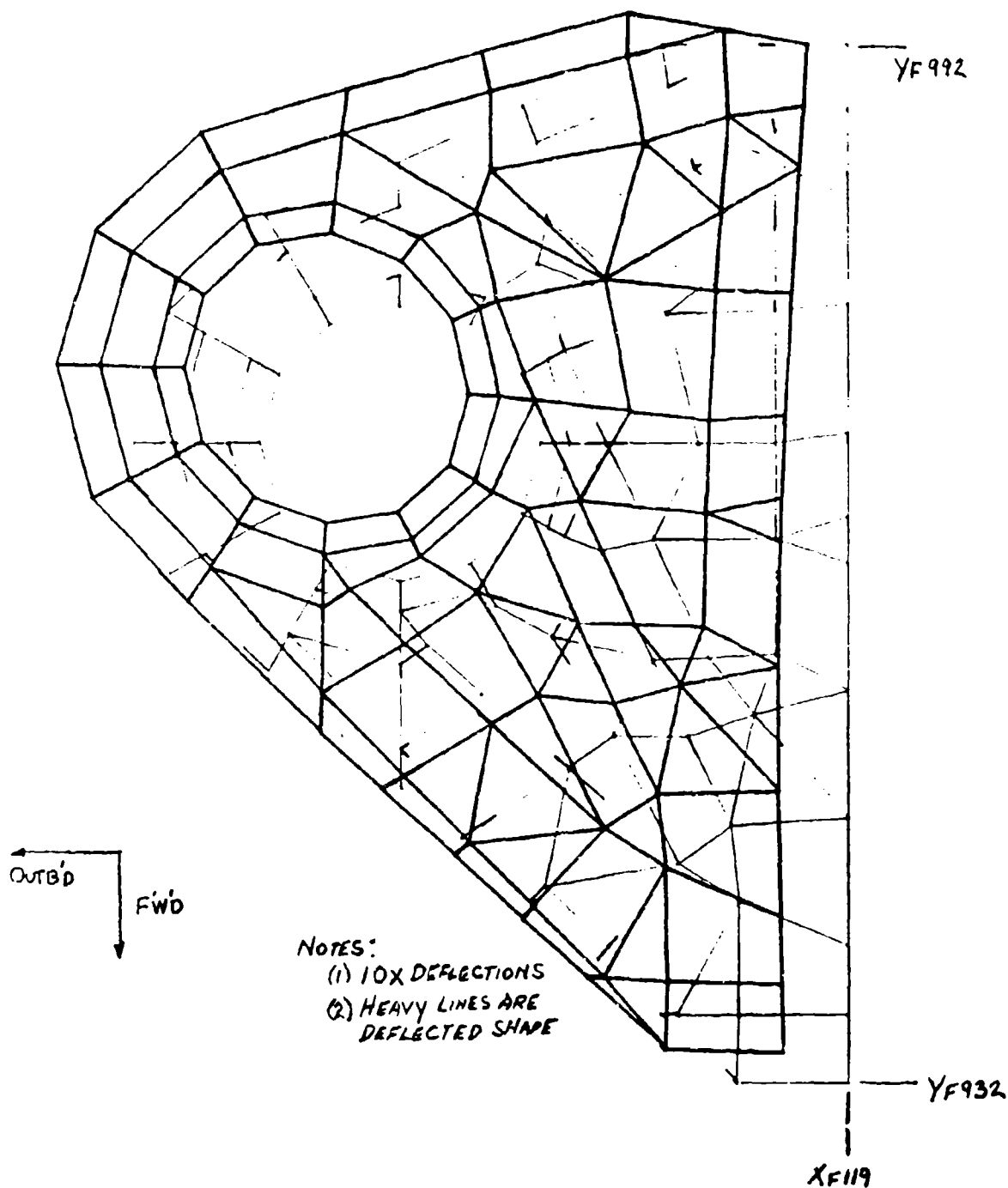


Figure 36 LOWER SURFACE DEFLECTIONS - ASKA 10

was that the weight was reduced considerably, apparently because the the load was spread fore and aft over the plate allowing the lug gages and the bulkhead cap areas at 932 and 992 to be reduced.

3. NBB-5

As a gross means of determining whether the weight reductions are primarily a result of more load being carried in the aluminum plate or of lug and bulkhead material removal, another run was made holding the aluminum constant at the values shown in Figure 33 with the steel portion allowed to vary during the resizing. This arrangement approximated the earlier design where all of the load was carried in the bulkhead caps in the outboard bay. Figure 32 shows that a considerable portion of the weight saving of 2 resulted from more efficient use of the steel since the weight saved for NBB-4 was 831 lbs while the weight saved for NBB-5 was 614 lbs.

4. NBB-6

The model was reconfigured to incorporate a four stiffener concept (15" - 10" - 10" - 10" - 15" spacing) needed to prevent compressive buckling in the outboard bay, X_{F84} to X_{F119} (See Figure 37). In addition, realistic minimum areas and gages for the rails, panels, and lug region were obtained. The iterative option of TR4 was set at 5 (6 cycles). It was found that the 0.20" steel panel (X_{F84} - X_{F119}) and rails were adequate at minimum gages and little iteration occurred. The .250 aluminum panel (X_{F39} to X_{F84}) increased to .30 to .50 required gage. The .187 aluminum inboard panel increased to .30" required gage. The analysis indicated that load was piled into the panel and removed from the rails. This situation required thick aluminum panels with unwieldy splices. A configuration appeared desirable that carried more load in the rails.

5. NBB-7

NBB-7 evolved from the results of NBB-6. In order to relieve load in the panels and to carry it in the rails, the X_{F84} to X_{F119} panel was reconfigured to incorporate a 9 stiffener gridwork with a .188 to .250 steel panel. In order to use the existing grid points to expedite the solution, the 9 stiffener areas were simulated with five stiffeners (9" - 10.5" - 10.5" - 10.5" - 10.5" - 9" spacing). All other structure was identical to NBB-6 including all minimum requirements. The model was allowed to iterate 3 times (4 cycles). See Figure 38 for stiffener arrangement.

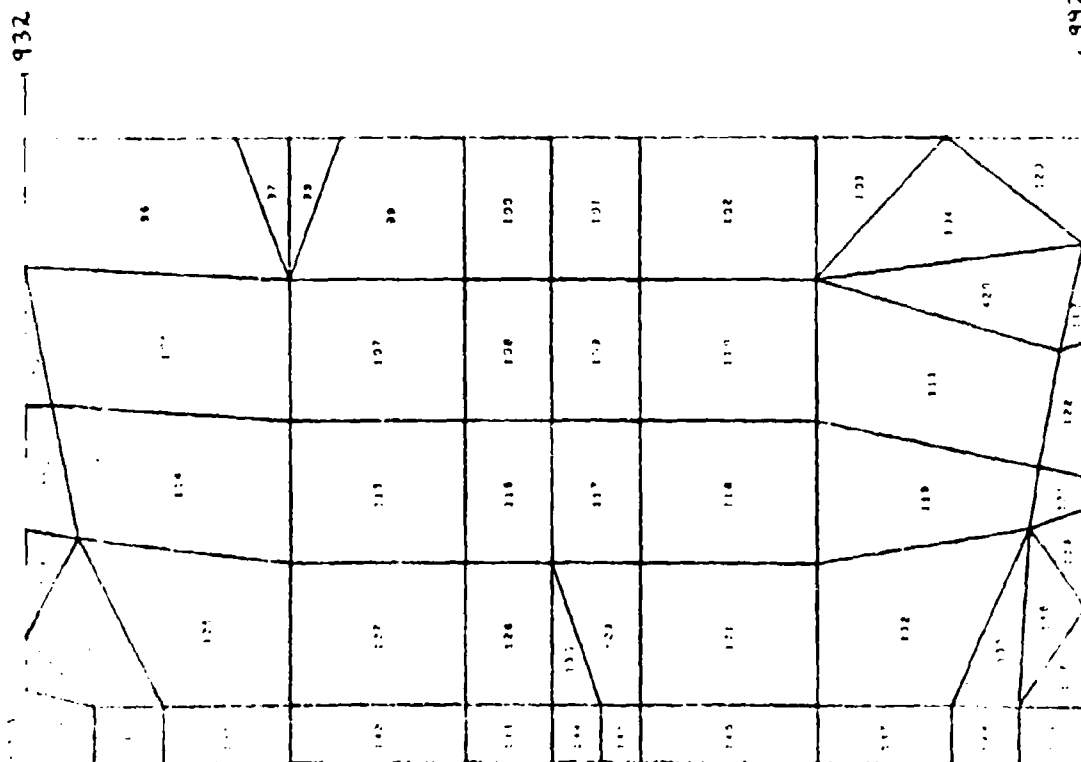
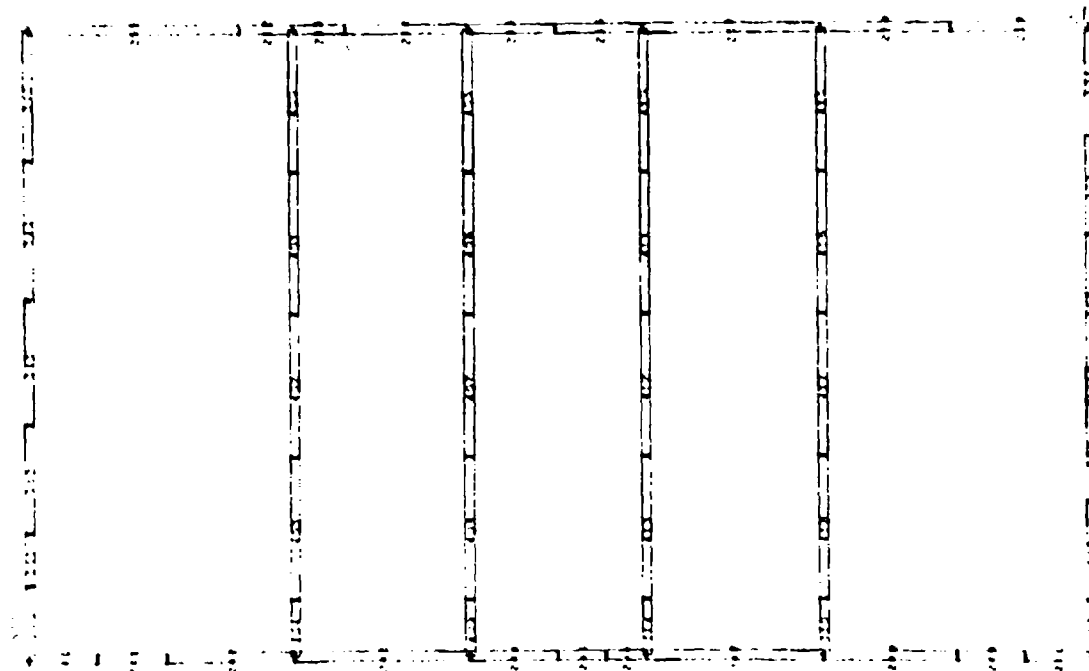


Figure 37 NBB-6 BAR AND PLATE ARRANGEMENT

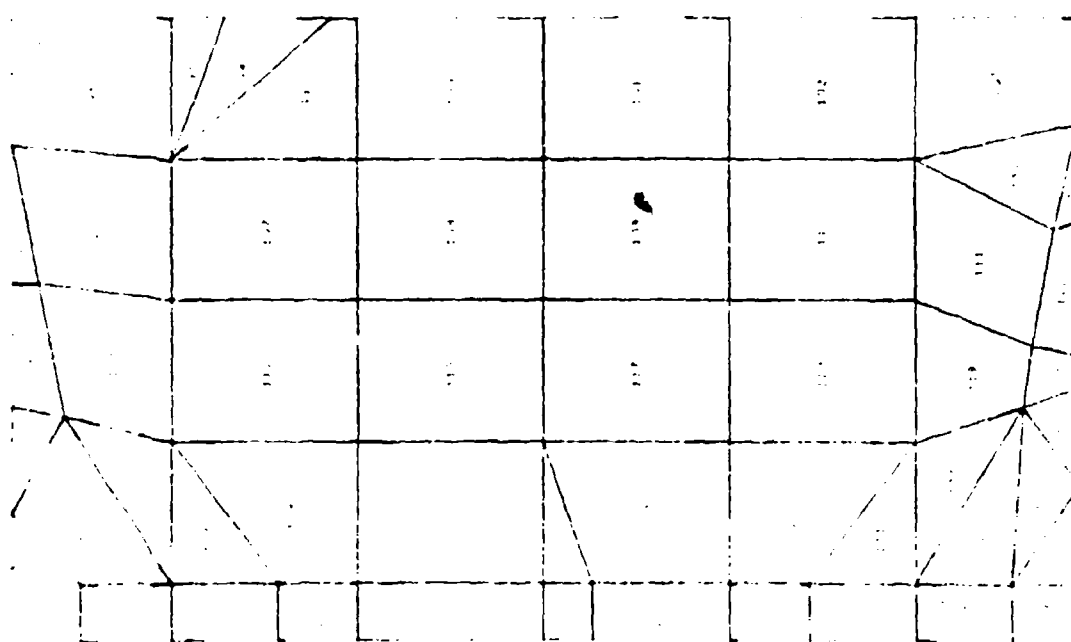
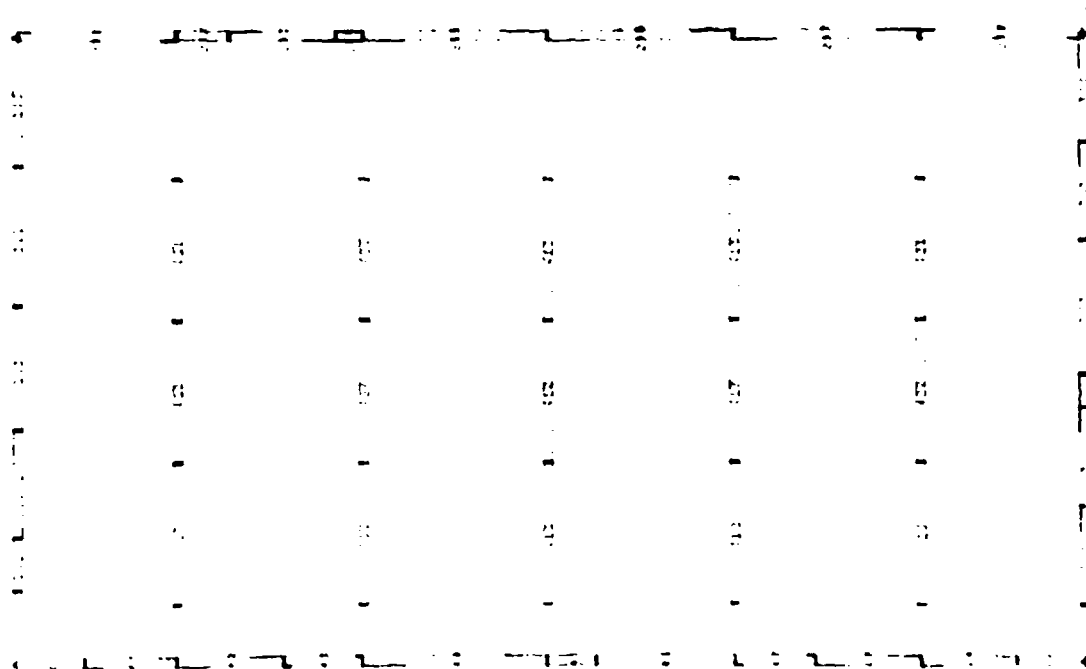


Figure 38 NBB-7 BAR AND PLATE ARRANGEMENT

The results were very similar to NBB-6; i.e., high panel loads and low rail loads. Thick aluminum panels were required inboard of $X_F 84$ with gages on the order of .30" to .50". NBB-7 also indicated the need for a thick aluminum panel inboard of $X_F 84$ which was not desirable from a manufacturing standpoint (unwieldy splices).

6. NBB-8

As a final attempt at a more efficient structural arrangement, NBB-7 was modified by incorporating a titanium panel inboard of $X_F 84$. The titanium panel inboard of $X_F 84$ allowed a 10 to 15 percent increase in rail loads. In addition, the required panel gages ranged from .100" to .200". This result indicated that a honeycomb panel was feasible from $X_F 0$ to $X_F 39$ and that plate structure could be utilized from $X_F 39$ to $X_F 84$ to tie in the landing gear drag brace structure. In addition, this structural arrangement produced the lightest computer-idealized structure for a realistic set of minimum sizes, Figure 39.

Updated Finite Element Overall Model - A large portion of the overall model was resized on the basis of results from the math model runs NBB-1-1 and 1-2. Design changes such as substitution of aluminum for titanium panels were incorporated.

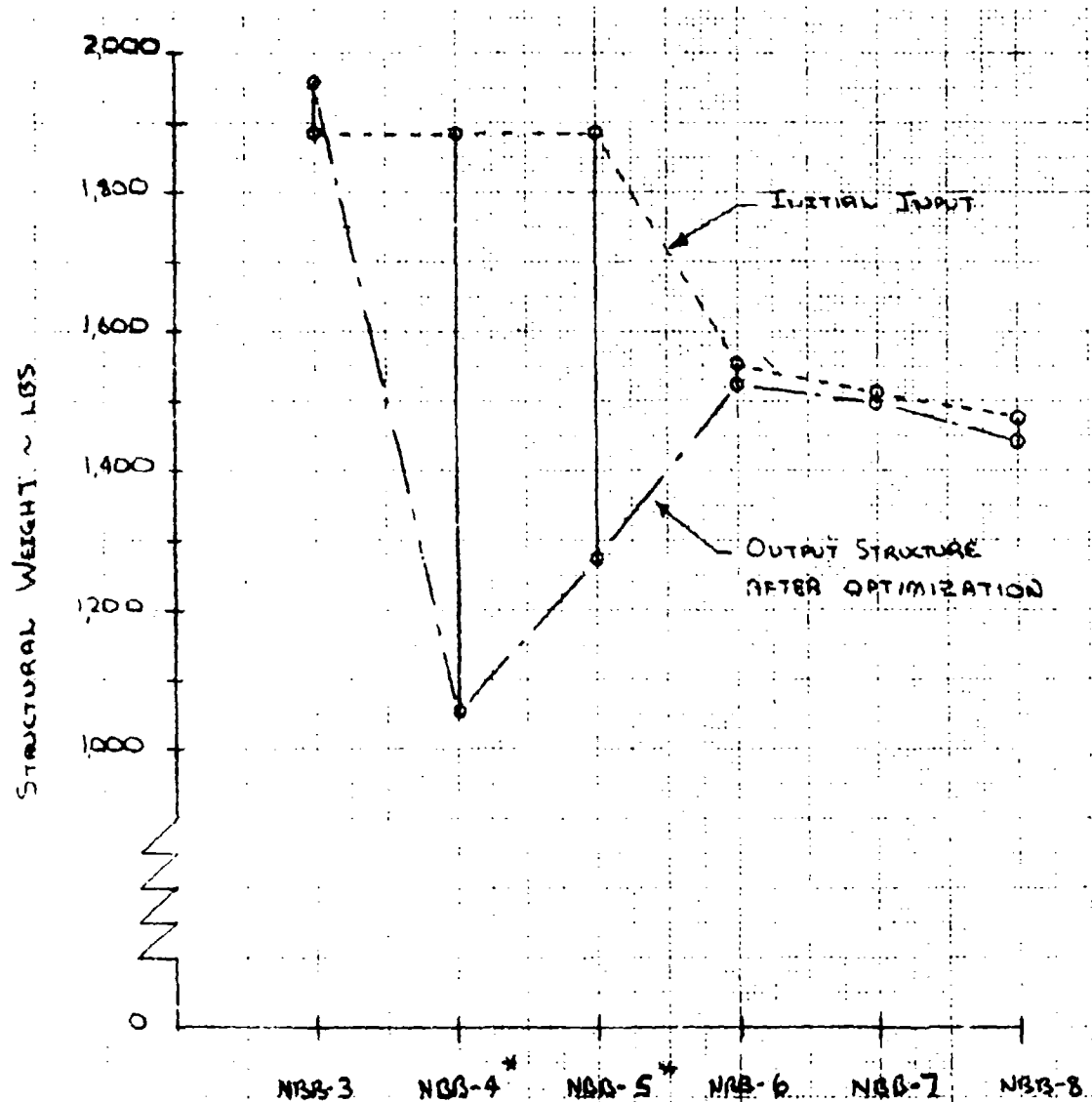
The model was revised to eliminate the step between the upper lug and upper panel at $X_F = 84$. This change will, with the use of orthotropic plate elements, make the evaluation of the magnitude of load transfer across the step possible.

Revision of the model to incorporate a lower plate at $Z_F = 0.0$ is in progress. This revision is extensive.

Upper Lug Buckling Study - A finite element model of the upper lug and cover (inboard to $X_F 84$) was run using Convair buckling analysis program A3S. This model utilized titanium as the material and was patterned after the FSRL upper lug design. The loads used were derived from the "No Box" Box TN1 model for condition ASKA 10.

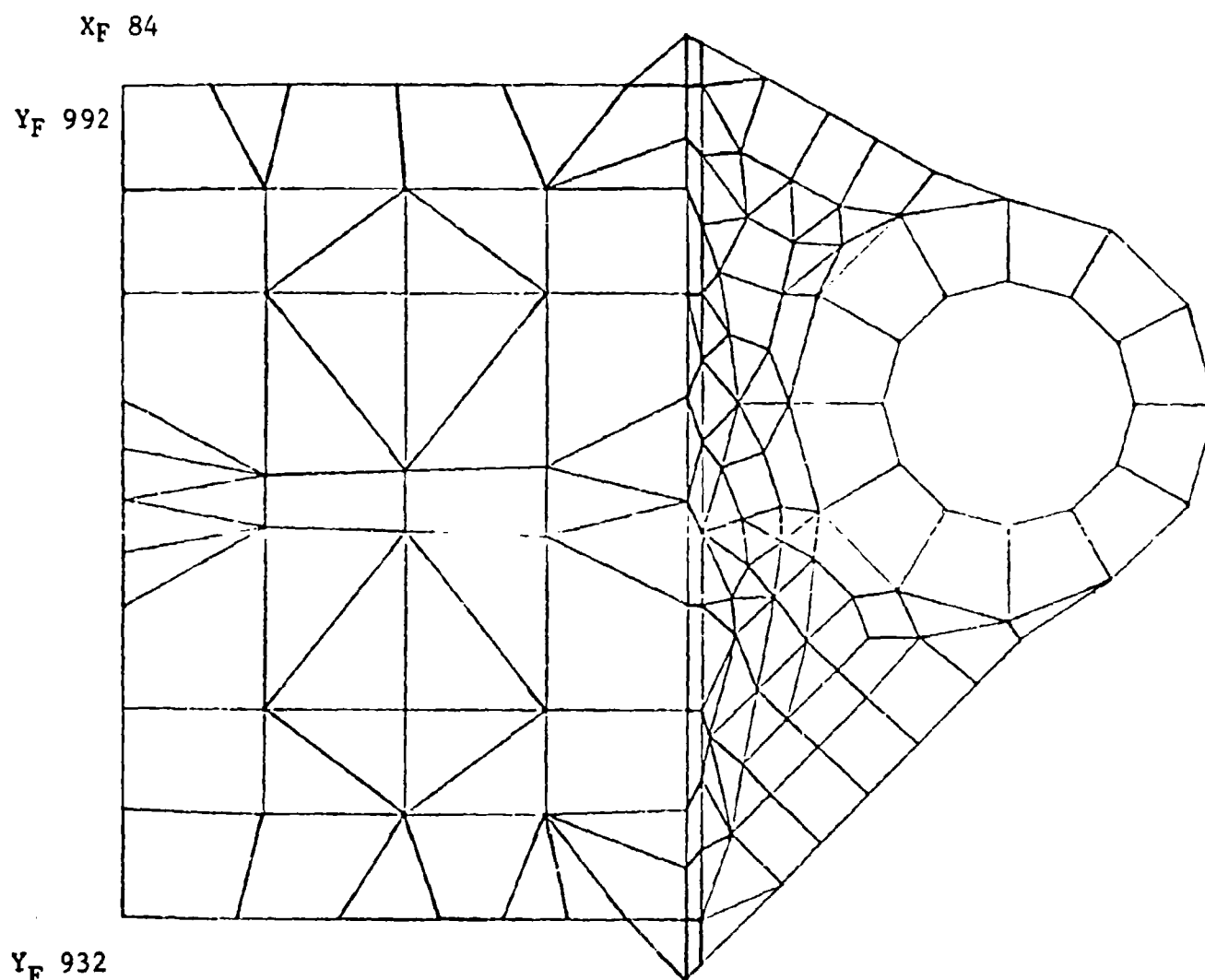
A plot of the arrangement of elements for this model is shown in Figure 40. The buckling mode shape is delineated in Figure 41.

The buckling ratio for this run was 0.941. This value is comparable to the buckling ratio (0.947) obtained earlier on the



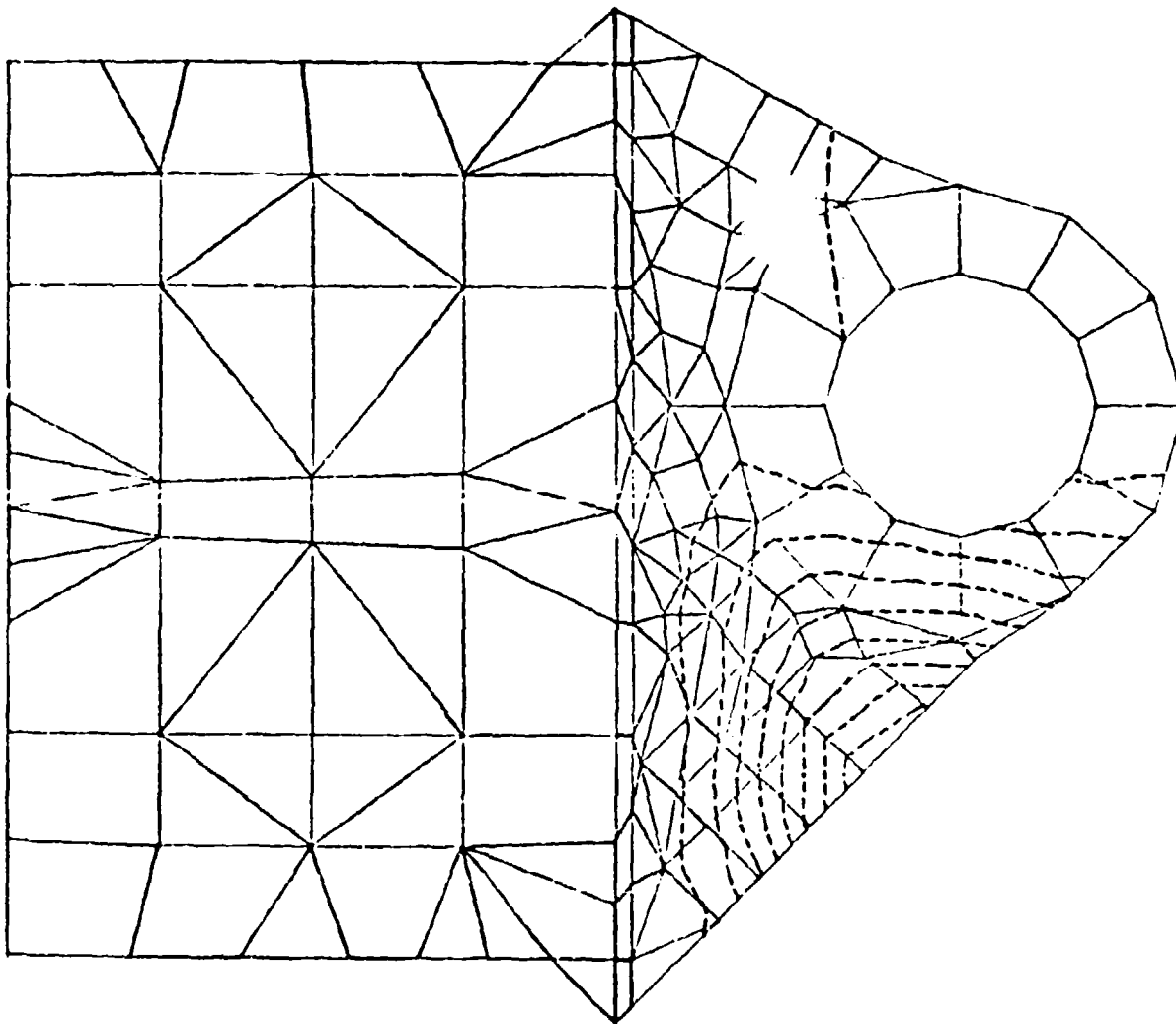
* QUALITATIVE STUDIES INVESTIGATING EFFECTS OF MINIMIZING STEEL AND ALUMINUM STRUCTURE

Figure 39 'NO BOX' BOX OPTIMIZATION STUDIES FOR LOWER PLATE CONFIGURATION AT $Z_F 0$



*** ELEMENT PLOT ***

Figure 40 "NO BOX" BOX UPPER LUG AND COVER - A3S BUCKLING MODEL



CONTOURS FOR BUCKLED MODE SHAPE

Figure 41 "NO BOX" BOX UPPER LUG AND COVER - BUCKLED MODE SHAPE FOR
CONDITION ASKA 10

10 Nickel steel "No Box" Box upper lug model (A3S computer run 177480A). This comparison indicated a possible weight saving through the redistribution of material to more closely approximate the FSRL upper lug thickness distribution.

Landing Gear Backup Structure - Loads and stress analysis were provided during the layout of the additional backup strut for the MLG side brace fitting which is required if the lower plate is below $Z_F = 0$.

Test Item - Stress data for component test planning was provided as required.

Model Data Transfer - Information concerning the "No Box" Box finite element model was furnished to AFFDL personnel as an aid to their model set up. The data furnished included computer generated geometry plots, a magnetic tape of the NBB-1 overall model input data, material properties, load and coordinate axes information, and miscellaneous drawings.

3.1.2.3 Simulated Fuselage

Math Model - As discussed in AFFDL-TR-73-40, several model iterations were made to obtain stiffnesses that gave loads applied to the carrythrough box as close to those from NARSAP as possible. The latest results at FM992 for plates including axial load capacity are shown in Tables III-2 and III-3 of AFFDL-TR-73-40. Although the results are mixed as compared with NARSAP, reasonable agreement was obtained in the more highly loaded areas.

Subsequent to running the axially loaded plate model, it was decided; because of extensive calculated plate buckling, offset plate load paths, and excessive effective widths of simulated fuselage acting to pick up loads which should have been in the box cover; that a run should be made with the plates carrying shear loads only. Such a model was run and the results are shown in Tables 10 and 11 which compare the results with NARSAP results. As in the case of panels carrying axial load, the results were mixed with the agreement with NARSAP being better in some cases and poorer in others. The amount of wing bending moment carried in the box did increase to nearer NARSAP values.

The model is currently being revised to include area and gage changes found to be necessary during the stress analysis. In addition, the carrythrough structure in the model is being updated to reflect the current design. The FSIL box is to be simulated first, followed by the NBB.

Table 10
PANEL SHEAR FLOW'S
LBS./IN

SHEAR FLOW	ASKA 2		ASKA 4		ASKA 5		ASKA 7		ASKA 9		ASKA 10		ASKA 11	
	CONVAIR	NARSAP	CONVAIR	NARSAP	CONVAIR	NARSAP	CONVAIR	NARSAP	CONVAIR	NARSAP	CONVAIR	NARSAP	CONVAIR	NARSAP
1	-635	-357	99	126	-332	-166	+232	-169	-644	-262	-881	-174	-237	40
2	+343	-68	-102	-137	442	12	-686	-674	+373	-4	+418	236	75	-74
3	-662	-973	55	326	-658	-764	-1099	-1099	-249	-540	+1847	1514	26	85
4	-2172	-1782	808	929	-1844	-1797	-583	-1006	-1917	-1867	-2033	-2241	173	346
5	-2367	-1782	870	763	-1995	-1476	-613	-826	-2100	-1533	-2222	-1841	167	284
6	+ 19	42	-90	-173	218	106	-859	-689	+101	100	+156	356	1	-76
7	-1529	-1444	310	509	-1080	-1053	-750	-819	-1330	-1282	-1204	-1450	-126	86
8	+1122	419	-399	92	954	388	+671	1000	+906	283	+740	-96	-149	111
9	+595	-409	-192	-4	545	-230	+ 88	26	+523	-323	+549	-293	-36	-44
10	-9	1010	124	-66	-103	689	+301	4	-36	818	-60	743	90	88
11	+419	-405	-71	172	163	-440	-695	-709	+356	-374	+378	-552	-21	40
12	+17	-287	-4	167	19	-265	-48	-346	+15	-230	-24	-326	8	134
13	+449	-194	-145	17	181	-250	-598	-470	+404	-200	+526	-215	-80	-99
14	+4293	77	-2468	-1018	4875	855	-753	-289	+3421	-695	-677	-5101	-695	-1557
15	-1404	5925	2232	-637	-3494	3009	+2941	4111	-742	5767	+6381	12102	784	713
16	17028	4911	-3625	-1967	7256	3975	+336	2522	+5793	4145	+1922	4769	-1068	-938
17	-7169	-4960	1775	1480	-5439	-3560	-826	-2510	-6834	-4990	-8935	-8820	-657	-330
18	+1533	102	-526	-200	1464	123	-2834	-1600	+1075	-73	-1628	-1214	-50	-270
19	-5573	-2020	1412	-282	-5331	-2595	+1921	3236	-4736	-1426	+1229	7720	-972	-188
20	-722	-98	-53	-99	-619	-196	+269	44	-588	-88	+1055	624	-559	-272
21	-777	-184	187	-185	-804	-367	-32	84	-656	-165	+429	1167	-230	-509
22	+2	-314	14	124	-31	-224	-126	-534	+4	-260	+44	-478	3	111
23	-606	-361	226	-65	-910	-653	+12	-163	-478	-341	+1097	868	-232	-484
24	-677	-297	67	6	-555	-365	+530	738	-550	-268	+15	428	-140	-260
25	+707	850	-111	-224	381	483	+1345	844	+647	746	+1495	1339	-39	-124
26	-731	-614	173	155	-400	-125	+229	-17	-632	-321	-912	-629	-92	195

NOTES: (1) PANELS CARRYING ONLY SHEAR

(2) SEE FIGURES 42 & 43

Table 11
LONGERON - FORE AFT COMPONENT
KIPS

NODE	ASKA 2		ASKA 4		ASKA 5		ASKA 7		ASKA 9		ASKA 10		ASKA 11	
	CONVAIR	NARSAP	CONVAIR	NARSAP	CONVAIR	NARSAP	CONVAIR	NARSAP	CONVAIR	NARSAP	CONVAIR	NARSAP	CONVAIR	NARSAP
141	166	198	10	2	102	151	46	76	139	160	101	79	66	49
146	-233	-216	38	34	-189	-170	-99	-87	-196	-181	-178	-168	-20	-12
148	-278	-234	58	43	-228	-197	-111	-110	-234	-195	-202	-164	-12	-13
150	-89	-103	33	78	-88	-95	-16	-30	-76	-84	-83	-77	17	5
157	232	99	-107	-57	194	76	4	26	231	103	421	291	-32	-36
162	202	256	-32	-50	209	235	176	125	135	198	-60	39	-19	7
256	334	336	-60	-60	245	226	228	213	291	290	341	364	21	6
257	30	17	-3	-2	26	14	-7	1	23	14	4	2	5	3
258	3	4	3	2	-1	1	1	-4	3	4	3	7	3	4
259	259	245	-50	-41	195	170	183	186	226	216	241	263	20	18
260	87	83	-11	-15	60	56	44	28	75	72	84	78	7	6
262	67	65	0	-6	36	41	47	45	60	58	75	60	16	12
266	113	39	-17	-4	86	17	63	59	109	41	119	103	22	6
267	171	308	-69	-128	26	189	213	261	215	329	1001	921	-75	-43
275	-590	-743	11	134	-270	-426	-399	-470	-579	-707	-1253	-1324	-84	-37
282	-308	-263	121	89	-250	-205	-225	-213	-279	-237	-431	-364	37	23
286	-165	-90	74	30	-155	-83	-142	-104	-145	-82	-184	-111	28	2

NOTES: (1) PANELS CARRYING ONLY SHEAR

(2) SEE FIGURES 42 & 43

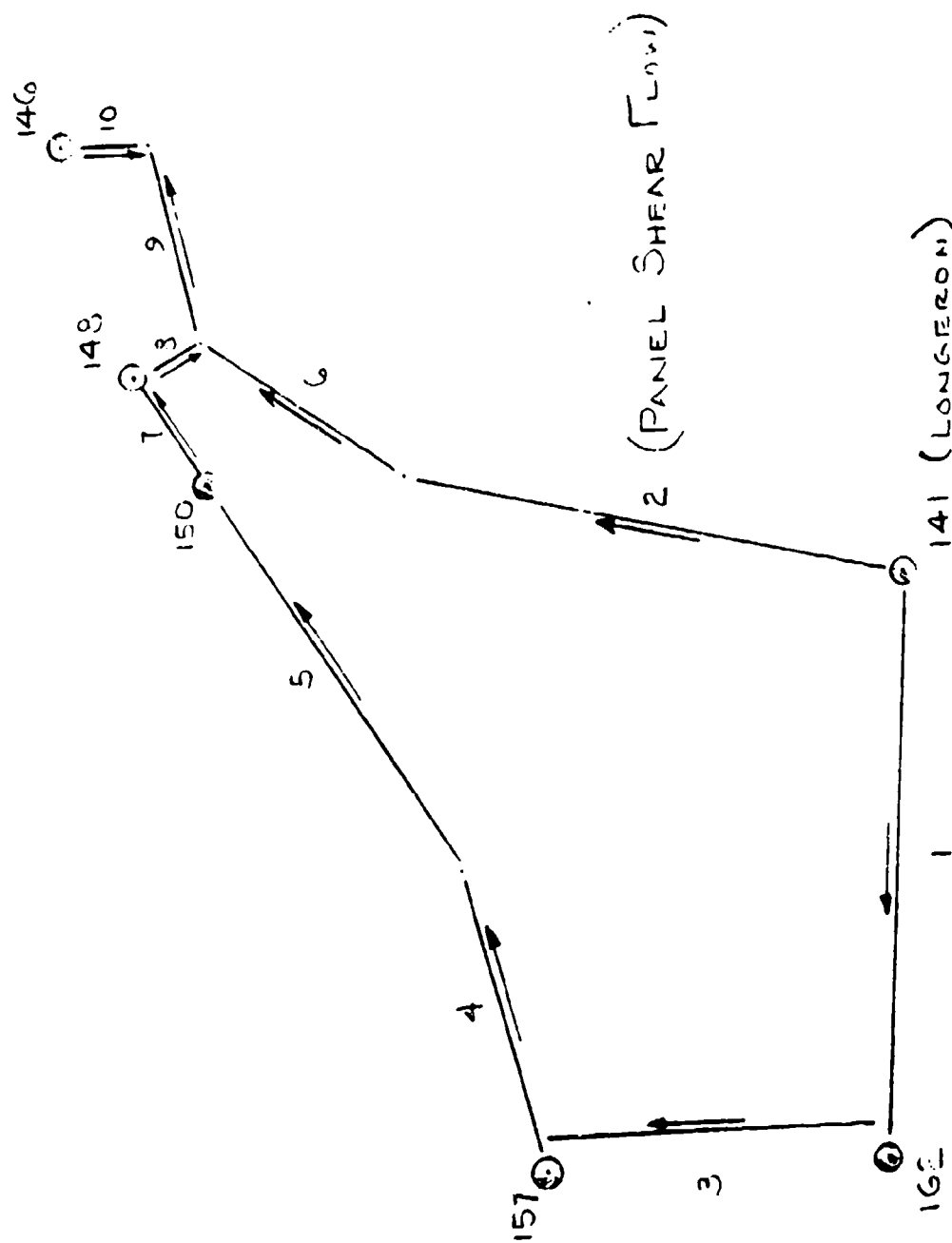


Figure 42 SECTION FORWARD OF STATION YF 992

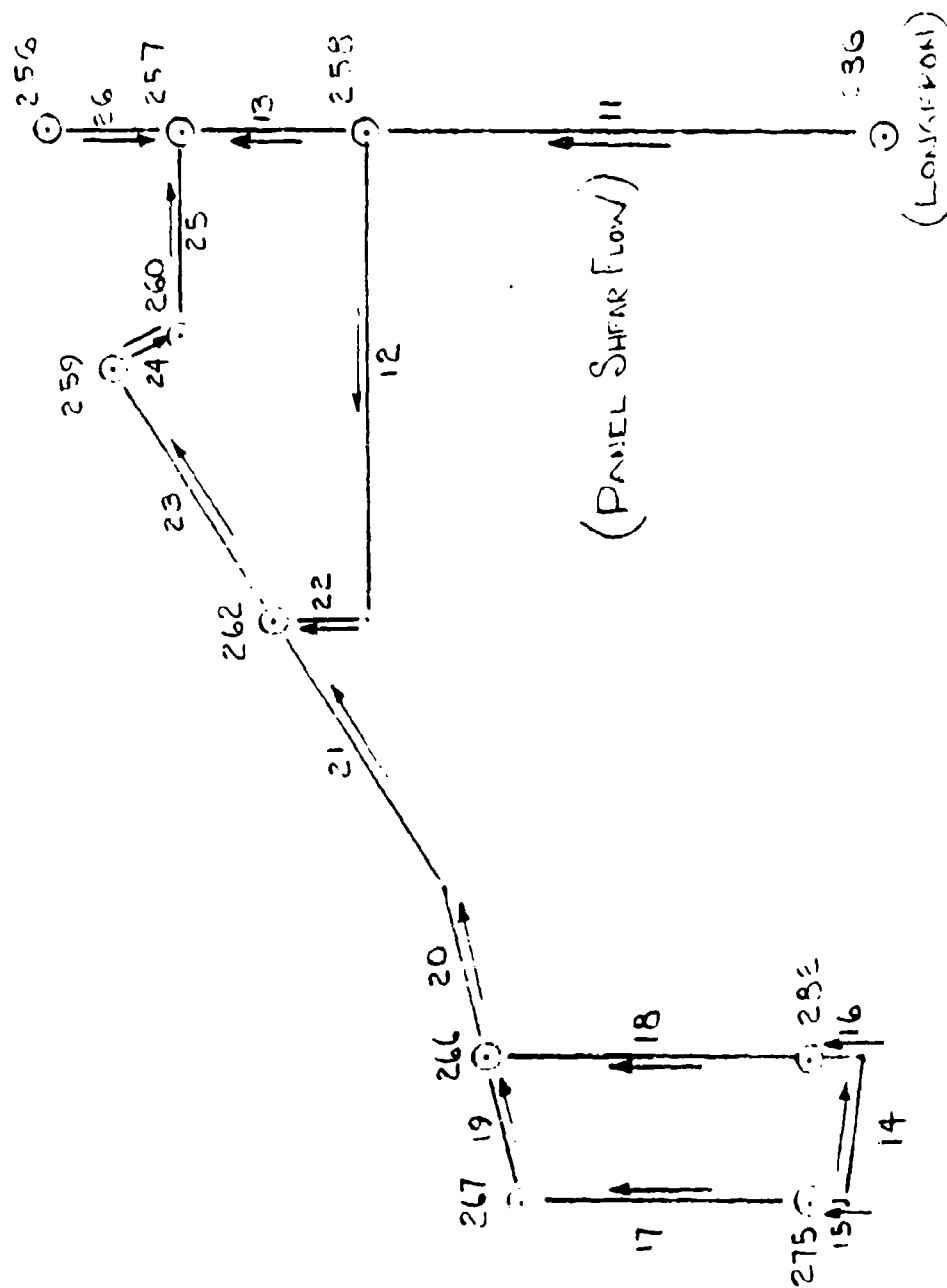


Figure 43 SECTION AFT OF STATION YF 992

Detail Stress Analysis - Analysis of the simulated fuselage drawings was started and is in progress. It was found that the original design would buckle at relatively low load levels so various stiffener and frame arrangements were studied and increased gages were determined such that buckling would not occur during fatigue testing. In order to provide increased fatigue resistance, longeron areas were increased where necessary to reduce stress levels. Preliminary analysis of various joints were accomplished.

Model Data Transfer - A deck of TN1 input data cards was furnished to AFFDL for running the model on ASOP.

3.1.2.4 Miscellaneous

Design Review Support (May, 1973)

Papers covering efficient computer usage for preliminary design and fail safe brazed structure were prepared and presented at the design review.

Computer Items

1. Programs TR4 and TN1 were modified to allow tape storage of joint displacements along with other output data. A program was written to allow SC 4020 plots to be made from the stored displacement data. Examples of the plots are shown in Figures 35 and 36
2. An IBM version of NASTRAN became available and indications are that the system charge time at Convair will be less than for the CDC version. The buckling studies previously discussed are being conducted using the IBM version. The IBM version has enough capacity to both restart and retain data for plotting.

3.1.3 Fatigue and Fracture Analysis

The fatigue and fracture analysis requirements for the AMAVS program are essentially the same as those specified for the base-line aircraft. The fatigue loads spectrum, the fatigue life requirements and the fracture analysis requirements are outlined in AFFDL-TR-73-1, the first 6-month interim report.

During this reporting period, most of the effort was directed toward reducing the results of the materials and component test programs to a form suitable for WCTS design. In addition, work was continued on the development and application of finite element fracture analysis procedures. Results to date are summarized in this section.

Significant effort was also directed toward the preparation of a Fracture Control Plan and a Component Test Plan. These plans were published as FZM-6068 (1 February 1973) and FZM-6054 (April 1973), respectively and will not be covered herein.

3.1.3.1 Fatigue Analysis - Preliminary fatigue allowables were determined for each WCTS configuration using the results of the stress analyses, the fatigue loads spectrum and available S-N data. The procedures employed and the preliminary results are presented in AFFDL-TR-73-40, the Phase Ib Preliminary Design Summary Report. Except for the FSRL lug, these allowables are still being used. Further analyses will be conducted upon completion of the stress analysis of the two WCTS configurations selected for detail design.

A revised fatigue allowable was developed for the FSRL lower lug using the lug analysis procedure and the S/N data for beta annealed 6Al-4V titanium reported in AFFDL-TR-73-40. The fatigue analysis results, shown in Figure 44, indicate an allowable of 78 ksi. The analysis procedure was validated by results of the first 3/8 scale lug test, 603FTB004. This specimen had a net section stress of 73 ksi and developed fatigue cracks after 6 lives of cycling. The second specimen was damage tolerance tested after 4 lives of fatigue cycling. Since cracks did not develop during the four lives, only partial validation of the fatigue analysis was obtained.

3.1.3.2 Crack Growth Analysis - Crack growth analyses based on linear elastic fracture mechanics are being conducted to determine the safe crack growth characteristics of the WCTS in accordance with the Baseline Fracture Mechanics Design Requirements. The

Ti 6Al-4V (β , MA)
 ALL NEGATIVE STRESSES SET = 0
 $K_T = 5$

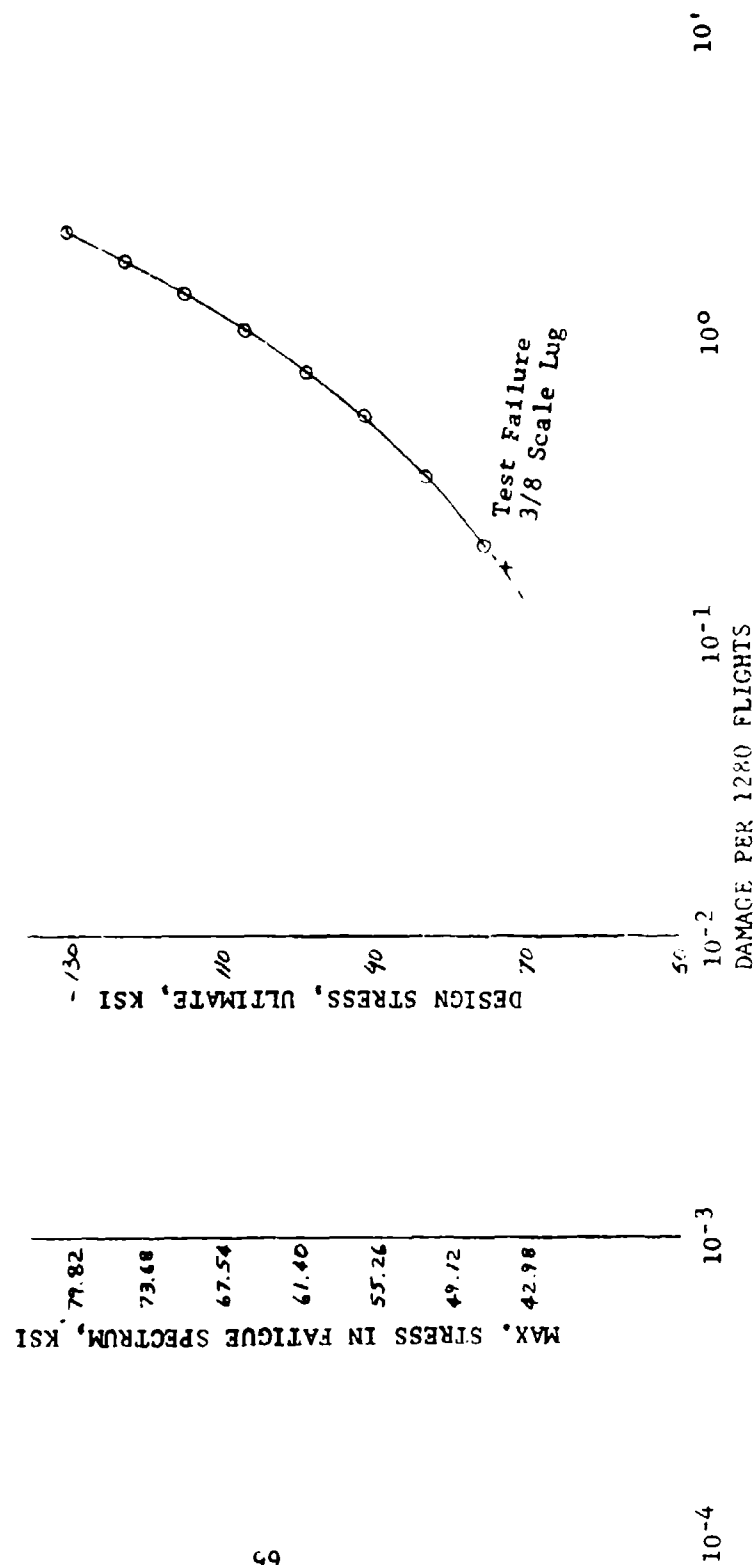


Figure 14 F5RL LOWER PLATE LUG

analyses are based on constant amplitude fatigue crack growth data developed for each of the materials selected for primary structure. Spectrum retardation and environmental effects are accounted for by use of the Wheeler crack growth model, Reference 1. The empirical parameter, m, needed to tune the Wheeler model for the case of interest is determined by correlation of spectrum/ environmental test results and analysis results using a series of m values. The m that leads to the best correlation of test and analysis is then used to determine the crack growth behavior of the WCTS.

3.1.3.2.1 Constant Amplitude Fatigue Crack Growth Data - The test plan and current status of the constant amplitude fatigue crack growth tests are shown in Table 12. The test data for 10 Ni steel and for beta annealed 6Al-4V titanium have been reduced to a form suitable for analysis. Testing on Beta C has just started, therefore, the appropriate equations have not yet been derived.

10 Ni Steel

The 10 Ni steel data have been expressed as Forman equations having the following form:

$$\frac{da}{dN} = \frac{C(\Delta K)^n \gamma}{(1-R)^{200-\Delta K}}$$

Where $\frac{da}{dN}$ = Crack growth rate

ΔK = Stress intensity range

γ = Environmental factor

R = Load ratio, Min load/max load

C, n = Empirical parameters

The empirical parameters used to fit the test data are summarized below:

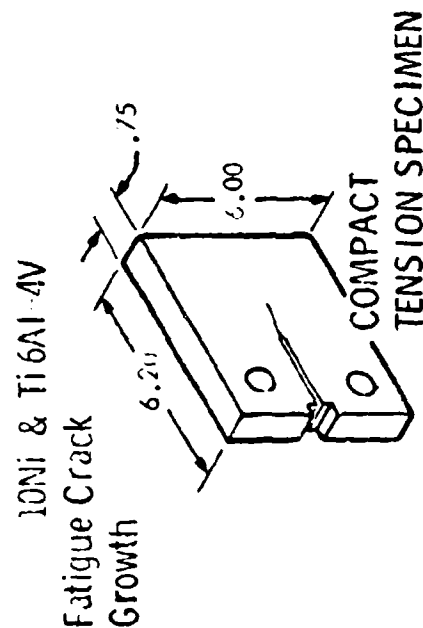
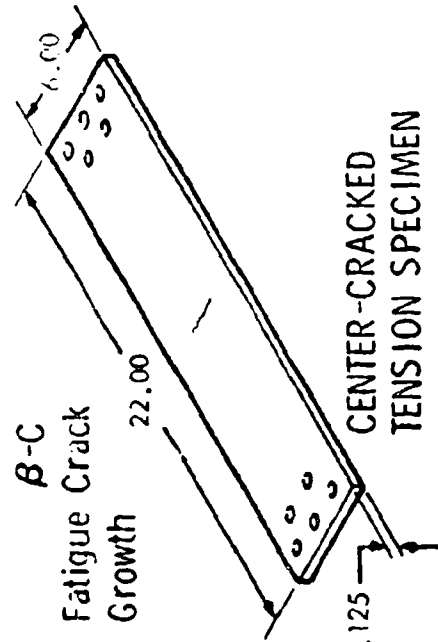
Stress Intensity Range		Parameters		Environmental Factor,		
R	ΔK Range	C	n	** DA	*** STW/6	*** STW/60
$R \leq 0.5^*$	$\Delta K < 15$	4.34×10^{-8}	3.3	1	1	1
$R \leq 0.5^*$	$\Delta K > 15$	2.94×10^{-6}	2.0	1	2	1.5
$R > 0.5$	All ΔK	2.52×10^{-7}	2.2	1	2	1.5

*For $0.3 < R < 0.5$, let $R = 0.3$ in Forman Equation.

Dry Air *Sump tank water, 6 cpm or 60 cpm as shown.

Table 12 FATIGUE CRACK GROWTH TESTS

MATERIALS	ENVIRONMENT	LOAD RATIO	CYCLIC FREQUENCY	GRAIN DIRECTION	NUMBER OF TESTS
ALL	↓	0.1	FAST	RW	2
ALL	↓	0.3	↓	↓	1
ALL	↓	0.5	↓	↓	1
β-C, 10Ni	↓	0.7	↓	↓	1
β-C, 10Ni	↓	0.1	6	RW	1
ALL	↓	0.5	6	↓	1
ALL	↓	0.1	60	↓	2 (2 Heats)
ALL	↓	0.5	↓	↓	1
β C, 10Ni	↓	0.1	↓	WR	2 (2 Heats)
β-C, 10Ni	↓	0.1	↓	TR	1
Ti6Al 4V	↓	0.1	↓	↓	1



FW 7-22-1-16 0739
ES 412 73

The analytical curves are shown with the test data in Figures 45 and 46. Note that for the $R = 0.1$ tests in sump tank water, there is a significant reduction (relative to corresponding tests in dry air) in growth rates at ΔK levels below about $20\text{ksi} \sqrt{\text{in}}$. The reduced growth rates are attributed to rust deposits on the fracture surface limiting the crack opening displacement range.

Beta Annealed 6Al-4V Titanium

The beta annealed 6Al-4V titanium data have been expressed as Paris equations having the following form:

$$\frac{da}{dN} = C(\Delta K)^n$$

The analytical curves are shown with the test data in Figures 47 and 48.

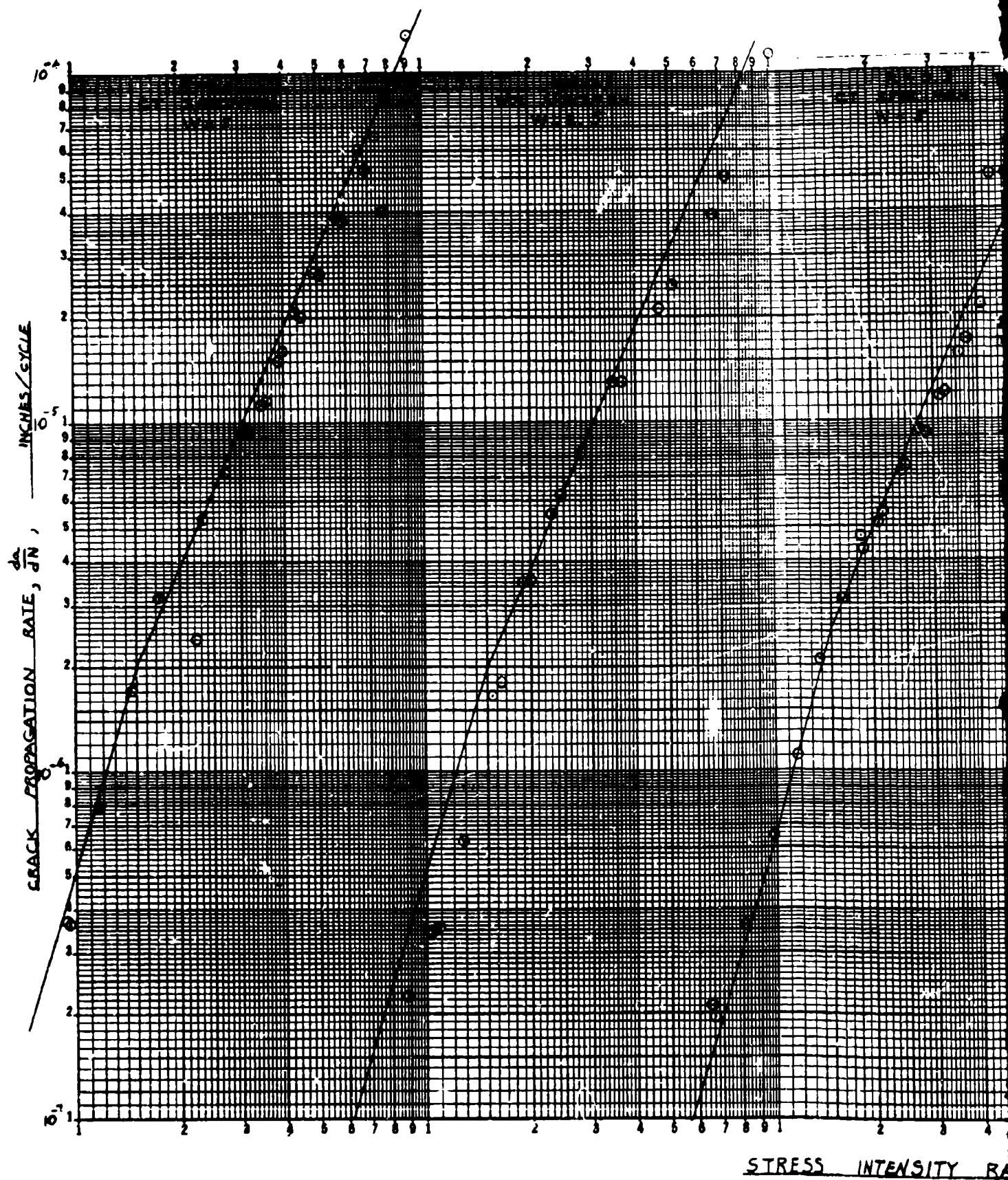
3.1.3.2.2 Spectrum - Environmental Crack Growth Tests - The test plan and current status of the spectrum environmental crack growth tests are shown in Table 13. Crack growth analyses based on the Wheeler model have been conducted to develop an analytical correlation for each set of test data. The experimental and analytical results are summarized for 10 Ni steel in Figures 49 through 53 and for beta annealed 6Al-4V titanium in Figures 54 through 58.

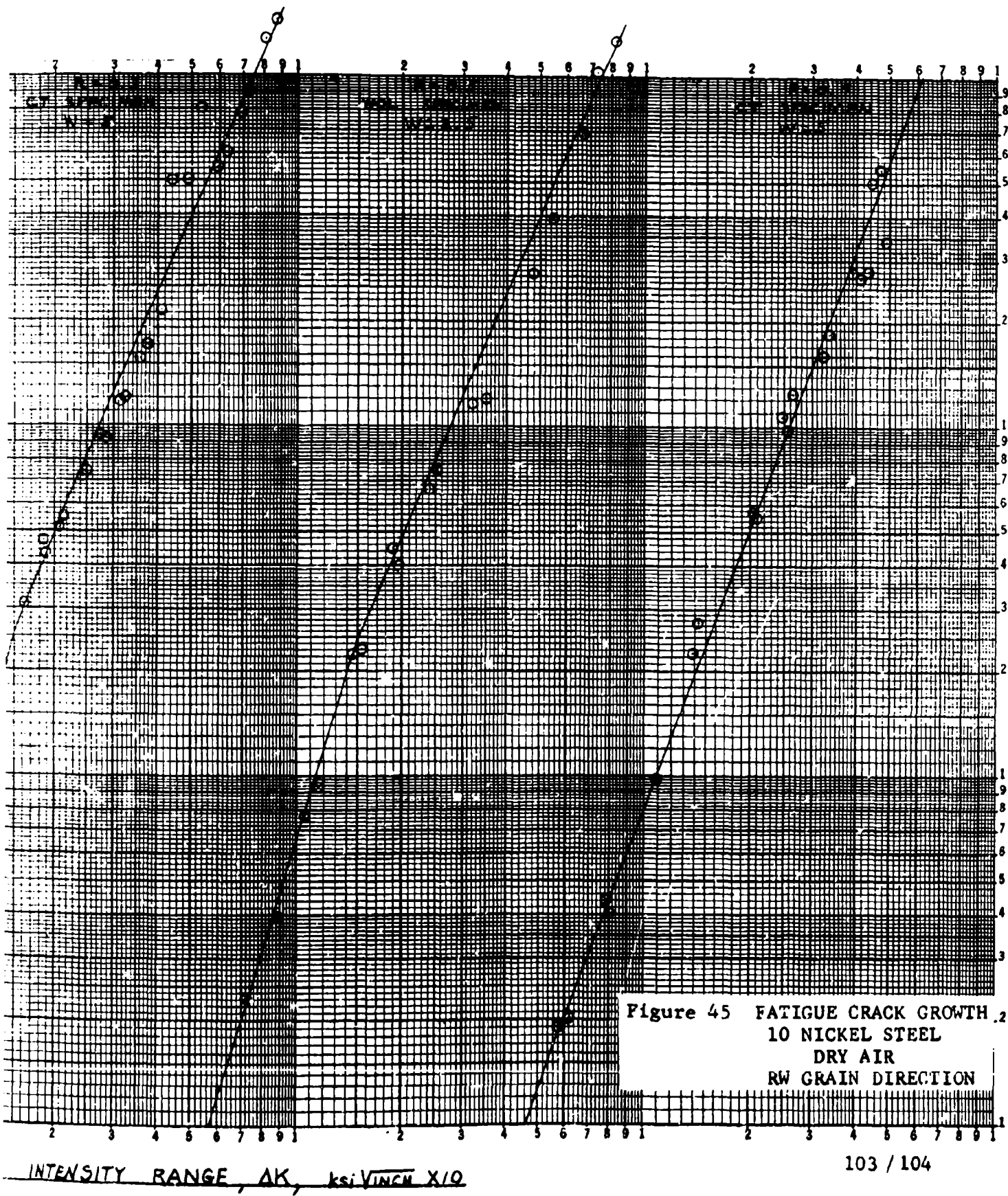
3.1.3.3 Finite Element Fracture Analysis - It was reported in Reference 1 that calculation for Mode I fracture had been coded and checked out. Within this reporting period the following tasks have been performed.

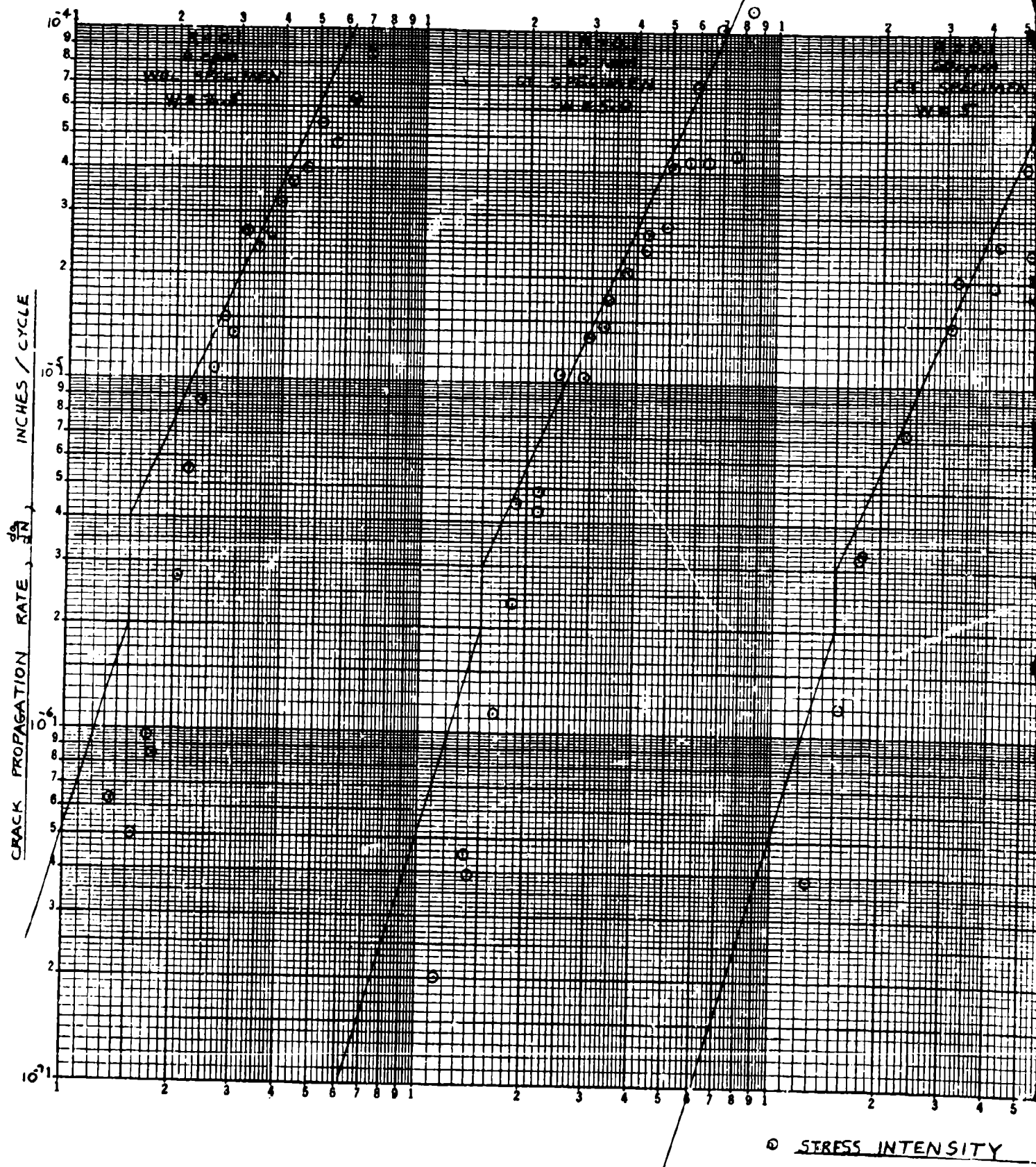
1. Mode II Analysis

Calculation of crack tip stress intensity factors for Mode II fracture has been programmed and checked out for computer procedure UD1. Therefore, UD1 is capable of calculating K_{II} and K_{II} simultaneously.

Test Problem 1 - Center-Cracked Plate Under Shear Load - A square sheet with a center crack under uniform shear load along its periphery was analyzed. Because of double skew-symmetry







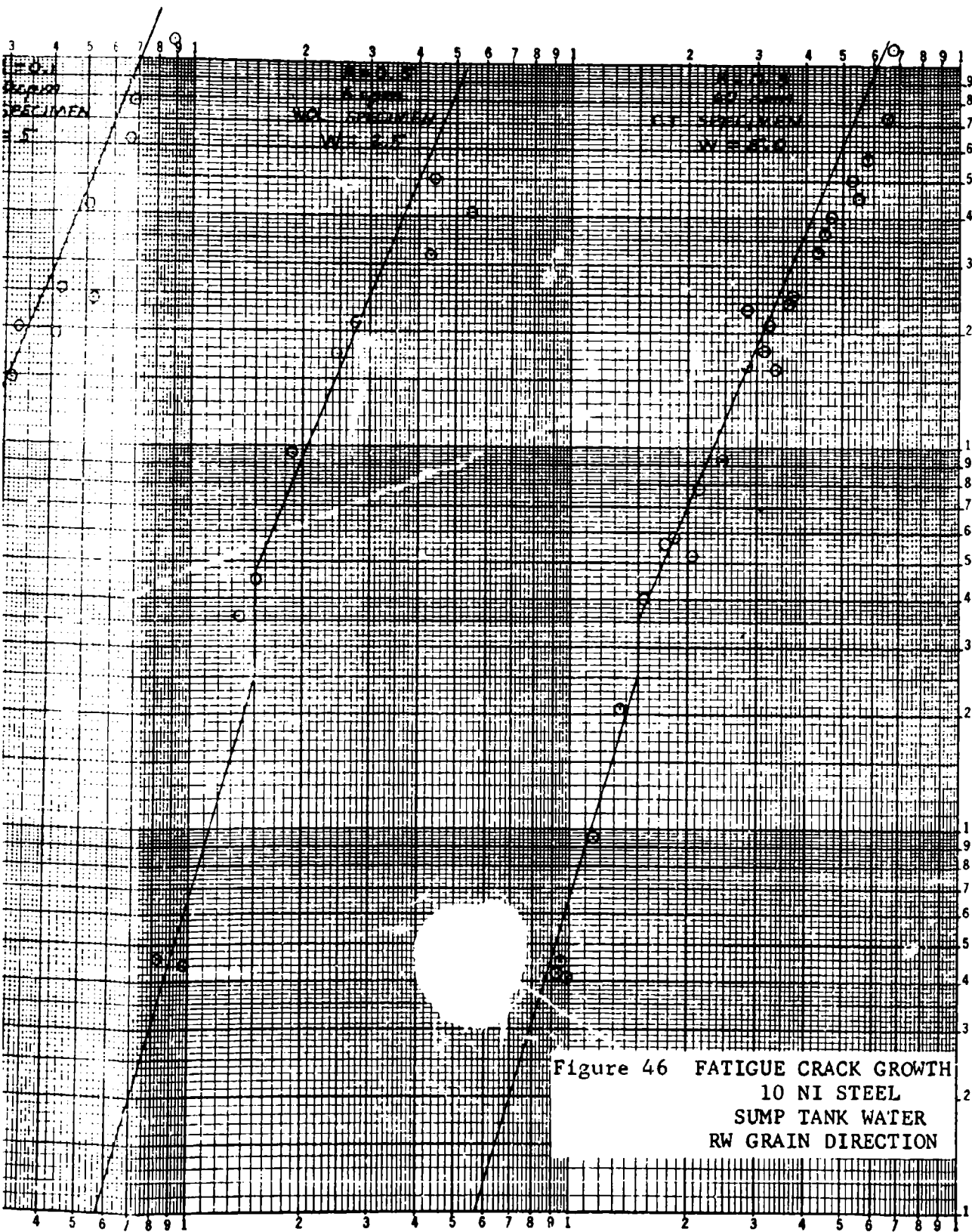
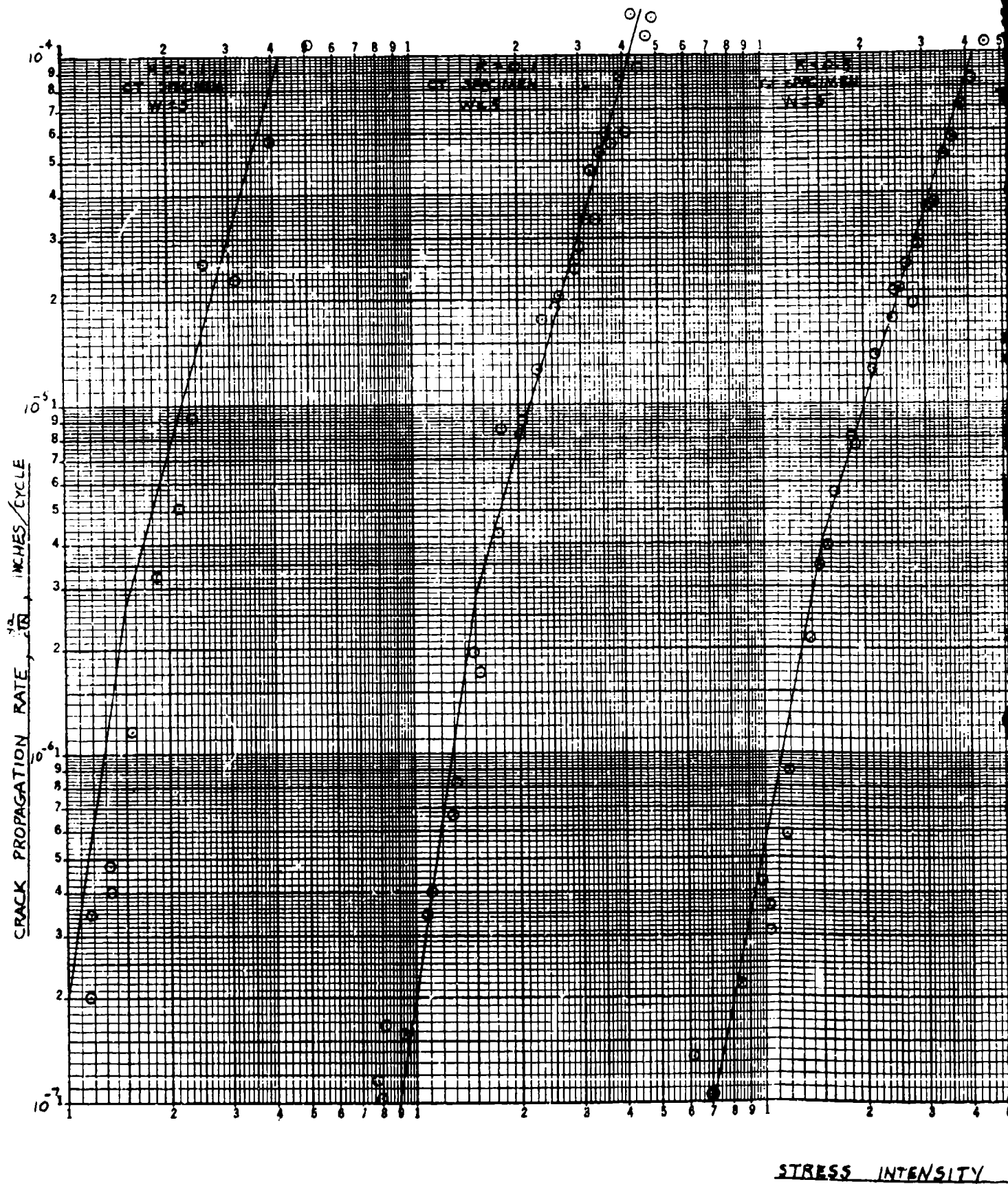


Figure 46 FATIGUE CRACK GROWTH
10 NI STEEL
SUMP TANK WATER
RW GRAIN DIRECTION

SITY RANGE, ΔK , KSI/VINCH X 10

105 / 106

2



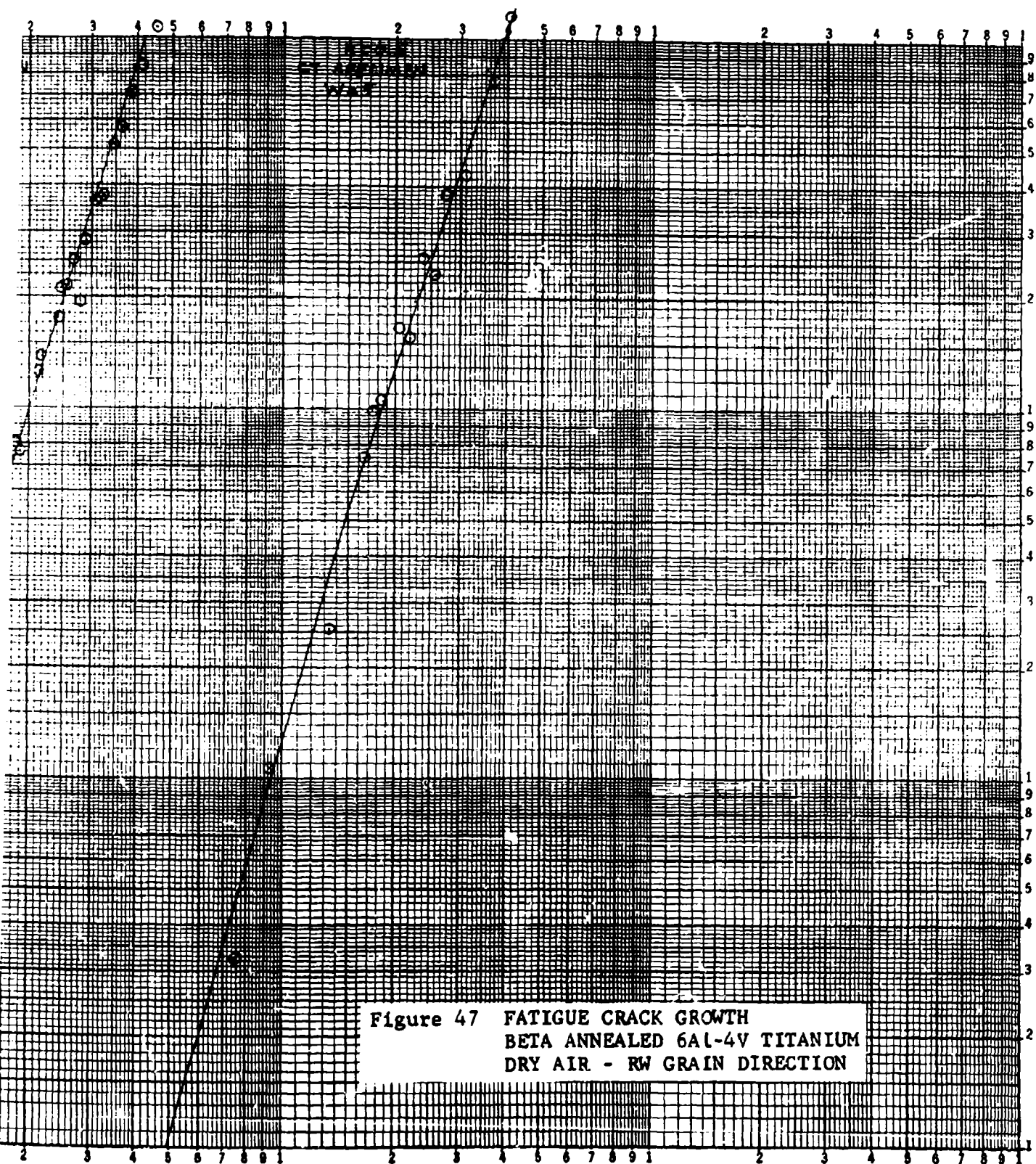
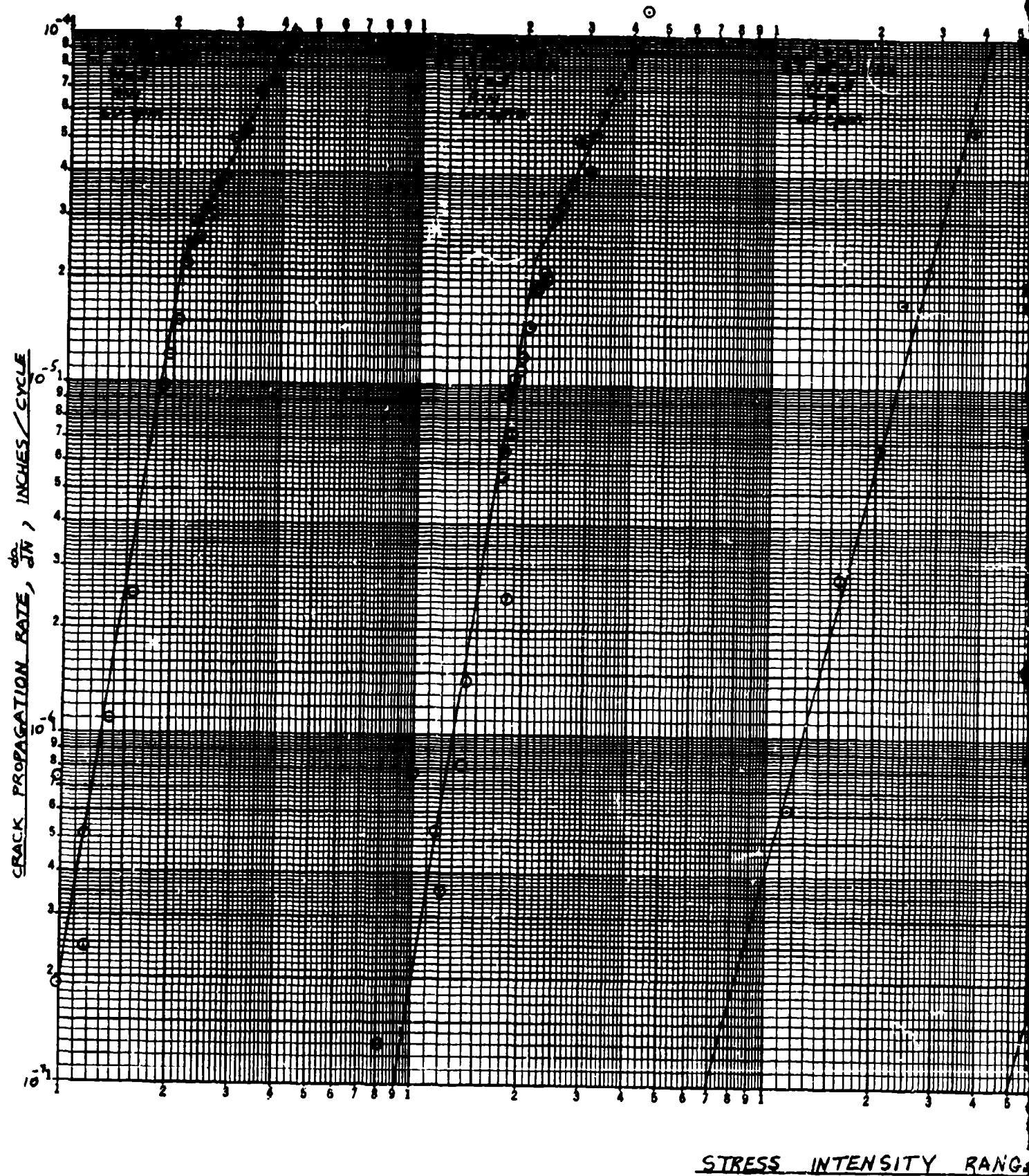


Figure 47 FATIGUE CRACK GROWTH
BETA ANNEALED 6Al-4V TITANIUM
DRY AIR - RW GRAIN DIRECTION



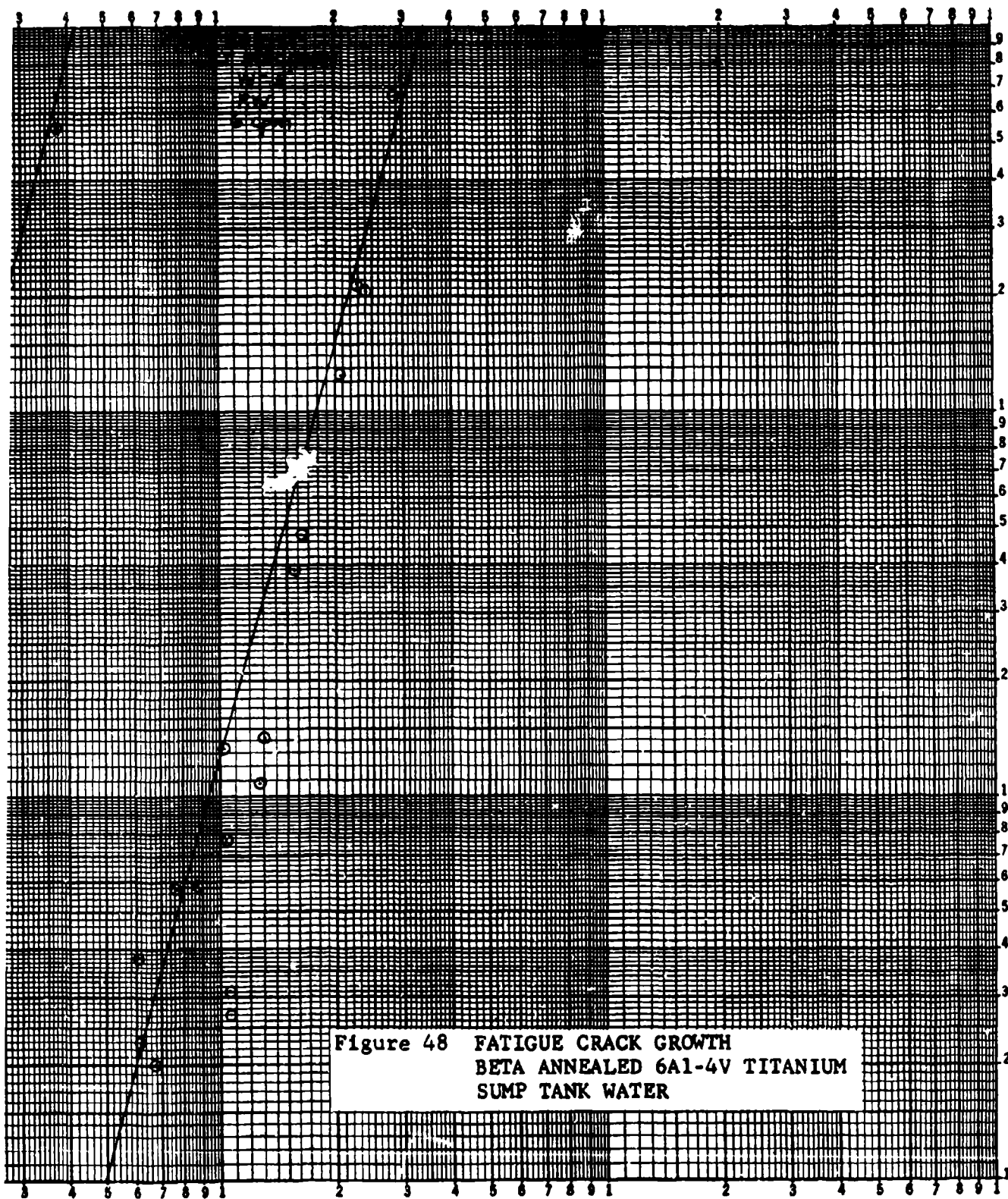


Table 13 SPECTRUM-ENVIRONMENTAL CRACK GROWTH TESTS

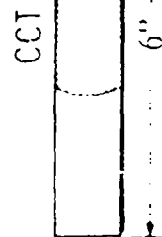
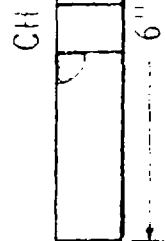
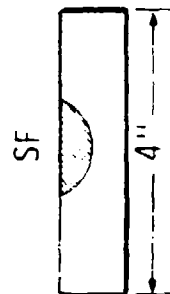
MATERIAL	ENVIRONMENT DA - Dry Air STW - Sump Water	SPECTRUM	SPECIMEN CCT - Center Crack SF - Surface Crack CH - Cracked Hole	NOTES
Beta "C"	DA	1	CCT	{ 1 Crack in DA { 1 Crack in STW/
	DA	2	CCT	
	DA/STW	1*	CCT	
	DA/STW	2*	CCT	
	STW	1	CCT	
Ti 6Al-4V and 10 Ni Steel	DA	1	SF	{ 1 Crack in DA { 1 Crack in STW/
	DA	2	SF	
	DA	1	CH	
	DA	2	CH	
	DA/STW	1*	SF	
	DA/STW	2*	SF	
	STW	1	SF	

SPECTRA: *1 180 Cycles, Flight Field Sweep Critical

*2 311 Cycles, Flight Air Sweep Critical

1 931 Cycles, Flight Version of *1

2 931 Cycles, Flight Version of *2



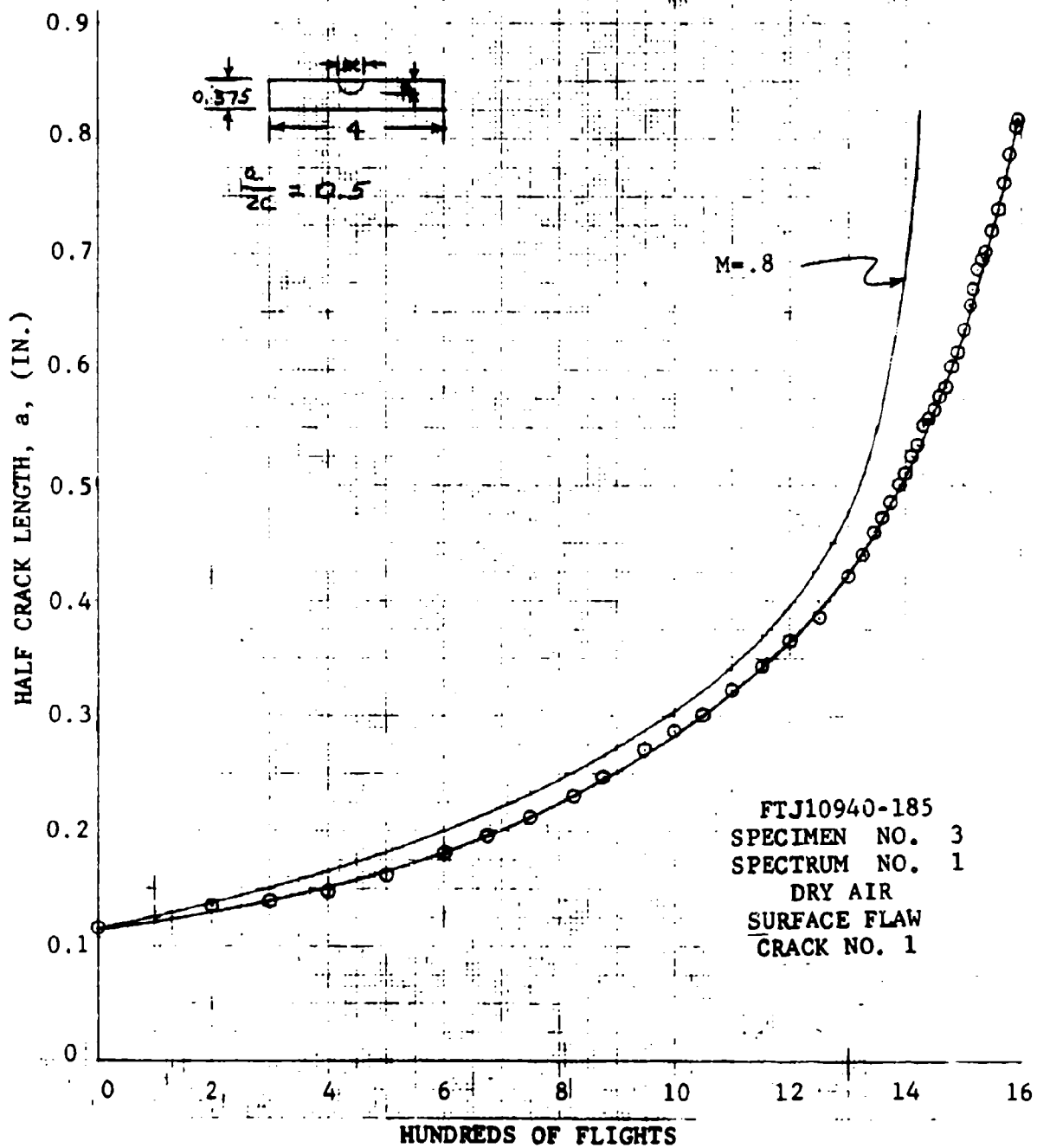


Figure 49 CRACK GROWTH TEST
10 NICKEL STEEL

FTJ10940-185
 SPECIMEN NO. 5
 SPECTRUM NO. 1
 SUMP TANK WATER
 SURFACE FLAW
 CRACK NO. 1

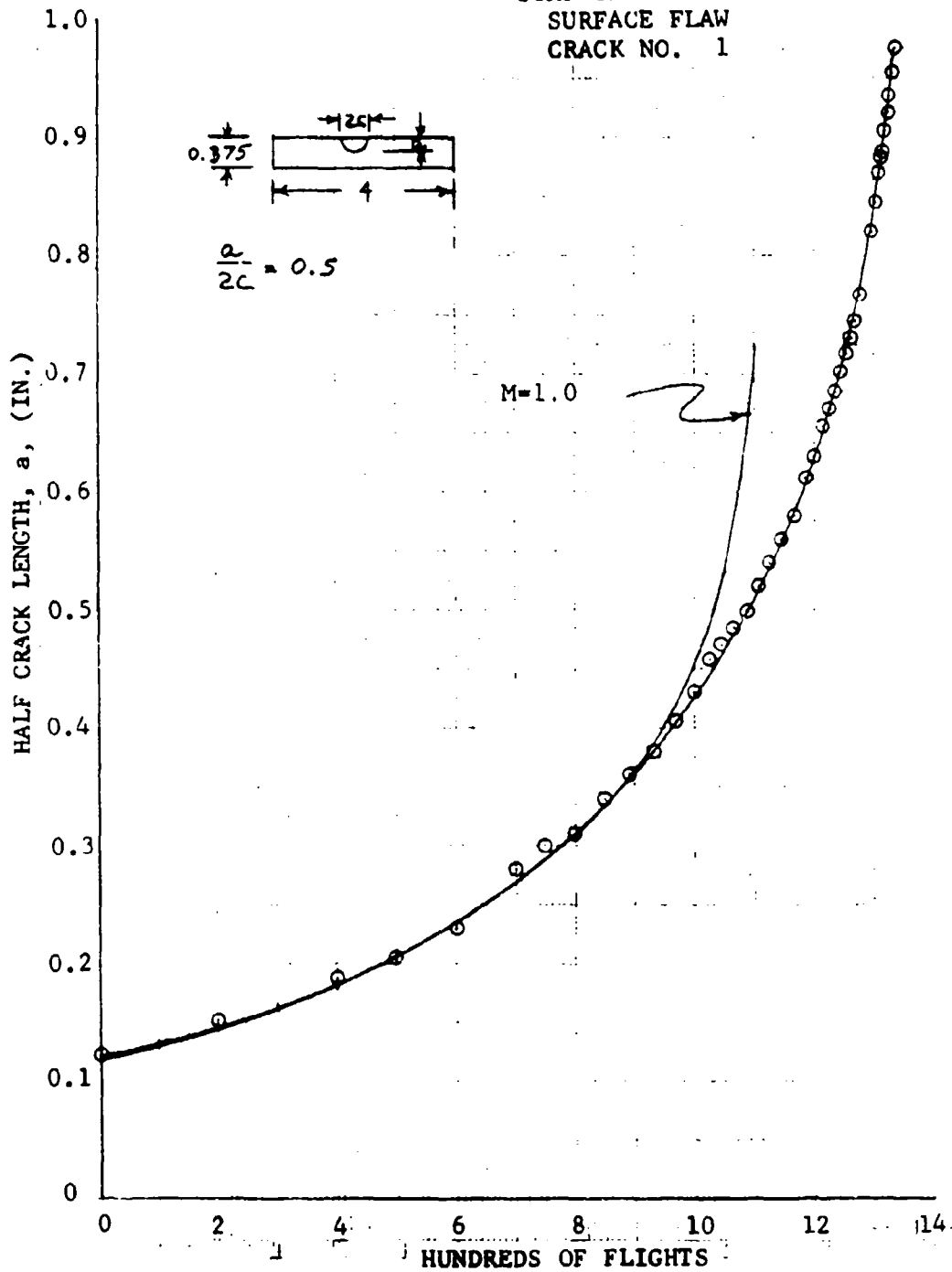


Figure 50 CRACK GROWTH TEST
 10 NICKEL STEEL

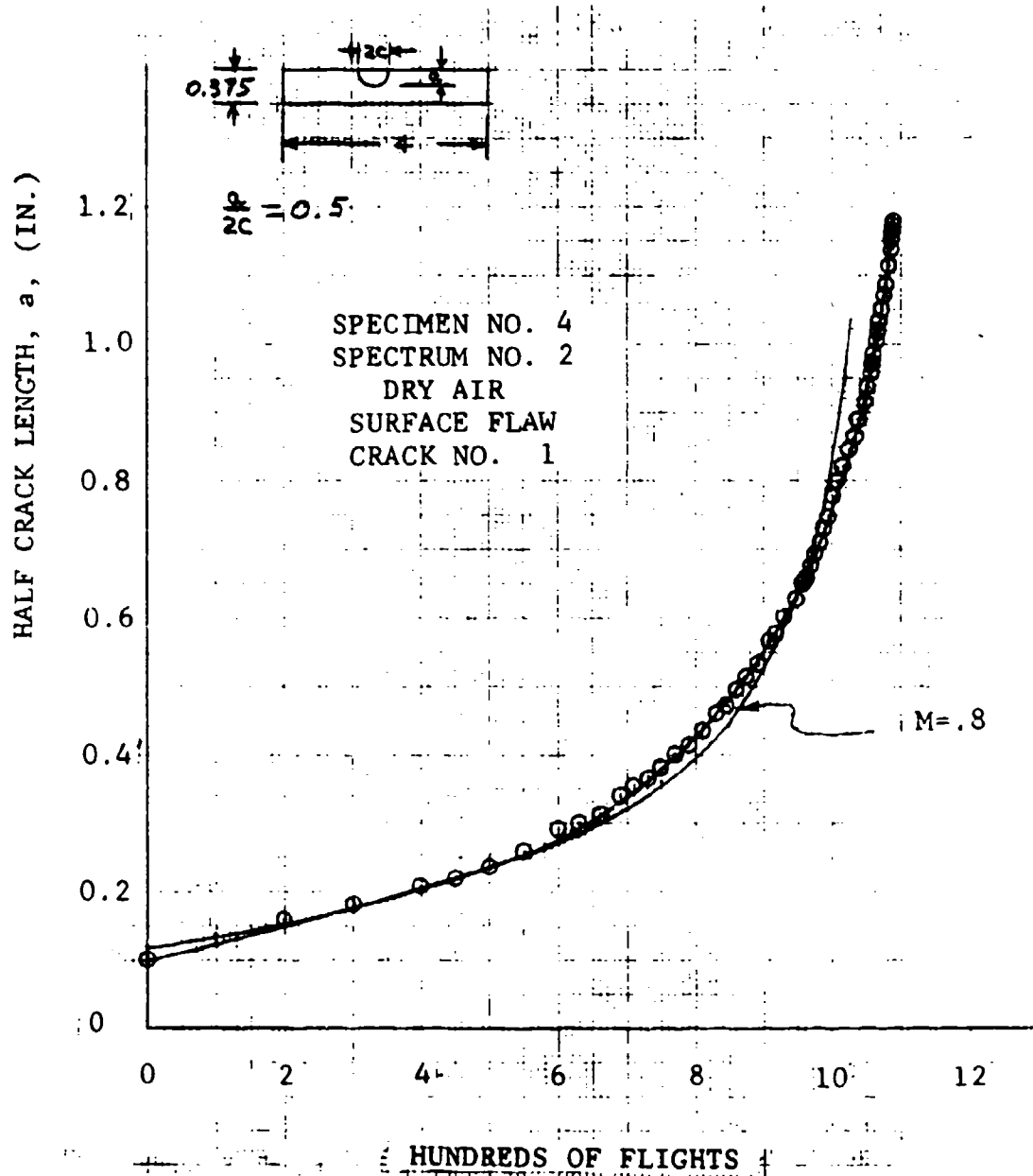


Figure 51 CRACK GROWTH TEST
10 NICKEL STEEL
FTJ10940-185

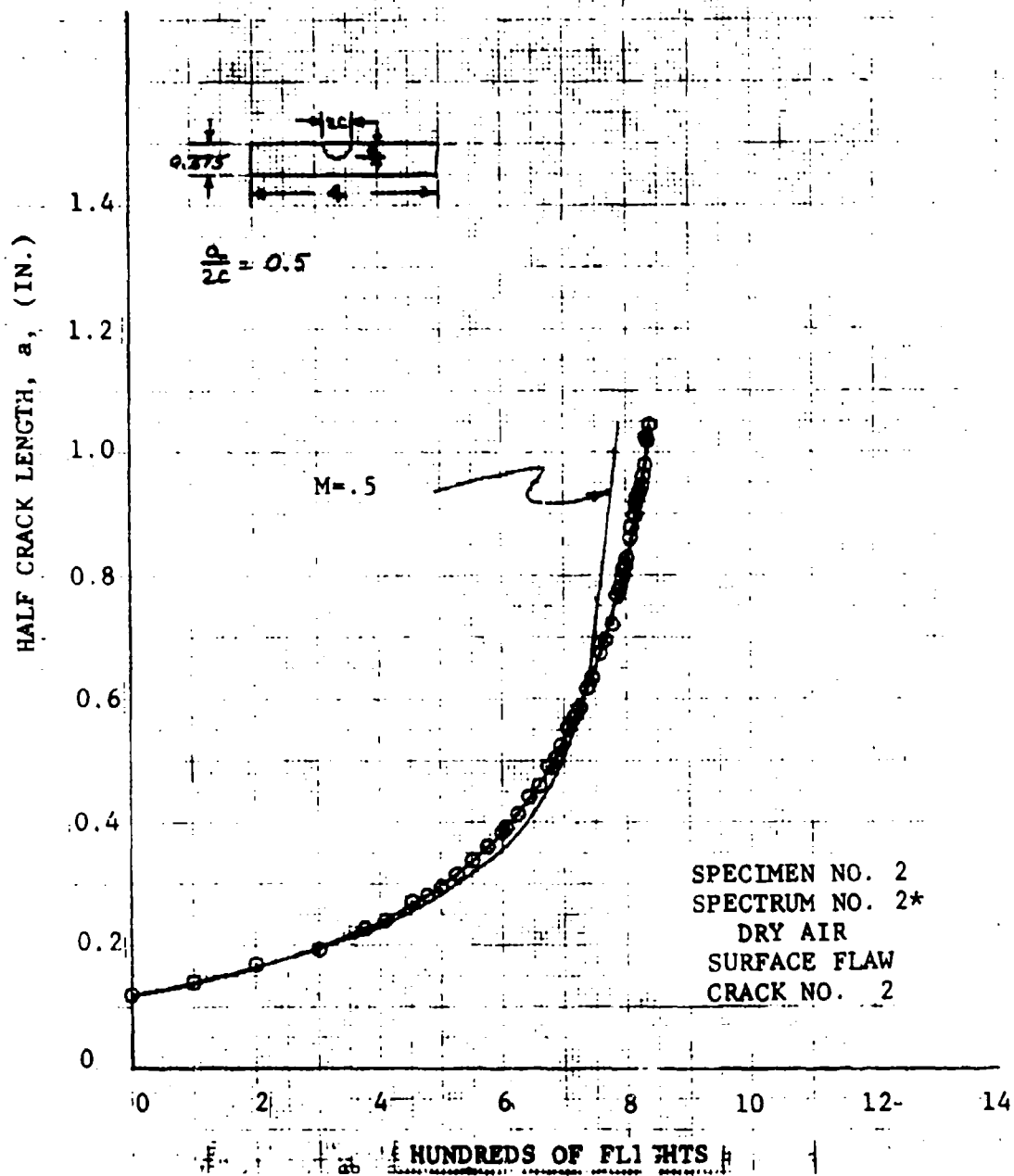


Figure 52 CRACK GROWTH TEST
10 NICKEL STEEL
FTJ10940-185

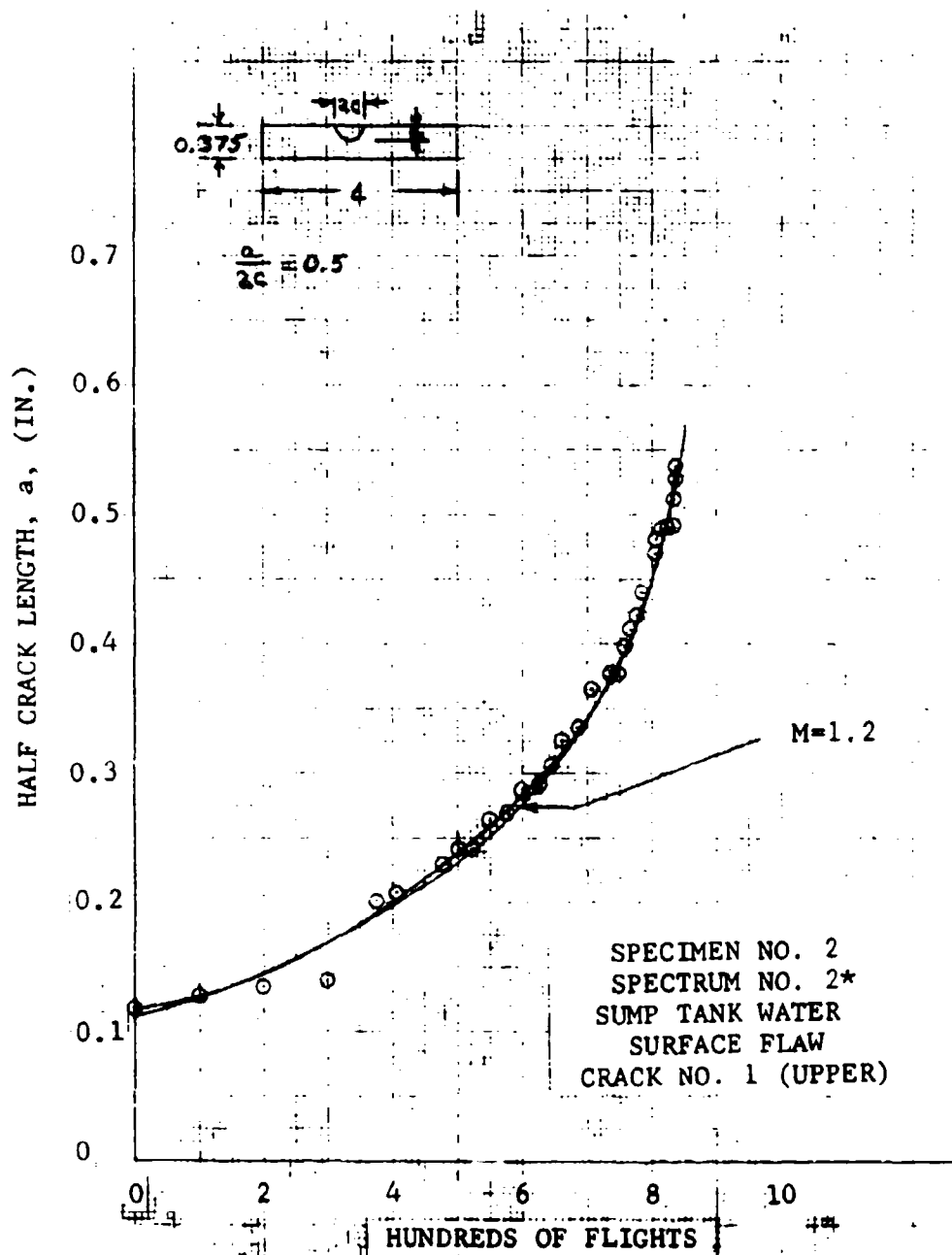


Figure 53 CRACK GROWTH TEST
10 NICKEL STEEL
FTJ10940-185

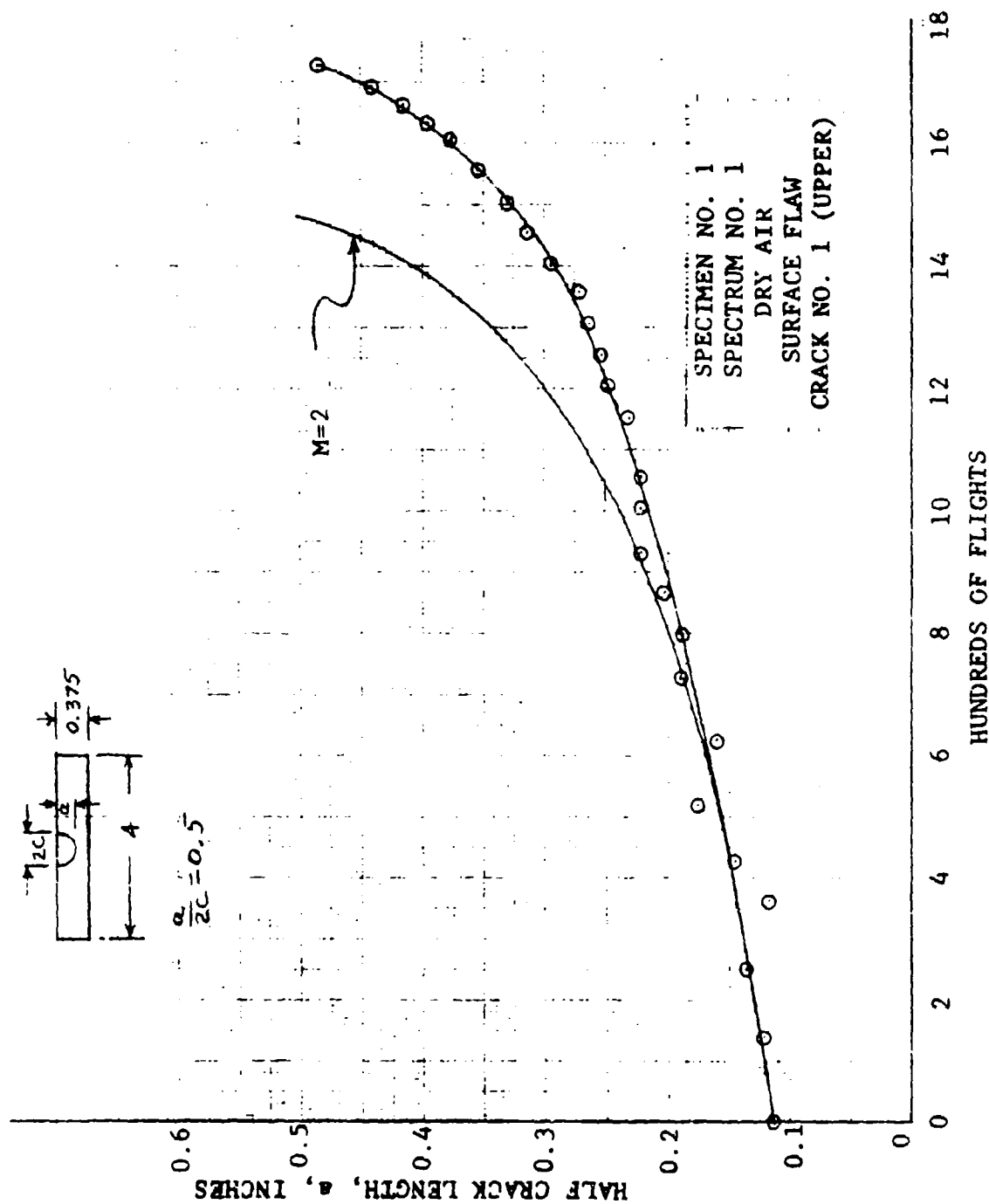


Figure 54 CRACK GROWTH TEST
BETA ANNEALED 6Al-4V TITANIUM
FTJ10940-153

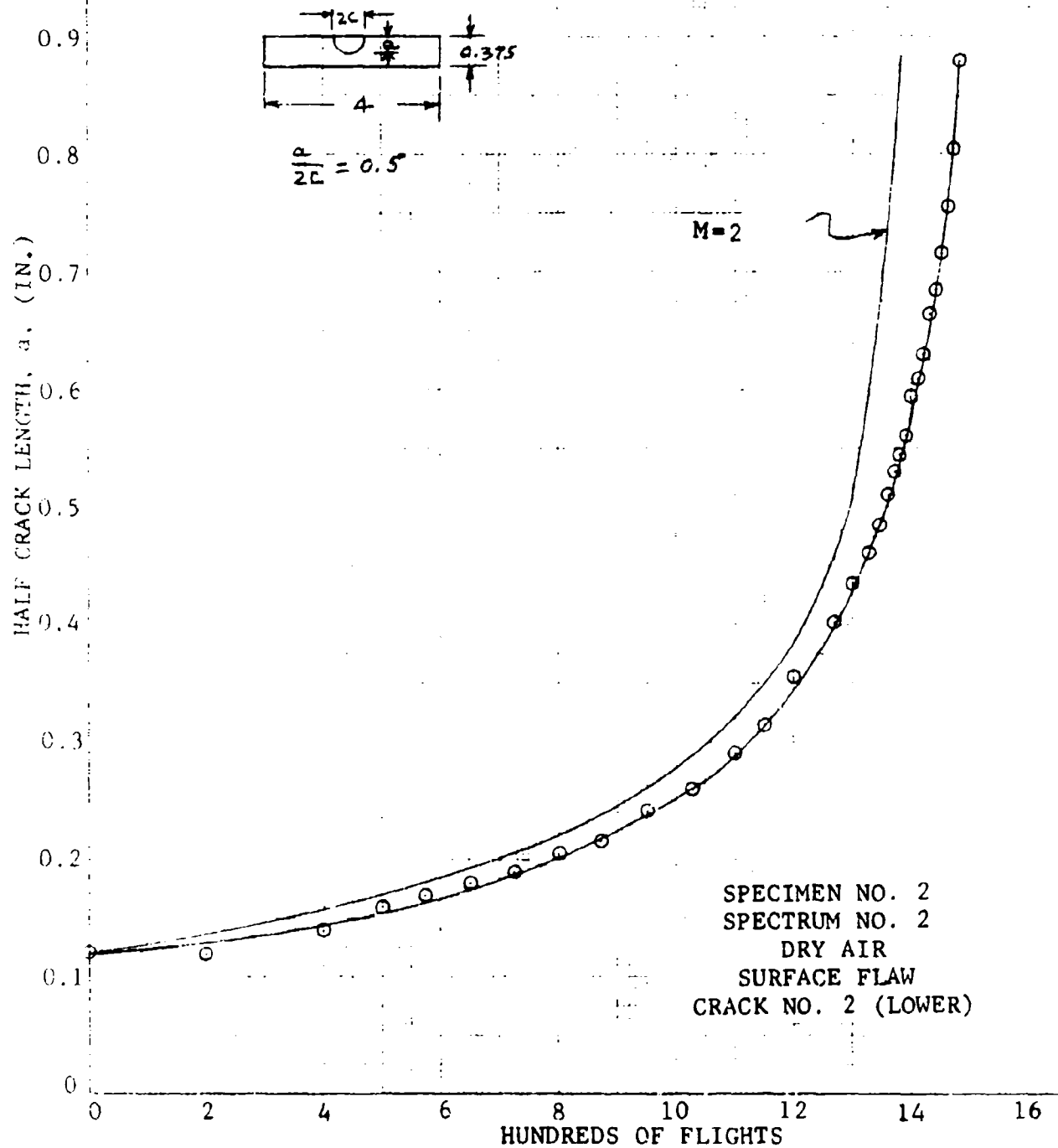


Figure 55 CRACK GROWTH TEST
BETA ANNEALED 6Al-4V TITANIUM
FTJ10940-153

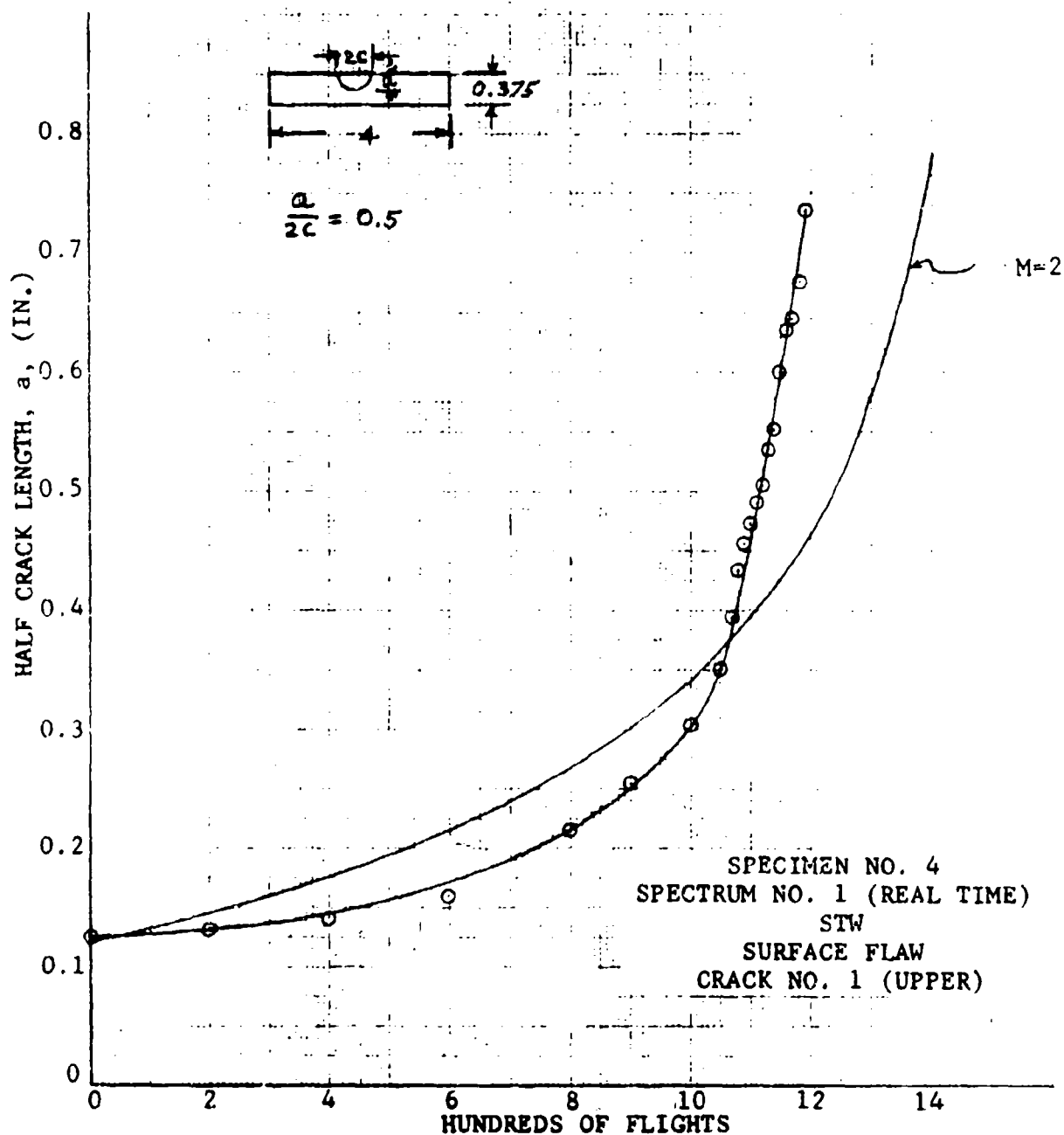


Figure 56 CRACK GROWTH TEST
BETA ANNEALED 6Al-4V TITANIUM
FTJ10940-153

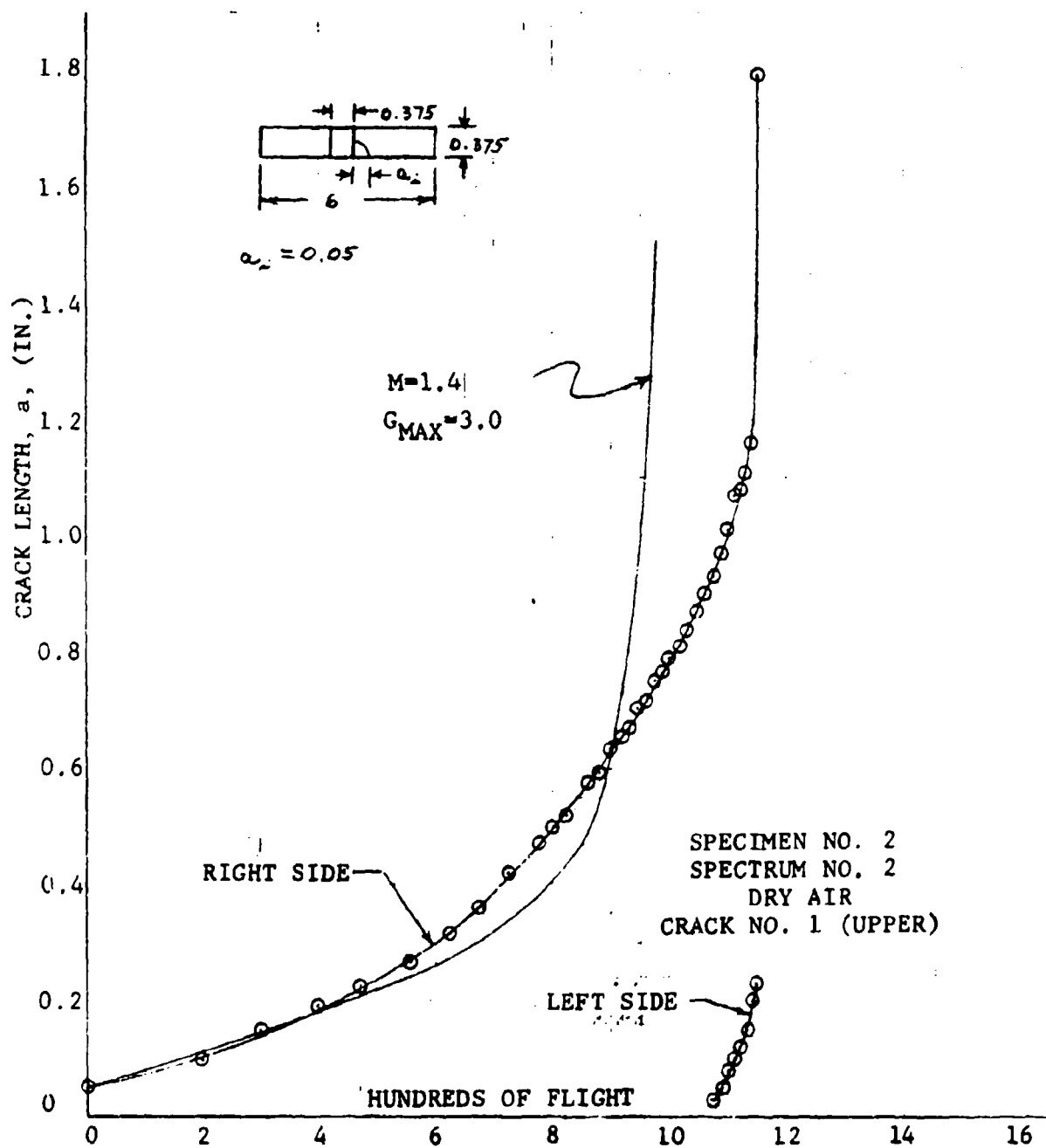


Figure 57 CRACK GROWTH TEST
BETA ANNEALED 6Al-4V TITANIUM
FTJ10940-152

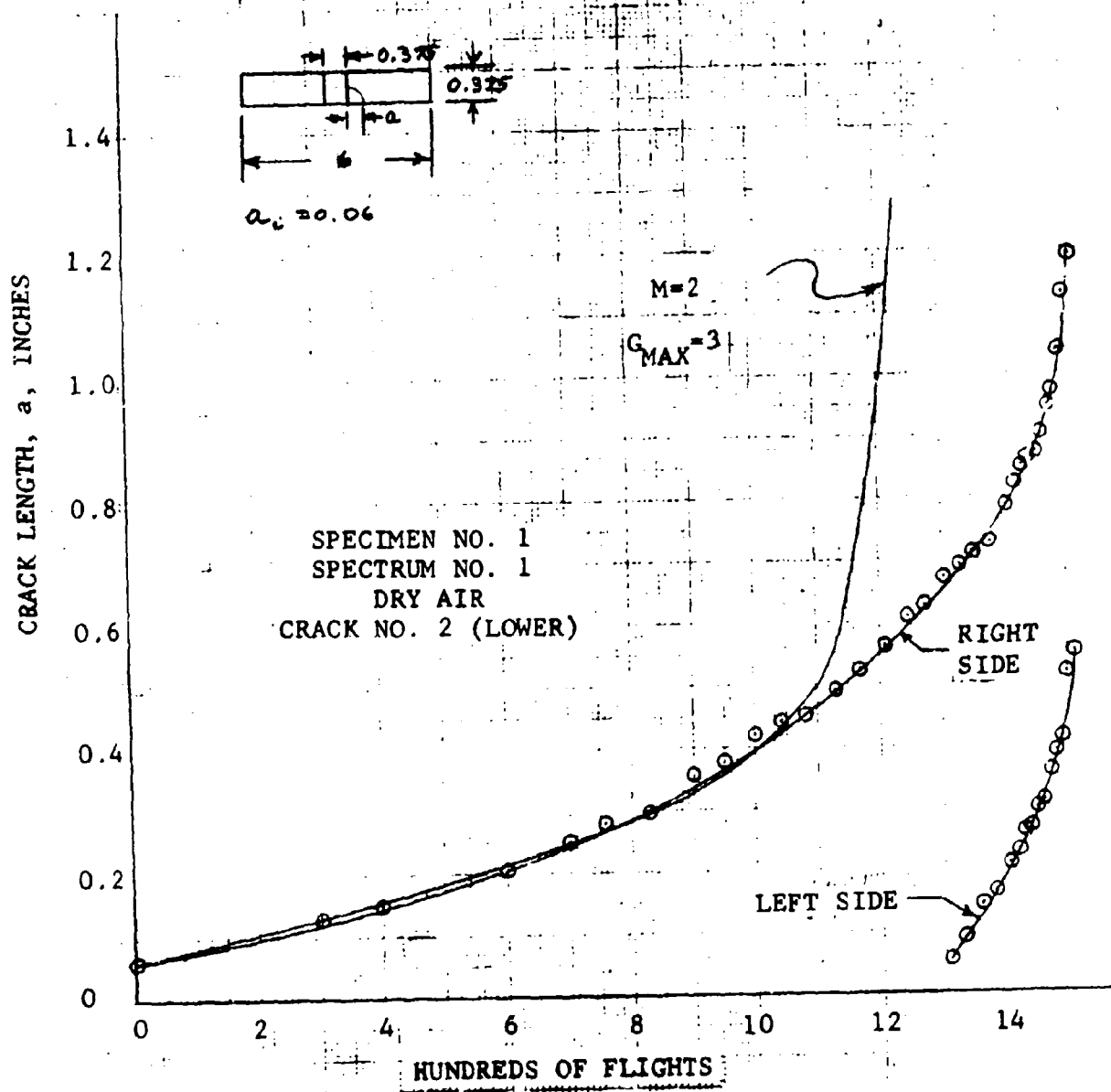


Figure 58 CRACK GROWTH TEST
BETA ANNEALED 6Al-4V TITANIUM
FTJ10940-152

only the upper right quarter needed to be simulated as shown in Figure 59. The K_{II} calculated by UD1 is 113.0 psi $\sqrt{\text{in}}$ while the solution for the crack in an infinite plate under same loading is:

$$K_{II} = a = 113.7 \text{ psi } \sqrt{\text{in}}.$$

The rather close correlation between the finite element solution and the theoretical solution for the infinite plate deserves some comments: (1) the coarse grid work used in the analysis should yield a solution about 5% too high as was observed and reported previously in the Mode I analysis (Reference 2), (2) there is no theoretical finite dimension correction factor for K_{II} calculation, however, it is reasonable to presume that the factor should be slightly greater than one. The effect from (1) tends to compensate that from (2). Thus the Mode II stress intensity factor calculation is shown to be satisfactory.

Test Problem 2 - Center-Cracked Plate Under Corner Load - The same square plate as in Problem 1 was loaded under antisymmetric corner loads as shown in Figure 60 and it was analyzed using computer procedure UD1. The purpose of this analysis was to demonstrate the capability of UD1 to calculate K_I and K_{II} simultaneously. There is no theoretical solution to this problem, yet the results seem in the right range.

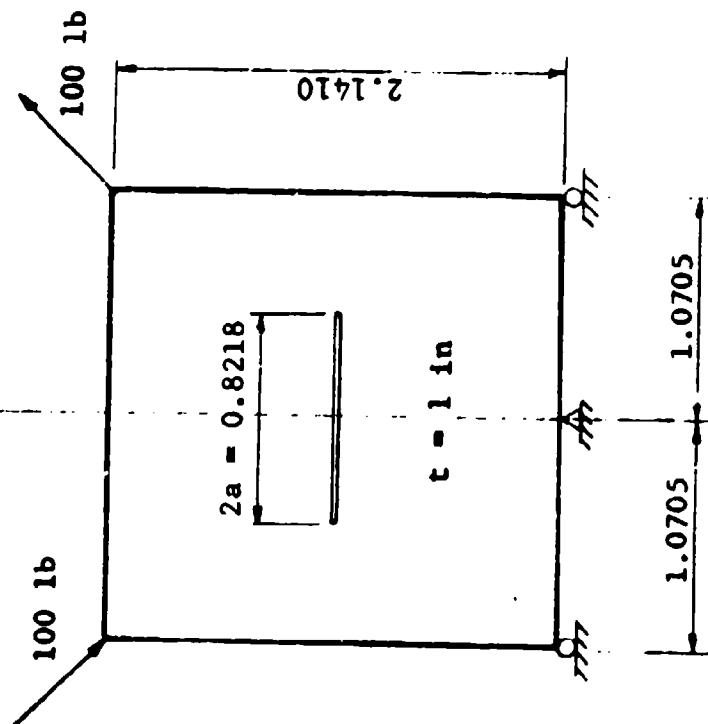
2. Structural Design Analysis

Three analysis problems were solved by computer procedure UD1. Results and discussion follow.

Problem 1 - Two Parallel Cracks in A Semi-Infinite Plate Under Uniform Tension - Two cases were studied to evaluate the two-crack test specimens used in the spectrum environmental effects test program. The results are summarized in Figure 61. With two equal cracks located 5 crack lengths apart along the load axis the stress intensity factor is magnified by a factor of 1.05. If one of the cracks is reduced to less than half of the other crack, the K_I of the smaller crack is slightly less than that of a single crack of the same length in a semi-infinite plate due to the "sheltering" effect of the larger crack. The K_I of the larger crack is virtually unchanged from that of a single crack in a semi-infinite plate.

Problem 2 - Damage Tolerance Test Specimen - Figure 62 shows the general arrangement of the damage tolerance test specimen, 603FTB033. Four computer runs were made for $a = 0.5$,

A SQUARE PLATE WITH A CENTER CRACK
UNDER ANTISYMMETRIC CORNER LOADS



$$K_I = 11.7 \text{ psi } \sqrt{\text{in}}$$

$$K_{II} = 126.2 \text{ psi } \sqrt{\text{in}}$$

Figure 60

A SQUARE PLATE WITH A CENTER CRACK UNDER ANTISYMMETRIC CORNER LOADS

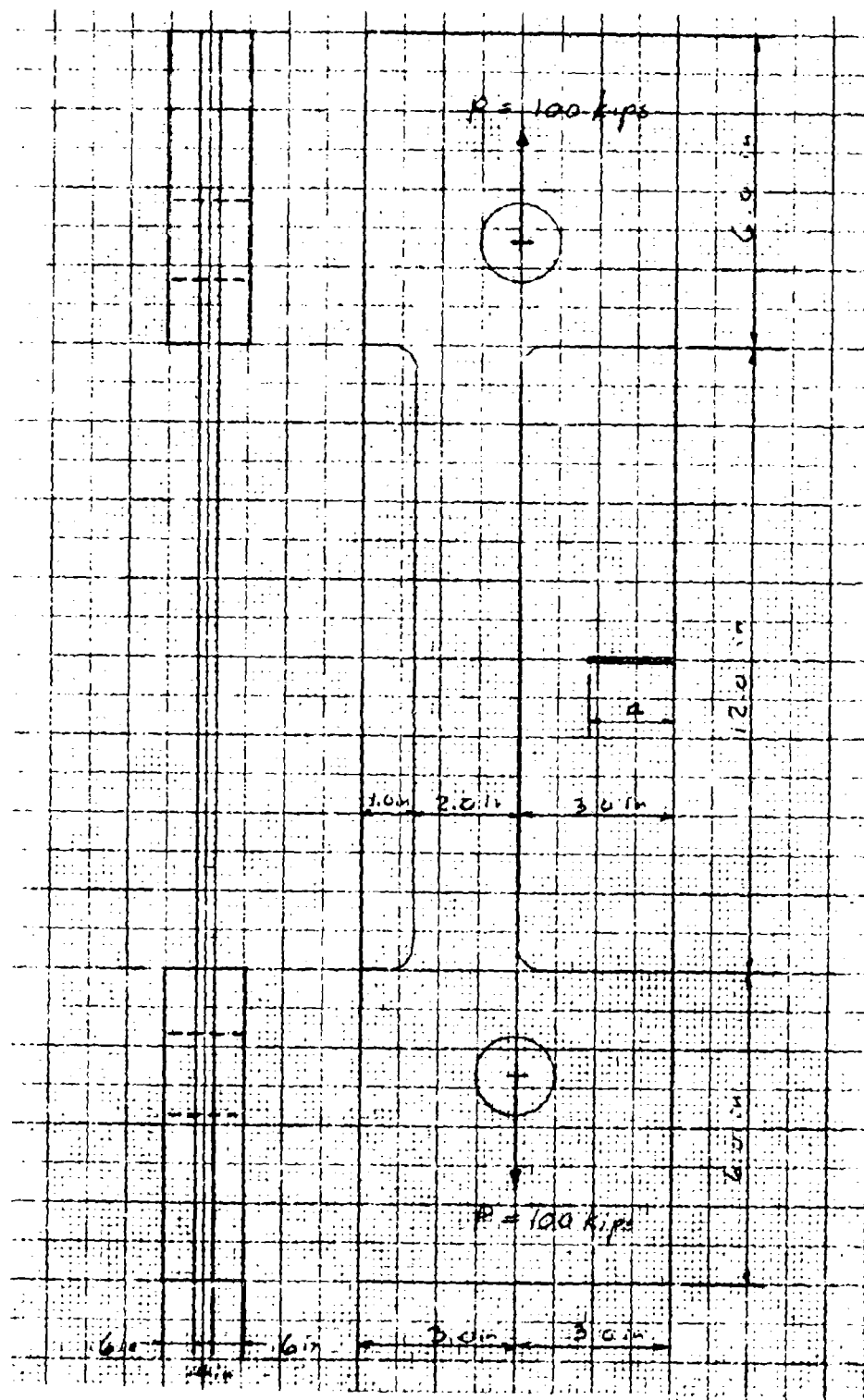


Figure 62 DAMAGE TOLERANCE TEST SPECIMEN

1.5, 2.5 and 3.0 in. The variation of K_I vs a is shown in Figure 63. The crack arrest characteristics are similar to those anticipated for a crack in a bay approaching a stiffener in the FSIL lower plate.

Problem 3 - Idealized Fail-Safe Brazed Lower Plate - A cracked sheet reinforced with brazed stringers was analyzed. The structural arrangement is shown in Figure 64. The analysis was conducted in order to gain some insight into the crack arrest behavior of the FSIL lower plate under tensile loads. The following assumptions were made prior to the analysis: (1) the bonding between the cracked sheet and the midstringers remains intact as long as $a \leq 1.0$ in, and (2) debonding between the cracked sheet and the midstringers occurs for $a > 1.0$ in. The stress intensity factors were calculated for $a = 0.5, 1.0, 2.0, 4.0, 6.0$ and 7.5 in. and were plotted in Figure 65. The abrupt increase of K_I at $a = 1.0$ in. is due to delamination of the midstringer along the braze line.

3. Triangular and Quadrilateral Plate Elements

The triangular and quadrilateral plate elements have been introduced into UDI in order to accommodate irregular geometry and configurations. The triangular element (Figure 66) stiffness matrix is based on the following displacement assumptions.

$$u_x = c_1x + c_2y + c_3$$

$$u_y = c_4x + c_5y + c_6$$

The stiffness matrix for a triangular plate element, derived in Reference 3, is of the following form:

$$k = k_n + k_s$$

where k_n represents stiffness due to normal stresses and k_s represents stiffness due to shearing stresses and

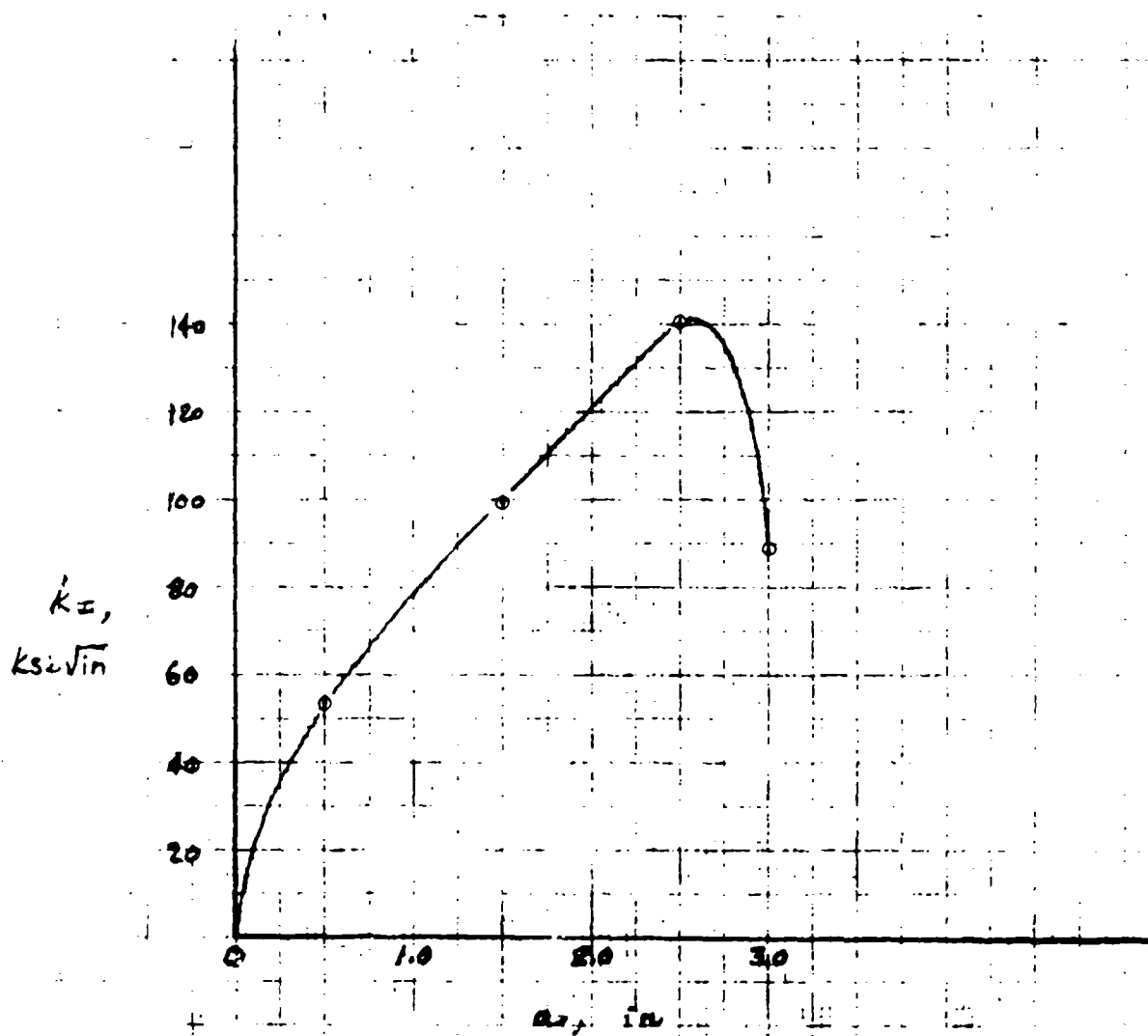


Figure 63 K_I vs a FOR THE DAMAGE TOLERANCE TEST SPECIMEN
UNDER TENSION

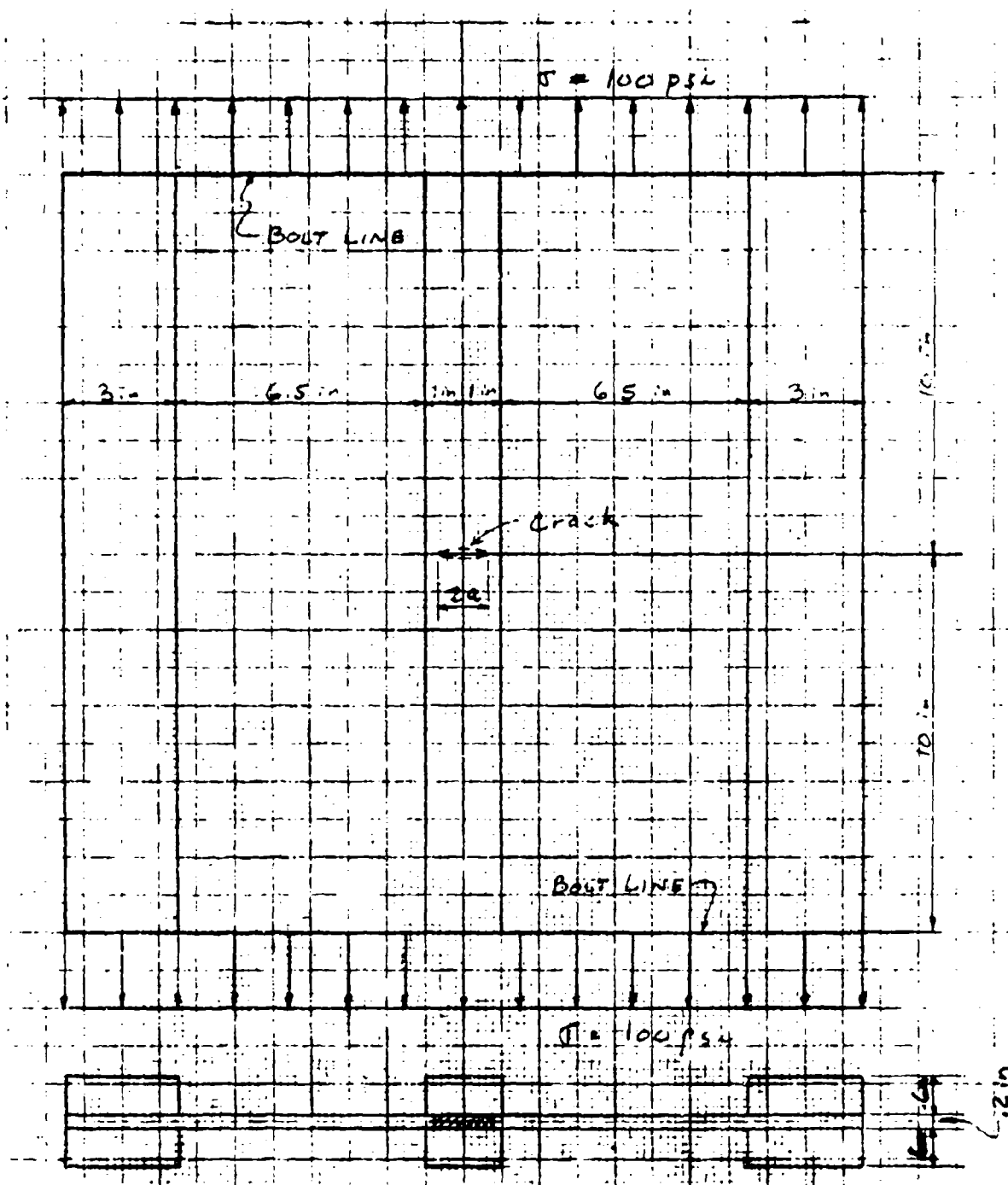


Figure 64 IDEALIZED FAIL-SAFE INTEGRAL LOWER PLATE

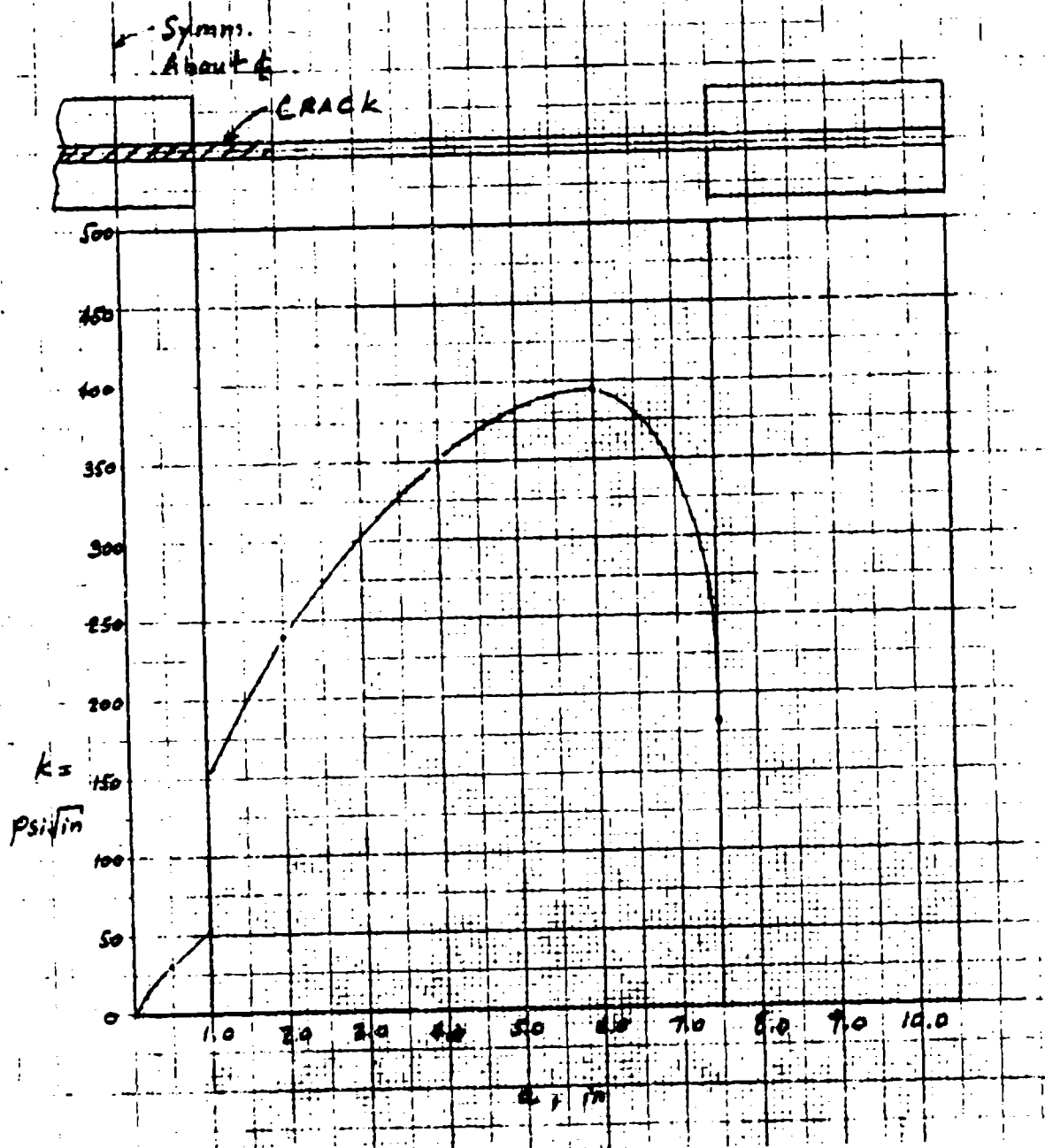


Figure 65 K_I vs a FOR THE IDEALIZED FAIL-SAFE BRAZED LOWER PLATE

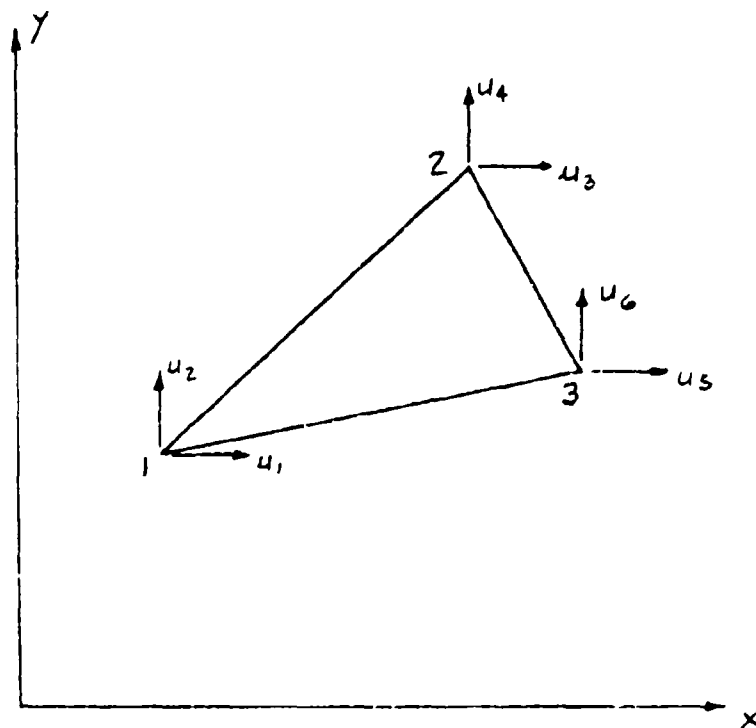


Figure 66 TRIANGULAR PLATE ELEMENT

$$k_n = \frac{Et}{4A_{123}(1-\nu^2)} \begin{bmatrix} y_{32}^2 & & & & \\ -\nu y_{32}x_{32} & x_{32}^2 & & & \\ -y_{32}y_{31} & \nu x_{32}y_{31} & y_{31}^2 & & \\ y_{32}x_{31} & -x_{32}x_{31} & -\nu y_{31}x_{31} & x_{31}^2 & \\ y_{32}y_{21} & -\nu x_{32}y_{21} & -y_{31}y_{21} & \nu x_{31}y_{21} & y_{21}^2 \\ -\nu y_{32}x_{21} & x_{32}x_{21} & y_{31}x_{21} & -x_{31}y_{21} & -\nu y_{21}x_{21} & x_{21}^2 \end{bmatrix} \quad \text{Symmetric}$$

$$k_s = \frac{Et}{8A_{123}(1+\nu)} \begin{bmatrix} x_{32}^2 & & & & \\ -x_{32}y_{32} & y_{32}^2 & & & \\ -x_{32}x_{31} & y_{32}x_{31} & x_{31}^2 & & \\ x_{32}y_{21} & -y_{32}y_{31} & -x_{31}y_{31} & y_{31}^2 & \\ x_{32}x_{21} & -y_{32}y_{21} & -x_{31}x_{21} & y_{31}x_{21} & x_{21}^2 \\ -x_{32}y_{21} & y_{32}y_{21} & x_{31}y_{21} & -y_{31}y_{21} & -x_{21}y_{21} & y_{21}^2 \end{bmatrix} \quad \text{Symmetric}$$

where A_{123} = Area $\Delta 123$

$$x_{ij} = x_i - x_j$$

$$\text{and } y_{ij} = y_i - y_j$$

A quadrilateral plate element is subdivided into four triangular elements by connecting its opposite vertices. The stiffness matrices of the triangular elements are assembled. The stiffness matrix of the quadrilateral element is then obtained by eliminating the mid-node coordinates.

3.1.4 Materials Engineering

3.1.4.1 Material Selection

The primary materials selected for the use in the AMAVS designs are 7050 aluminum, Beta C titanium, beta annealed 6Al-4V titanium and 10 Nickel steel. Tentative design allowables have been established and were included in AFFDL-TR-72-75 and AFFDL-TR-73-1. Based on tests that have now been completed final design allowables are now available for the beta annealed 6Al-4V titanium and are shown in Table 14 .

The test plans for the selected materials are included in the following test plan charts:

603R100-1 "D"	6Al-4V Beta Annealed - Welding
603R100-2 "F"	10 Ni Steel - Welding
603R100-3 "J" Sheet 1	6Al-4V Beta Annealed - Braze
603R100-3 "F" Sheet 2	
603R100-4 "F"	Beta C Titanium Base Material
603R100-5 "F"	6Al-4V Beta Annealed Base Material
603R100-6 "G"	10 Ni Steel Base Material
603R100-7 "F"	Beta C Titanium Bonding

The latest revisions to 603R100-2, -3, and -6 are shown in this report as Figures 67 , 68 , 69 . The rest of the test plan charts with their latest revisions are included in AFFDL-TR-73-40.

3.1.4.2 Material Procurement

10 Nickel Steel - All material for the materials test program has been received. The only procurement now active is the 10 Nickel steel to support Group II component tests, NDI tests and weld parameter studies. One piece of steel, size 2½" X 60" X 128", is being produced by U. S. Steel Corporation from a slab available from a Navy order identified as being from Heat No. C52106 Slab F4619. Test data from three different 1" thick plates from this same heat of material are reported in Table 15 .

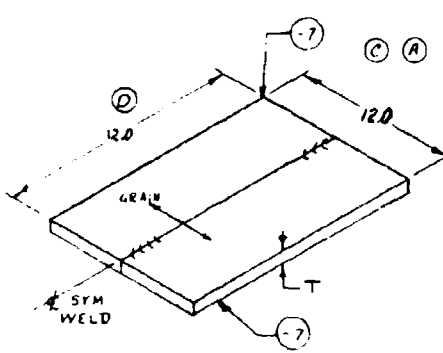
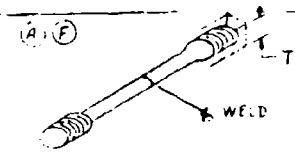
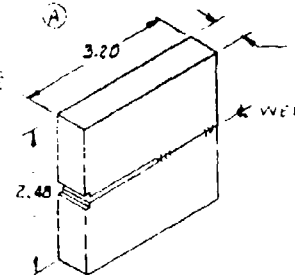
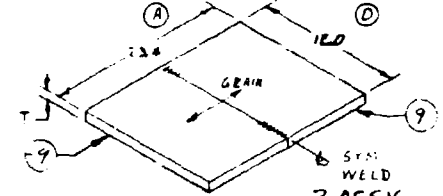
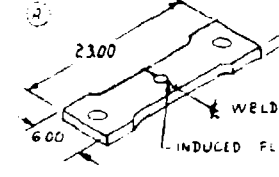
Beta Annealed 6Al-4V Titanium - All materials have been received and acceptance test data reported in Table 16 . The last two (2) pieces of 1.75" X 46½" X 80" received is reported on the last two (2) items of acceptance data. This table has been revised to include additional data generated since it was originally published in AFFDL-TR-73-1.

Table 14

DESIGN ALLOWABLES
For Ti 6Al-4V
Beta Annealed Condition
(Ref. FMS-1109A)

FORM	PLATE					
	THICKNESS (Inches)	.188 - .500	.501 - 1.000	1.001 - 2.000	2.001 - 2.500	2.501 - 4.000
PROPERTY:						
F_{tu} (KSI)		130	127	125	122	120
F_{ty} (KSI)		115	115	112	110	110
F_{cy} (KSI)		121	121	118	116	116
F_{su} (KSI)		87	85	83	81	80
F_{bru} (KSI)						
$e/D = 1.5$		208	203	200	195	192
$e/D = 2.0$		267	260	256	250	246
F_{bry} (KSI)						
$e/D = 1.5$		140	140	136	134	134
$e/D = 2.0$		170	170	166	163	163
$\%Elong(L \text{ or } LT)$		10	10	8	8	8
E (10^6 psi)				16.0		
E_c (10^6 psi)				16.4		
K_{IC} (KSI inch)				90 (TYP) 80 (MIN)		
K_{Isc} (KSI inch) typ (lbs/in ³)				60+ .160		

10 NI STEEL

MANUFACTURING RESEARCH	NONDESTRUCTIVE INSPECTION DEVELOPMENT	ENGINEERING
SPECIMEN	T. STOCK THICKNESS ASSY QUANTITY	SPECIMEN
 <p>-1 ASSY</p>	<p>.625</p> <p>(A) 14</p> <p>RADIOGRAPHIC (X-RAY) MAGNETIC PARTICLE</p>	  <p>-2 ASSY</p> <p>-3 ASSY</p>
 <p>-3 ASSY</p>	<p>.625</p> <p>(A) 2</p> <p>RADIOGRAPHIC (X-RAY) MAGNETIC PARTICLE</p>	 <p>-4 ASSY</p>

3. ALL TESTING TO BE ACCOMPLISHED BY ETL.

2. ALL WELDING TO BE ACCOMPLISHED BY MFG ENGR.

1. ALL MACHINING TO BE ACCOMPLISHED BY ETL.


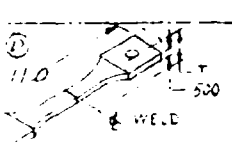
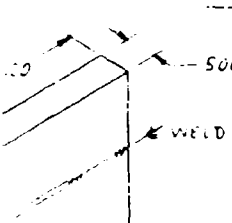
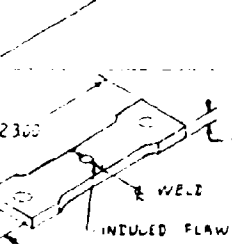
NOTES:

SYM	20
A	
B	
C	
D	
E	
F	

FOR REVISION SEE BELOW

ENGINEERING TEST

(A)

DIMEN	TYPE OF TEST	TEST SPECIMEN PART NUMBER	QUANTITY	T	TYPE OF WELD	SPECIMEN IDENTIFICATION
	TENSION	FTJ10940-1 (F)	6	.625	GAS TUNGSTEN ARC	NI-T-1 THRU 6
	FATIGUE TEST: R 0.1 Kt-I R 0.5 Kt-I	-124 (B) -124	24 12	.625		NI-F-1 THRU 36
	FATIGUE CRACK GROWTH	-147	2	.625		NI-CG-1 -2
	FRACTURE TOUGHNESS	FTJ10940-121	3	.625	GAS TUNGSTEN ARC	NI-FT-1 THRU 3

REVISIONS			
SYM	ZONE	DESCRIPTION	DATE
A		MFG RES SPEC: DIM 13 WAS 18, 11.4 WAS 13, 28.4 WAS 20, 13 WAS 20, REVISED QTY. ENGR TEST SPEC ADDED OVER ALL DIMS IN SPEC ID	8-3-78 1-2-78
B		ADDED GEN NOTES 1, 2, 4, 8; REVISED QTY OF -124 TO 24 (WAS 22) & 12 (WAS 14)	9-18-78 1-2-78
C		CHGD DIM 11 IN MFG RES. 12.0 WAS 11.4, DIM 12.00 WAS 10.5 FOR FTJ10940-124 CREATED -1 (1-3 ASSY) -7, 7-10-78	10-1-78 1-2-78
D		FOR -10-3 12.00 WAS 13.0. FOR FTJ10940-124 DIM 11.0 WAS 12.0	1-8-79 1-2-78
E		REVISED DIMS OF FTJ10940-147	2-26-79 1-2-78
F		ENGR TEST SPECIMEN FTJ10940-1 WAS FTJ10940-143	4-10-79 1-2-78

Figure 67

PRELIMINARY DESIGN DRAWING

10 NI STEEL-
WELDING PROPERTIES-
DEVELOPMENT TEST PROGRAM

BY D. L. ...	APPROVED	SCALE	DATE 7-7-78
GENERAL DYNAMICS		603R100-2F	
Convair Aerospace Division		REV 1 0 1	
Fort Worth Operation		REV 1 0 1	

2

MANUFACTURING RESEARCH SPECIMENS

NON-DESTRUCTIVE INSPECTION DEVELOPMENT

END-NOTCHED TEST SPECIMENS REMOVAL, REMOVED SPECIMENS NUMBERS, DIRECTIONS, AND TESTING, STRESS, AND TEST DATA

TYPE OF ENGINEERING TEST SPECIMEN

TEST SPECIMEN	TEST SPECIMEN	TEST SPECIMEN	TEST SPECIMEN	TEST SPECIMEN
1000	1000	1000	1000	1000
1000	1000	1000	1000	1000
1000	1000	1000	1000	1000

1000 1000 1000 1000 1000

TEST SPECIMEN	TEST SPECIMEN	TEST SPECIMEN	TEST SPECIMEN	TEST SPECIMEN
1000	1000	1000	1000	1000
1000	1000	1000	1000	1000
1000	1000	1000	1000	1000

1000 1000 1000 1000 1000

TEST SPECIMEN	TEST SPECIMEN	TEST SPECIMEN	TEST SPECIMEN	TEST SPECIMEN
1000	1000	1000	1000	1000
1000	1000	1000	1000	1000
1000	1000	1000	1000	1000

1000 1000 1000 1000 1000

TEST SPECIMEN	TEST SPECIMEN	TEST SPECIMEN	TEST SPECIMEN	TEST SPECIMEN
1000	1000	1000	1000	1000
1000	1000	1000	1000	1000
1000	1000	1000	1000	1000

1000 1000 1000 1000 1000

TEST SPECIMEN	TEST SPECIMEN	TEST SPECIMEN	TEST SPECIMEN	TEST SPECIMEN
1000	1000	1000	1000	1000
1000	1000	1000	1000	1000
1000	1000	1000	1000	1000

1000 1000 1000 1000 1000

TEST SPECIMEN	TEST SPECIMEN	TEST SPECIMEN	TEST SPECIMEN	TEST SPECIMEN
1000	1000	1000	1000	1000
1000	1000	1000	1000	1000
1000	1000	1000	1000	1000

1000 1000 1000 1000 1000

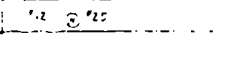
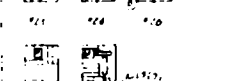
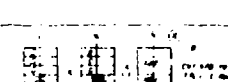
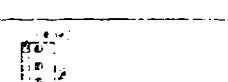
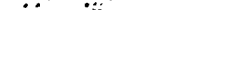
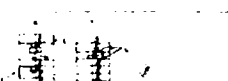
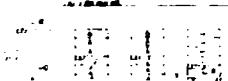
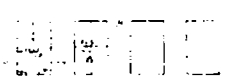
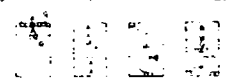
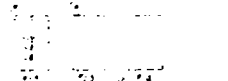
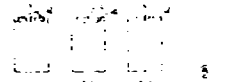
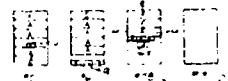
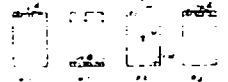
TEST SPECIMEN	TEST SPECIMEN	TEST SPECIMEN	TEST SPECIMEN	TEST SPECIMEN
1000	1000	1000	1000	1000
1000	1000	1000	1000	1000
1000	1000	1000	1000	1000

1000 1000 1000 1000 1000

TEST SPECIMEN	TEST SPECIMEN	TEST SPECIMEN	TEST SPECIMEN	TEST SPECIMEN
1000	1000	1000	1000	1000
1000	1000	1000	1000	1000
1000	1000	1000	1000	1000

1000 1000 1000 1000 1000

1000 1000 1000 1000 1000



FATIGUE (RELIABLE)



FATIGUE (EXCESSIVE)



FATIGUE CRACK



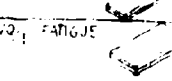
FATIGUE



FATIGUE



FATIGUE



25-A
26-A
27-A
28-A
29-A
30-A
31-A
32-A
33-A
34-A
35-A
36-A
37-A
38-A
39-A
40-A
41-A
42-A
43-A
44-A
45-A
46-A
47-A
48-A
49-A
50-A
51-A
52-A
53-A
54-A
55-A
56-A
57-A
58-A
59-A
60-A
61-A
62-A
63-A
64-A
65-A
66-A
67-A
68-A
69-A
70-A
71-A
72-A
73-A
74-A
75-A
76-A
77-A
78-A
79-A
80-A
81-A
82-A
83-A
84-A
85-A
86-A
87-A
88-A
89-A
90-A
91-A
92-A
93-A
94-A
95-A
96-A
97-A
98-A
99-A
100-A
101-A
102-A
103-A
104-A
105-A
106-A
107-A
108-A
109-A
110-A
111-A
112-A
113-A
114-A
115-A
116-A
117-A
118-A
119-A
120-A
121-A
122-A
123-A
124-A
125-A
126-A
127-A
128-A
129-A
130-A
131-A
132-A
133-A
134-A
135-A
136-A
137-A
138-A
139-A
140-A
141-A
142-A
143-A
144-A
145-A
146-A
147-A
148-A
149-A
150-A
151-A
152-A
153-A
154-A
155-A
156-A
157-A
158-A
159-A
160-A
161-A
162-A
163-A
164-A
165-A
166-A
167-A
168-A
169-A
170-A
171-A
172-A
173-A
174-A
175-A
176-A
177-A
178-A
179-A
180-A
181-A
182-A
183-A
184-A
185-A
186-A
187-A
188-A
189-A
190-A
191-A
192-A
193-A
194-A
195-A
196-A
197-A
198-A
199-A
200-A
201-A
202-A
203-A
204-A
205-A
206-A
207-A
208-A
209-A
210-A
211-A
212-A
213-A
214-A
215-A
216-A
217-A
218-A
219-A
220-A
221-A
222-A
223-A
224-A
225-A
226-A
227-A
228-A
229-A
230-A
231-A
232-A
233-A
234-A
235-A
236-A
237-A
238-A
239-A
240-A
241-A
242-A
243-A
244-A
245-A
246-A
247-A
248-A
249-A
250-A
251-A
252-A
253-A
254-A
255-A
256-A
257-A
258-A
259-A
260-A
261-A
262-A
263-A
264-A
265-A
266-A
267-A
268-A
269-A
270-A
271-A
272-A
273-A
274-A
275-A
276-A
277-A
278-A
279-A
280-A
281-A
282-A
283-A
284-A
285-A
286-A
287-A
288-A
289-A
290-A
291-A
292-A
293-A
294-A
295-A
296-A
297-A
298-A
299-A
300-A
301-A
302-A
303-A
304-A
305-A
306-A
307-A
308-A
309-A
310-A
311-A
312-A
313-A
314-A
315-A
316-A
317-A
318-A
319-A
320-A
321-A
322-A
323-A
324-A
325-A
326-A
327-A
328-A
329-A
330-A
331-A
332-A
333-A
334-A
335-A
336-A
337-A
338-A
339-A
340-A
341-A
342-A
343-A
344-A
345-A
346-A
347-A
348-A
349-A
350-A
351-A
352-A
353-A
354-A
355-A
356-A
357-A
358-A
359-A
360-A
361-A
362-A
363-A
364-A
365-A
366-A
367-A
368-A
369-A
370-A
371-A
372-A
373-A
374-A
375-A
376-A
377-A
378-A
379-A
380-A
381-A
382-A
383-A
384-A
385-A
386-A
387-A
388-A
389-A
390-A
391-A
392-A
393-A
394-A
395-A
396-A
397-A
398-A
399-A
400-A
401-A
402-A
403-A
404-A
405-A
406-A
407-A
408-A
409-A
410-A
411-A
412-A
413-A
414-A
415-A
416-A
417-A
418-A
419-A
420-A
421-A
422-A
423-A
424-A
425-A
426-A
427-A
428-A
429-A
430-A
431-A
432-A
433-A
434-A
435-A
436-A
437-A
438-A
439-A
440-A
441-A
442-A
443-A
444-A
445-A
446-A
447-A
448-A
449-A
450-A
451-A
452-A
453-A
454-A
455-A
456-A
457-A
458-A
459-A
460-A
461-A
462-A
463-A
464-A
465-A
466-A
467-A
468-A
469-A
470-A
471-A
472-A
473-A
474-A
475-A
476-A
477-A
478-A
479-A
480-A
481-A
482-A
483-A
484-A
485-A
486-A
487-A
488-A
489-A
490-A
491-A
492-A
493-A
494-A
495-A
496-A
497-A
498-A
499-A
500-A
501-A
502-A
503-A
504-A
505-A
506-A
507-A
508-A
509-A
510-A
511-A
512-A
513-A
514-A
515-A
516-A
517-A
518-A
519-A
520-A
521-A
522-A
523-A
524-A
525-A
526-A
527-A
528-A
529-A
530-A
531-A
532-A
533-A
534-A
535-A
536-A
537-A
538-A
539-A
540-A
541-A
542-A
543-A
544-A
545-A
546-A
547-A
548-A
549-A
550-A
551-A
552-A
553-A
554-A
555-A
556-A
557-A
558-A
559-A
560-A
561-A
562-A
563-A
564-A
565-A
566-A
567-A
568-A
569-A
570-A
571-A
572-A
573-A
574-A
575-A
576-A
577-A
578-A
579-A
580-A
581-A
582-A
583-A
584-A
585-A
586-A
587-A
588-A
589-A
590-A
591-A
592-A
593-A
594-A
595-A
596-A
597-A
598-A
599-A
600-A
601-A
602-A
603-A
604-A
605-A
606-A
607-A
608-A
609-A
610-A
611-A
612-A
613-A
614-A
615-A
616-A
617-A
618-A
619-A
620-A
621-A
622-A
623-A
624-A
625-A
626-A
627-A
628-A
629-A
630-A
631-A
632-A
633-A
634-A
635-A
636-A
637-A
638-A
639-A
640-A
641-A
642-A
643-A
644-A
645-A
646-A
647-A
648-A
649-A
650-A
651-A
652-A
653-A
654-A
655-A
656-A
657-A
658-A
659-A
660-A
661-A
662-A
663-A
664-A
665-A
666-A
667-A
668-A
669-A
670-A
671-A
672-A
673-A
674-A
675-A
676-A
677-A
678-A
679-A
680-A
681-A
682-A
683-A
684-A
685-A
686-A
687-A
688-A
689-A
690-A
691-A
692-A
693-A
694-A
695-A
696-A
697-A
698-A
699-A
700-A
701-A
702-A
703-A
704-A
705-A
706-A
707-A
708-A
709-A
710-A
711-A
712-A
713-A
714-A
715-A
716-A
717-A
718-A
719-A

1	100-154	100-154	100-154
2	100-154	100-154	100-154
3	100-154	100-154	100-154
4	100-154	100-154	100-154
5	100-154	100-154	100-154
6	100-154	100-154	100-154
7	100-154	100-154	100-154
8	100-154	100-154	100-154
9	100-154	100-154	100-154
10	100-154	100-154	100-154
11	100-154	100-154	100-154
12	100-154	100-154	100-154
13	100-154	100-154	100-154
14	100-154	100-154	100-154
15	100-154	100-154	100-154
16	100-154	100-154	100-154
17	100-154	100-154	100-154
18	100-154	100-154	100-154
19	100-154	100-154	100-154
20	100-154	100-154	100-154
21	100-154	100-154	100-154
22	100-154	100-154	100-154
23	100-154	100-154	100-154
24	100-154	100-154	100-154
25	100-154	100-154	100-154
26	100-154	100-154	100-154
27	100-154	100-154	100-154
28	100-154	100-154	100-154
29	100-154	100-154	100-154
30	100-154	100-154	100-154
31	100-154	100-154	100-154
32	100-154	100-154	100-154
33	100-154	100-154	100-154
34	100-154	100-154	100-154
35	100-154	100-154	100-154
36	100-154	100-154	100-154
37	100-154	100-154	100-154
38	100-154	100-154	100-154
39	100-154	100-154	100-154
40	100-154	100-154	100-154
41	100-154	100-154	100-154
42	100-154	100-154	100-154
43	100-154	100-154	100-154
44	100-154	100-154	100-154
45	100-154	100-154	100-154
46	100-154	100-154	100-154
47	100-154	100-154	100-154
48	100-154	100-154	100-154
49	100-154	100-154	100-154
50	100-154	100-154	100-154
51	100-154	100-154	100-154
52	100-154	100-154	100-154
53	100-154	100-154	100-154
54	100-154	100-154	100-154
55	100-154	100-154	100-154
56	100-154	100-154	100-154
57	100-154	100-154	100-154
58	100-154	100-154	100-154
59	100-154	100-154	100-154
60	100-154	100-154	100-154
61	100-154	100-154	100-154
62	100-154	100-154	100-154
63	100-154	100-154	100-154
64	100-154	100-154	100-154
65	100-154	100-154	100-154
66	100-154	100-154	100-154
67	100-154	100-154	100-154
68	100-154	100-154	100-154
69	100-154	100-154	100-154
70	100-154	100-154	100-154
71	100-154	100-154	100-154
72	100-154	100-154	100-154
73	100-154	100-154	100-154
74	100-154	100-154	100-154
75	100-154	100-154	100-154
76	100-154	100-154	100-154

[illegible][illegible]

- [illegible]

Figure 68

PRELIMINARY DESIGN DRAWING

6AL-4V Ti BRAZED LAMINA
MECHANICAL PROPERTIES TEST
DEVELOPMENT TEST PROGRAM

DATE: 10-1-73

SPECIAL DYNAMICS

General Dynamics Corporation
Aircraft Division

603R100-95

2

10 NI STEEL MATERIAL PROPERTIES

DESIGN ALLOWABLES			FATIGUE					
SPECIMEN	STOCK THICKNESS	NUMBER OF SPECIMENS	SPECIMEN	STOCK THICKNESS	TEST CONDITIONS			
					NUMBER OF SPECIMENS	R	GRAIN	SEE NOTE
TENSION (PLATE) FTJ-10380-1	250	GE DA L LT HEAT NO 1 2 3 4 2 3 4 5 3 4 5 6	 FTJ-10340-183	625	22	0.1	L	2
COMPRESSION (PLATE) FTJ-10380-18	250	GR DR L HEAT NO 1 2 3 4 2 3 4 5 3 4 5 6	 FTJ-10340-133	500	22	0.1	L	2
SHEAR-DOUBLE (PLATE) FTJ-10340-161	250	GR DR L HEAT NO 1 2 3 4 2 3 4 5 3 4 5 6	 FTJ-10340-134	500	22	0.1	L	2
BEARING FTJ-10340-163	250	GR DR L HEAT NO 1 2 3 4 2 3 4 5 3 4 5 6	 FTJ-10340-135	500	22	0.1	L	2
				SEAM, DIRECTION FTJ-10340-135 SPECTRUM				
				ALL TESTS CONDUCTED UNDER CERTAIN CONDITIONS: 1. TEST 5 SPECIMENS AT EACH OF 8 STRESS LEVELS 2. TEST 5 SPECIMENS AT EACH OF 8 STRESS LEVELS AND 7 SPECIMENS TO DEFINE ENDURANCE LIMIT NOTES				

SPECIMEN	
FRACTURE TOUGHNESS FTJ-10340-1	
FATIGUE CRACK GROWTH FTJ-10340-100	
SPECTRUM/ENVIRONMENTAL FATIGUE CRACK GROWTH FTJ-10340-1	
SEE NOTE 6 FTJ-10340-1	

SPECIMEN	
FRACTURE TOUGHNESS FTJ-10340-1	
FATIGUE CRACK GROWTH FTJ-10340-100	
SPECTRUM/ENVIRONMENTAL FATIGUE CRACK GROWTH FTJ-10340-1	
SEE NOTE 6 FTJ-10340-1	

SPECIMEN	
FRACTURE TOUGHNESS FTJ-10340-1	
FATIGUE CRACK GROWTH FTJ-10340-100	
SPECTRUM/ENVIRONMENTAL FATIGUE CRACK GROWTH FTJ-10340-1	
SEE NOTE 6 FTJ-10340-1	

SPECIMEN	
FRACTURE TOUGHNESS FTJ-10340-1	
FATIGUE CRACK GROWTH FTJ-10340-100	
SPECTRUM/ENVIRONMENTAL FATIGUE CRACK GROWTH FTJ-10340-1	
SEE NOTE 6 FTJ-10340-1	

SPECIMEN	
FRACTURE TOUGHNESS FTJ-10340-1	
FATIGUE CRACK GROWTH FTJ-10340-100	
SPECTRUM/ENVIRONMENTAL FATIGUE CRACK GROWTH FTJ-10340-1	
SEE NOTE 6 FTJ-10340-1	

SPECIMEN	
FRACTURE TOUGHNESS FTJ-10340-1	
FATIGUE CRACK GROWTH FTJ-10340-100	
SPECTRUM/ENVIRONMENTAL FATIGUE CRACK GROWTH FTJ-10340-1	
SEE NOTE 6 FTJ-10340-1	

SPECIMEN	
FRACTURE TOUGHNESS FTJ-10340-1	
FATIGUE CRACK GROWTH FTJ-10340-100	
SPECTRUM/ENVIRONMENTAL FATIGUE CRACK GROWTH FTJ-10340-1	
SEE NOTE 6 FTJ-10340-1	

SPECIMEN	
FRACTURE TOUGHNESS FTJ-10340-1	
FATIGUE CRACK GROWTH FTJ-10340-100	
SPECTRUM/ENVIRONMENTAL FATIGUE CRACK GROWTH FTJ-10340-1	
SEE NOTE 6 FTJ-10340-1	

SPECIMEN	
FRACTURE TOUGHNESS FTJ-10340-1	
FATIGUE CRACK GROWTH FTJ-10340-100	
SPECTRUM/ENVIRONMENTAL FATIGUE CRACK GROWTH FTJ-10340-1	
SEE NOTE 6 FTJ-10340-1	

SPECIMEN	
FRACTURE TOUGHNESS FTJ-10340-1	
FATIGUE CRACK GROWTH FTJ-10340-100	
SPECTRUM/ENVIRONMENTAL FATIGUE CRACK GROWTH FTJ-10340-1	
SEE NOTE 6 FTJ-10340-1	

SPECIMEN	
FRACTURE TOUGHNESS FTJ-10340-1	
FATIGUE CRACK GROWTH FTJ-10340-100	
SPECTRUM/ENVIRONMENTAL FATIGUE CRACK GROWTH FTJ-10340-1	
SEE NOTE 6 FTJ-10340-1	

SPECIMEN	
FRACTURE TOUGHNESS FTJ-10340-1	
FATIGUE CRACK GROWTH FTJ-10340-100	
SPECTRUM/ENVIRONMENTAL FATIGUE CRACK GROWTH FTJ-10340-1	
SEE NOTE 6 FTJ-10340-1	

SPECIMEN	
FRACTURE TOUGHNESS FTJ-10340-1	
FATIGUE CRACK GROWTH FTJ-10340-100	
SPECTRUM/ENVIRONMENTAL FATIGUE CRACK GROWTH FTJ-10340-1	
SEE NOTE 6 FTJ-10340-1	

SPECIMEN	
FRACTURE TOUGHNESS FTJ-10340-1	
FATIGUE CRACK GROWTH FTJ-10340-100	
SPECTRUM/ENVIRONMENTAL FATIGUE CRACK GROWTH FTJ-10340-1	
SEE NOTE 6 FTJ-10340-1	

SPECIMEN	
FRACTURE TOUGHNESS FTJ-10340-1	
FATIGUE CRACK GROWTH FTJ-10340-100	
SPECTRUM/ENVIRONMENTAL FATIGUE CRACK GROWTH FTJ-10340-1	
SEE NOTE 6 FTJ-10340-1	

SPECIMEN	
FRACTURE TOUGHNESS FTJ-10340-1	
FATIGUE CRACK GROWTH FTJ-10340-100	
SPECTRUM/ENVIRONMENTAL FATIGUE CRACK GROWTH FTJ-10340-1	
SEE NOTE 6 FTJ-10340-1	

SPECIMEN	
FRACTURE TOUGHNESS FTJ-10340-1	
FATIGUE CRACK GROWTH FTJ-10340-100	
SPECTRUM/ENVIRONMENTAL FATIGUE CRACK GROWTH FTJ-10340-1	
SEE NOTE 6 FTJ-10340-1	

SPECIMEN	
FRACTURE TOUGHNESS FTJ-10340-1	
FATIGUE CRACK GROWTH FTJ-10340-100	
SPECTRUM/ENVIRONMENTAL FATIGUE CRACK GROWTH FTJ-10340-1	
SEE NOTE 6 FTJ-10340-1	

SPECIMEN	
FRACTURE TOUGHNESS FTJ-10340-1	
FATIGUE CRACK GROWTH FTJ-10340-100	
SPECTRUM/ENVIRONMENTAL FATIGUE CRACK GROWTH FTJ-10340-1	
SEE NOTE 6 FTJ-10340-1	

SPECIMEN	
FRACTURE TOUGHNESS FTJ-10340-1	
FATIGUE CRACK GROWTH FTJ-10340-100	
SPECTRUM/ENVIRONMENTAL FATIGUE CRACK GROWTH FTJ-10340-1	
SEE NOTE 6 FTJ-10340-1	

SPECIMEN	
FRACTURE TOUGHNESS FTJ-10340-1	
FATIGUE CRACK GROWTH FTJ-10340-100	
SPECTRUM/ENVIRONMENTAL FATIGUE CRACK GROWTH FTJ-10340-1	
SEE NOTE 6 FTJ-10340-1	

SPECIMEN	
FRACTURE TOUGHNESS FTJ-10340-1	
FATIGUE CRACK GROWTH FTJ-10340-100	
SPECTRUM/ENVIRONMENTAL FATIGUE CRACK GROWTH FTJ-10340-1	
SEE NOTE 6 FTJ-10340-1	

SPECIMEN	
FRACTURE TOUGHNESS FTJ-10340-1	
FATIGUE CRACK GROWTH FTJ-10340-100	
SPECTRUM/ENVIRONMENTAL FATIGUE CRACK GROWTH FTJ-10340-1	
SEE NOTE 6 FTJ-10340-1	

SPECIMEN	
FRACTURE TOUGHNESS FTJ-10340-1	
FATIGUE CRACK GROWTH FTJ-10340-100	
SPECTRUM/ENVIRONMENTAL FATIGUE CRACK GROWTH FTJ-10340-1	
SEE NOTE 6 FTJ-10340-1	

SPECIMEN	
FRACTURE TOUGHNESS FTJ-10340-1	
FATIGUE CRACK GROWTH FTJ-10340-100	
SPECTRUM/ENVIRONMENTAL FATIGUE CRACK GROWTH FTJ-10340-1	
SEE NOTE 6 FTJ-10340-1	

SPECIMEN	
FRACTURE TOUGHNESS FTJ-10340-1	
FATIGUE CRACK GROWTH FTJ-10340-100	
SPECTRUM/ENVIRONMENTAL FATIGUE CRACK GROWTH FTJ-10340-1	
SEE NOTE 6 FTJ-10340-1	

SPECIMEN	
FRACTURE TOUGHNESS FTJ-10340-1	
FATIGUE CRACK GROWTH FTJ-10340-100	
SPECTRUM/ENVIRONMENTAL FATIGUE CRACK GROWTH FTJ-10340-1	
SEE NOTE 6 FTJ-10340-1	

SPECIMEN	
FRACTURE TOUGHNESS FTJ-10340-1	
FATIGUE CRACK GROWTH FTJ-10340-100	
SPECTRUM/ENVIRONMENTAL FATIGUE CRACK GROWTH FTJ-10340-1	
SEE NOTE 6 FTJ-10340-1	

SPECIMEN	
FRACTURE TOUGHNESS FTJ-10340-1	
FATIGUE CRACK GROWTH FTJ-10340-100	
SPECTRUM/ENVIRONMENTAL FATIGUE CRACK GROWTH FTJ-10340-1	
SEE NOTE 6 FTJ-10340-1	

SPECIMEN	
FRACTURE TOUGHNESS FTJ-10340-1	
FATIGUE CRACK GROWTH FTJ-10340-100	
SPECTRUM/ENVIRONMENTAL FATIGUE CRACK GROWTH FTJ-10340-1	
SEE NOTE 6 FTJ-10340-1	

SPECIMEN	
FRACTURE TOUGHNESS FTJ-10340-1	
FATIGUE CRACK GROWTH FTJ-10340-100	
SPECTRUM/ENVIRONMENTAL FATIGUE CRACK GROWTH FTJ-10340-1	
SEE NOTE 6 FTJ-10340-1	

SPECIMEN	
FRACTURE TOUGHNESS FTJ-10340-1	
FATIGUE CRACK GROWTH FTJ-10340-100	
SPECTRUM/ENVIRONMENTAL FATIGUE CRACK GROWTH FTJ-10340-1	
SEE NOTE 6 FTJ-10340-1	

SPECIMEN	
FRACTURE TOUGHNESS FTJ-10340-1	
FATIGUE CRACK GROWTH FTJ-10340-100	
SPECTRUM/ENVIRONMENTAL FATIGUE CRACK GROWTH FTJ-10340-1	
SEE NOTE 6 FTJ-10340-1	

SPECIMEN	
FRACTURE TOUGHNESS FTJ-10340-1	
FATIGUE CRACK GROWTH FTJ-10340-100	
SPECTRUM/ENVIRONMENTAL FATIGUE CRACK GROWTH FTJ-10340-1	
SEE NOTE 6 FTJ-10340-1	

SPECIMEN	
FRACTURE TOUGHNESS FTJ-10340-1	
FATIGUE CRACK GROWTH FTJ-10340-100	
SPECTRUM/ENVIRONMENTAL FATIGUE CRACK GROWTH FTJ-10340-1	
SEE NOTE 6 FTJ-10340-1	

SPECIMEN	
FRACTURE TOUGHNESS FTJ-10340-1	
FATIGUE CRACK GROWTH FTJ-10340-100	
SPECTRUM/ENVIRONMENTAL FATIGUE CRACK GROWTH FTJ-10340-1	
SEE NOTE 6 FTJ-10340-1	

SPECIMEN	
FRACTURE TOUGHNESS FTJ-10340-1	
FATIGUE CRACK GROWTH FTJ-10340-100	
SPECTRUM/ENVIRONMENTAL FATIGUE CRACK GROWTH FTJ-10340-1	
SEE NOTE 6 FTJ-10340-1	

SPECIMEN	
FRACTURE TOUGHNESS FTJ-10340-1	
FATIGUE CRACK GROWTH FTJ-10340-100	
SPECTRUM/ENVIRONMENTAL FATIGUE CRACK GROWTH FTJ-10340-1	
SEE NOTE 6 FTJ-10340-1	

SPECIMEN	
FRACTURE TOUGHNESS FTJ-10340-1	
FATIGUE CRACK GROWTH FTJ-10340-100	
SPECTRUM/ENVIRONMENTAL FATIGUE CRACK GROWTH FTJ-10340-1	
SEE NOTE 6 FTJ-10340-1	

SPECIMEN	
FRACTURE TOUGHNESS FTJ-10340-1	
FATIGUE CRACK GROWTH FTJ-10340-100	
SPECTRUM/ENVIRONMENTAL FATIGUE CRACK GROWTH FTJ-10340-1	
SEE NOTE 6 FTJ-10340-1	

SPECIMEN	
FRACTURE TOUGHNESS FTJ-10340-1	
FATIGUE CRACK GROWTH FTJ-10340-100	
SPECTRUM/ENVIRONMENTAL FATIGUE CRACK GROWTH FTJ-10340-1	
SEE NOTE 6 FTJ-10340-1	

SPECIMEN	
FRACTURE TOUGHNESS 	

FATIGUE

TEST CONDITIONS

Figure 69

277-100000 (277-100000) GENERAL DYNAMICS Convair Aerospace Division For your records	603R100-61 277-100000
------------------------------------------------------------------------------------------------------	--------------------------

Table 15

10 Nickel Steel Test Data

Heat No. C52106
Plate Size 1" X 48" X 72"

<u>Chemical Composition percent</u> [*]												
<u>C</u>	<u>Mn</u>	<u>P</u>	<u>S</u>	<u>Si</u>	<u>Ni</u>	<u>Cr</u>	<u>Mo</u>	<u>Co</u>	<u>O</u>	<u>Al**</u>	<u>N</u>	<u>Ti</u>
0.12	0.09	0.004	0.007	0.03	10.12	2.01	0.98	7.81	0.00005	0.002	0.002	0.01

*Plate check analyses.

**Total.

Tensile Properties

<u>Plate No.</u>	<u>Test Orientation</u>	<u>Yield Strength (0.2% Offset), psi</u>	<u>Tensile Strength, psi</u>	<u>Elongation in 2 Inches, %</u>	<u>Reduction of Area, %</u>
OF4617A	L*	183,500	198,900	16.5	70.7
	L	182,200	198,700	16.5	70.5
	T*	183,200	200,200	15.5	68.4
	T	183,500	200,100	16.0	69.4
OF4617B	L	183,000	198,000	16.0	70.9
	L	181,800	196,900	16.5	71.5
	T	179,300	196,400	15.5	68.7
	T	183,000	197,000	15.5	68.9
OF4617C	L	181,500	197,000	16.5	70.9
	L	183,200	197,000	16.5	71.5
	T	185,000	198,700	15.5	67.9
	T	185,200	199,200	16.5	70.1

(Continued)

Table 15 (Continued)

Tensile Properties (Continued)

Plate No.	Test Orientation	Yield Strength (0.2% Offset), psi	Tensile Strength, psi	Elongation in 2 Inches, %	Reduction of Area, %
OF4617D	L	181,000	197,000	16.5	71.4
	L	181,000	196,000	16.5	71.6
	T	182,000	197,000	16.5	69.7
	T	182,000	196,000	16.5	69.6

CVN Impact Values at 0 F

Plate No.	Test Orientation	Energy Ft-lb	Lateral Expansion, mils	Hardness RC
OF4617A	L	81, 81, 79	35, 35, 34	42
	T	76, 75, 78	34, 34, 34	43
OF4617B	L	77, 78, 78	34, 35, 34	43
	T	81, 80, 80	37, 38, 37	41
OF4617C	L	76, 81, 77	36, 36, 33	43
	T	80, 80, 75	32, 35, 32	44
OF4617D	L	85, 85, 90	42, 41, 40	43
	T	83, 90, 89	37, 39, 40	43

* L = Longitudinal and T = Transverse.

Heat Treatment: 1625 F WQ
1500 F WQ
950 F (5 hr.) WQ

Table 16 ACCEPTANCE DATA 6A1-4V TITANIUM BETA ANNEALED

CUTTING Spec. No.	Heat No.	REACTIVE METALS, INC., DATA										CONVAIR DATA										GSA Claim Number
		C	N	Fe	Al	V	O	H (PPM)	Tensile (Ksi) L/T	Yield (Ksi) L/T	el (%) L/T	RA	R _w Kic (Ksi/in)	RQ (Ksi/in)	(%) al	(%) V	(PPM) H ₂	Tensile (Ksi) (L)	Yield (Ksi) L	(%) al	(%) V	
A270-1-1	295398-02	.02	.02	.17	6.2	4.0	.140	127	138.1 142.8	122.1 125.0	10/10	-			5.7	4.1	110	136.0	125.5	10		-4-33
A295-3-1	295501-02	.02	.009	.20	6.2	4.0	.114	81	139.4 140.3	128.2 129.4	12/11				5.7	3.7		134.6	128.8	6		-4-33
A330-6-1	295553-02	.02	.009	.18	6.1	4.0	.112	105	140.0 141.5	123.9 127.0	11/11				5.5	3.6	94					-4-33
-2	Same								135.7 140.7	128.0 125.0	11/10											
-3	Same								138.8 138.8	123.8 124.5	10/10											
-4	Same								138.5 140.5	123.1 126.5	11/10											
A370-7-1	295561-02	.010	.20	5.1	4.0	.126		77	132.6 135.8	120.5 122.8	12/13				5.5	3.8	56	137.4	122.6	11.8		-8-75
-2	Same								139.0 140.5	124.9 126.1	12.0/10.0		58.8	99.6	5.6	3.8	91	139.4	120.9	9.3		-4-40
A590-1-1	295549-02	.010	.19	5.9	3.9	.107		98	137.8 139.4	124.2 126.0	12.0/11.0											
A675-5-1	295551-02	.010	.21	6.1	4.0	.108		73	135.8 136.0	122.5 133.7	10/10	26/25		75.9	5.5	3.7	72	136.1	121.5	9*		-4-66
-2	Same								135.1 136.8	122.0 122.3	10/10	23/25										
A760-8-1	304581-02	.011	.22	6.0	3.9	.110		60	134.1 135.1	123.0 124.5	10/11		67.6	97.2	5.5	3.8	60	132.6	112.7	9.3		-3-21
-2	Same								133.7 134.1	123.7 123.2	11/10											
-3	Same								134.9 135.3	126.1 125.1	10/10											
-4	Same								133.0 136.3	123.7 123.8	12/11											
-5	Same								133.4 133.8	124.7 123.1	12/10											
-6	Same								134.1 135.7	123.9 125.1	12/10											
-7	Same								133.6 134.8	125.0 126.0	10/10											

Table 16 (Contd)

REACTIVE METALS INC. DATA															CONVAIR DATA										GSA (claim Number
Cutting Spec. No.	Heat No.	Z					H (PPM)	Tensile (Ksi)		Yield (Ksi) L/T	e1 (%) L/T	7RA	RW Kic (Ksi in)	RW RO (Ksi in)	(2) u1 V	(2) H2	Tensile (Ksi) (L)	Yield (Ksi) (L)	(2) e1	Kic (Ksi in)					
		C	N	Fe	al	V		O	L/T												L/T				
A760-8-8	304581	.02	.011	.22	6.0	3.5	.110	60	132.4 132.2	123.6 123.7	11/10														
-9		Same							135.8 136.3	126.7 124.6	11/11														
A760-6-1	295353	.02	.009	.18	6.1	4.0	.112	74	131.4 132.8	123.5 119.2	12/12		67.6	97.2	5.6	3.8	80	130.1	122.2	12.9		-4-71			
A1030-7-1	295361	.02	.010	.20	6.1	4.0	.126	45	132.3 134.7	118.4 121.4	10/11			78.3*	5.5	3.8	41	131.4	122.4	11.0		-8-86			
A2290-9-1	304383	.02	.011	.21	5.8	3.8	.116	62	131.1 132.4	113.4 115.9	10/9		88.2	106.0	5.5	3.8	38				93 (RW)	-8-102			
A2567-4-1	295349	.02	.010	.19	5.9	3.9	.114	35	125.2 128.9	120.6 118.8	10/9			80.7*	5.5	3.6	50	129.6	122.8	6.3	113 (RW)	-5-86			
-2		Same																							
A2780-7-1	295399	.02	.011	.17	6.1	4.0	.103	30	132.3 133.6	117.8 120.0	11/10			76.4	5.5	4.0	60	130.3	122.5	9.3	109 (RW)	-8-13			
A1750-10-1	304400	.02	.009	.21	6.1	4.0	.112	64	129.5 131.3	116.5 118.5	11/10			106.0*								-8-22			
A1750-10-2		.02	.009	.21	6.1	4.0	.112	115	131.3 132.3	117.9 119.9	10/10														

* Added 29 May 1973

Beta C Titanium - All the required materials for the test programs have been received. A total list of the materials received is included in Table 17. The chemical composition of the three (3) different heats are as follows:

Element	Specification	Weight Percent		
		Heat No. 304324	Heat No. 600393	Heat No. 690507
Carbon	.05	.02	.02	.01
Nitrogen	.03	.011	.014	.012
Iron	.30	.06	.06	.06
Aluminum	3.0-4.0	3.4	3.4	3.4
Vanadium	7.5-8.5	8.3	8.2	8.1
Chromium	5.5-6.5	5.8	5.9	5.6
Molybdenum	3.5-4.5	4.2	4.1	3.6
Zirconium	3.5-4.5	3.9	3.4	4.3
Oxygen	.12	.110	.093	.102
Hydrogen	.02*	*		

*All heats are within specification values. Each product of each was inspected.

The requirements for 90 inches wide Beta C was eliminated when the DTIL design configuration was eliminated at the end of Phase Ib. The orders for the material was cancelled and no further evaluation or studies of wide sheet are planned during the AMAVS program.

Table 17
Beta C Titanium Received

SIZE	QUANTITY	RMI HT NO
.040 X 38.5 X 113	2	304324
.050 X 38.5 X 101	2	
.125 X 36 X 99	1	
.125 X 37 X 100	1	
.125 X 38 X 103*	2	
.125 X 38 X 97	1	
.125 X 38 X 97	1	
.125 X 36 X 97	1	
.125 X 38 X 101	1	
.125 X 38 X 97	1	
.125 X 38 X 96	1	
.125 X 37 X 97	2	304324

Table 17 (Continued)

SIZE	QUANTITY	RMI HT NO
.160 X 11 X 21	1	304324
.625 X 25 X 37	1	↓
2.500 X 24 X 24	1	304324
.062 X 36 X 92	1	600393
.062 X 36 X 94	1	↓
.100 X 36 X 96	2	↓
.125 X 36 X 96	16	↓
.375 X 36 X 96	1	↓
2.500 X 24 X 24	1	600393
.125 X 36 X 96	2	690507
2.500 X 24 X 24	1	690507

* Rolled and Pickled to size, all other sheet product rolled, grounded and pickled

Brazing Alloy - Approximately 51 pounds of Dynabraz B brazing has been received. The chemical composition and certification are included in AFFDL-TR-73-40. Additional alloy will be required for Phase II component tests.

3.1.4.3 Materials Testing

Materials Data Report - Convair Report No. FZM-6148 has been prepared covering the majority of the test data that has been generated. This report is the first of four (4) interim reports and a final report which are to be prepared for this program. The scope of the test program, the test procedures used, test equipment description, test specimen configurations and test data are included.

Significant Data - The first Beta C titanium spectrum crack growth test was completed. The specimen had two .12 inch long center cracks; one in sump tank water and one in dry air. The crack in sump tank water grew to critical size (1.6 inches) in twelve flights while the crack in dry air did not grow a measurable amount. The cause of the early failure is being investigated. Crack propagation tests (da/dN) and stress corrosion tests (K_{Isc}) have been given priority in the test program. Metallurgical examinations indicate intergranular crack growth with possible signs of stress corrosion. Data on weldments and brazed joints are included later in this section.

3.1.4.4 Brazing Development

A list of brazed specimens with details of the braze cycling and comments are listed in Table 18 . Twenty seven (27) braze assemblies have been cycled since 15 March 1973 without a leaking retort with no contamination, good wetting, and predictable NDI results. The 603R100-3 test plan has been maintained with changes to the plan as noted on the "J" revision, Figure 68 . One of the overlapping plank specimens has been dropped since this design concept has been abandoned. The surface finish of the interface surfaces remains the most critical factor. Steps of over .001 in. result in braze raids. Non contacting surfaces between silver and titanium between layers of silver is susceptible to contamination by whatever atmosphere is present.

The second 603FTB005 panel brazed on 2 March 1973, originally reported as a good braze, was found to have approximately 10% braze at the interface. Two layers of braze alloy (.002" and .005") were used to supplement steps at plank intersections due to slight variations in plank thicknesses. The .002" silver brazing alloy foil was tack welded to one layer of planks and the .005 foil was tack welded to the other layer of planks. A subsequent destruction test showed the braze alloy to have wet the titanium surfaces consistently but due to the atmosphere contamination trapped in the pockets in the center of the panel, the interfaces of the two (2) layers of silver alloy oxidized and did not wet at the brazing temperature. Prior and subsequent test plates did not have pockets and excellent braze joints resulted. Note the VQ/I bend shear results of panels No. 2 and 19 in Table 19 . It is reasonable to assume some contamination occurred on the interfaces of the silver braze foil next to the titanium but the reaction at the braze temperature was sufficient to overcome the oxidation and produce wetting. The radiograph results did not agree with the ultrasonic inspection results. The radiograph indicated a 98% braze based on the presence of silver. The ultrasonic inspection indicated fair correlation with the destruction test results. See Figure 70 for microsection of the B005 brazed panel. Note the lack of wetting between the two layers of silver alloy. The configuration of the panel contributed to the lack of correlation. Correlation on other panels and brazed specimens have increased confidence in ultrasonic inspection to the point that it should be mandatory (in conjunction with X-ray) to insure reliability of any brazed assembly. In the future, brazed assemblies with pockets will be tooled to insure the removal of atmosphere from all portions of the assembly.

Table 18

BRAZED SPECIMENS

PRIORITY	MS&D BZ PANELS TEST	BRAZE TIME MIN.	TEMP. C _F	VAC.	CFH ARGON	AG, AL, NO., ALLOY	BUTTONS	BRAZE DATE	REMARKS
603R100-1	16	2	1575	15"	10	0.005	.002 X 1/8	12/22/72	
Brazing Temperature	17	2	1575	15"	10		.002 X 1/8	12/28/72	
	15	2	1550	15"	10			1/1/73	
NDI (ND3187-1, -2)	18	2	1600	15"	10			1/4/73	
Braze Time	11	2	1575	15"	10			1/25/73	
	2	2	1575	15"	10			1/8/73	
NDI	14A	30	1530	25"	10			1/30/73	Good BZ
603FTB001	1st	5	1575	15"	10		.002 X 1/8"	2/3/73	1/2" Fiberfrax on top, poor braze
603FTB004	1st	2	1530	10"	10-OFF @ 600°F		.002 X 1/8" X 1/4"	2/2/73	Retort 2/3/73
	1st	1 (hr) @	1350	25"	10-OFF @ 1400°F				1/2" Fiberfrax
603FTB013	1st	2	1530		10		.002 X 1/8" X 1/4"	1/10/73	
	2nd	2	1575	20"	10		.002 X 1/8" X 1/4"	1/12/73	
603R100-3	36-37	2	1575	20"	10-OFF/600°F	0.005	.002 X .125	2/6/73	First re' forced weld; very clean parts.
			1540	10"					
603R100-1 H.T. Cycle	1st	10	1650	3	10	NO	NO	1/24/73	
603R100-1 Weld Plates	2nd	10	1650	3	10	NO	NO	2/2/73	
603R100-1	4	5	1530	25"	10-OFF/600°F	0.005	.002 X .125	1/26/73	Sanded surfaces, Good BZ
Surface Finish	12	2	1575	20"	10		.002 X .125	1/16/73	Poor Braze
603R100-3	25	5	1530	20"	10		.002 X .125	1/18/73	Poor Braze (.002 X .125 Cres Steel Boundary)
							.002 X .125		Good Braze (.002 X .125 Cres Steel Boundary)
(Double Cycle Preform)		5	1530	20"	10-OFF/600°F			1/24/73	Very Good Braze
(Single Cycle Preform)	14	5	1550	25"	10-OFF/600°F		.002 X .125	1/25/73	2 Panels Brazed in B005
	12A	5	1550	10"	5		.002 X .125	2/22/73	Retort for dummy run.
	25A	5	1550	10"	5		.002 X .125	2/22/73	Good braze on both panels.
	44	5	1550	10"	10-OFF/800°F		.002 X .125	2/27/73	2 Panels brazed in B005
	45	5	1550	10"	10-OFF/800°F		.002 X .125	2/27/73	Retort for 2nd dummy run.
603R100-3	1st	5	1550	10"	10-OFF/800°F		.002 X .125	2/27/73	Good braze on both panels.
	2nd	5	1550	10"	10-OFF/800°F	0.005	.002 X .125	2/17/73	Good braze - Crack arrest demonstration specimen.
603FTB05C							.002 X .125 & .250	3/5/73	Good Braze

TABLE 18 (Cont.)

BRAZED SPECIMENS

PRIORITY	MSD BZ PANELS TEST	BRAZE TIME MIN.	TEMP. C _F	VAC.	CFH ARGON	Ag, Al, Mn, Alloy	BUTTONS	BRAZE DATE	REMARKS
603FTB015 603FTB014 603FTB100-3	2nd	2	1550	10"	10-OFF/800°F	.001/.005	.002 X .125	3/2/73	Poor Braze
	2nd	5	1550	10"	10-OFF/800°F	.005	.002 X .125 + .250	3/9/73	Good Braze
	30	2	1550	10"	10-OFF/800°F	.002	.001 X .125	2/14/73	Poor Braze
	31, 32						NO	3/15/73	
	33, 34						NO	3/15/73	
	35, 40					.005	.002 X .125	3/19/73	
	38, 39					.002	NO	3/19/73	
	41, 42					.005	.002 X .125	3/20/73	
	43							3/22/73	Poor Braze
	13A	10		10"				3/23/73	1500/Hr Slow Cool
(Gaps) (Gaps) (Preplaced Voids) (Preplaced Voids) 603RI00-3 (Plan) NDI, MD 3208-1 3209-1 603RI00-3 603RI00-3	8	2		5"			.002 X .125	3/27/73	Good Braze
	1			10"		.005	NO	3/28/73	63 RMS, Good Braze
	2					.007	.002 X .125	3/28/73	125 RMS, Good Braze
	3					.005		4/11/73	250 RMS, Poor Braze
	5							3/29/73	125 RMS
	6					.005		3/30/73	125 RMS, Good Braze
	7			15" to 13750F		.005		3/30/73	Brazed 1 day after cleaning
	19			5"		.007		4/13/73	125 RMS, Good Braze
	20					.005		4/6/73	Good Braze
	23							5/18/73	Good Braze
603RI00-3 NDI, MD 3208-1 3209-1 603RI00-3 603RI00-3	24							5/23/73	Good Braze
	21			10"				4/23/73	Poor Braze
	26							5/14/73	Preplaced Voids
	10	2	1550	5"	10-OFF/800°F	.005	.002 X .125	5/30/73	In X-Ray
	7B			10"				4/18/73	250 RMS Planer Finish Good Braze

Table 19

BRAZED PANEL (603R100-3)
VQ/I SHEAR DATA*

SPECIMEN NO.	SPECIMEN DIMENSIONS			SUPPORT SPACING	LOAD (LBS)	SHEAR (PSI)	BZ JOINT FAILURE	COMMENT
	L	W	T					
BZ16-J1C -J2C -J3C -J4C -J5C -J6C	2.5	.5 .5	.25/.25	1.625	14,800 12,250 12,950 14,250 11,400 12,700	59,000 49,000 51,700 57,000 45,500 50,800	Yes	No Void 20% Void 10% Void No Void 20% Void No Void
BZ17-J1C -J2C -J3C -J4C -J5C -J6E	 2.5 4.0	.45		 1.625 3.5 1.625	12,200 12,000 8,900 11,800 15,950 13,700	53,800 52,800 39,200 52,000 60,200	 Yes No Yes	No Void No Void 20% Void 5% Void Bending demonstration No Void
BZ15-Q1E -Q2E -Q3E -Q4E -Q5E -Q6E -Q7E -Q8E -Q9E	 4.0	 .45		 1.625 3.5 1.625	10,900 10,500 10,100 12,490 12,100 11,000 9,850 10,400 10,000	48,000 46,200 44,500 55,000 53,100 48,400 45,800 44,000	 Yes No Yes Yes No	No Void 10% Void 10% Void 5% Void No Void 20% Void 20% Voids bending demonstration 5% scattered void 5% scattered void
BZ18-Z1C -Z2C -Z3C					12,000 10,000 11,500	52,800 44,000 51,500	Yes	No Void 20% Void 15% Void
BZ11-Q1E -Q2E -Q3E -Q4E -Q5E -Q6E -Q7E	 4.0	 .45		 1.625 3.5	10,500 10,600 10,000 10,900 9,600 10,800 15,350	46,200 46,600 44,000 48,000 42,200 47,500	 Yes No	No Void No Void No Void - bending demonstration
BZ13-J1E -J2E -J3E -J4E		.40 .40		1.625	8,000 9,400 8,000 9,300	40,000 47,000 40,000 46,500	Yes	27% Void 27% Void 27% Void 27% Void
BZ14-N1E -N2E -N3E -N4E	 4.0	.45 .45	 .25/.25	 1.625	9,800 9,000 9,200 9,300	44,000 40,500 41,400 41,700	 Yes	10% Void 10% Void 10% Void 10% Void

TABLE 19 (Continued)

SPECIMEN NO.	SPECIMEN DIMENSIONS			SUPPORT SPACING	LOAD (LBS)	SHEAR (PSI)	BZ JOINT FAILURE	COMMENT
	L	W	T					
BZ4-Q1E -Q2E -Q3E	2.5	.50	.25/.25	1.625	16,000 16,100 16,400	64,000 64,400 65,600	Yes Yes No	No void 3% void No void
BZ1-Q1E -Q2E -Q3E					11,700 11,400 10,400	46,700 45,500 45,500	Yes	No void
BZ2-Q1E -Q2E -Q3E					11,500 10,800 11,500	46,000 43,200 46,000		2% void, button No void
BZ5-J1C -J2C -J3C					11,800 11,300 11,600	47,200 45,200		, thin braze
BZ-Q1E -Q2E -Q3E					10,600 11,000 11,900	42,400 44,000 47,500		
BZ7-M1C -M2C -M3C					11,150 11,400 12,400	44,500 45,600 49,600		No void 5% void No void
BZ8-Q1E -Q2E -Q3E					12,200 12,050 12,500	48,700 48,100 50,000	Yes	5% void No void No void
BZ-12A-J1C -J2C -J3C		.50 .45 .45			10,700 8,800 8,800	35,500 35,500	No Yes	Failed in bending No void No void
BZ13A-P1E -P2C -P3C		.50			9,600 10,500 9,800	38,400 42,000 39,100		10% void, (Lines) No void 50% void, (Lines)
BZ14-Q1C -Q2C -Q3C					12,900 12,300 10,700	51,500 49,100 42,800		3% void No void 30% scattered void
BZ19-L1E -L2C -L3C					12,300 10,500 11,800	49,200 42,000 47,200		10% void, (groove) 20% void, (groove) 15% void, (groove)
BZ25A-Q1C -Q2C -J1E	2.5	.50	.25/.25	1.625	11,000 10,700 10,100	44,000 42,800 40,400	Yes	3% void No void 5% void

- *1. Strips were sawed from panels. Dim. are $\pm .03$
2. Loads are maximum at braze line failure - Yielding was noted prior to failure.
3. Specimens not failed had load removed after yielding.
4. VQ/I shear stress based on fully plastic bending stress distributions which are not applicable at the failure loads shown.
5. Estimated percentage void listed in "comment" based on interface area of specimens delaminated and X-ray of specimens not delaminated.
6. "C" denotes specimen removed from other than edge of panel.
"E" denotes specimen removed from edge of panel.

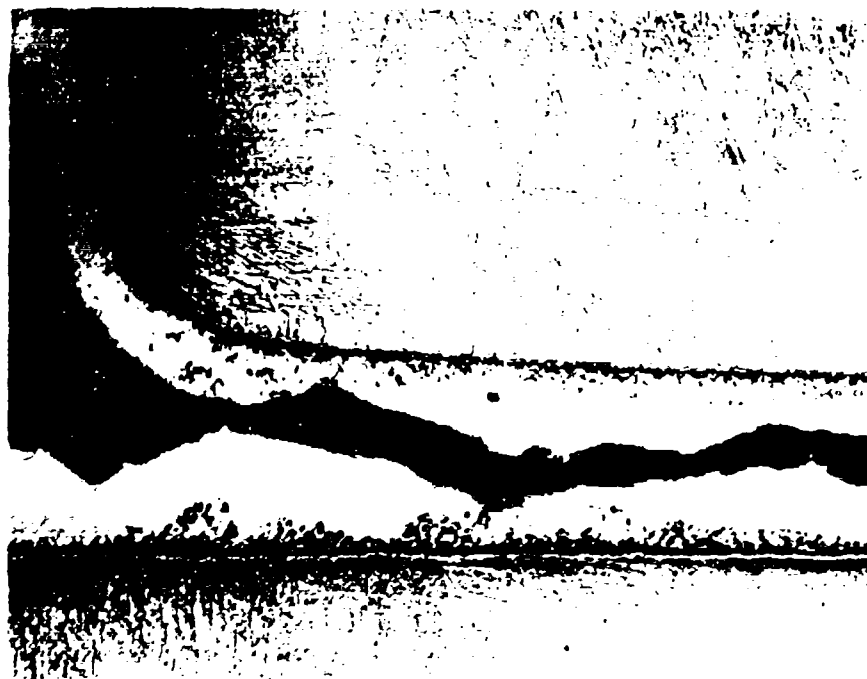


Figure 70 603FTB005 NUMBER 2 BRAZE ASSEMBLY 200X
(1% HF, 2% HNO₃ ETCH)

The VQ/I shear data is shown in Table 19 for specimens from 19 panels. Shear data from the last 11 panels was very consistent and high. It is interesting to note that even with large voids created by the .002, .005, .020 grooves cut in one plate lamina (panel 19) the shear strength was high.

The sustained load stress corrosion resistance lap shear testing is listed in Table 20. All but one of the single lap shear specimen from panel 11 have failed at less than 1000 hours. Specimens from panels 14, 7, 1, 4, and 8 have indicated no early failures with the exception of specimen BZ1-12 from panel 1 in Group IV. Metallography will be performed on representative specimens to establish cause of failure. The data from double-double lap shear specimens has been inconsistent. With four interface braze joints per specimen good fit was impractical and overall specimen braze shear strength is inconsistent at best. These tests are in process and will characterize the stress corrosion resistance of titanium brazed with silver-aluminum-manganese alloy.

The environmental sensitivity testing has indicated thus far that the corrosion resistance of the brazed specimen is very good. See Figure 71 for update of data generated to date.

3.1.4.5 Welding Development

The electron beam welded 6Al-4V titanium tensile and fatigue specimens have been tested. See Tables No. 21 and 22 and Figure 72 for tabular and plotted data, respectively. As can be noted on Figure 72 the endurance of EB welded specimen follows closely the fatigue resistance of the parent metal. Only the failure that occurred in the parent metal, weld and heat affected zone, are plotted. A high percentage of specimens were radius and loading hole failures. These failures were of sufficient number of cycles to compare with the weld area failures.

The GTA welding of the 10 Nickel steel (HY180) plates have been completed. Tensile specimens have been prepared and tested (see Table 23). Additional tensile and CVN specimens are being prepared for testing.

3.1.4.6 Adhesive Bonding and Development Tests

A summary of the adhesives test program is presented in AFFDL-TR-73-40. All tests shown in test plan chart 603R100-7 have been completed except items 5, 7, 8, and 13. Items 5 and 7, the environmental effects (sump water) on adhesive shear strength and cleavage, are undergoing exposure. Item 8, the dog-bone fatigue test, is in a hold status pending a decision on whether to conduct the test. Data from Items 9 (large area bond strength and VQ/I shear) and 2 (adhesive shear modulus), and a discussion of the adhesives program to 15 March 1973 are also presented in the AFFDL-TR-73-40.

TABLE 20
SUSTAINED LOAD S.C.C. TESTS - BRAZED LAP SHEAR SPECIMENS

Status as of 5/31/73

SPECIMEN NUMBER	SINGLE OVERLAP	DOUBLE OVERLAP	OVERLAP LENGTH	SPECIMEN WIDTH	SHEAR STRESS (KSI)	CUMULATIVE		COMMENTS
						TIME (HRS)	FAIL TIME (HRS)	
GROUP I								
BZ111-21	X		.250	1.000	12		475	No corr. attach along sides
BZ111-29	X		.250	"	"		838	No corr. attach along sides
BZ111-25	X		.375	"	"		626	No Corr. attach along sides
BZ111-28	X		.375	"	"		346	No Corr. attach along sides
BZ111-24	X		.500	"	"	1006		No Failure
BZ111-26	X		.500	"	"		296	No corr. attach along sides
BZ14A-43	X		.250	"	"		818	
BZ14A-44	X		.250	"	"		818	
BZ14A-41	X		.375	"	"		835	
BZ14A-42	X		.375	"	"		835	
BZ14A-47	X		.500	"	"		812	
BZ14A-48	X		.500	"	"		812	
BZ 7-41	X		.250	"	"		578	
BZ 7-42	X		.250	"	"		578	
BZ 7-45	X		.375	"	"		574	
BZ 7-46	X		.375	"	"		574	
BZ 7-43	X		.500	"	"		573	
BZ 7-44	X		.500	"	"		573	

TABLE 20
SUSTAINED LOAD S.C.C. TESTS - BRAZED LAP SHEAR SPECIMENS
(Sheet 2 of 4)

SPECIMEN NUMBER	SINGLE OVERLAP	DOUBLE OVERLAP	OVERLAP LENGTH	SPECIMEN WIDTH	SHEAR STRESS (KSI)	CUMULATIVE TIME (HRS)	FAIL TIME (HRS)	COMMENTS
GROUP II MILLED SPECIMENS								
BZ41-15-5		X	.250	.500	12	"	0	Broke in assy; milling dang.
BZ41-16-5		X	.250	"	"	"	883	
BZ41-15-2		X	.375	"	"	"	867	
BZ41-15-4		X	.375	"	"	"	9	Damaged braze
BZ41-16-2		X	.375	"	"	"	882	
BZ41-16-3		X	.375	"	"	"	26	Bad Braze
BZ41-15-3		X	.500	"	"	"	1	Damaged Braze
BZ41-16-4		X	.500	"	"	"	134	Bad Braze
GROUP III SAWED SPECIMENS								
BZ42-18-3		X	.250	.500	12	"	693	
BZ43-20-3		X	.250	"	"	"	693	
BZ42-18-3		X	.375	"	"	"	641	Bad Braze
BZ43-20-1		X	.375	"	"	"	676	
BZ42-17-3		X	.250	"	"	"	527	
BZ43-19-2		X	.250	"	"	"	527	
BZ43-19-3		X	.250	"	"	"	578	
BZ43-19-5		X	.250	"	"	"	578	
BZ42-17-2		X	.375	"	"	"	530	
BZ43-19-4		X	.375	"	"	"	530	

TABLE 20
SUSTAINED LOAD S.C.C. TESTS - BRAZED LAP SHEAR SPECIMENS
(Sheet 3 of 4)

SPECIMEN NUMBER	SINGLE OVERLAP	DOUBLE OVERLAP	OVERLAP LENGTH	SPECIMEN WIDTH	SHEAR STRESS (KSI)	CUMULATIVE TIME (HRS)	FAIL TIME (HRS)	COMMENTS
<u>GROUP IV</u>								
BZ1-12	X		.250	1.000	8		304	50% Braze
BZ1-17	X		.250	1.000	8	333		
BZ4-17	X		.250	1.000	8			
BZ8-19	X		.250	1.000	8	333		
BZ8-17	X		.250	1.000	8			
BZ8-19	X		.250	1.000	8			
BZ1-16	X		.500	1.000	8	333		
BZ1-112	X		.500	1.000	8	332		
BZ4-16	X		.500	1.000	8	332		
BZ4-111	X		.500	1.000	8	243		
BZ8-14	X		.500	1.000	8		239	Bad Braze
BZ8-15	X		.500	1.000	8	243		
<u>GROUP V</u>								
BZ1-14	X		.250	1.000	4	332		
BZ1-19	X		.250	1.000	4	332		
BZ4-12	X		.250	1.000	4			
BZ4-18	X		.250	1.000	4	332		

TABLE 20

SUSTAINED LOAD S.C.C. TESTS - BRAZED LAP SHEAR SPECIMENS
(Sheet 4 of 4)

SPECIMEN NUMBER	SINGLE OVERLAP	DOUBLE OVERLAP	OVERLAP LENGTH	SPECIMEN WIDTH	SHEAR STRESS (KSI)	CUMULATIVE		FAIL TIME (HRS)	COMMENTS
						TIME (KSI)	TIME (KSI)		
GROUP V (Continued)									
BZ3-11	X		.250	1.000	4				
BZ3-111	X		.250	1.000	4				
BZ1-15	X		.500	1.000	4	333			
BZ1-111	X		.500	1.000	4	333			
BZ4-14	X		.500	1.000	4	333			
BZ4-110	X		.500	1.000	4	172			
BZ8-12	X		.500	1.000	4	172			
BZ8-16	X		.500	1.000	4	172			

Table 21

TENSILE TEST RESULTS
(FLAT TYPE, 2.0" G.L.)

Transverse Welds in Beta Annealed
6Al-4V Titanium, FTJ10940-149

Specimen Test No.	Welded Plate Thickness (inches)	Specimen Thick Width (inches)		YTS (KSI)	UTS (KSI)	%E	%RA
(1)							
64T0-1	.675	.379	.7210	114.5	124.8	13.5	23.1
64T0-2	.675	.378	.7088	115.7	126.2	12.5	21.4
64T0-3	.675	.377	.7215	114.3	125.7	13.0	22.4
(2)							
64T1-1	1.0	.376	.7305	116.1	126.7	13.0	21.7
64T1-2	1.0	.378	.7280	115.9	125.7	13.0	20.5
64T1-3	1.0	.375	.7210	115.0	125.4	13.0	22.5
(3)							
64T2-1	2.0	.378	.7225	111.7	120.8	12.0	17.9
64T2-2	2.0	.376	.7188	113.6	122.8	12.0	16.7
64T2-3	2.0	.375	.7188	110.9	120.9	12.0	18.9
Averages	.675			115.0	125.6	13.0	22.3
	1.0			115.7	125.9	13.0	21.6
	2.0			112.1	121.5	12.0	17.8

(1) Heat Number - RMI 295551

(2) Heat Number - RMI 295561

(3) Heat Number - RMI 304583

Table 22

Fatigue Test Results of Beta Annealed 6Al-4V Titanium
Welded on 3 Plate Thickness, Tested at $R = 0.1$, $\sigma_{\max} = 80$ KSI

Specimen	Plate Thickness	w (in)	t (in)	Max P (KIPS)	Cycles To Fail	Cycles To Stop	Comments
64F0-1	5/8	.652	.335	17.5	600,303		Radius Fracture
-2		.649	.332	17.2	206,981		Radius Fracture
-5		.661	.326	17.4	59,446		Radius Fracture
-6		.655	.315	16.5		273,218	Failed through Hole
-10		.655	.334	17.5	96,201		Radius Fracture
-11	5/8	.623	.332	16.5		513,716	Failed through Hole
64F1-2	1	.657	.323	17.0	317,401		HAZ
-3		.651	.328	17.1		171,603	Failed through Hole
-5		.652	.326	17.0	314,342		Radius Fracture
-7		.649	.320	16.6	348,651		Weld Fracture
-9		.654	.324	17.0		614,092	Failed through Hole
-10	1	.6615	.331	17.5		122,282	Failed through Hole
64F2-5	2	.652	.325	17.0	131,473		Weld Fracture
-8		.651	.324	16.9		128,249	Failed through Hole
-9		.651	.324	16.9		161,955	Failed through Hole
-10		.653	.315	16.5		252,193	Failed through Hole
-11		.650	.325	16.7		152,661	Failed through Hole
-12	2	.648	.324	16.8	81,443		Radius Fracture

Table 22 (Continued)

 $\sigma_{\max} = 110 \text{ KSI}$

Specimen	Plate Thickness	w (in)	t (in)	Max P (KIPS)	Cycles to Fail	Comments
64F0-3	5/8	.326	.652	23.7	14,073	HAZ
-4		.333	.657	24.1	15,000	Radius Fracture
-7		.332	.654	23.9	17,280	HAZ
-8		.332	.654	23.9	14,788	Radius Fracture
-9		.325	.648	23.5	21,218	Radius Fracture
-12	5/8	.323	.651	23.1	17,210	HAZ
64F1-1	1	.324	.652	23.2	13,793	Radius Fracture
-4		.321	.650	22.9	17,467	Radius Fracture
-6		.335	.652	24.0	15,784	HAZ
-8		.325	.652	23.3	15,827	Parent Metal Fracture
-11		.324	.648	23.1	14,615	Parent Metal
-12	1	.332	.655	23.9	14,404	Radius Fracture
64F2-1	2	.322	.658	23.3	11,563	Radius Fracture
-2		.325	.654	23.4	9,380	Weld Fracture
-3		.326	.652	23.4	14,666	HAZ
-4		.322	.649	23.0	10,389	Parent Metal
-6		.327	.656	23.6	9,000	Parent Metal
-7		.320	.650	22.9	13,847	HAZ

NOTES: 1. HAZ = Heat Affected Zone

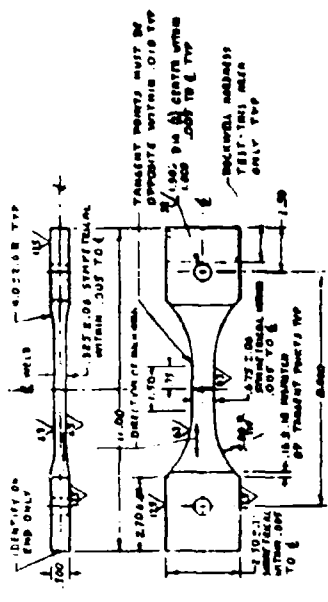
2. Plate Thickness shown is thickness at time of Welding

3. Welded Plate Assemblies Stress Relieved at 1250°F/1 hour

Int. No.
 Fny =

Form: 736

SPECIMEN (Sketch and Dimensions)



TEST CONDITIONS: Machine

R = .1; Mean Stress = ; A =
Notched Fatigue Specimen F₀₁ =
Temp
Speed
Date: N₁ (Net Section) = 1

6Al-4V Titanium
Parent Material

quantity of specimens
failing at one point

Figure 72 ELECTRON BEAM WELDED 6Al-4V TITANIUM FATIGUE DATA

STICK

Table 23

10 Nickel Steel Weldments - Mechanical Properties

SPECIMEN NO.	YIELD POINT (KSI)	ULTIMATE (KSI)	ELONG- ATION %	R. A. %
N1-T-1	186.1	188.7	14.0	71.7
N1-T-2	186.2	190.1	14.5	72.3
N1-T-3	183.5	186.7	14.0	72.4
N1-T-4	183.4	188.5	14.5	71.1
N1-T-5	185.8	192.1	14.0	69.1
N1-T-6	185.8	191.3	14.0	69.5

PL-717B from the B. F. Goodrich Company has been selected as the adhesive to be used for the remainder of the AMAVS Program. The decision was based primarily upon the failure mode of L/t lap shear specimens and the VQ/I beams. There was no major difference in various adhesive shear strength levels.

The failure mode difference indicated an advantage of the PL-717B over AF-66 in an apparent crack stopping ability after the bond line was initially ruptured. This was shown in the L/t specimens where AF-66 specimens, following metal yield, ruptured the bond line through peel and/or shear forces under continued load applications. The PL-717 in some cases broke the metal even though the large degree of area reduction in the titanium during yield had created a rupture in the bond line (up to 3/8" deep) at the end of the lap joint. This extended load carrying ability was also shown in the VQ where specimens of AF-66 had a distinct failure point whereas the PL-717 specimens continued to carry load.

Details of significant tests completed since 15 March 1973 are presented in the following paragraphs.

4t Data - PL-717 and AF66 Adhesive; 6-6-2 Titanium Adherends

Empirical data was generated for four different overlap dimensions for one thickness of titanium sheet. The test panel geometry is shown in Figure 73. For each overlap dimension, two panels were bonded to permit a comparison between bond cycles. Bond cycle consisted of curing 1 hour at 260°F under 30 psi pressure. The adherends were cleaned by grit blasting followed by a 15 minute room temperature immersion in Pasa-Jell 107M, a commercial acid solution from Semco Corporation.

Tests were conducted at three temperatures, -65, 80, and 180 degrees F for each overlap and adhesive material. The results are given in Tables 24 and 25 for each specimen tested. The data is presented graphically in Figures 74 through 79 in terms of load versus overlap dimension for each temperature and adhesive. The load level corresponding to average yield strength of the titanium substrates is superposed on each figure for reference. Both adhesives exceeded the yield strength of the metal for 1.5- and 2.0- inch overlaps at -65 and 80 degrees F. The data shown in Figure 79 indicates that the PL-717 adhesive might be capable of exceeding the reference yield strength at 180°F for an overlap greater than 2.0 inches. AF-66 (Figure 76) would probably not be capable of yielding the metal since the load-lap length relationship appears to have reached an asymptotic load level near 2.0-inches overlap.

The failure modes of PL-717 and AF-66 bonded specimens were dissimilar for the larger overlaps. Following metal yield,

TABLE II

THICKNESS			
0.050		0.100	
DASH NO	B	DASH NO	B
-9	4.50	-15	3.40
-11	3.50	-13	4.60
-17	5.00	-23	2.90
-19	3.00	-21	5.10
-25	4.70	-31	3.10
-27	3.30	-29	4.90
-33	4.30	-39	3.70
-35	3.70	-37	4.30

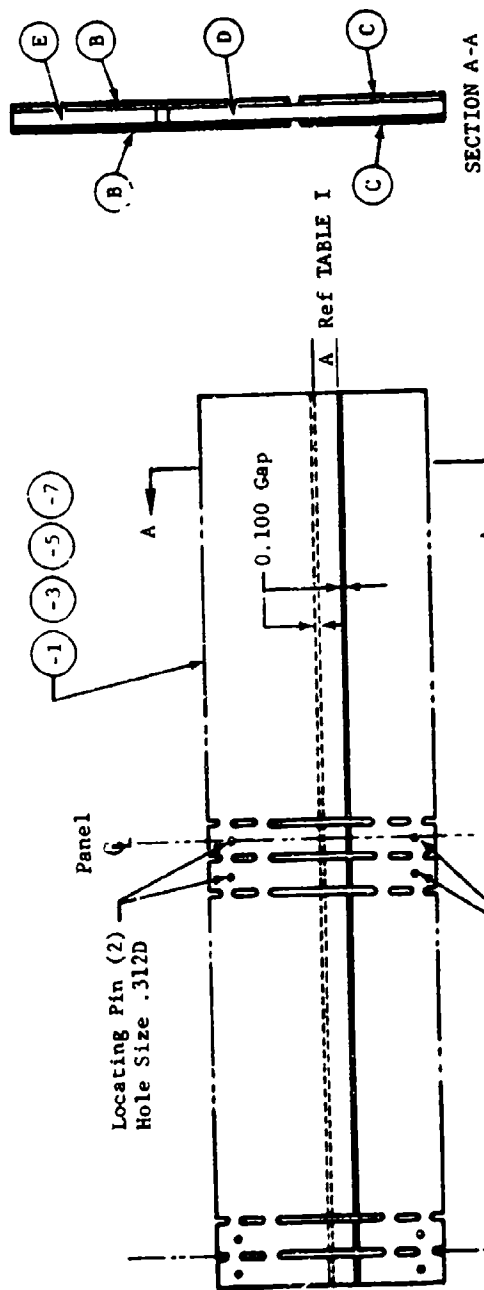
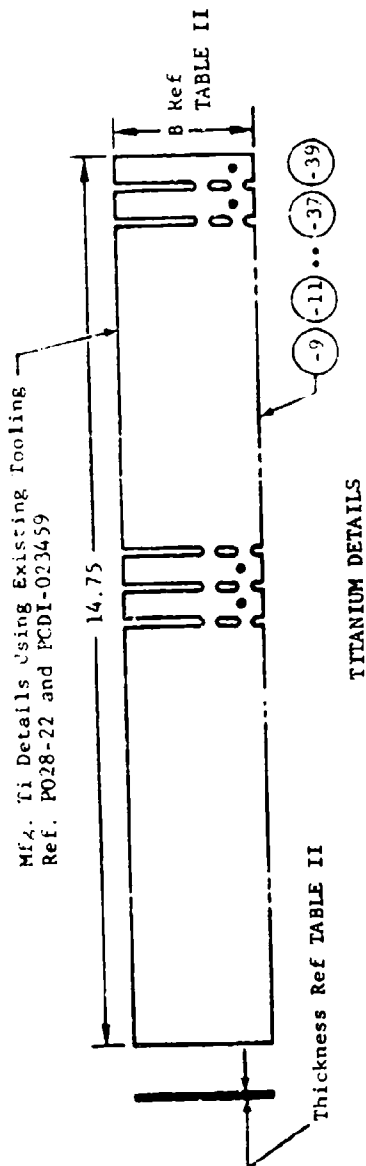


TABLE I

ASS'Y	A	B	C	D	E
-1	1.00	-9	-11	-13	-15
-3	2.00	-17	-19	-21	-23
-5	1.50	-25	-27	-29	-31
-7	0.50	-33	-35	-37	-39

Figure 73 Test Panel Geometry

Table 24
AF66 ADHESIVE BONDED TITANIUM ALLOY 6A1-6V-2Sn

Bond Operation	Lap Length (Inches)	Test Temperature		Bond Operation	Lap Length (Inches)	Test Temperature		
		-65°F	80°F (Pounds/Inch)			-65°F	80°F (Pounds/Inch)	180°F
1	0.5	10,600 10,450 10,250	7,500 7,400 7,300 6,800	1	2.0	19,200 (2) 19,100 (2) 19,300 (2) 17,000	17,600 (2) 17,200 (2) 16,600 (2) 17,000	13,660 12,680 13,380
2	0.5	10,700 10,750 10,000	6,900 6,800 6,900 7,200	2	2.0	18,500 (2) 19,000 (2) 18,500 (2)	15,400 15,800 15,030 15,820	11,080 11,240 11,340
1	1.0	16,250 17,000 16,100	12,400 13,200 12,600 13,200			7,560 7,750 7,780		
2	1.0	16,550 16,950 16,200	13,400 14,030 14,000 13,480			8,000 8,300 8,840		
1	1.5	19,050 (2) 18,950 (2) 18,100 (2)	16,400 (2) 15,500 15,700 15,400			10,800 11,310 10,400		
2	1.5							

Notes:

- (1) All failures within bond line
(2) Exceeded metal yield load level

Table 25
PL 717 ADHESIVE BONDED TITANIUM ALLOY 6Al-6V-2Sn

Bond Operation	Lap Length (Inches)	Test Temperature			Bond Operation	Lap Length (Inches)	Test Temperature		
		-65°F	80°F (Pounds/Inch)	180°F			-65°F	80°F (Pounds/Inch)	180°F
1	0.5	9,900 9,750 10,050	6,800 6,400 7,000 6,700	3,810 3,660 3,780	1	2.0	18,500 (1) 19,000 (1) 18,000 (1)	16,500 (1) 17,000 (1) 16,750 (1) 16,250 (1)	14,630 15,100 15,300
2	0.5	9,700 9,500 9,750	7,030 7,180 7,300 7,200	4,260 4,160 4,080	2	2.0	18,200 (1) 18,000 (1) 17,500 (1)	15,980 (1) 16,800 (2) 17,200 (2)	13,640 13,000 13,640
1	1.0	17,500 17,000 17,600	11,750 12,500 12,750 13,000	8,320 8,400 8,100					
2	1.0	17,600 17,500 16,500	13,240 13,000 12,600 12,600	7,600 7,740 7,600					
1	1.5	18,400 (1) 17,750 (1) 18,800 (1)	16,000 (2) 16,960 (2) 16,500 (2) 16,550 (2)	11,320 11,640 11,680					
2	1.5								

Notes:
(1) Metal rupture, all other failures in bond line
(2) Exceeded metal yield load level

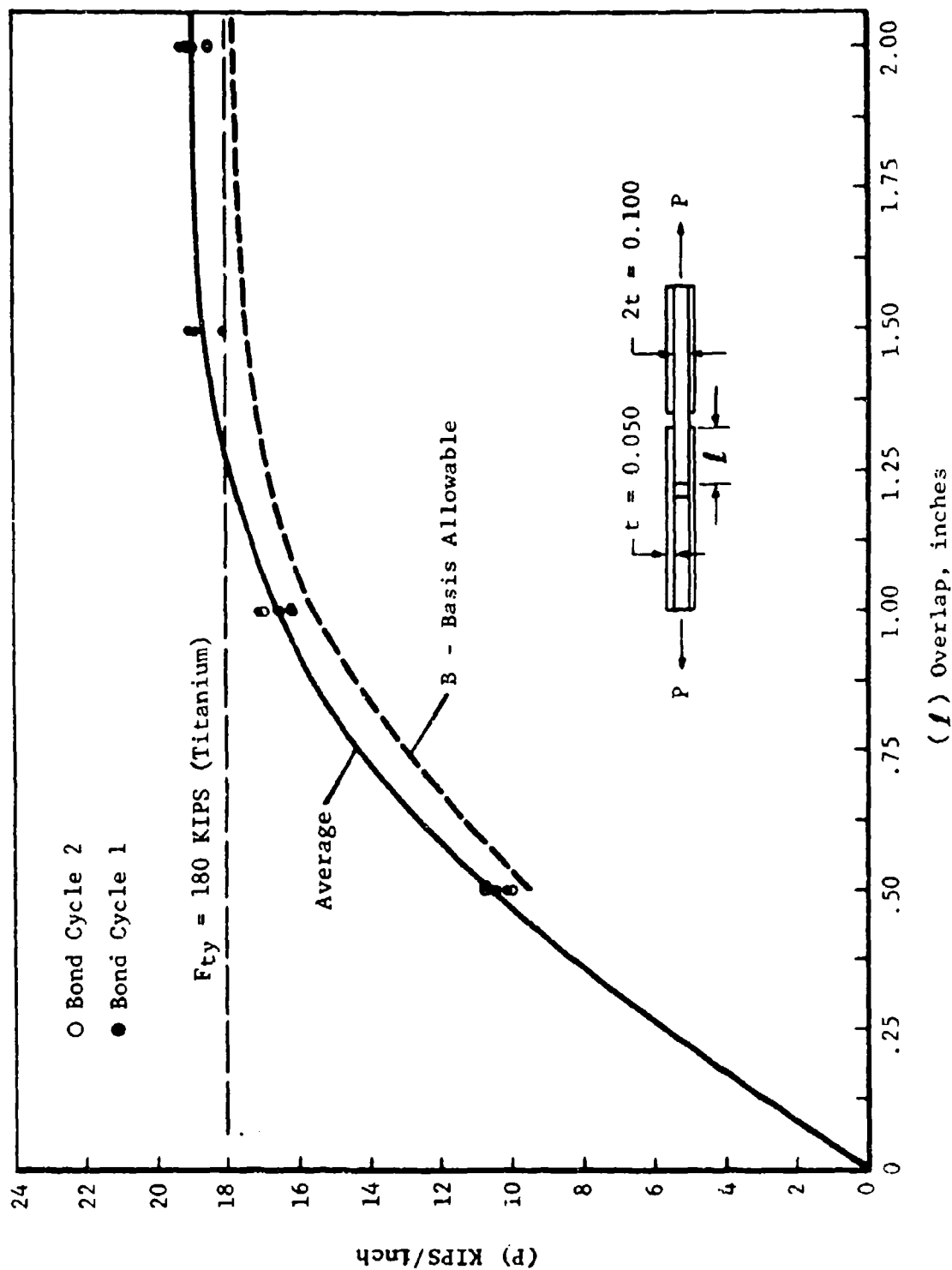


Figure 74 Overlap Shear Results Bonded 6Al-6V-2Sn Titanium Alloy/AF66 Adhesive (-65°F)

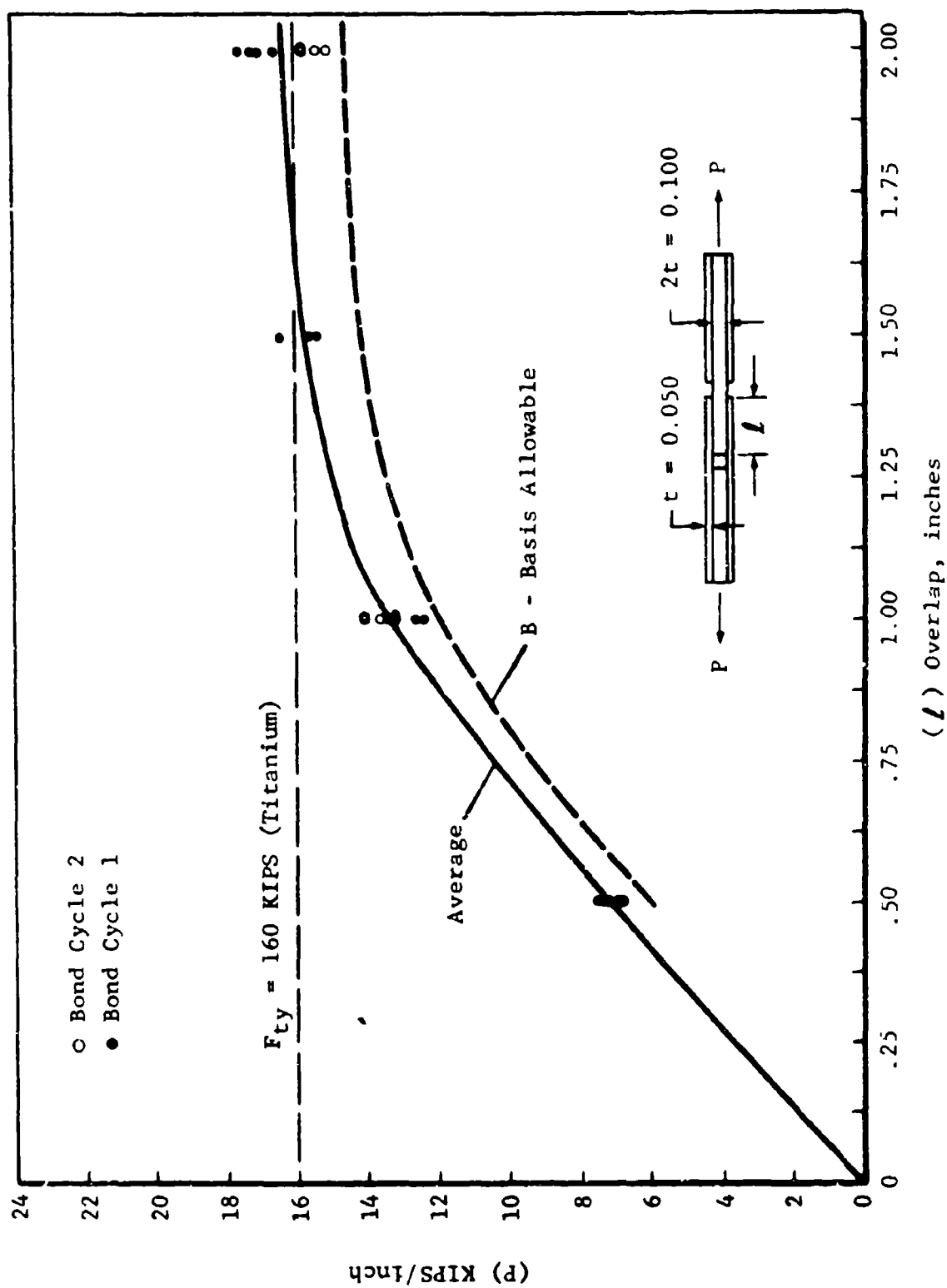


Figure 75 Overlap Shear Results Bonded 6Al-6V-2Sn Titanium Alloy/AF 66 Adhesive (80°F)

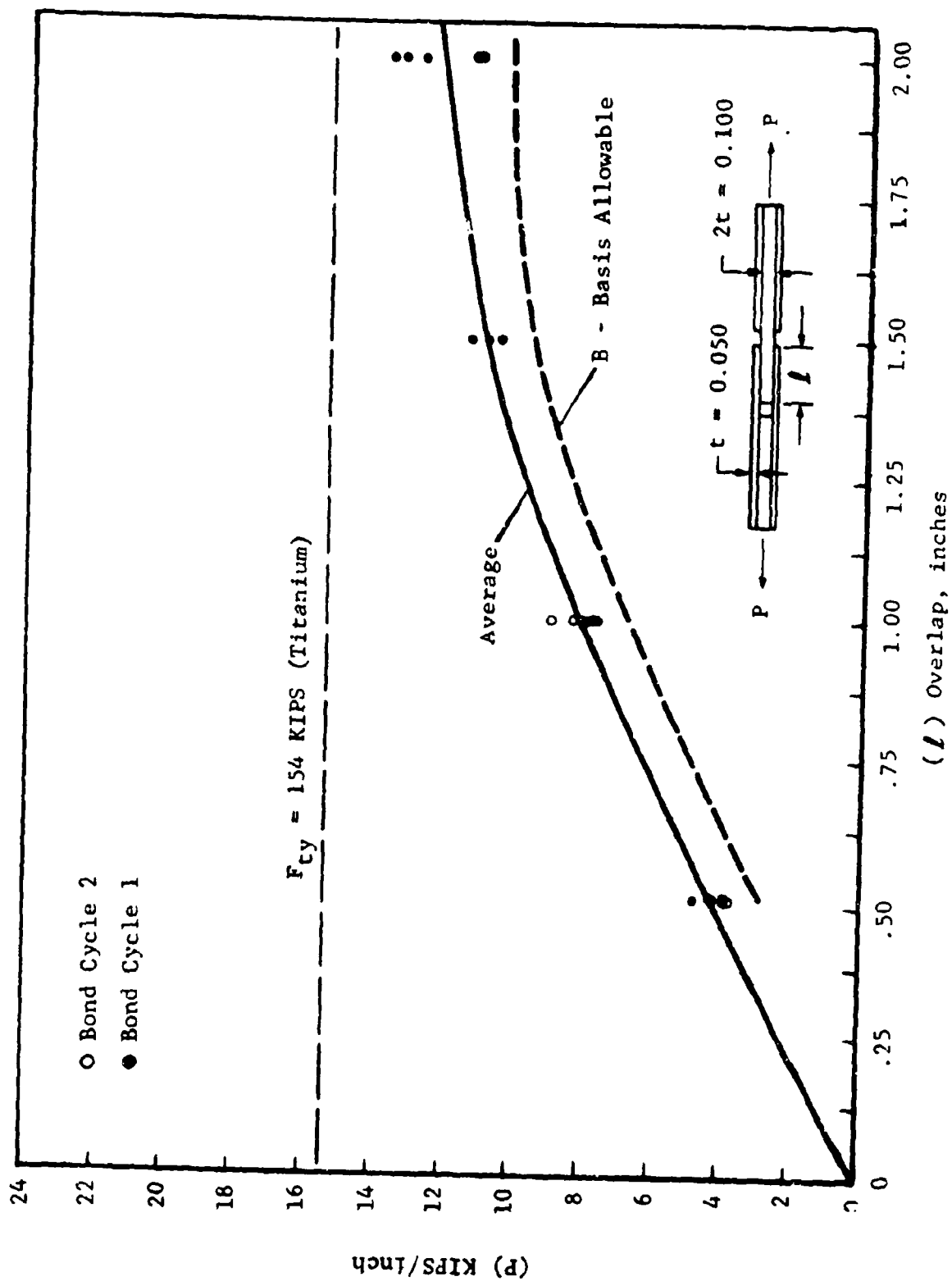


Figure 76 Overlap Shear Results Bonded 6Al-6V-2Sn Titanium Alloy/AF 66 Adhesive (180°F)

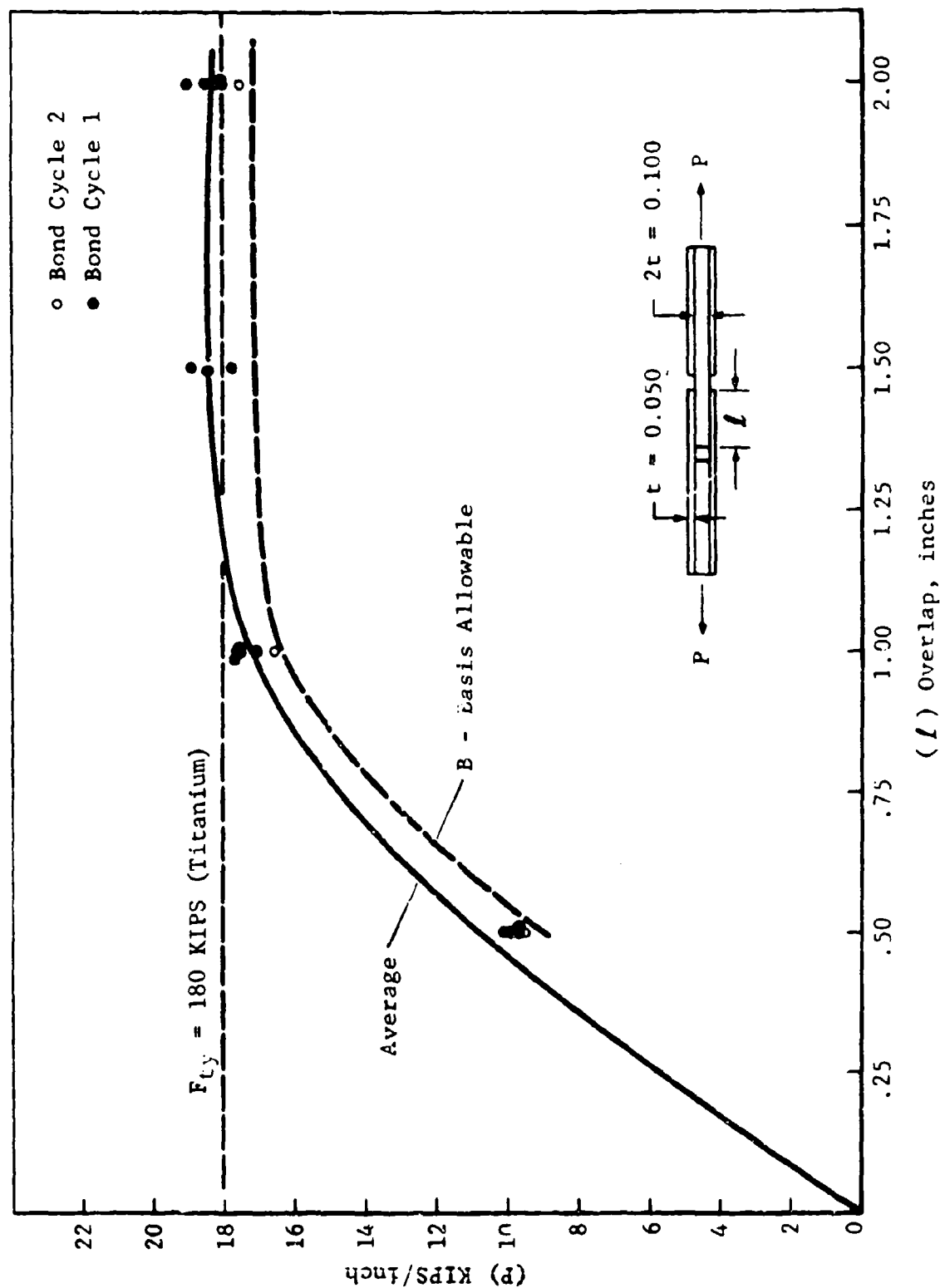


Figure 77 Overlap Shear Results Bonded 6Al-6V-2Sn Titanium Alloy/PL-717 Adhesive (-65°F)

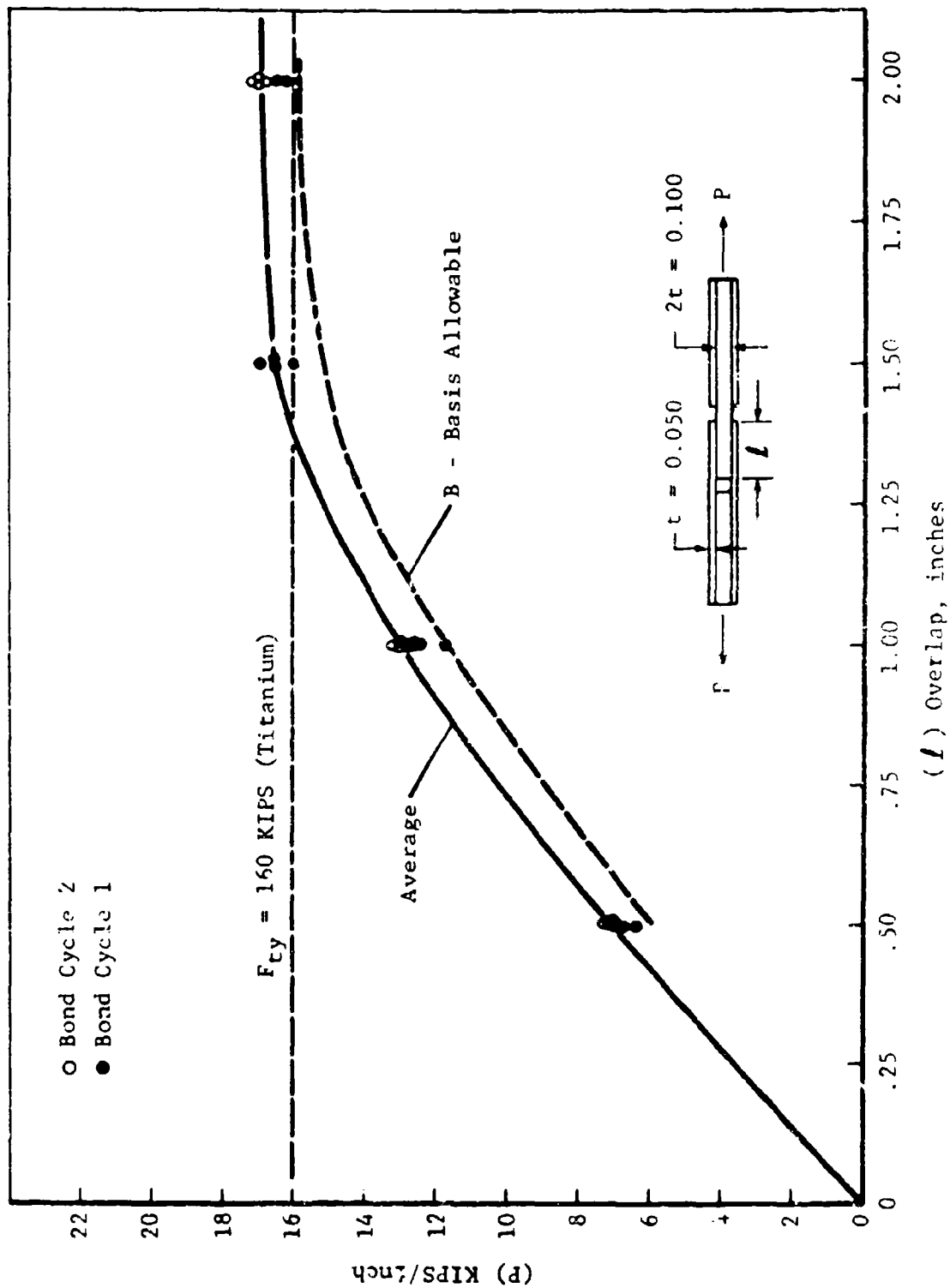


Figure 78 Overlap Shear Results Bonded 6Al-6V-2Sn Titanium Alloy/PL-717 Adhesive (80°F)

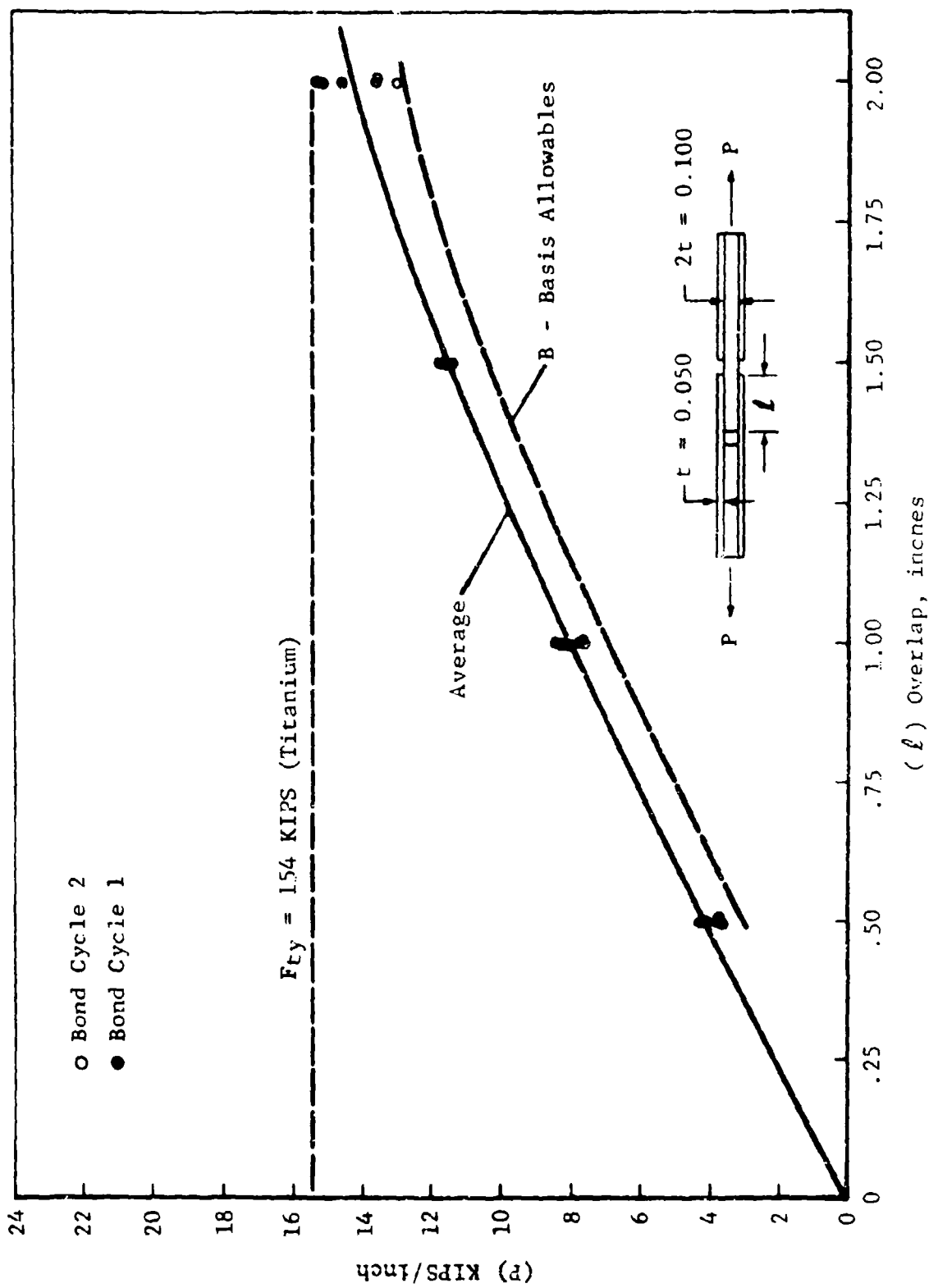


Figure 79 Overlap Shear Results Bonded 6Al-6V-2Sn Titanium Alloy/PL-717 Adhesive (180°F)

specimens bonded with AF-66 under continued load application ultimately ruptured the bond line through peel and/or shear forces. Specimens bonded with PL-717 under continued load application following metal yield in some cases ruptured the metal. The titanium sheet exhibited a large degree of "necking down" prior to ultimate rupture. These differences in failure modes are probably due to the differences in adhesive makeup. AF-66 is an unsupported film with flow controlled through filler-additives; PL-717 is a supported film where flow is controlled using a nylon knit scrim cloth.

The data above was used to develop shear strength allowables. The allowables are presented in the form of shear strength versus (l/t) curves as a function of temperature. Since shear strength results obtained for a similar adhesive i.e. Hysol's EA-9601 was represented by a single strength versus l/t curve for aluminum skins of .032 to .080-inch thickness, it is believed that these curves can be used for other gages of titanium not too different from the .050-inch gage. The allowables are presented in the form of shear strength versus (l/t) curves as a function of temperature. Since shear strength results obtained for a similar adhesive i.e. Hysol's EA-9601 was represented by a single strength versus l/t curve for aluminum skins of .032 to .080-inch thickness, it is believed that these curves can be used for other gages of titanium not too different from the .050-inch gage. The allowables are presented in graphical form in Figures 80 and 81. (The allowables were actually derived in terms of load versus lap length and then converted to strength versus (l/t) curves). These allowables were obtained for each adhesive material in accordance with the following equations

$$(\text{Allowable})_{ij} = (\text{Average Result})_{ij} - K_{\nu, 1-\alpha} S_p \quad (1)$$

where i = overlap

j = test temperature

ν = degrees of freedom = 30

α = "risk" = .05 for B-allowable

= .01 for A-allowable

K = One-side tolerance limit for
95-percent confidence level

S_p = pooled standard deviation

$$S_p = \left[\frac{\sum \nu_{ij} S_{ij}^2}{\sum \nu_{ij}} \right]^{\frac{1}{2}} \quad (2)$$

where ν_{ij} = degrees of freedom for each test condition

S_{ij} = standard deviation for each test condition

The value of 30 degrees of freedom was selected for use in obtaining K in Equation (1) because this value corresponds to the sample size required to set a distribution free B-allowable. The calculated values of allowables, averages, S_{ij} , and S_p are also included in Table 26. The A-allowables are not plotted.

The average result used in Equation (1) was the lower result of \bar{X}_1 and \bar{X}_2 of Table 26 which are the averages of the first and second bonding operations, respectively. The lower results was used since there appears to be a significant variation in mean strength due to the different bonding operations. Since there was only one set of data available for the 1.5-inch overlap the allowables (shown in Table 26) were determined graphically from curves drawn through the calculated allowables for the other three overlap conditions.

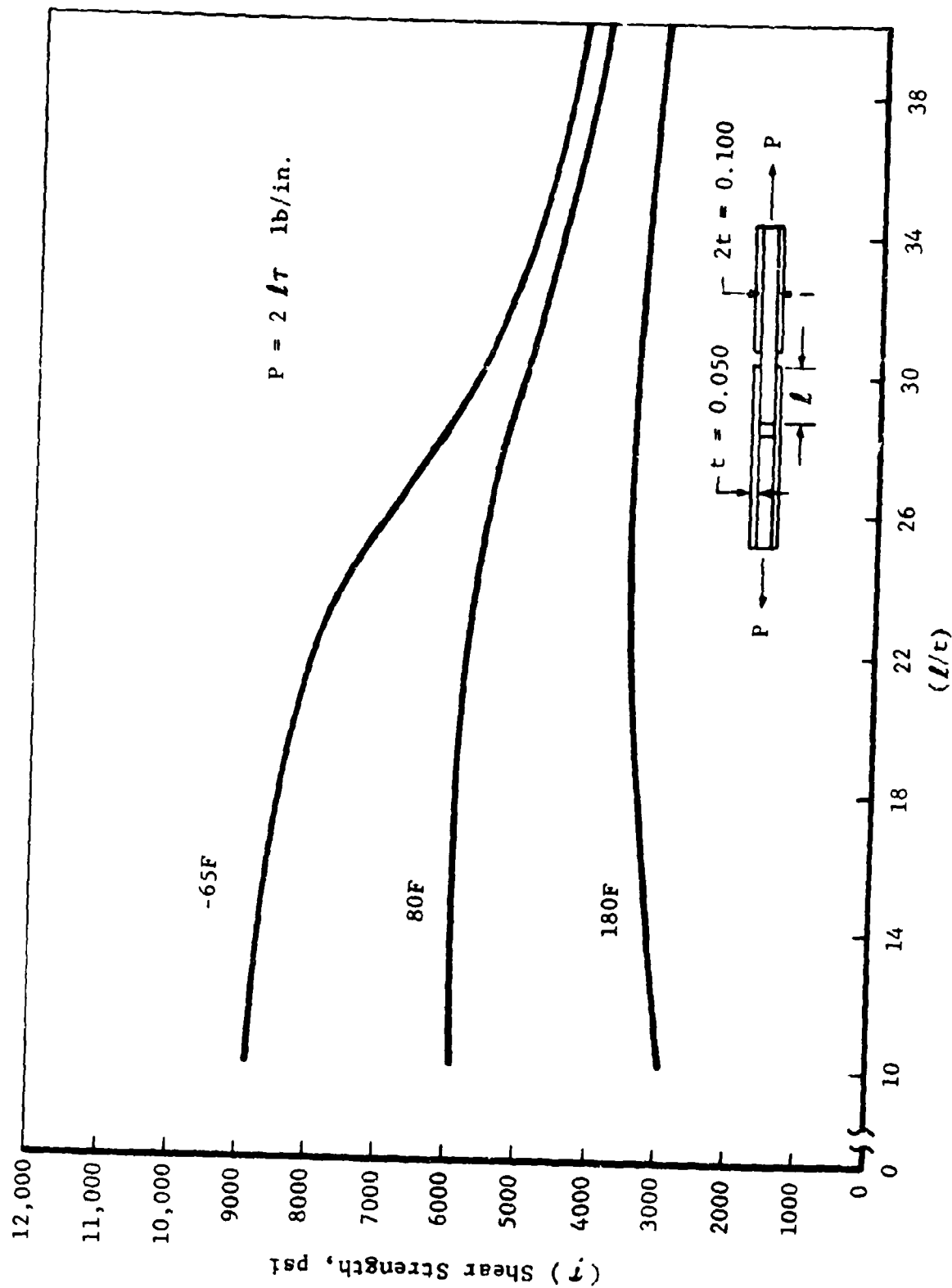


Figure 80 B-Allowables Bonded 6Al-6V-2Sn Titanium Alloy/PL-717 Adhesive

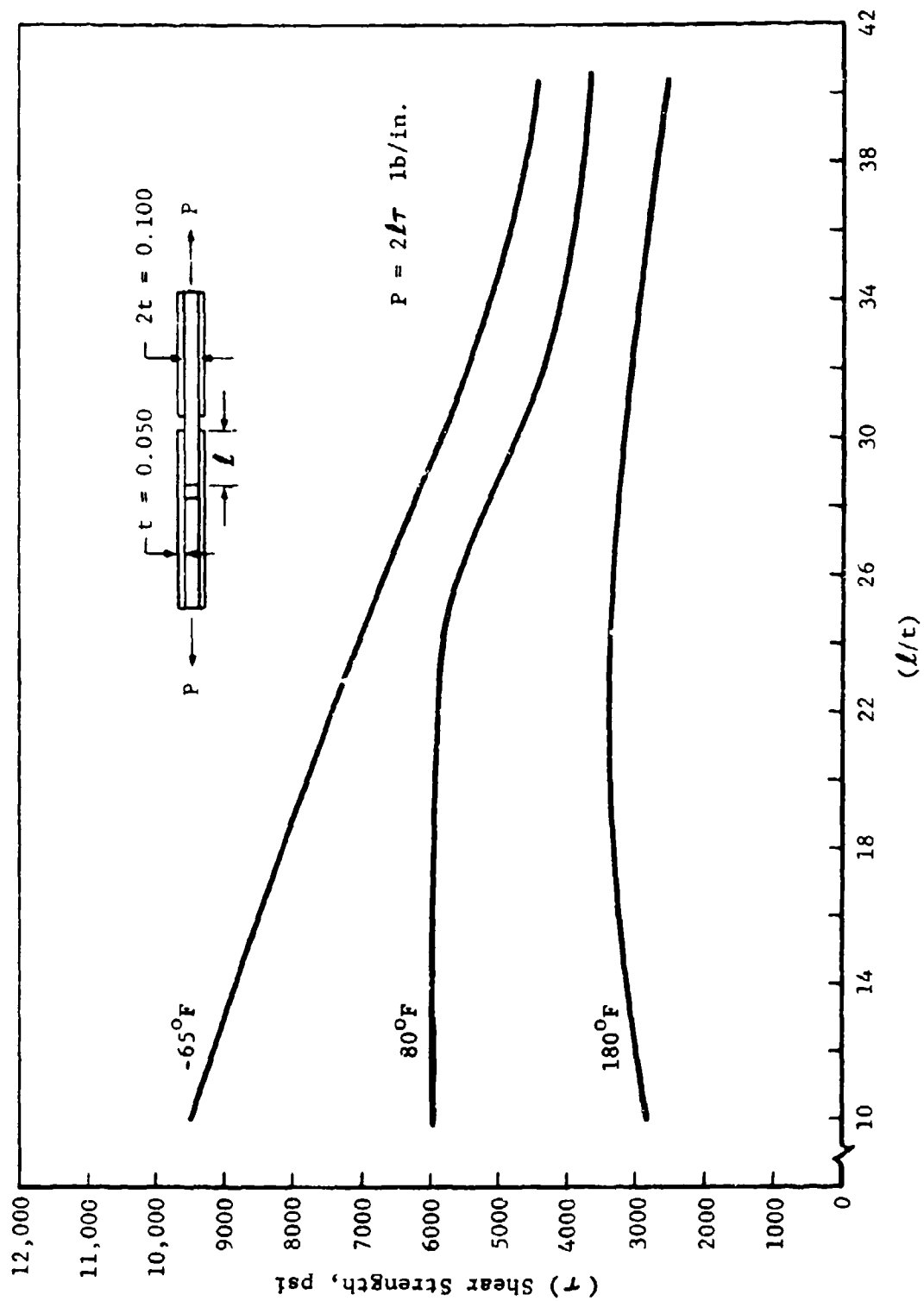


Figure 81 B-Allowables Bonded 6Al-6V-2Sn Titanium Alloy/AF 66 Adhesive

Table 26

ADHESIVE ALLOWABLES CALCULATIONS

Adhesive	Temp (°F)	Lap Length (In.)	n	Xi _j (Lb/In.)	Si _j (Lb/In.)	Sp (Lb/In.)	X ₁ (Lb/In.)	X ₂ (Lb/In.)	B-allow ⁽²⁾ (Lb/In.)	A-allow ⁽²⁾ (Lb/In.)
PL-717	-65	0.5	6	9,775	186	432	9,900	9,650	8,880	8,330
		1.0	6	17,283 (1)	444		17,370	17,200	16,430	15,880 (3)
		1.5	3	18,317 (1)	530		18,320	-	17,130	16,580 (3)
		2.0	6	18,200 (1)	510		18,500	17,900	17,130	16,580
	80	0.5	8	6,951	301		6,720	7,180	5,950	5,400
		1.0	8	12,680 (1)	453		12,500	12,860	11,730	11,180 (3)
		1.5	4	16,502 (1)	393		16,730	-	15,100	14,540 (3)
		2.0	7	16,783 (1)	323		16,620	17,000	15,850	15,300
	180	0.5	6	3,958	241		3,750	4,170	2,980	2,430
		1.0	6	7,960	361		8,270	7,650	6,880	6,330 (3)
		1.5	3	11,547	197		11,550	-	10,300	9,740 (3)
		2.0	6	14,218	924		15,010	13,430	12,660	12,110
AF-66	-65	0.5	6	10,458	289	555	10,433	10,483	9,447	8,730
		1.0	6	16,508 (1)	392		16,450	16,550	15,460	14,750 (3)
		1.5	3	18,700 (1)	522		18,700	-	17,400	16,680 (3)
		2.0	6	18,933	350		19,200	18,667	17,680	17,000
	80	0.5	8	7,100	283		7,250	6,950	5,960	5,250
		1.0	8	13,288	584		12,850	13,730	11,860	11,150 (3)
		1.5	4	14,750 (1)	451		15,750	-	14,100	13,380 (3)
		2.0	8	16,306 (1)	924		17,100	15,510	14,520	13,810
	180	0.5	6	4,097	365		4,390	3,810	2,820	2,110
		1.0	6	8,038	467		7,700	8,380	6,710	6,000 (3)
		1.5	3	10,837	456		10,840	-	9,500	8,780 (3)
		2.0	6	12,230	1,154		13,240	11,220	10,230	9,520

Notes: (1) Average load above yield strength of metal

(2) To obtain shear strength divide lb/in by 21 where 1 is lap length.

(3) Allowables determined graphically based on curve fit through allowables calculated for other lap lengths.

4t Data - PL-717 Adhesive and Beta C Titanium

Empirical data was generated for four different overlap dimensions and one thickness of Beta C titanium sheet (3Al-8V-6Cr-4Mo-4Zr). The test panel geometry was the same as for the 6-6-2 titanium data except the .12" sheet was not slotted into "finger" pods. Bond cycle and cleaning of adherends was also the same.

Tests were conducted at three temperatures, -65, 80, and 180 degrees F for each overlap and adhesive batch. The results are given in Table 27 for each specimen tested. The data is presented graphically in Figures 82 through 84 in terms of load versus overlap dimension for each temperature and batch. The load level corresponding to average ultimate strength of the titanium substrates is superposed on each figure for reference. Certain specimens of the 2-inch overlap test series failed within the 0.050 metal at -65F and 80F; several others of this same series failed at the loading hole in net section tension. All other specimens tested failed within the adhesive bond line.

One of the test panels which was bonded with a 1-inch overlap yielded several low test results. At some point in the fabrication process the panel details became misaligned sufficiently to cause a larger gap between the two (0.125 thick) center details than was normally obtained. The wider gap allowed the epoxy matrix of the adhesive material to flow or "bleed-out" more than the other panels. The high flow characteristic of PL-717 adhesive is a shortcoming of the system for small area bonding and careful attention must be exercised to prevent excessive bleed-out in bonding. Five test specimen from this panel gave low results which were related to excessive flow; these are noted as applicable on Figures 82 , 83 , and 84 .

The data above was used to develop shear strength allowables. The allowables are presented in the form of shear strength versus (L/t) curves as a function of temperature. The allowables are presented in graphical form in Figure 85 . (The allowables were actually derived in terms of load versus lap length and then converted to strength versus L/t curves). The allowables were obtained in accordance with the procedure used for the 6-6-2 titanium data above.

A comparison of the B-allowables for the subject alloy with 6Al-6V-2Sn is given in Figure 86 . The allowables for Beta C alloy equal or exceed the allowables for the latter alloy at all test conditions.

Table 27
OVERLAP SHEAR RESULTS (3)
BETA C TITANIUM ALLOY AND PL-717 ADHESIVE

Overlap (in.)	-65°F			80°F			180°F		
	Bond #1 (4) (LB/INCH)	Bond #2 (4)		Bond #1 (4) (LB/INCH)	Bond #2 (4)		Bond #1 (4) (LB/INCH)	Bond #2 (4)	
0.50	10225	9400		7400	7080		4700	3900	
	10380	9600		7320	7200		4900	4200	
	10800	9400		7400	7200		4850	4100	
				7300	6800				
1.00	18320	17000 (6)		12900	11400 (6)		8720	7400 (6)	
	17980	14800		13000	12200 (6)		8660	7640 (6)	
	18200	16100		13200	11400		8300	8220	
1.50	21400	19900		18000	17000		12600	10800	
	21400	20000		17200	16800		12400	10920	
	21600	20750		17800	17000		12540	10640	
				17700	16400				
2.00	22200 (2)	22150 (2)		19600 (1)	19400 (1)		12840 (5)	14440	
	20000+	21450		19900 (2)	19350 (1)		14200	13660	
	20000+	21650		19800 (2)	19000 (1)		15040	13680	
				20020 (1)	19400 (1)				

NOTES

(1) NET SECTION TENSION ACROSS LOADING HOLE

(2) METAL FAILED

(3) BOND FAILURES UNLESS NOTED

(4) BOND #1 USED ADHESIVE BATCH #8011; BOND #2 USED ADHESIVE BATCH #8152

(5) BEARING FAILURE AT LOADING HOLE ALLOWED EXCESSIVE PEEL ON SPECIMEN

(6) GAP BETWEEN METAL CENTER PIECES OF SPECIMEN PERMITTED EXCESS ADHESIVE FLOW COMPARED TO OTHER SPECIMEN OF THIS SERIES.

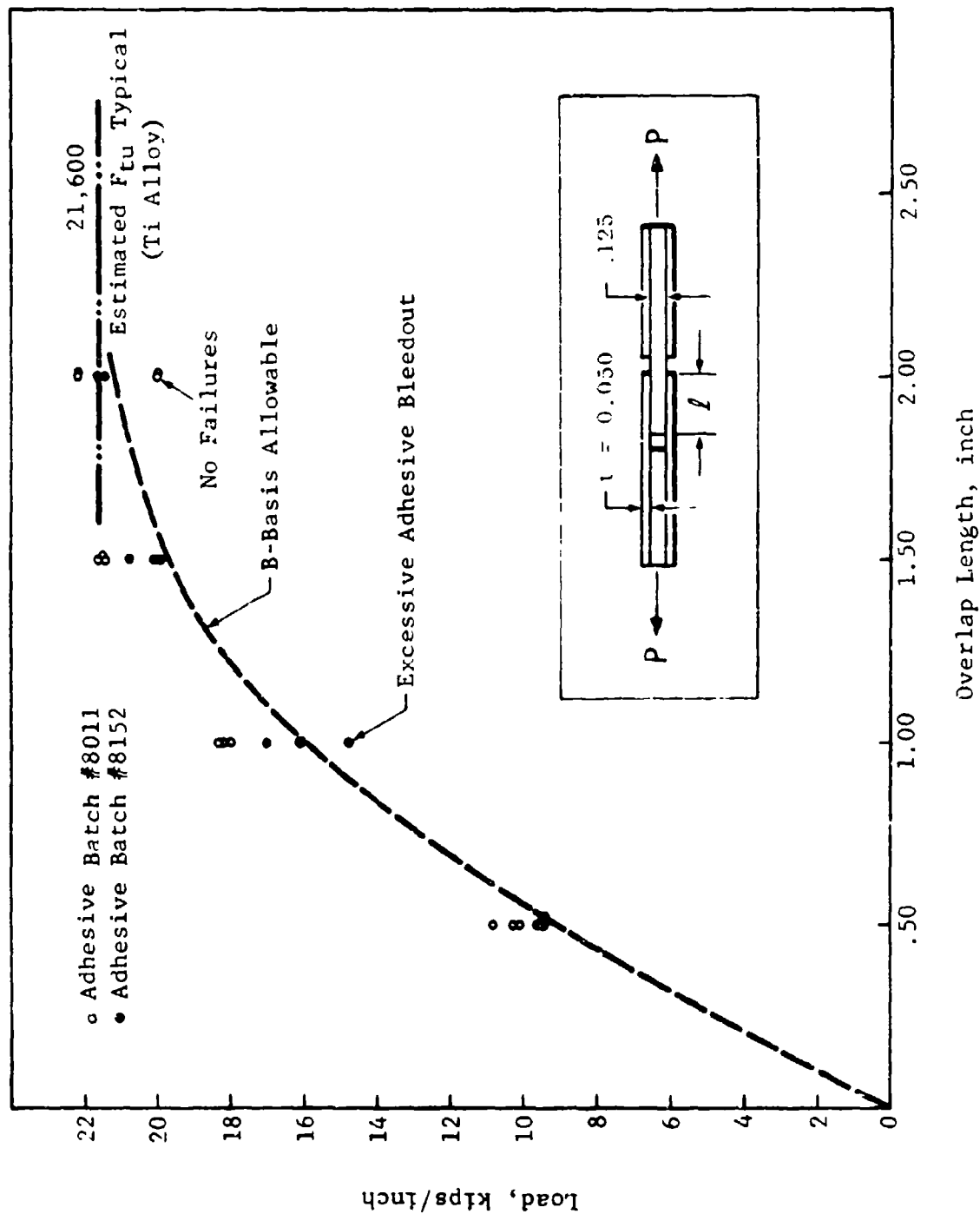


Figure 82 PL 717 Adhesive and Beta C Titanium Alloy Test at -65F

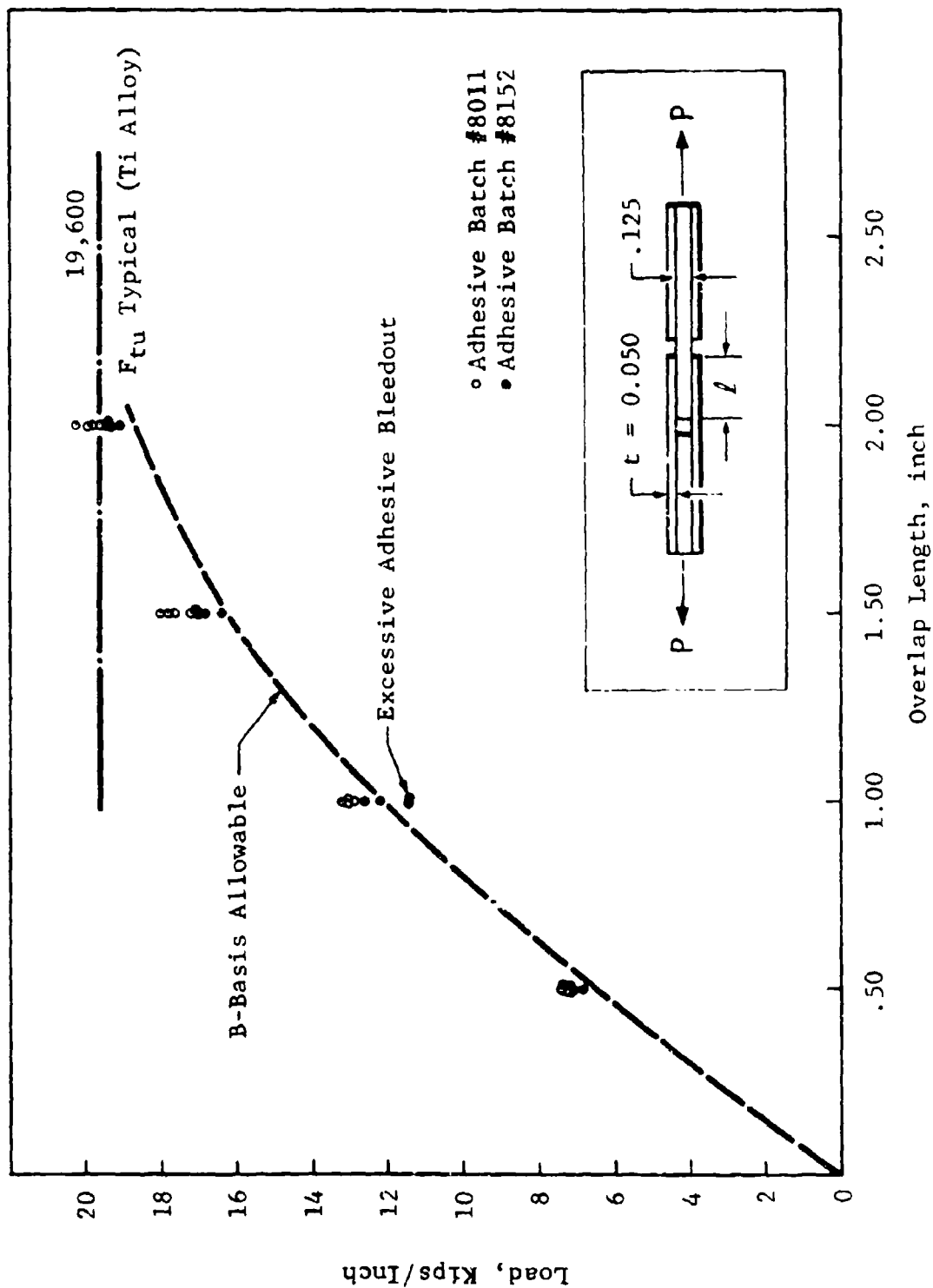


Figure 83 PL 717 Adhesive and Beta C Titanium Alloy Test at 80F

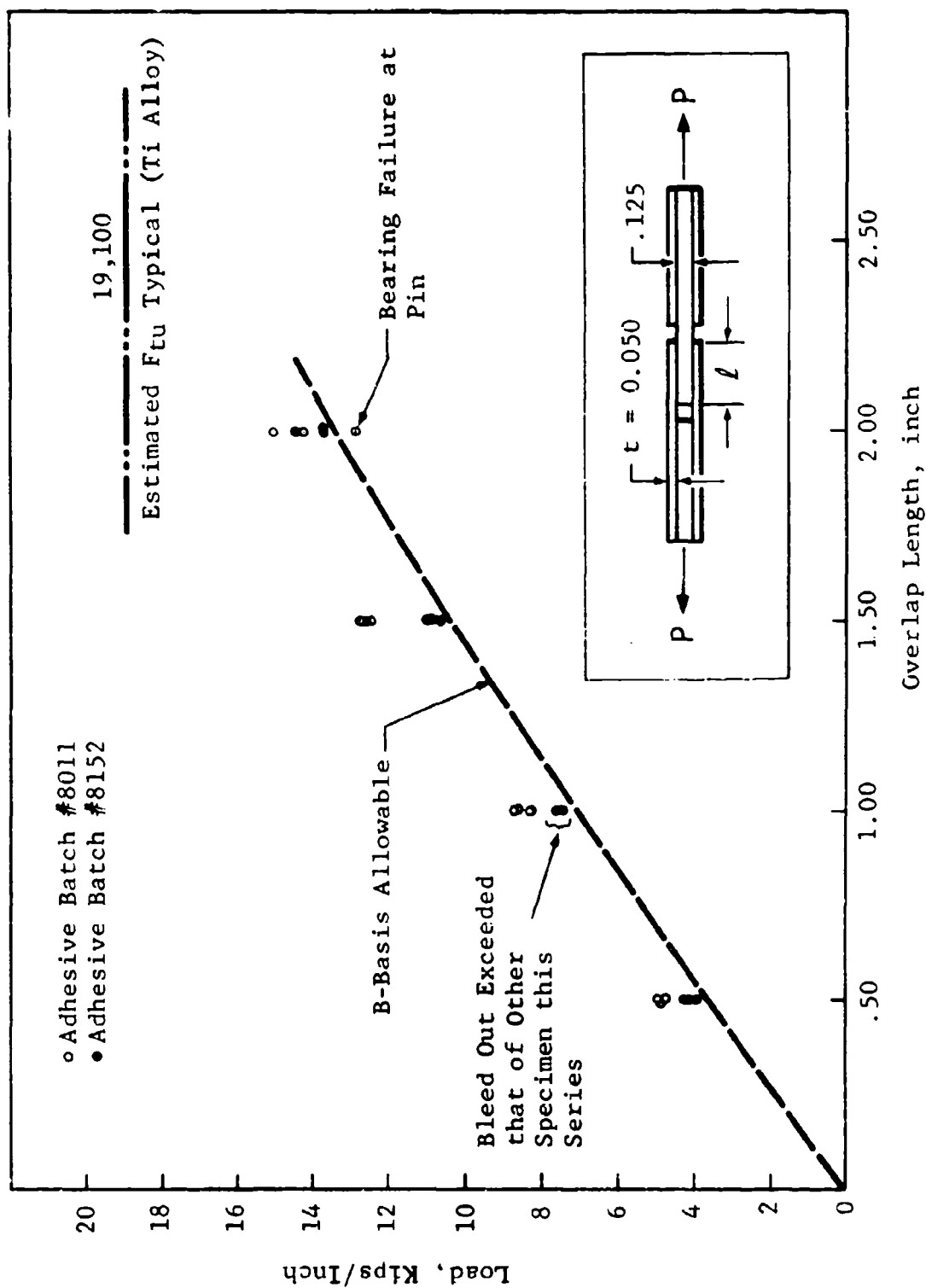


Figure 84 PL 717 Adhesive and Beta C Titanium Alloy Test at 180F

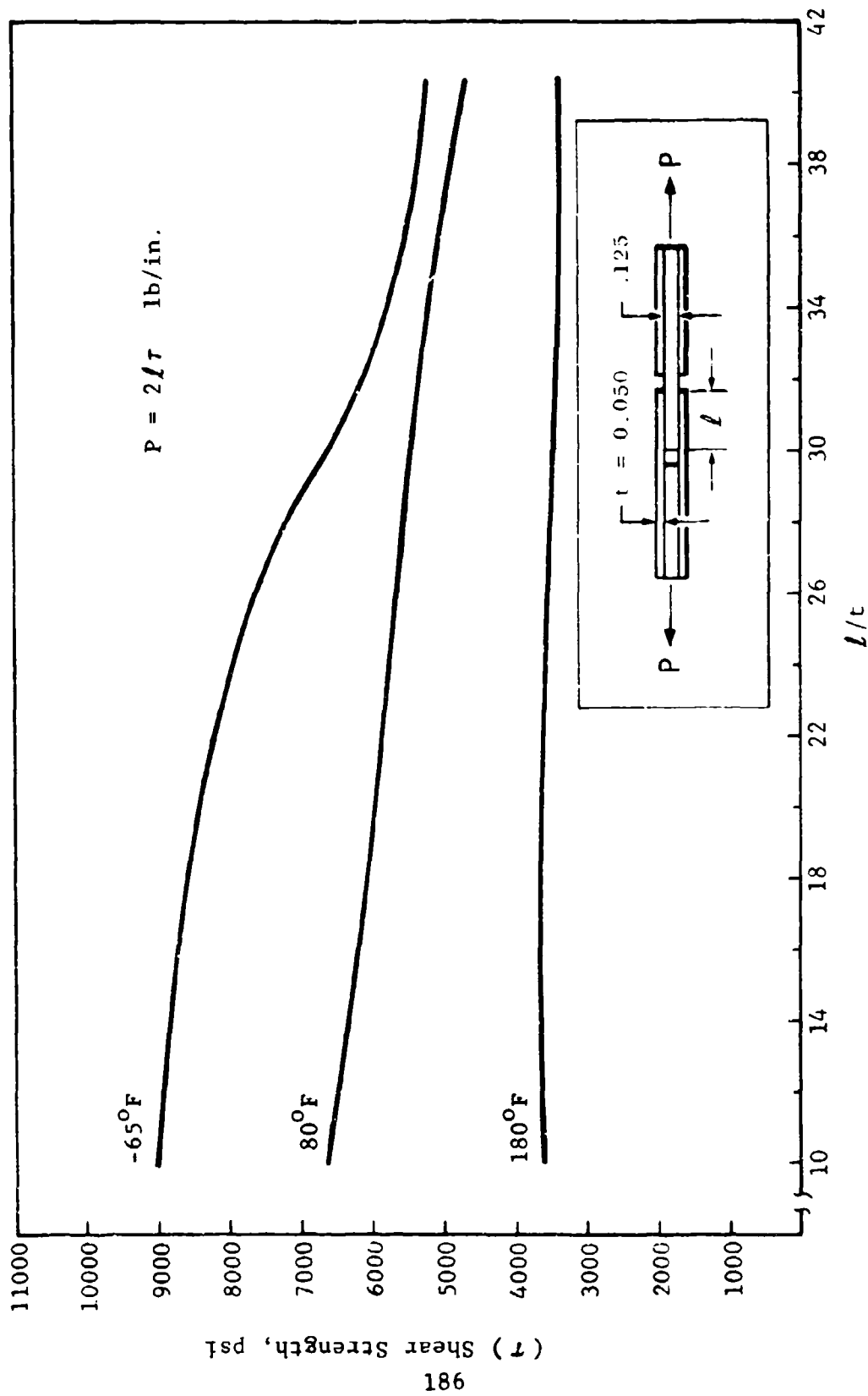


Figure 85 B-Allowables Bonded "Beta C" (3Al-8V-6Cr-4Mo-4Zr) Titanium Alloy/PL 717 Adhesive

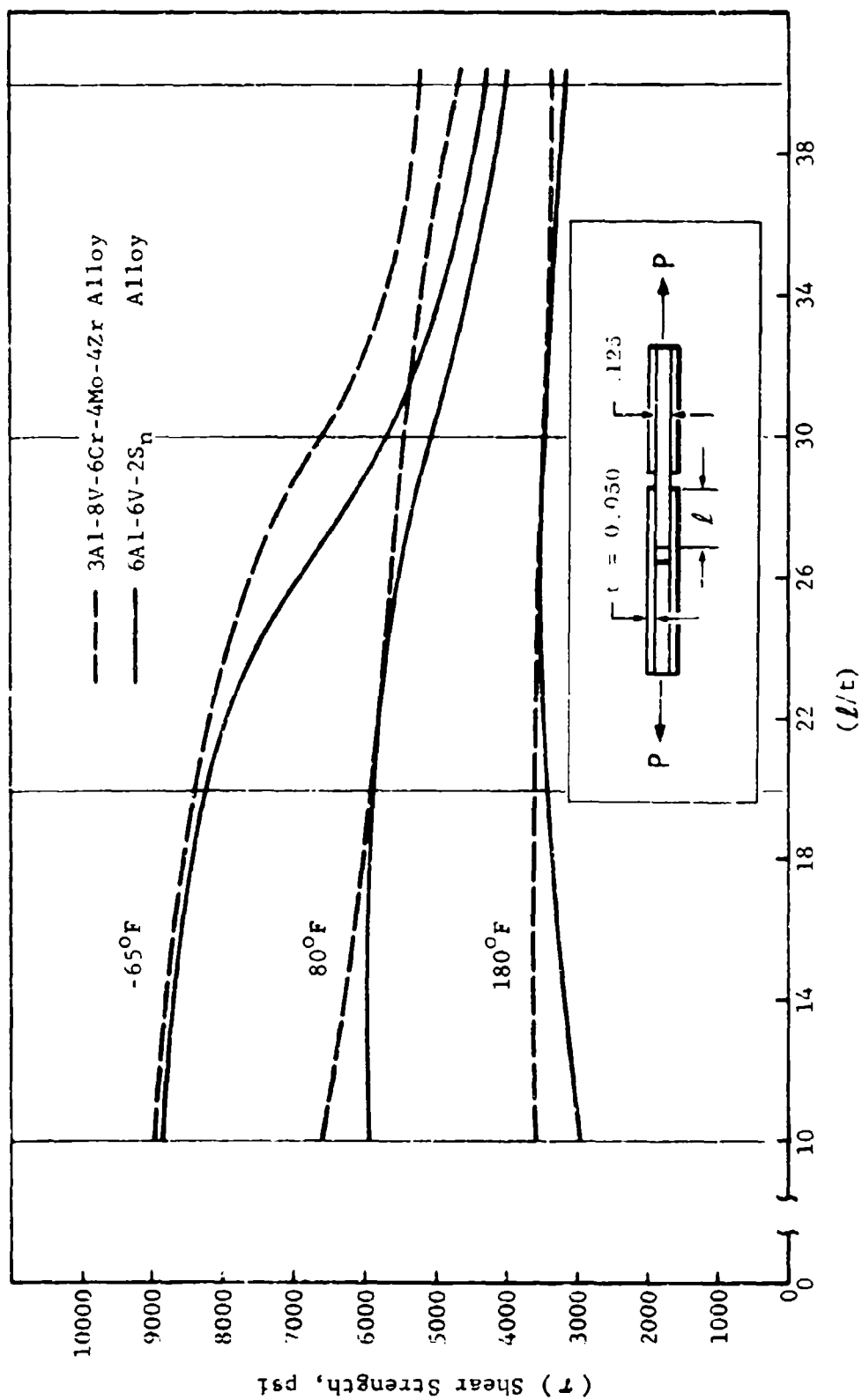


Figure 86 Comparison of B-Allowables for Two Titanium Alloys Bonded with PL 717 Adhesive

3.1.4.7 Specifications

Procurement Specifications - Convair specification numbers have been assigned to the procurement specifications which are being prepared for the program. A list of specifications are as follows:

FMS-1108	Aluminum Alloy (7050) Sheet and Plate
FMS-1109	Titanium Alloy, 6Al-4V Beta Annealed, Bar & Plate
FMS-1111	Steel Alloy, 10Ni-2Cr-1Mo-8Co (10 Nickel) Bar, Forged Billet and Plate
FMS-1112	Wire, Welding, Type 10 Nickel Steel
FMS-1113	Titanium Alloy, 3Al-8V-6Cr-4Mo-4Z (Beta C), Sheet, Strip and Plate
FMS-1114	Brazing Alloy, Ag-Al-Mn, Strip
FMS-1115	Wire, Welding, 6Al-4V Titanium Alloy, Extra Low Interstitial
FMS-1116	Adhesive, 250°F Cure, 180°F Service

All of these specifications are in some stage of preparation except FMS-1108 which is being held pending the results of design and stress studies to determine actual need for this material. Process specification to cover welding, brazing, and adhesive bonding processes will also be performed and are scheduled to start into preparation in August after more processing data becomes available.

Non-Destructive Inspection Specifications - Presently prepared Convair specifications will be used as applicable for the inspection of raw materials and components. The following is a list of the specification numbers and the type of inspection they cover:

FPS-1084	Penetrant Inspection (A modification of MIL-I-6866)
FPS-0040	Magnetic Particle Inspection (A modification of MIL-I-6868)
FPS-0018	Longitudinal Wave Ultrasonic Inspection (Similar to MIL-I-8950)

- FPS-1086 Delta Scan Ultrasonic Inspection (No existing Military specification)
- FPS-0065 Weld Joint Inspection - Combine penetrant, magnetic particle and radiographic inspection (No existing single Military specification)
- FPS-1076 Magnetic Rubber Inspection (no existing Military specification)

All of the above specifications have been written with the exception of FPS-1086 which is presently being written. All require that an NDTS be prepared for general use and for individual parts when specified by Engineering.

Fracture Acceptance Criteria - A fracture acceptance criteria for inclusion in procurement specifications is being formulated. The major problem is to establish an acceptance criteria for the two very tough materials, beta annealed 6Al-4V titanium and 10 Nickel steel. Acceptable test procedures to determine a valid K_{IC} value for the 6Al-4V alloy in thicknesses less than 1.50 inch and 4.00 inches for 10 Nickel steel do not presently exist. As a result, only procuring, chemical composition and microstructural controls combined with some supplemental type of test can be used for material acceptance testing. Present plans are to require these controls and add Charpy V-notch impact testing as a supplement. The material procurement specifications will reflect this philosophy except for Beta C titanium. Valid K_{IC} values can be obtained down to as low as $\frac{1}{2}$ inch thick and perhaps to as thin as $\frac{3}{8}$ inch.

3.1.4.8 Corrosion Prevention System

The corrosion prevention finish system selected for use on metallic materials proposed for the AMAVS Program is described in the Phase Ib Summary Report, AFFDL-TR-73-40. These finishes are compatible with those required by Rockwell International for the B-1, except that the top coats of paint, for exterior surfaces of the test articles will be MIL-L-81352 acrylic lacquer in lieu of MIL-C-83286 polyurethane coating.

3.2 TESTING

During the second six-month period of this program, most materials testing and all Group I component testing were accomplished. Additionally, Group II component test requirements were finalized and significant progress was made in preparing for full scale testing.

3.2.1 Materials Testing

Materials testing requirements were established prior to the reporting period and are presented in AFFDL-TR-73-1. Most of the required testing has been accomplished during the reporting period as indicated in Table 28. Significant test results are summarized in this paragraph and Section 3.1.3 and 3.1.4.

3.2.2 Component Testing

The Group I component test program was completed during the reporting period.

The following paragraphs describe the results obtained from each of the component test specimens. Note: Report Number FZM-6054 describes the specimens.

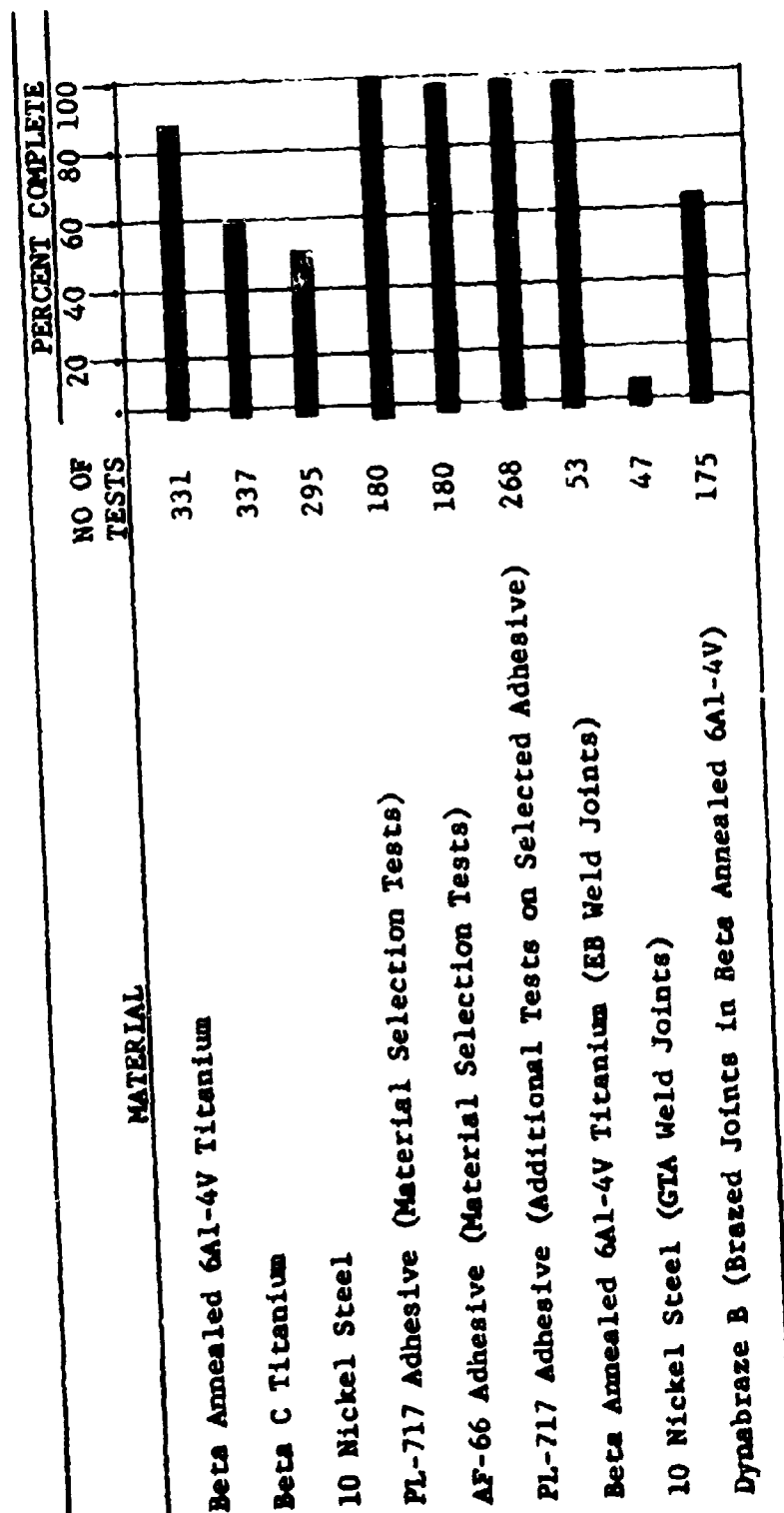
3.2.2.1 Fastener Comparison Tests - Brazed Laminates - Drawing Number 603FTB013

Tests completed and results are shown in AFFDL-TR-73-40, Phase Ib Summary Report.

3.2.2.2 3/8 Scale Brazed Lower Plate - First Specimen - Drawing Number 603FTB005

Tests completed and results are shown in AFFDL-TR-73-40, Phase Ib Summary Report.

Table 28 Materials Test Program



3.2.2.3 3/8 Scale Brazed Lower Plate - Second Specimen

Specimen was put into test with a 48.32 cycles per flight fatigue spectrum. After two service lives were completed, inspection revealed possible delamination occurring. The testing was continued for an additional 400 flights, then stopped for another inspection. The inspection revealed delamination occurring at two of the braze splices. Testing was discontinued and the specimen was removed from the fixture and subjected to destructive inspection. The inspection and the associated Engineering investigation disclosed that the failure was probably due to a poor brazed joint which had been caused by inadequate purging during the braze operation. A possible aggravating cause was joint eccentricity. As a result of this test, the configuration of the lower plate has been changed to eliminate the joint eccentricity and to improve the brazing parameters. Refer to Section 3.1.4 for further discussion of purging problem.

3.2.2.4 Interim Crack Stopper Test - First Specimen - Drawing Number 603FTB051

Tests completed and results are shown in AFFDL-TR-73-40, Phase Ib Summary Report.

3.2.2.5 Interim Crack Stopper Test - Second Specimen

This specimen was configured the same as the first specimen except that the eloxed notch was only 0.60 inch long and 0.30 inch deep (half-moon shaped) and was completely contained in one of the center bars. Where the first specimen would be categorized as fast crack growth, this specimen would be categorized as slow crack growth. The specimen was fatigue cycled, first by spectrum loading, then with constant amplitude loading until a crack appeared at the ends of the notch. At this point the loading was changed back to spectrum cycling and continued until the crack completely traversed the bar. This took 1075 flights, or approximately 0.84 service lives. Following this, the bar was cut away and the web under the bar was examined. Examination showed that the braze between the bar and the web had failed, and that the crack had not penetrated into the web.

3.2.2.6 3/8 Scale Brazed Lower Lug - First Specimen - Drawing Number 603FTB004

The specimen was fatigue loaded for four service lives using a 38.32 cycles per flight fatigue spectrum. One hundred percent limit load was 9/64 of the full size airplane load. The specimen was

thoroughly examined after four lives of testing, and no defect was found other than some galling between the steel bushing and the lug. The bushing was smoothed slightly, greased and reinstalled. Testing was continued for two more lives. After the sixth life the bushing was again removed and the part was inspected. Inspection revealed several cracks in the interior of the pivot pin hole, in all three layers. The bushing was again reinstalled and testing resumed, but the spectrum was changed to the 179.32 cycles per flight crack growth spectrum. The specimen failed in the 650th flight after six service lives.

3.2.2.7 3/8 Scale Brazed Lower Lug - Second Specimen

This specimen was the same as the first except that a 16 RMS finish was created on the interior of the pivot pin hole, and the exterior surface of the bushing was dry-film lubricated.

The specimen was fatigue cycled for four fatigue lives in the same manner as the first specimen. After the four lives of testing, the bushing was removed and the specimen was inspected. No cracks were found, and there was no galling on the inside of the hole.

The specimen was removed from the test fixture and was elox notched 0.12 inch x 0.12 inch across the edge of the pivot pin hole in one of the outside layers of material.

The part was replaced in the test machine and spectrum cycled using the 179.32 cycles per flight spectrum. After 260 flights no crack had appeared so the loading was changed to constant amplitude, using a loading of 3.7% to 65.4% of limit. After 1200 cycles a crack was detected at the end of the elox slot on the surface of the specimen. Spectrum testing was resumed. As the crack progressed along the outside layer, a separate crack initiated in the opposite surface. The two cracks continued to propagate until failure occurred at 998 flights after crack initiation.

The total test history on the part at the time of failure was: Four lives, 1200 constant amplitude cycles and 1258 flights.

3.2.2.8 Fastener Comparison Tests - Bonded Beta C Laminate - Drawing No. 603FTB014

Test results are as follows:

Specimen	Fasteners	Test Type	Failing Load	No. of Cycles	Type of Failure
1	2-7/16 Bolts	Static	87,300 #		Net Section
2	2-7/16 Bolts	Static	86,000 #		Net Section
3	2-7/16 Bolts	Static	85,100 #		Net Section
4	2-7/16 Taperloks	Static	84,100 #		Net Section
5	2-7/16 Taperloks	Static	84,700 #		Net Section
6	2-7/16 Taperloks	Static	79,000 #		Net Section
7	2-7/16 Bolts	Fatigue*		62,348	
8	2-7/16 Bolts	Fatigue*		42,515	
9	2-7/16 Bolts	Fatigue*		44,207	
10	2-7/16 Taperloks	Fatigue*		157,644**	
11	2-7/16 Taperloks	Fatigue*		201,700**	
12	2-7/16 Taperloks	Fatigue*		53,000***	

*1170 Lbs-To-23,400 Lbs.

**Failed In Grips

***Nontest Bolts Failed - Bolts were reused

3.2.2.9 Bonded Shear Web Stability Tests - Dwg. No. 603FTB012

Two specimens, each consisting of two plies of 0.125" thick Beta C titanium bonded together, were tested to failure in a "picture frame" shear fixture. The failing loads of the two specimens were within 2% of each other. Shear stress at failure was approximately 93,000 psi.

The test results showed that the adhesive (PL-717) successfully held the two plies together until monolithic buckling took place. The actual buckling stress agreed well with the buckling stress predicted by standard analytical techniques using the combined thicknesses of the two plies as a single thickness.

One specimen consisting of three plies of 0.125" thick Beta C titanium bonded together was also tested. In this case, the adhesive held the plies together until rupture of the part occurred at a shear stress of 96,500 psi.

3.2.3 Full Scale Testing

Testing is to be accomplished on a full-scale WCTS of the configuration to be chosen at the end of Phase II. This testing will be accomplished at AFFDL in the test setup shown in Figure 87. Convair will provide test planning, test fixtures and the test article, and AFFDL will provide test equipment and perform the testing. A definition of the planned testing is presented in AFFDL-TR-73-40 along with a description of the physical setup to be used for this testing.

3.2.3.1 Progress During Six-Month Period

A plan was developed for manufacturing the full scale test fixture, shipping it to AFFDL and reassembling it. This plan involves two shipments of hardware as shown in Figures 88 and 89. The initial shipment will allow early installation and checkout of loading systems and of some data systems elements. The final shipment will complete the setup and will facilitate final checkout and testing. Design of the test fixture is nearing completion, as is the procurement of fixture materials and hardware. Manufacture of the frame for the initial hardware shipment is approximately 50% complete. Status at the end of the reporting period is shown in Table 29 for the main elements of the test fixture.

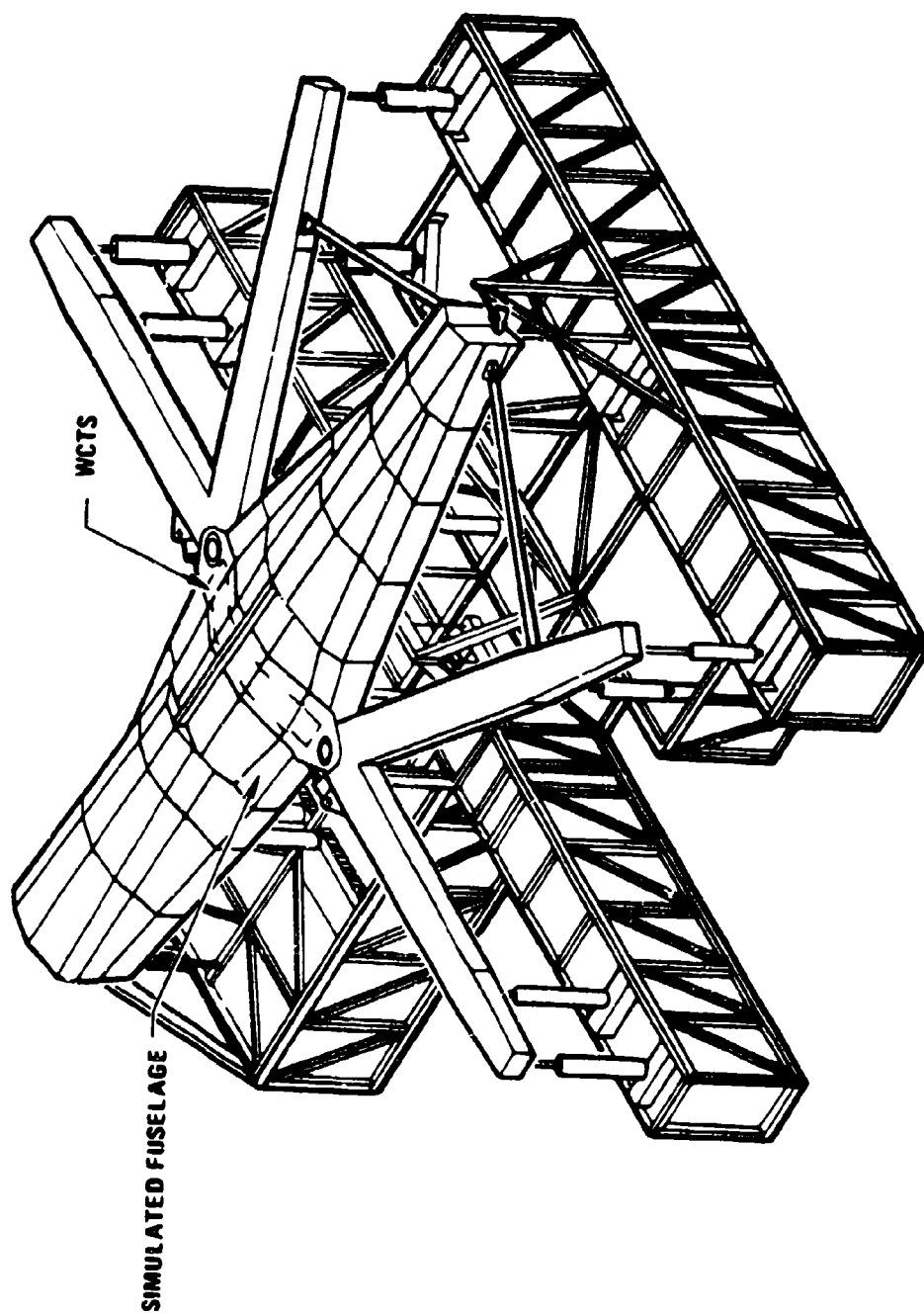
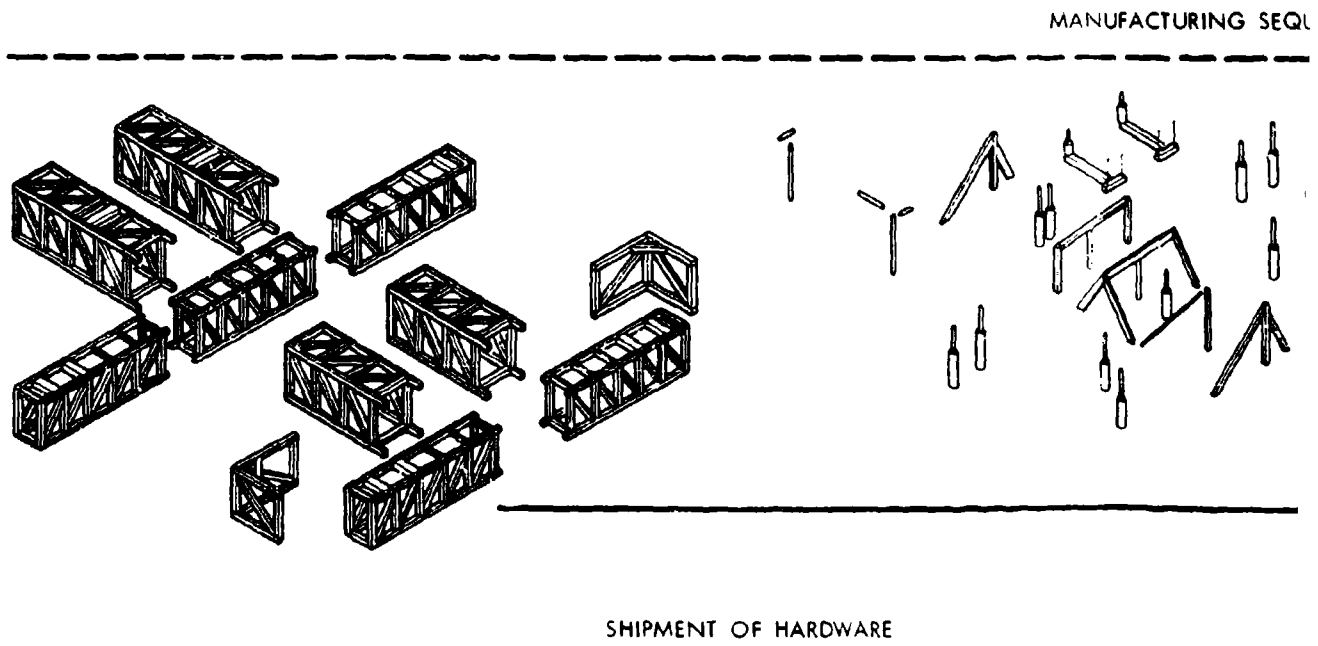
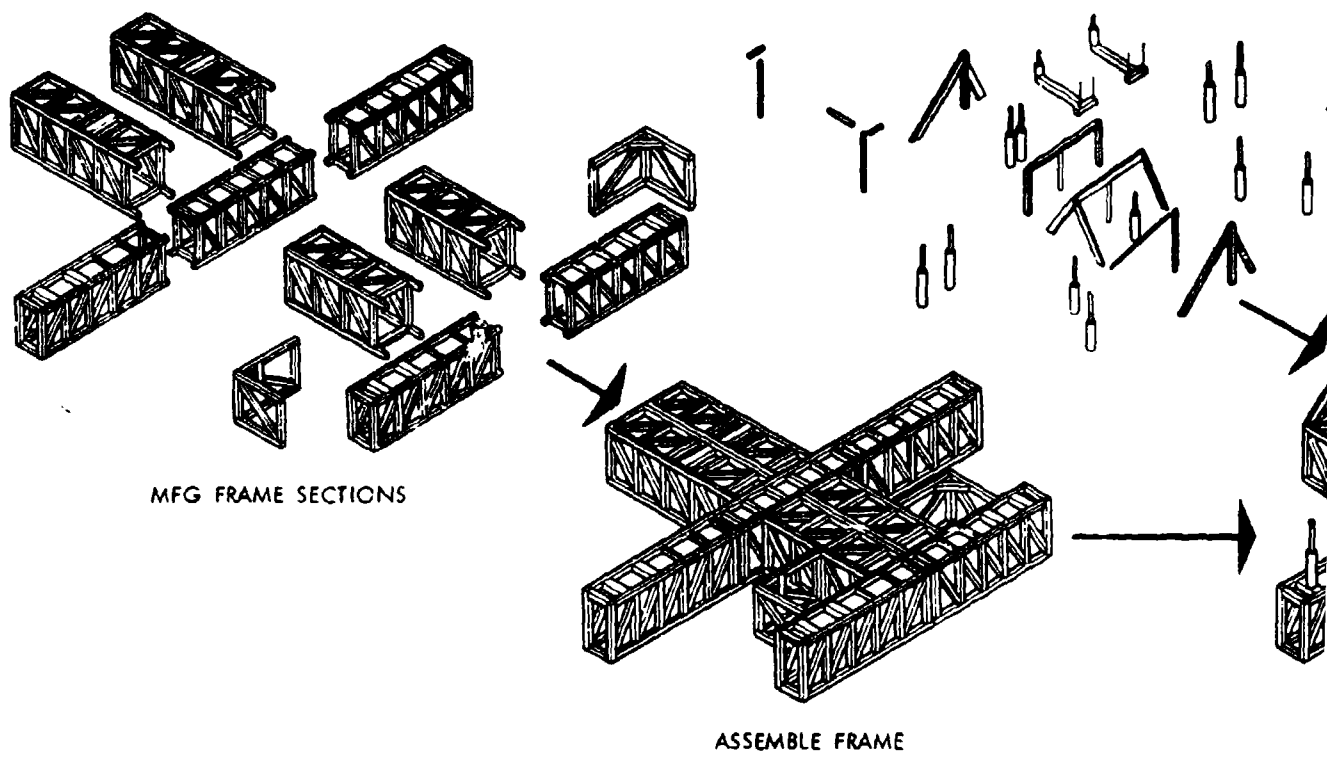


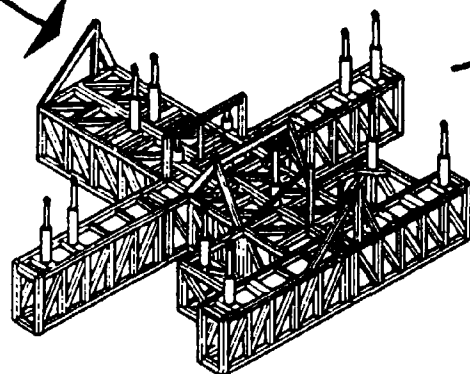
Figure 87 AMAVS FULL SCALE TEST (OVERALL VIEW)



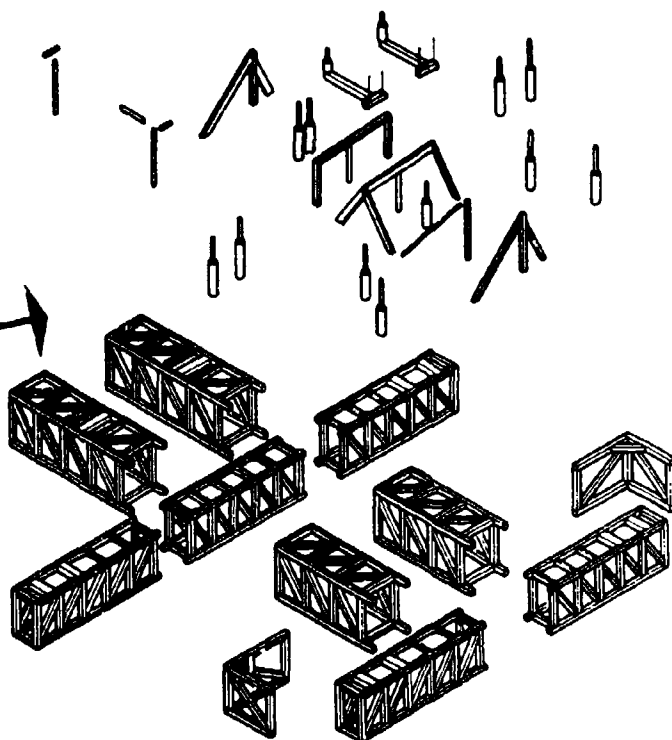
REASSEMBLY SEQU

Figure 88 INITIAL

MFG/PROCURE LOAD
SYSTEM ELEMENTS

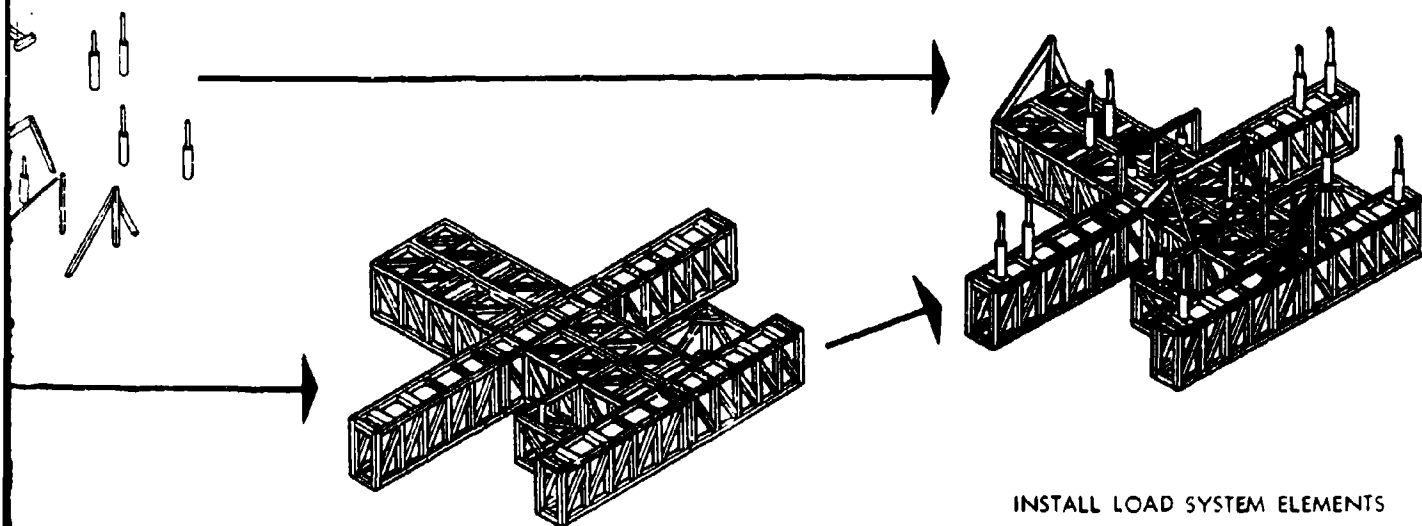


PRE-FIT LOAD SYSTEM ELEMENTS



DISASSEMBLE FOR SHIPPING

CTURING SEQUENCE - LOWER FIXTURE



ASSEMBLY FRAME

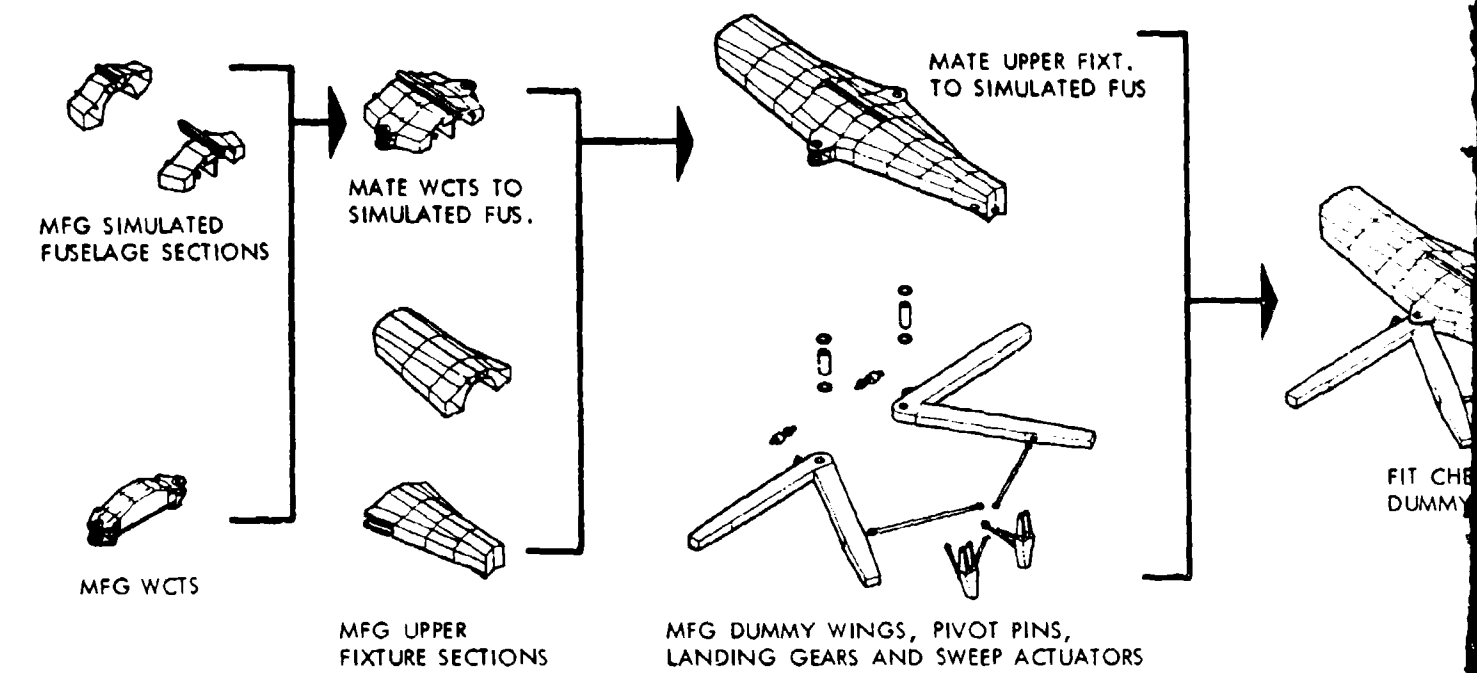
INSTALL LOAD SYSTEM ELEMENTS

SEMBLY SEQUENCE - LOWER FIXTURE

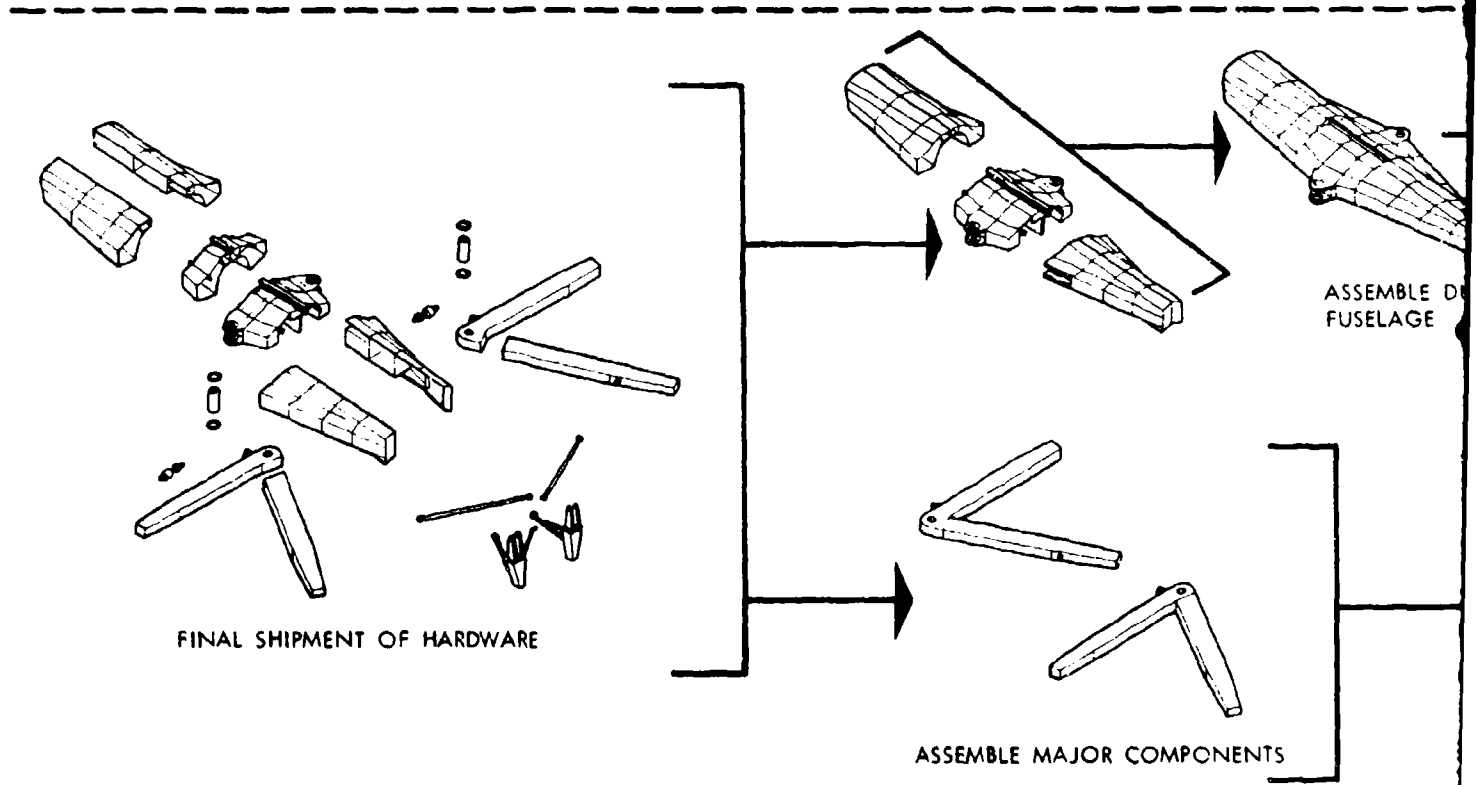
INITIAL SHIPMENT OF HARDWARE

197/198

2

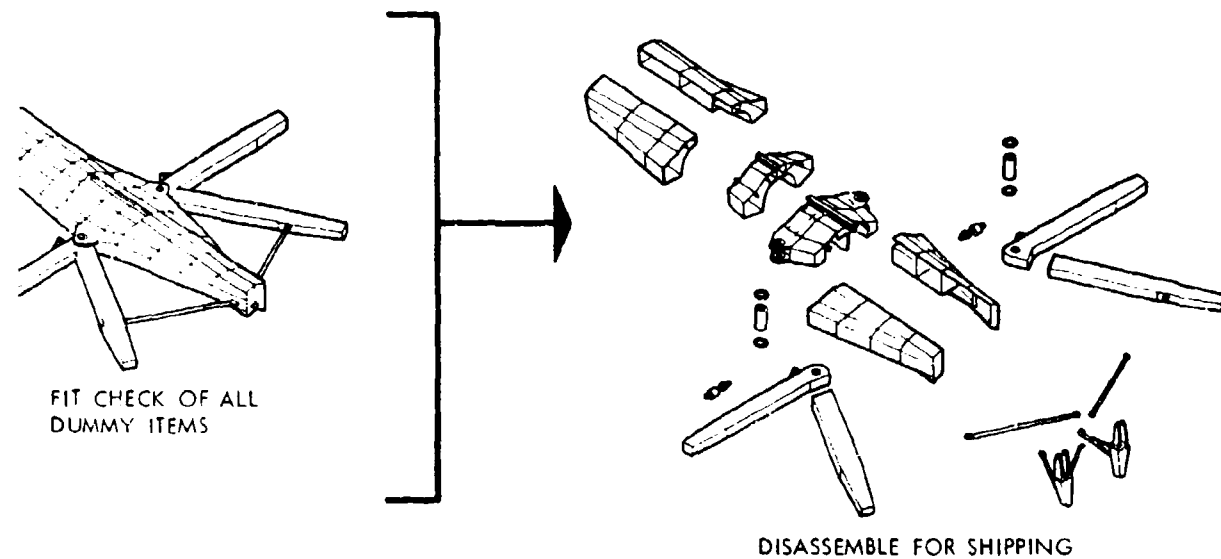


MANUFACTURING SEQUENCE - FINAL HARDWARE

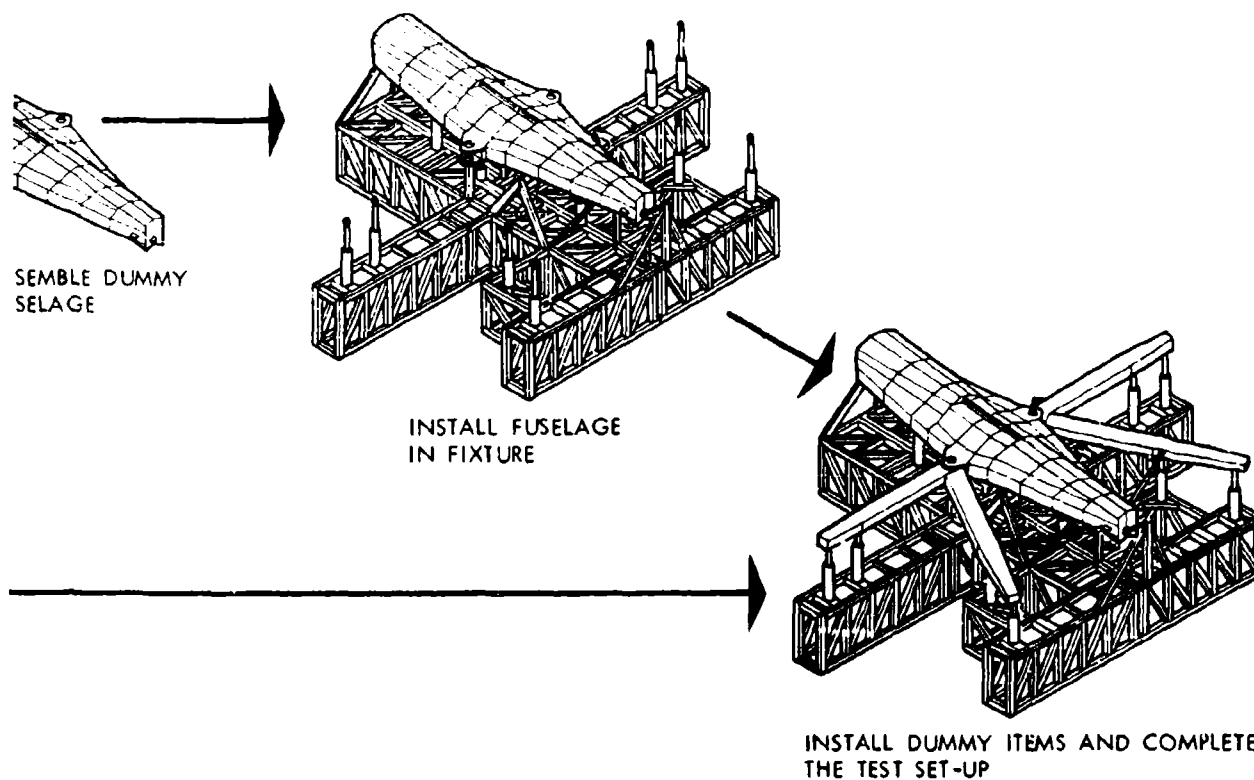


REASSEMBLY SEQUENCE - FINAL HARDWARE

Figure 89 FINAL SHIPMENT



FINAL HARDWARE SHIPMENT



INAL HARDWARE SHIPMENT

SHIPMENT OF HARDWARE

2

Table 29 Full Scale Test Fixture Status

ITEM	DESIGN & ANALYSIS					STATUS - PERCENT COMPLETE					MFG./ASSEMBLY				
	20	40	60	80	100	20	40	60	80	100	20	40	60	80	100
<u>INITIAL SHIPMENT OF HARDWARE</u>															
Load Systems Hardware															
Flat Trusses for Base Frame															
Assembly of Flat Trusses into Box Section															
Assembly of Box Sections into Base Frame															
Prefit Load Systems Hdw. on Base Frame															
Disassemble for Shipping															
<u>FINAL SHIPMENT OF HARDWARE</u>															
Dummy Wings															
Dummy Pivot Pin System															
Dummy Sweep Actuators															
Dummy Main Landing Gears															
Simulated Fuselage Sections															
Upper Fixture Sections															
Fixture for Assembly & Mating															
Mating															
Prefit Dummy Hardware															
Disassemble for Shipping															

3.3 QUALITY ASSURANCE AND NDI

The NDI applications development program has been redefined to parallel the recent changes in the configuration designs. As a result, the NDI specimen requirements were reidentified and have been outlined in the following drawings.

<u>NDI SPECIMEN TYPE</u>	<u>DRAWING</u>	<u>FIGURE</u>
EB and GTA Welding	603R231	90
Bonded Sandwich	603R232	91
Bonded Laminate	603R233	92
Raw Material and Brazing	603R234	93

3.3.1 Brazed Joint Evaluation

Six 7.5 x 12 inch NDI flaw induction and technique development specimens have been fabricated to investigate various means of inducing controllable flaws into a braze line. Specimens MD3189-1, MD3189-2, MD3208 and MD3209, sketches shown in Figures 94 through 97, were built on the basis of results obtained from previous specimens.

A specific objective of the flaw induction program is to achieve a nonwetted surface. It is anticipated that this condition will be the most difficult to detect (see Section 4.3.3 of AFFDL-TR-73-40). Responses obtained by nondestructive methods from nonwetted areas will be compared to responses from voids (which are easily induced) and inclusions such as stainless steel buttons. If the responses from the two types of defects are identical, only the most easily applied method will be used in producing reference part defects.

The specimens are also being used to determine suitable inspection methods. The NDI techniques evaluated on the specimens thus far are: ultrasonic pulse-echo, both contact and immersion ultrasonics, through transmission, a ring pattern application (Slik Bond Tester) and X-ray. All of the techniques except X-ray have been effective on all the induced flaws. One large area in specimen MD3208 (see Figure 98) was not detected by X-ray and is believed to be a nonwetted surface.

Based on work completed thus far, four conclusions can be drawn:

- (1) No detectability problems have been encountered with any of the ultrasonic techniques in the .25 inch thick laminate specimens. All techniques have readily detected the defects.
- (2) The results from ultrasonic pulse-echo tests run from opposite sides of specimens are identical. Experience has shown that in some cases pulse-echo responses from one side of a part are not identical to those from the opposite side.
- (3) Corrosives such as acids do induce flaws, but flaw shape and size are difficult to control.
- (4) "Stop-off" materials such as Everlube T-50 or tungsten disulfide are effective in creating a void condition (alloy completely missing in an area). They are not effective in producing a nonwetted surface.

All of the scheduled brazed manufacturing and engineering specimens have been inspected using X-ray and ultrasonic pulse echo. These specimens include the following.

603R100-3-30, -31, -32, -33, -34, -35, -38, -39, -40, -41,
-42, -43

BZ500-1, -2, -3, -4, -5, -6, -7, -7A, -8, -10, -11, -12,
-12A, -13, -13A, -14, -14A, -15, -17, -18, -19,
-20, -21, -23, -24, -25, -25A, -44, -45

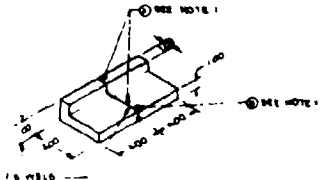
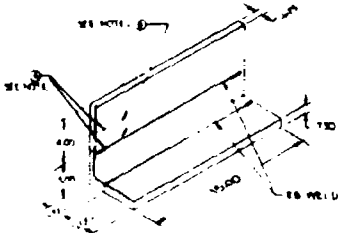
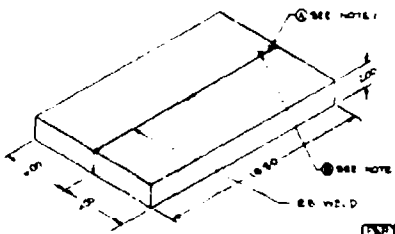
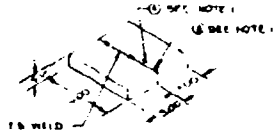
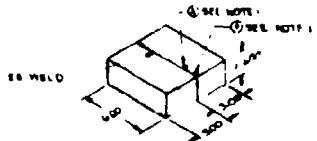
603FTB004-13 #1 and #2

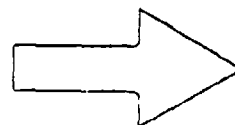
603FTB005-13 #1, #2 before and after test

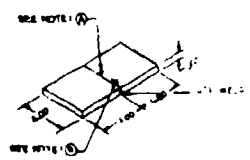
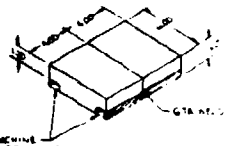
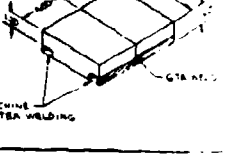
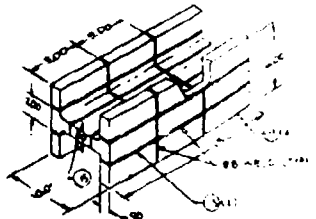
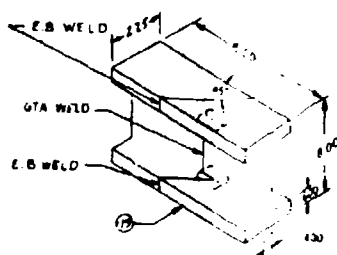
603FTB050-100BZ #1 before and after test, #2 before test.

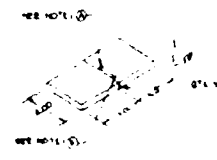


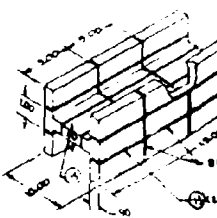
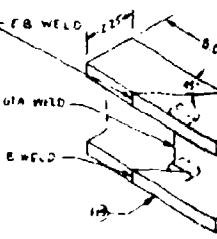

All of the manufacturing and engineering specimens were inspected using X-ray and ultrasonic pulse-echo.

The 603R100-3 and BZ500 specimens evaluated the effects of variables in the manufacturing process. All of these specimens had .25 inch thick laminates. Results obtained from the two methods generally agree with each other.

SPECIMEN	MATERIAL	REQUIREMENTS	
		NDI	TYPE
	6AL-4V BETA TITANIUM	1	3
	6AL-4V BETA TITANIUM	1	3
	6AL-4V BETA TITANIUM	1	
	10 AL-9		
	20 AL-9	2	



SPECIMEN	
	PART 1A MD322
	PART 1B MD323
	PART 1C MD324
	PART 1D MD325
	PART 1E MD326

SPECIMEN	MATERIAL	REQUIREMENTS	
		NDI	INSPECTION
	10 MI STEEL	2	
	10 MI STEEL	2	
	10 MI STEEL GTA WELD	2	
	10 MI STEEL GTA WELD	2	
	10 MI STEEL		SEE NOTE 1
	10 MI STEEL		SEE NOTE 2

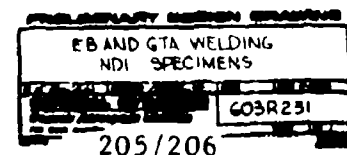


1. NRC PRODUCEABILITY SPECIMEN WILL BECOME NDI SPECIMEN UPON COMPLETION
2. NRC PRODUCEABILITY SPECIMEN MAY BECOME NDI SPECIMEN UPON COMPLETION

INDUCED FLAWS		
HOLE	TYPE	SIZE
8	PH	1/4 DIA
8	PH	2/4 DIA

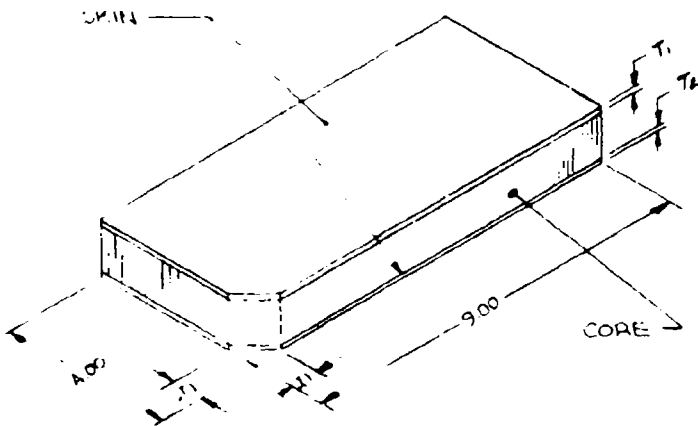
NOTES (EXCEPT AS SHOWN)

Figure 90

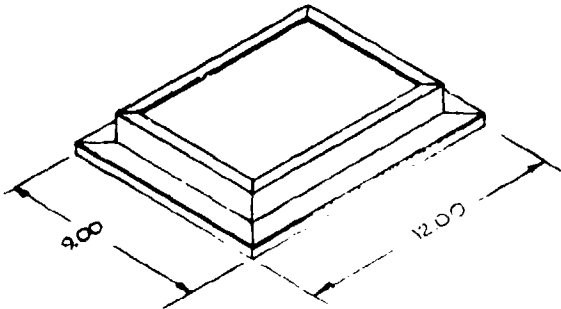
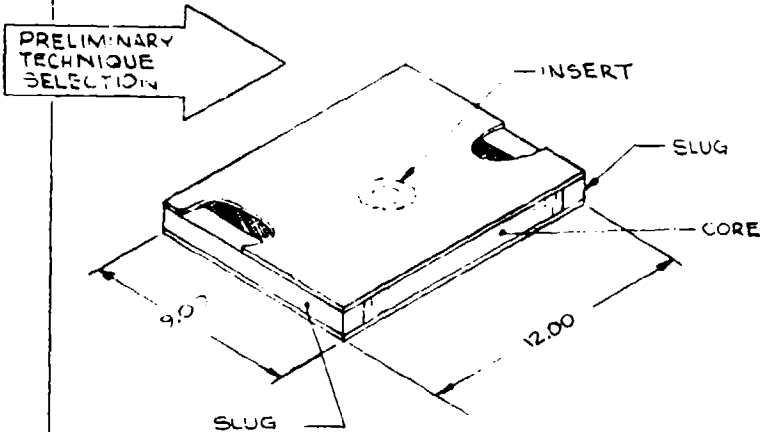
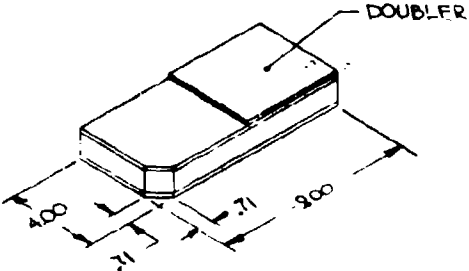


205/206

2

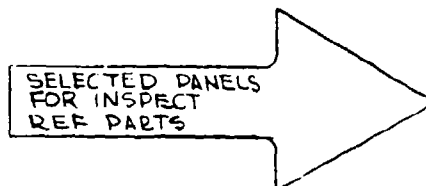
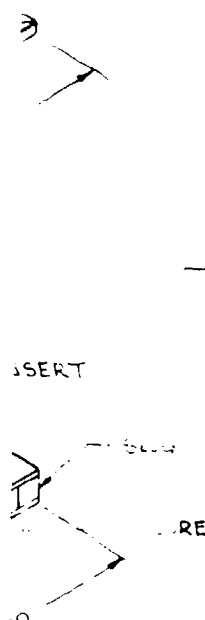
SPECIMEN	PART NO.	MATERIAL		T
		SKIN	CORE	
	MD3196	6AL-4V MILL ANNEALED		.063
	MD3195	6AL-4V MILL ANNEALED		.090
	MD3249	BETA C		.125
	MD3266	2024 ALUMINUM		.200
	MD3256			.125
	MD3267			.080
	MD3258			.035
	MD3268			.125
	MD3260			.190
	MD3272			.130
	MD3269			.050
	MD3262			.300
	MD3271			.250
	MD3270			.150
	MD3264			.090
	MD3257			.300
	MD3261			.213
	MD3263	2024 ALUMINUM		.125
	MD3257	6AL-4V MIL ANNEALED		.250
	MD3265			.135
	MD3278			.060
	MD3279			.135
	MD3280			.185
	MD3281	6AL-4V MIL ANNEALED		.300

GAGE		QUANTITY REQUIRED
T ₁	T ₂	
.063	.063	1
.090	.032	1
.125	.040	3
.200	.075	3
.125	.025	2
.080	.025	3
.035	.025	2
.125	.040	3
.190	.032	2
.130	.032	3
.050	.032	2
.300	.050	3
.250	.050	2
.150	.050	3
.090	.050	2
.300	.063	3
.213	.063	2
.125	.063	3
.250	.030	2
.135	.030	3
.060	.030	2
.135	.060	3
.185	.060	2
.300	.060	3

SPECIMEN	PART NO.	MATERIAL	QUANTITY REQUIRED
		2024 ALUMINUM	30
		6AL-4V MILL ANNEALED T1	10
		2024 ALUMINUM	10
		TITANIUM AND ALUMINUM AS REQUIRED TO EXTEND PRELIMINARY DEVELOPMENT	15

9

	PART NO.	MATERIAL	QUANTITY REQUIRED
		2024 ALUMINUM	30
		6AL-4V MILL ANNEALED TI	10
		2024 ALUMINUM	10
		TITANIUM AND ALUMINUM AS REQUIRED TO EXTEND PRELIMINARY DEVELOPMENT	15

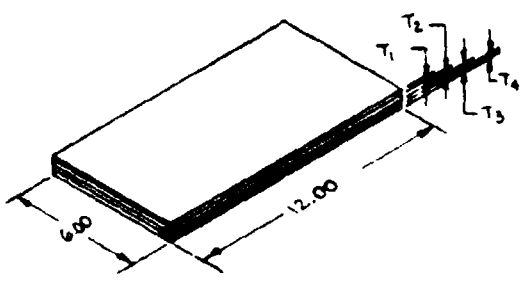
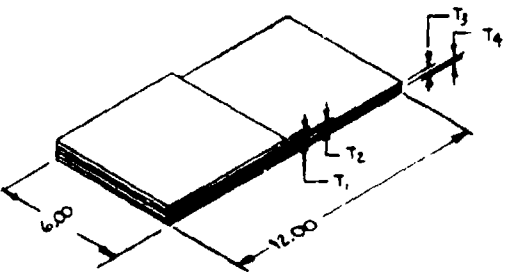


3. DETAILED CONSTRUCTION AND QUANTITY DETERMINED BY PRELIMINARY RESULTS, DESIGN ITERATION AND INSPECTION CRITERIA
 2. FLAW TYPES - TEFLON TAPE INSERTS, OTHER TYPES AS REQUIRED
 1. USE PLTIT ADHESIVE FOR ALL PANELS
- NOTES (EXCEPT AS SHOWN)

Figure 91

PRELIMINARY DESIGN DRAWING

BONDED SANDWICH NDI SPECIMENS			
BY <i>L. Brundage</i>	DESIGNED <i>Chet</i>	SCALE	DATE 5-20-73
GENERAL DYNAMICS Convair Aerospace Division Fort Worth Operation		603R232	
		SHEET	OF

SPECIMEN	PART NO.	MATERIAL	LAMINA				QUANTITY REQD
			T ₁	T ₂	T ₃	T ₄	
 <p>SIMPLE LAMINATE</p>	MD3204	BETA C	.125	.125	.125	.125	3
	MD3203	BETA C	.062	.125	.125	.062	2
	MD3253	BETA C	.100	.100	.100	.100	3
	MD3255	BETA C	.100	.100			3
	MD3254	BETA C	.06	.06			1
 <p>STEPPED LAMINATE</p>	MD3261	BETA C	.125	.125	.125	.100	2
	MD3252	BETA C	.125	.125	.100		3

PRELIMINARY
TECHNIQUE
SELECTION

THICKNESS/ MATERIAL		QUANTITY REQD
EDGE MEMBER	SKIN	
.016 / 2024 AL	.200 / 2024 AL	10
.016 / 2024 AL	.150 / 2024 AL	
.016 / 2024 TI	.300 / 6AL-4V TI	
.016 / 2024 TI	.125 / 6AL-4V TI	
SEE NOTE 3	SEE NOTE 3	SEE NOTE 3

3. CONSTRUCTION AND QUANTITY OF PHASE SPECIMEN
WILL BE DETERMINED BY PRELIMINARY RESULT, DESIGN
ITERATION AND INSPECTION CRITERIA

2. FLAW TYPES- TEFLON TAPE AND OTHERS IF REQUIRED

1. USE PLTIT ADHESIVE FOR ALL SPECIMENS

Figure 92

PRELIMINARY DESIGN DRAWING

BONDED LAMINATE NDI SPECIMENS			
BY <i>R. B. ...</i>	DESIGNED <i>...</i>	DATE	DATE 5-29-73
GENERAL DYNAMICS		603R233	
Convair Aerospace Division			
Fort Worth Operation			

209 / 210

3

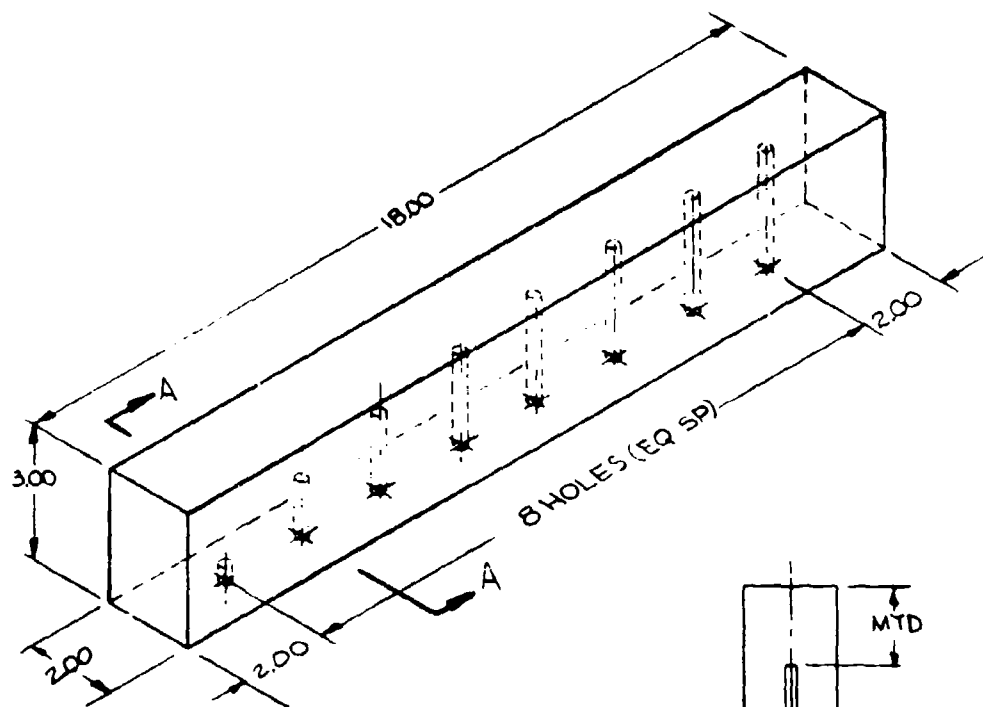
RAW MATERIAL SPECIMENS

PART NO.

MD3201

MD3220

MD3206



SECT. A-A

ESTABL
REFER
SPECIF
REQUI
ADDIT

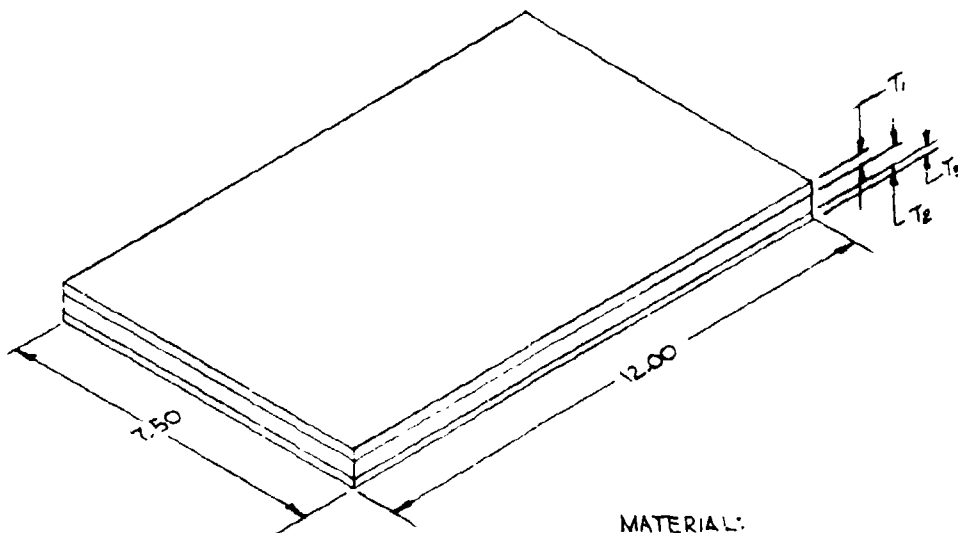
2. HOLES TO BE FLAT BOTTOMED & 5/64 DIA
1. PARTS TO HAVE MTD (METAL TRAVEL DISTANCE) OF: 2.275, 1.750, 1.250, 0.875, 0.625, 0.500, 0.375 & 0.250

NOTES (EXCEPT AS SHOWN)

PART NO.	MATERIAL	QUANTITY REQD
MD3201	6AL-4V Ti	1
MD3220	10 NI STEEL	1
MD3206	BETA C	1

ESTABLISH NEED FOR
REFERENCE BLOCKS;
SPECIFY DESIGN
REQUIREMENTS FOR
ADDITIONAL BLOCKS

BRAZED SPECIMENS



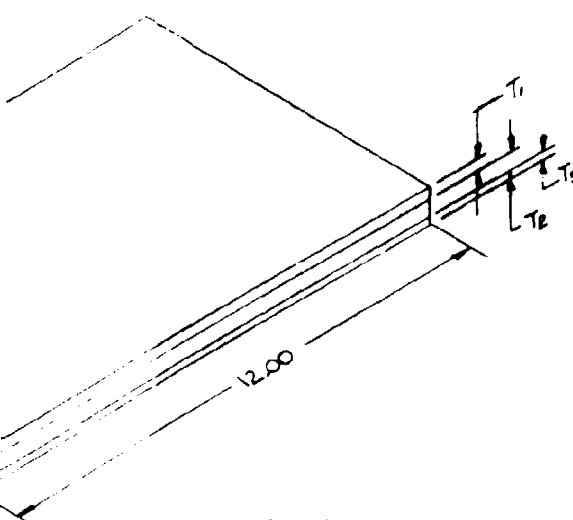
MATERIAL:
BETA ANNEALED 6AL-4V TITANIUM

1. FLAW TYPE W
OF PRELIMIN
NOTES (EXCE

PRELIMIN

RAW N
N
ST. 2.000
GENERAL
Convair Aerospace
Fort Worth Operations

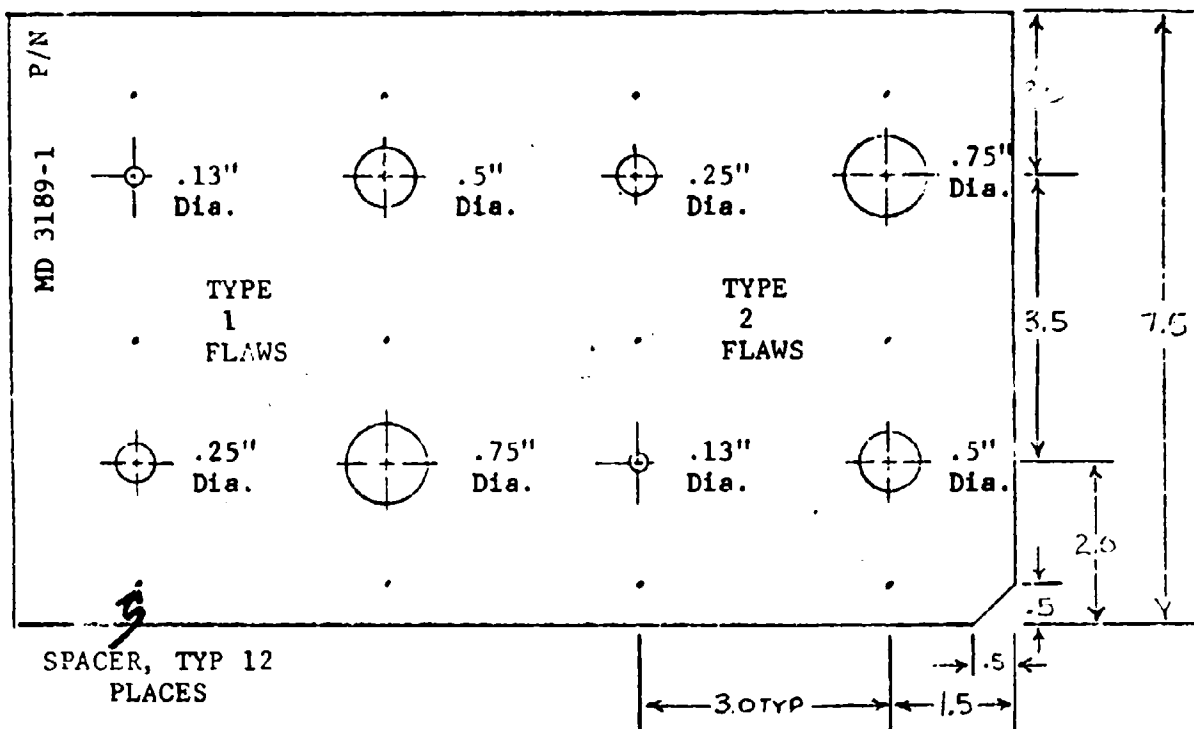
2

D SPECIMENS	PART NO.	LAMINA			TYPE FLAW	QTY REQD
		T ₁	T ₂	T ₃		
 <p>MATERIAL: BETA ANNEALED 6AL-4V TITANIUM</p>	MD3187-1-1	.250	.250		CORROSIVE	1
	MD3187-1-2	.250	.250		INCLUSION	1
	MD3189-1-1	.250	.250		CORROSIVE	1
	MD3189-1-2	.250	.250		INCLUSION	1
	MD3188-1	.250	.250		CORROSIVE	1
	MD3188-2	.250	.250		CORROSIVE	1
	MD3205	.250	.250		CORROSIVE	1
	MD3209	.250	.250		INCLUSION	1
	MD3210	.400	.600		CORROSIVE	1
	MD3211	.400	.600		CORROSIVE	1
	MD3212-1	.250	.250		SEE NOTE 1	1
	MD3213-1	.250	.250			1
	MD3215	.400	.600			1
	MD3222	.400	.400	.400		1
	MD3223	.400	.400	.400	SEE NOTE 1	1

1. FLAW TYPE WILL BE DEFINED AS A RESULT
OF PRELIMINARY STUDIES
NOTES (EXCEPT AS SHOWN)

Figure 93

PRELIMINARY DESIGN DRAWING			
RAW MATERIAL AND BRAZED NDI SPECIMENS			
BY <i>L. B. Shaw</i>	APPROVED <i>W. H. Shaw</i>	DATE	SEP 5-19-73
GENERAL DYNAMICS		603R234	
Convair Aerospace Division			
Fort Worth Operations			



		T1
		T2
		T3

SPECIMEN NO. MD 3189-1

REFERENCE B/P 603R100-3 "B"

MATERIAL: 6Al - 4V Beta Processed Titanium

BRAZE ALLOY: Dynabrazz B (Ag - 5.0 Al - .03 Mn)

PART NUMBER: To be vibroetched at location shown

SPACERS: To be .12" diameter, .002" thick stainless steel placed in hole punched in alloy

FLAWS: TYPE 1 Everlube T-10

TYPE 2 Tungsten Disulfide

LAMINATE THICKNESS: T1 .25"

T2 .25"

T3

Figure 94 ROUGH SKETCH OF NDI SPECIMEN MD3189-1

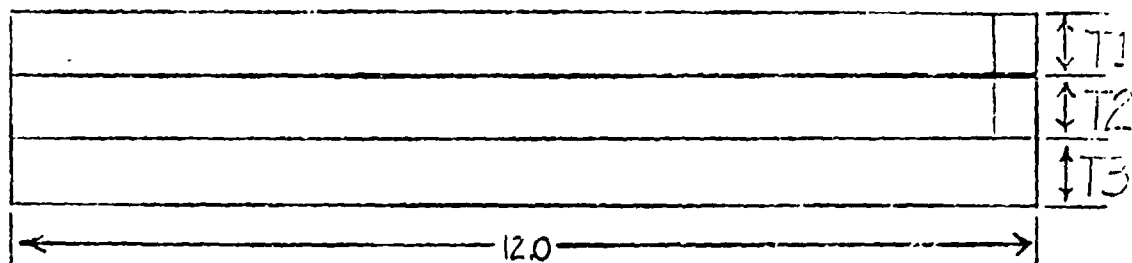
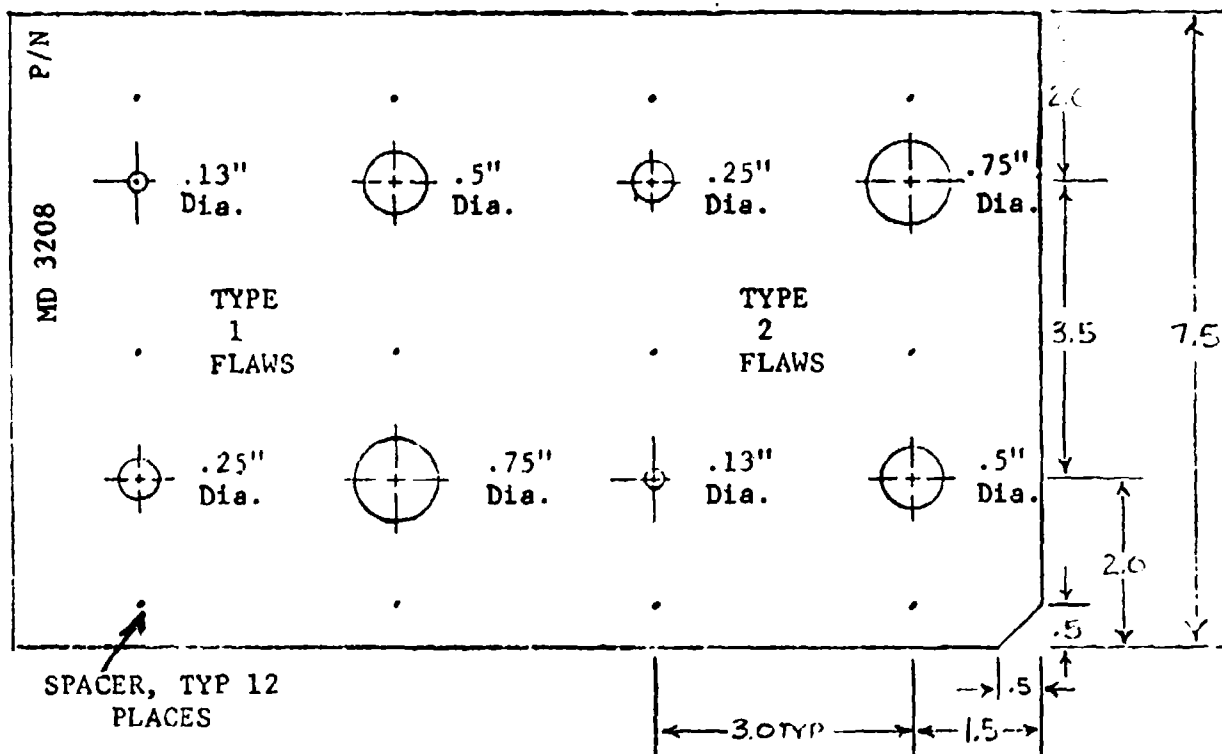


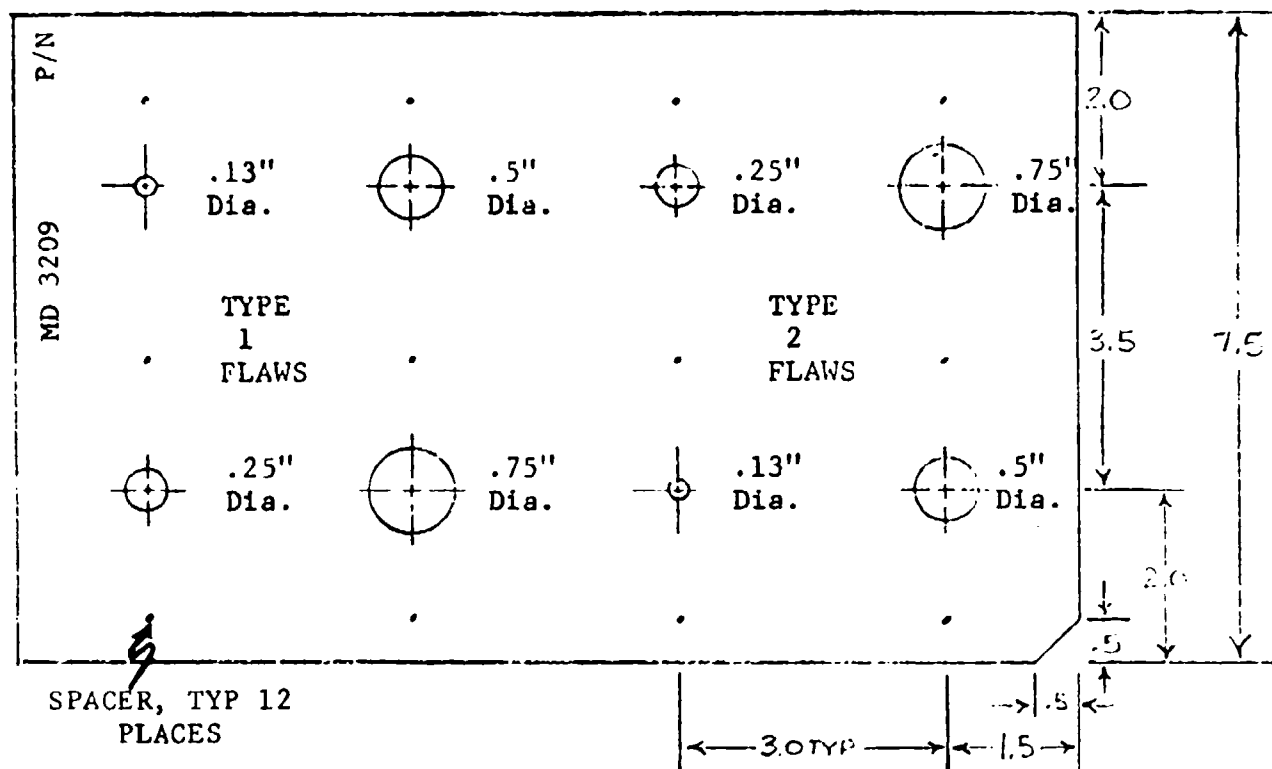
Figure 95 ROUGH SKETCH OF NDI SPECIMEN MD3189-2



		T1
		T2
		T3
12.0		

SPECIMEN NO. MD3208
REFERENCE B/P 603R100-3 "B"
MATERIAL: 6Al - 4V Beta Processed Titanium
BRAZE ALLOY: Dynabraz B (Ag - 5.0 Al - .03 Mn)
PART NUMBER: To be vibroetched at location shown
SPACERS: To be .12" diameter, .002" thick stainless steel placed in hole punched in alloy
FLAWS: TYPE 1 Sulfuric Acid
TYPE 2 Nitric Acid
LAMINATE T1 .25"
THICKNESS: T2 .25"
T3

Figure 96 ROUGH SKETCH OF NDI SPECIMEN MD3208



		↑T1
		↑T2
		↑T3
←12.0→		

SPECIMEN NO. MD 3209

REFERENCE B/P 603R100-3 "B"

MATERIAL: 6Al - 4V Beta Processed Titanium

BRAZE ALLOY: Dynabrazo B (Ag - 5.0 Al - .03 Mn)

PART NUMBER: To be vibroetched at location shown

SPACERS: To be .12" diameter, .002" thick stainless steel placed in hole punched in alloy

FLAWS:

TYPE 1 Everlube T-10

TYPE 2 Tungsten Disulfide

LAMINATE THICKNESS:

T1 .25"

T2 .25"

T3

Figure 97 ROUGH SKETCH OF NDI SPECIMEN MD3209

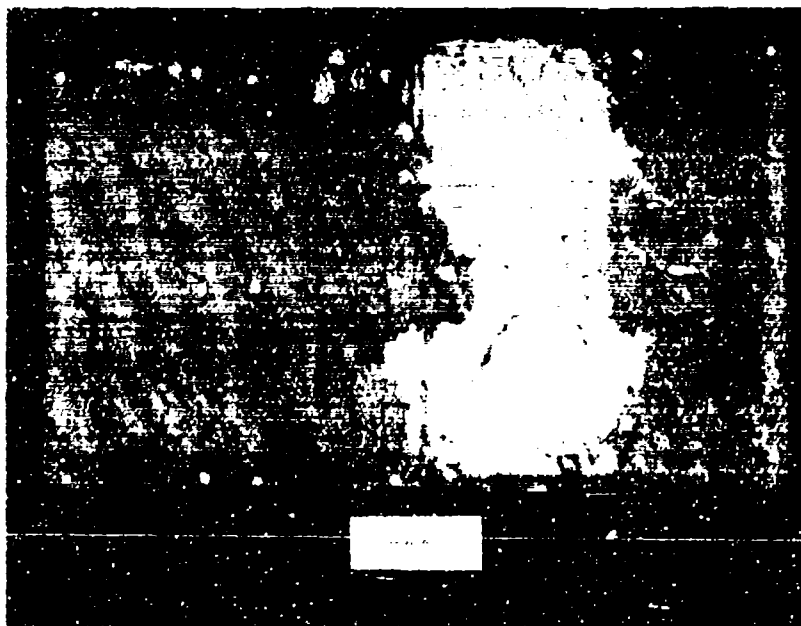


Figure 98 ULTRASONIC C-SCAN OF NDI SPECIMEN MD3208

The first 603FTB005-13 (representative of the lower plate) produced drastically different X-ray and ultrasonic results. The part was later shown to have very large areas of nonwetted surface, see Section 4.3.3.1 of AFFDL-TR-73-40.

A second 603FTB005-13 was built and tested. The part was built of components which were warped in manufacturing. To compensate for this warpage, shims and multiple layers of braze alloy were used. Ultrasonic pulse-echo evaluations of the part before test (Figure 99) showed the part to be relatively free of defects. The part was then fatigue tested until it failed (prematurely). A second ultrasonic test showed the part to be extensively damaged (Figure 100).

Two 603FTB004 simulations of the lower lug were inspected. Ultrasonic inspection was made difficult by the abrupt thickness changes in the parts. Acceptable recordings were obtained, however.

Two crack arrest demonstration specimens were inspected before and after test.

3.3.2 Bonding Evaluations

Four engineering test specimens were evaluated with through transmission ultrasonic technique during this reporting period. These specimens were the four and five layer laminate shear panels outlined on 603R100-8; detail drawing 603FTB012.

Only small indications were obtained in inspecting three of the panels -1-2, -2-1 and -2-2. These indications were resolved by successive increases in instrument sensitivity to determine the relative change in the amount of energy required to eliminate the responses. Thick adhesive areas or other material changes will attenuate the response only about 5 decibels but a void will decrease the detected energy by 10 decibels or more. As a result of applying this procedure the foregoing panels were accepted.

A very large void was detected in inspecting the fourth panel 603FTB012-1-1 as shown in Figure 101 . As a result of the inspection, the panel was disassembled for defect verification and to reuse the detail parts. Figures 102 and 103 show the two internal bond lines. Note that, in general, the voids in the two bond lines correlate with the ultrasonic test.



Figure 99 ULTRASONIC C-SCAN OF 603FTB005#2
BEFORE FATIGUE TESTING

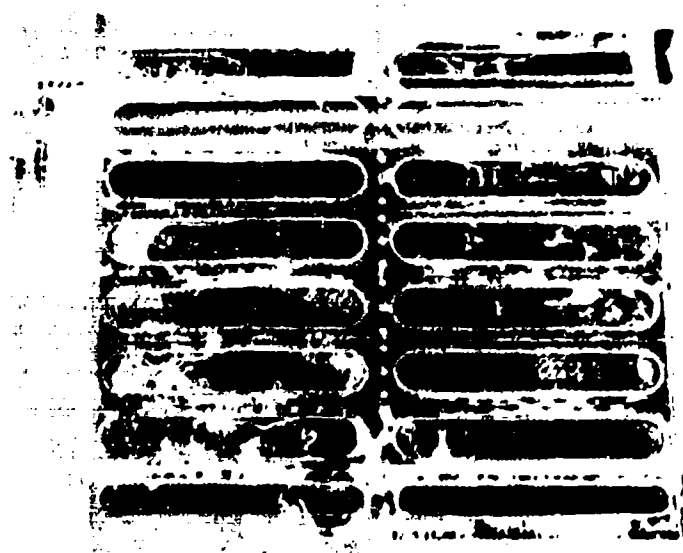


Figure 100 ULTRASONIC C-SCAN OF 603FTB005#2
AFTER FATIGUE TESTING



Figure 101 THROUGH TRANSMISSION C-SCAN RECORDING
OF 603FTB012-1-1



Figure 102 DISASSEMBLY OF 603FTB012-1-1
SECOND BOND LINE



Figure 103 **DISASSEMBLY OF 603FTB012-1-1**
THIRD BOND LINE

The NDI evaluation specimens were fabricated from either 6Al-4V Mill Annealed Titanium or Beta III Titanium. Each specimen had three or four induced flaws of 1.0", 3/4", 1/2" and 1/4" diameter teflon tape in each bond line.

Two of the specimens, MD3195 and MD3196, were sandwich type panels of different skin gage thickness. Through transmission ultrasonic tests showed all but one of the induced flaws (Figures 104/105). Also, numerous other areas were recorded same as the induced flaws.

The other two NDI specimen, MD3197 and MD3198, were three and four layer laminate type panels with .050 and .070 skin gages. Through transmission tests showed all of the induced flaws but failed to record all flaws to their known sizes. Several additional areas were also recorded in Figure 106 , 107 , 108 , 109 , and 110 .

Both types of specimens were evaluated with other techniques; resonance and a energy summing ultrasonic technique. Investigations with these techniques have not progressed to a point where final technique comparisons are realistic.

These specimens were disassembled for bond line analysis and NDI/DT correlations.

The two sandwich panels, MD3195 and MD3196, were cut in half before disassembly. One half was disassembled and the visual inspection showed well defined induced flaws with no unintentional defect area. The through transmission recording and the contact methods showed many additional areas; Figure 104 and 105 . The reasons for the additional indications have not been determined at this time.

Figures 106 through 110 , show each bond line and the through transmission recording. Note that, in general, the natural defect correlates with the NDI results except the recorded sizes were larger.

3.3.3 EB and GTA Welding Evaluations

It is the intended objective of the welding evaluations to examine and select ultrasonic NDT approaches for the inspection of Beta titanium 6Al-4V and 10 Ni steel weldments. For this purpose Pulse-Echo-Longitudinal, Pulse-Echo-Shear and Delta techniques will be and are being investigated.

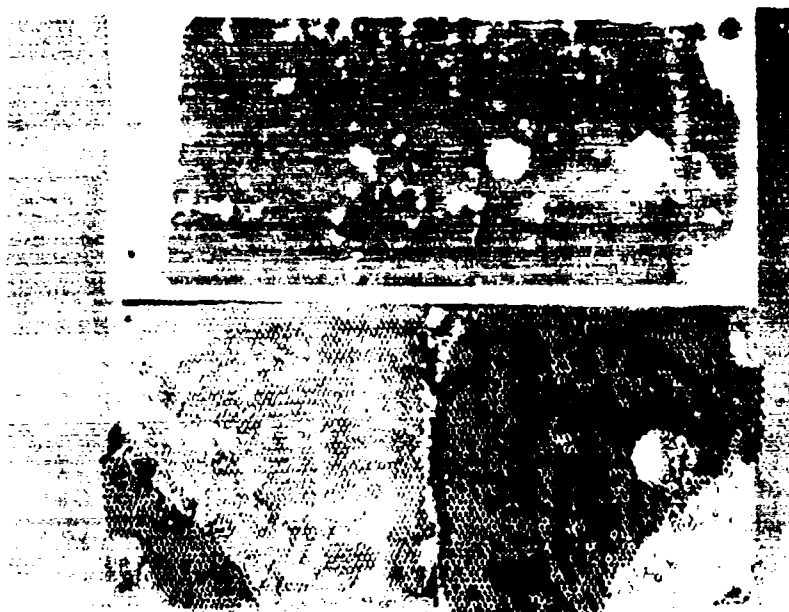


Figure 104 SANDWICH PANEL MD3195, THROUGH TRANSMISSION
RECORDING WITH DISASSEMBLY OF HALF "A"

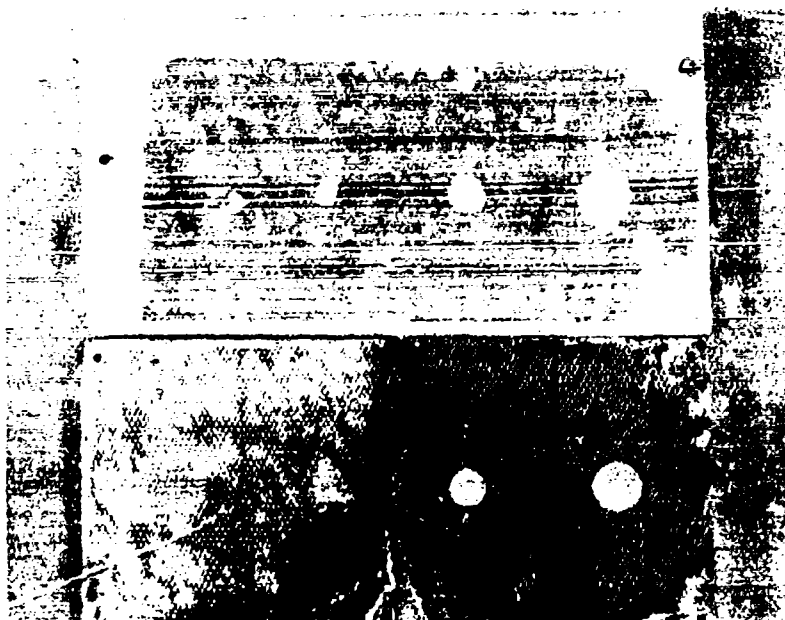


Figure 105 SANDWICH PANEL MD3196, THROUGH TRANSMISSION
RECORDING WITH DISASSEMBLY OF HALF "A"



Figure 106 SPECIMEN MD3197, THROUGH TRANSMISSION RECORDING
WITH DISASSEMBLY OF FIRST BOND LINE

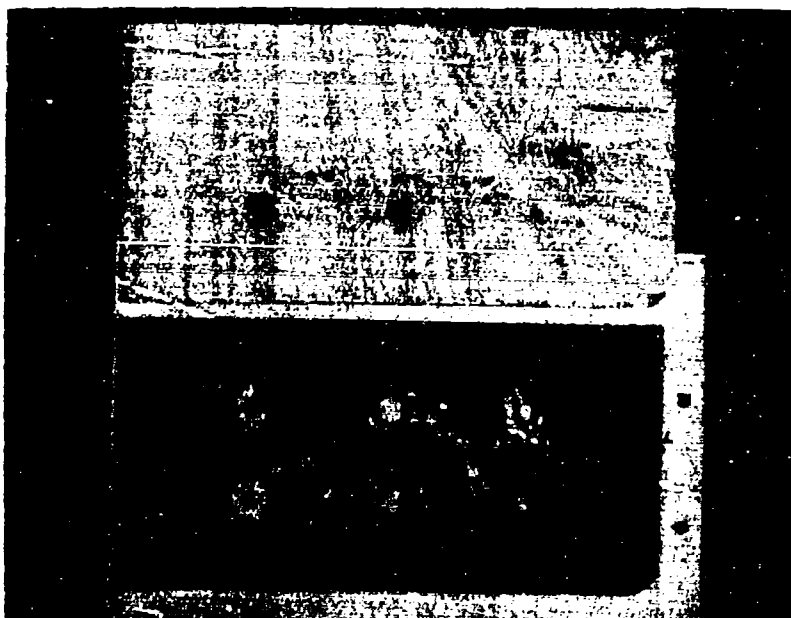


Figure 107 SPECIMEN MD3197 THROUGH TRANSMISSION RECORDING
WITH DISASSEMBLY OF SECOND BOND LINE

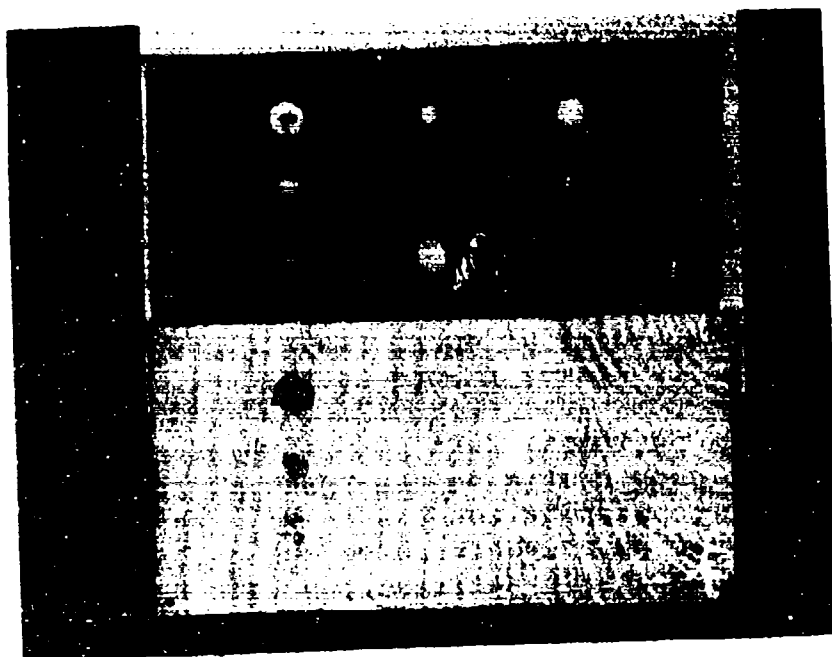


Figure 108 SPECIMEN MD3198, THROUGH TRANSMISSION RECORDING
WITH DISASSEMBLY OF FIRST BOND LINE

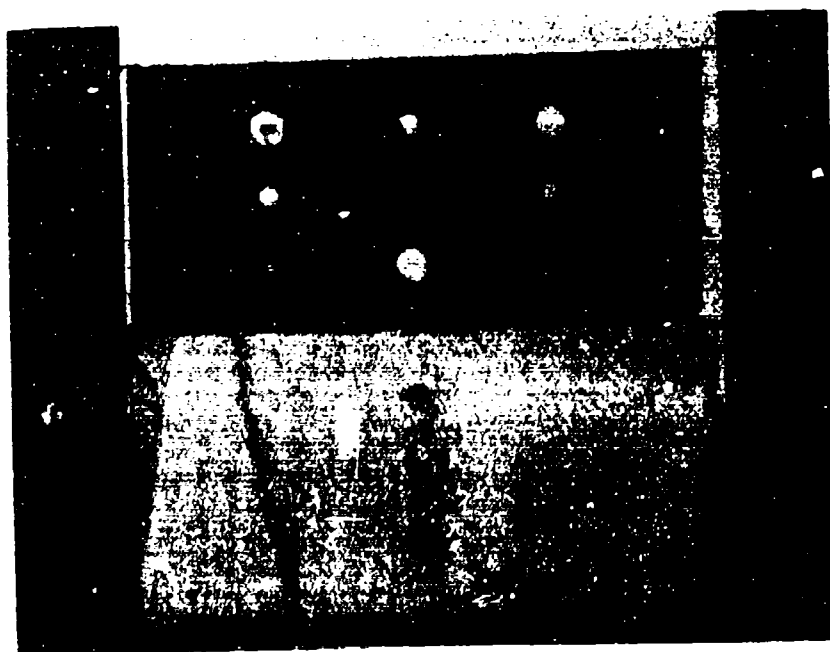


Figure 109 SPECIMEN MD3198, THROUGH TRANSMISSION RECORDING
WITH DISASSEMBLY OF SECOND BOND LINE

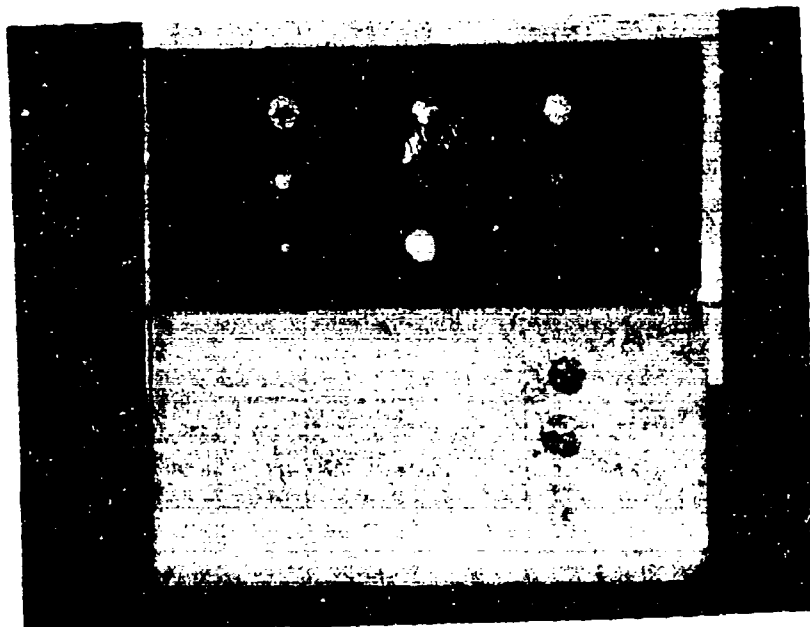


Figure 110 SPECIMEN MD3198, THROUGH TRANSMISSION RECORDING
AND DISASSEMBLY OF BOND LINE #3

3.3.3.1 Titanium 6Al-4V Beta Welds (Pulse-Echo-Longitudinal)

The pulse-echo-longitudinal NDT evaluation has been completed. Flaw response vs depth profiles have been compiled for transducer frequencies 5, 10 and 15 MHZ. These response curves, plotted relative to 2/64 flat bottom holes, (FBH), proved invaluable in tailoring transducer selection and equipment settings. No evaluations were conducted on transducers or frequencies (i.e.: 2MHZ) where preliminary examination and prior experience indicated unsatisfactory potential.

Four 6Al-4V, Ti Beta, one-inch thick angle welds and one, two inch flat plate specimens were inspected and data recorded. From these tests it has been established that 15MHZ focused transducers (SIL and SIJ) produce best ultrasonic penetration and detection compatible with optimum front surface resolution (FSR). (One inch weld, .180 in. FSR; 1/2 inch weld, .100 in. FSR) Pending final evaluation thru specimen sectioning and metallographic examination, 2/64 discontinuity area is a fair estimate of detection capability for this pulse-echo-longitudinal approach. Particularly significant are the apparent sensitivity to narrow vertical flaws and the detection of apparent discontinuity areas not shown in X-rays. In addition, the technique is straightforward using the UM 721 reflectoscope.

The following gives an estimate of inspection potential, defining approximate inspectability, accessibility, thickness and sensitivity factors:

(1) Flat Plate Vertical Weld:

- Accessibility: Two side inspection required due to FSR depth loss.
- Thickness: 2 inch (max) inch depth scanned from each side.
- Inspectability: 80% effectiveness estimated.
20% uncertainty factor due primarily to flaw orientation and geometry plus FSR loss.
- Sensitivity: 2/64" dia. discontinuity area (est).

these welds also, 15 MHZ transducers have permitted the best obtainable responses. Data recorded in the preliminary "best effort" inspections will be used in conjunction with, and to corroborate, the evaluation of the forthcoming NDI test specimens.

(2) Tee Weld:

Accessibility: Inspection possible from either of two sides; from the flat traverse element or thru the perpendicular arm.

Thickness: One inch to and including weld area.

Inspectability: 80% effectiveness estimated.
20% uncertainty factor due to flaw orientation and geometry (no FSR loss).

Sensitivity: 2/64" dia. discontinuity area (est).

(3) Angle Weld:

Accessibility: Any of four side potential approaches.

Thickness: One inch to and including weld area.

Inspectability: 80% effectiveness estimated.
20% uncertainty factor due primarily to flaw orientation and geometry plus FSR loss.

Sensitivity: 2/64" dia. discontinuity area (est).

3.3.3.2 Titanium 6Al-4V Beta Welds (Delta and Shear)

Shear evaluation test will be conducted at the end of this program. Delta NDI preliminary tests have been initiated. Negative results have been obtained with available D6 delta probes (GD QC 127, 148 and 149). Some satisfactory results have been obtained utilizing SIJ 15 and SIL 5 MHZ transducers. Number 3 eloxed slots have produced satisfactory responses. At the present time bottom and top elox response ratios are not satisfactory (6 to 7 optimum). This is deemed correctable by optimizing transducer depths and angles or by transducer selection. A primary handicap of this technique that must be overcome is the higher than usual "noise" responses from the weld area. This is the determining factor in minimum area discontinuity detectability.

3.3.3.3 10 Nickel Steel Welds

Only preliminary inspections have been performed with these type of welds. Evaluation was conducted in 12, 1/2 inch, flat weld plates. In preparation for further testing work, eloxed slots and flat bottom hole (FBH) references are being prepared. For

these welds also, 15 MHZ transducers have permitted the best obtainable responses. Data recorded in the preliminary "best effort" inspections will be used in conjunction with, and to corroborate, the evaluation of the forthcoming NDI test specimens.

3.4 MANUFACTURING DEVELOPMENT

The manufacturing effort during this reporting period was primarily concerned with manufacturing methods development, fabrication of engineering test specimens and design support consultation. Tasks accomplished through March 15, 1973 and reported in detail in the Phase Ib report (AFFDL-TR-73-70), are summarized herein and detail results presented for the period of March 15 - June 15, 1973.

3.4.1 Adhesive Bonded Metal Laminated Structure Process Development

The plan for adhesive bonding manufacturing process development has been realigned and rescheduled due to the decision made at the January 15-18 design review conference. The adhesive bonded (DTIL) configuration was removed from AMAVS carry through box competition. The realigned plan is directed toward identification and solution of the manufacturing problems associated with adhesive bonding laminated titanium components using 1/8 inch Titanium alloy. Such structures are included in current designs of the FSIL and "No Box" Box configuration as bulkheads and ribs.

Manufacture of the bulkheads, and ribs involve adhesive bonding of relatively large area laminates up to four ply thickness (rather than the 10 ply thickness involved in the DTIL lower plate). Many of the processing problems anticipated are the same as those involved in bonding a 10 ply laminate. All effort towards development of processes for bonding 10 ply metal laminates has been stopped. The 10 ply laminates and the laminate data already obtained will be utilized, wherever possible, in development of the manufacturing processes for the 4 ply adhesive bonded elements.

3.4.1.1 Realigned Test Plan

The new adhesive bonding manufacturing development plan embodies the following elements:

1. Bonding of a simulated bulkhead, involving manufacture of lamina details containing machined pockets, cut outs, and fingers from measured Beta C titanium 1/8 inch ground sheet. The effect of manufacturing

operations on the curvature and adhesive bonding characteristics of the details will be determined. The details will be adhesive bonded into an assembly; and the assembly evaluated for thickness, warp, and adhesive bond characteristics. Assessment of chemical etching of Beta C as a method of metal removal for manufacturing operations is included.

2. Continued tool planning and manufacturing engineering support of the manufacture of adhesive bonded design verification test panels.
3. Support of the raw material evaluation and adhesive selection and verification test programs.
4. Initial development work on techniques and methods for repair of voids in adhesive bonded titanium metal laminated structure.

3.4.1.2 Program Summary and Status

To develop the manufacturing process for adhesive bonding bulkheads, a bonding tool (BNFM) was built and plans were made for processing and adhesive bonding four simulated bulkhead panels using "ground" (current) 1/8" Beta C alloy sheet for 2 panels and "rolled and pickled" 1/8 inch Beta C alloy sheet for 2 panels.

On receipt of the 1/8 inch Beta C alloy sheet in late March, material for details for one 4 ply simulated bulkhead panel (40 inch x 36 inch) was sheared and released for measurement and machining of pockets, cutouts and fingers in preparation for adhesive bonding. Also, a single lamina (40 inch x 36 inch) was sheared and sent to chemical etch for etching pockets, cut outs and fingers for assessment of chemical etching as a method of metal removal.

All details for completion of the adhesive selection and adhesive evaluation programs have been completed and have been delivered to Process Control for preparation and testing of specimens.

Planning for marking and first-cut operations on all incoming Beta C alloy material has been completed and all Beta C material has been received, marked, the required first cut

operations performed, and remnants placed in stock. Thickness and flatness measurements of three "rolled and pickled" and five "ground" sheets of Beta C alloy 1/8 inch sheet (as received) have been completed. The "rolled and pickled" sheets show greater thickness variation, wider thickness range, and possibly slightly less curvature than the "ground" sheets.

All adhesive bonded design verification test panels (603FTB012 and 603FTB014) have been manufactured and delivered to engineering test laboratory for test. All fastener tests (603FTB014) have been completed and three of the four bonded shear specimens (603FTB012) have been completed.

Initiation of the program for void repair technique development is awaiting approval by AMAVS Program Management. Preliminary plans for task accomplishment have been made.

3.4.1.3 Manufacturing Problem Area - Summation to Date

The data at present indicates that the major road block to successful adhesive bonding of laminated structures is the high degree of non-flatness of the metal used for lamination. Flat metal can easily be bonded without voids. Curved metal can easily be bonded without voids provided the pressure applied during cure of the adhesive brings the two metal surfaces together sufficiently close, without air entrapment, so that adhesive fills all space between them. Compensation for metal curvature can be provided by increasing the volume of adhesive between the plies. This results in thicker adhesive bondlines in the finished structure and may result in a void condition due to local lamina curvature mating conditions.

3.4.1.4 Program Data

3.4.1.4.1 Beta C Alloy Sheet Raw Material Evaluation Data

Sheet Thickness - A comparison of the sheet thickness characteristics of current marketed (ground) sheet and special "rolled and pickled" sheet (significantly lower in cost than the ground) is given in Table 30. The data shows that the thickness range of the "rolled" material is much greater than the "ground" material, as expected, and indicates that the grinding operation merely "knocks off" the sheet surface peaks.

The rolled and pickled material could be used in adhesive bonding, provided allowance is made for tolerance of thicker

Table 30

BETA C TITANIUM ALLOY 1/8-INCH SHEET THICKNESS

	GROUND VS ROLLED & PICKLED						ROLLED & PICKLED **		
	GROUND *						1-3	1-4	1-5
Sheet	1-1	1-2	1-6	1-7	1-8				
Average	.1257	.1273	.1255	.1219	.1271		.1304	.1275	.1295
Maximum	.128	.130	.128	.125	.1305		.1385	.1345	.1350
Minimum	.122	.123	.1205	.1175	.118		.1215	.118	.1205
Range	.0060	.0070	.0075	.0075	.0125		.0170	.0165	.0145
Std. Dev.	.00197	.0062	.0009	.0101	.0018		.0032	.0069	.0029
Dimension	37x100	37x99.5	39x98	37x97.5	39x101		39x103	39x97	39x103.5
No. Points	408	408	429	396	442		442	429	455

*HT 304324-19

**HT 304324-25

All dimensions - inches

adhesive bondlines, resulting from space due to possible mating of peaks on individual lamina. From the range noted in the Table, the space between the lamina could be as much as .035" due to peaks on the surface.

Contour diagrams showing sheet thickness variation within each measured sheet are included in the Appendix. Pages 276 through 280 show thickness variation within the ground sheets. Pages 281 through 283 show thickness variation within the rolled and pickled sheets.

Sheet Flatness - Table 31 gives a comparison of the flatness characteristics of the two types of sheet materials. This data indicates individual sheet waviness of the two materials is similar, i.e., both "ground" and "rolled and pickled" material contain sheets having high waviness and sheets which are relatively flat. However, the "rolled" sheets may have slightly less curvature than the "ground" sheets.

Contour Diagrams showing waviness of the individual sheets are also included in Appendix. Pages 284 through 288 show waviness of the ground sheets; pages 289 through 291 show waviness of the rolled and pickled sheets.

3.4.1.4.2 Engineering Design Verification Test Panel Manufacture

603FTB014 - Fastener Comparison Test - To manufacture the adhesive bonded 603FTB014 Assembly, a four ply, 1/8 inch Beta C alloy titanium laminate was laid up using PL717 adhesive and cured using the deaeration processing technique. The 16 x 36 inch bonded panel was sawed into sections, approximately 5 inch x 12 inch, and the test specimens were machined to shape and drawing dimensions. Load and fastener holes were drilled and reamed in the finish machined specimens to prepare them for test. The deaeration processing technique and specimen machining and hole preparation were accomplished as previously reported in the Summary report AFFDL-TR-73-40.

The waviness of each Beta C alloy sheet used in the 4 ply bonded panel was measured on the "as received" sheet and after shear and grit blast to determine degree of contour change caused by these operations. Thickness of the bonded panel, as well as the flatness of each surface, was also measured. The bonded panel thickness varied only .026 inch, from .504 inch minimum to .530 inch maximum, with the center area being thicker as shown in Figure 111.

Table 31

BETA C TITANIUM ALLOY 1/8-INCH SHEET FLATNESS

GROUND VS ROLLED & PICKLED

	Ground					Rolled & Pickled		
	1-1	1-2	1-6	1-7	1-8	1-3	1-4	1-5
Sheet								
Average	.2243	.1706	.1782	.1862	.1948	.1764	.1735	.1827
Maximum	.557	.274	.375	.396	.396	.374	.221	.507
Minimum	.130	.129	.123	.125	.132	.132	.126	.130
Range	.427	.148	.252	.271	.264	.242	.095	.377
Std. Dev.	.0777	.0304	.0451	.0486	.0160	.0467	.0230	.0590
Dimension								
Width	37	37	38.7	36.7	38.7	38.8	38.8	38.9
Length	100.	99.5	97.7	97.5	101	103.3	97.0	103.5
No. Points	408	408	429	396	442	455	429	455

Panel surfaces were relatively flat as shown by the flatness contour maps in Figure 111 varying .017" on the bag side and .028" on the tool side.

The ultrasonic "C" scan on the bonded panel indicated it possibly contained some small localized voids; however, no voids were detected during subsequent machining and drilling operations.

The flatness comparison of the individual sheet lamina, in the original sheet (Figure 112) after shearing (Figure 113) and after grit blast (Figure 114), indicate these manufacturing operations cause no significant change in the general shape of the metal. However, "cans" or high curvature in the large sheet are, for the most part, trapped within the piece cut from the large sheet and the curvature magnitude may be greater or less than was present in the large sheet. Grit blasting tends to reduce the magnitude of curvature of the pieces.

603FTB012 - Bonded Shear Web - Except for one assembly, the four 603FTB012 bonded shear web panels were processed through detail cutting, machining and adhesive bonding without difficulty. Cutting and machining of the Beta C titanium alloy sheet was readily accomplished using current titanium metal working procedures. Adhesive bonding the net machined details into an assembly was very successful using make-up rivets to maintain lamina alignment. This indicates the technique is applicable for bonding bulkhead, rib and cover panels for the selected box configuration.

Bonded panel thickness variation and surface flatness variation, both within a panel and between duplicate panels, was relatively small as shown in Table 32 . The maximum doubler area thickness variation within a panel was .019 inch and variation between the panels in the doubler areas was less than .019 inch. Web area thickness variation, except for one assembly, was approximately the same. The panel thickness measurements reflected the presence of adhesive bondline thicknesses of up to .020 inch in the web areas of the panels, except for the one assembly which indicated adhesive bondline thicknesses of up to .030 inch.

Surface flatness variation was also in the range of .015 to .025 inch with tool side variations being less than the variation on the bag side. Contour maps of the bonded panel surfaces indicate the flatness of one surface is independent of the other surface, which shows that there was no significant warpage (rack) in the bonded panels.

4 PLY 16" x 36" 1/8" BETA C TITANIUM ALLOY
PL717 ADHESIVE

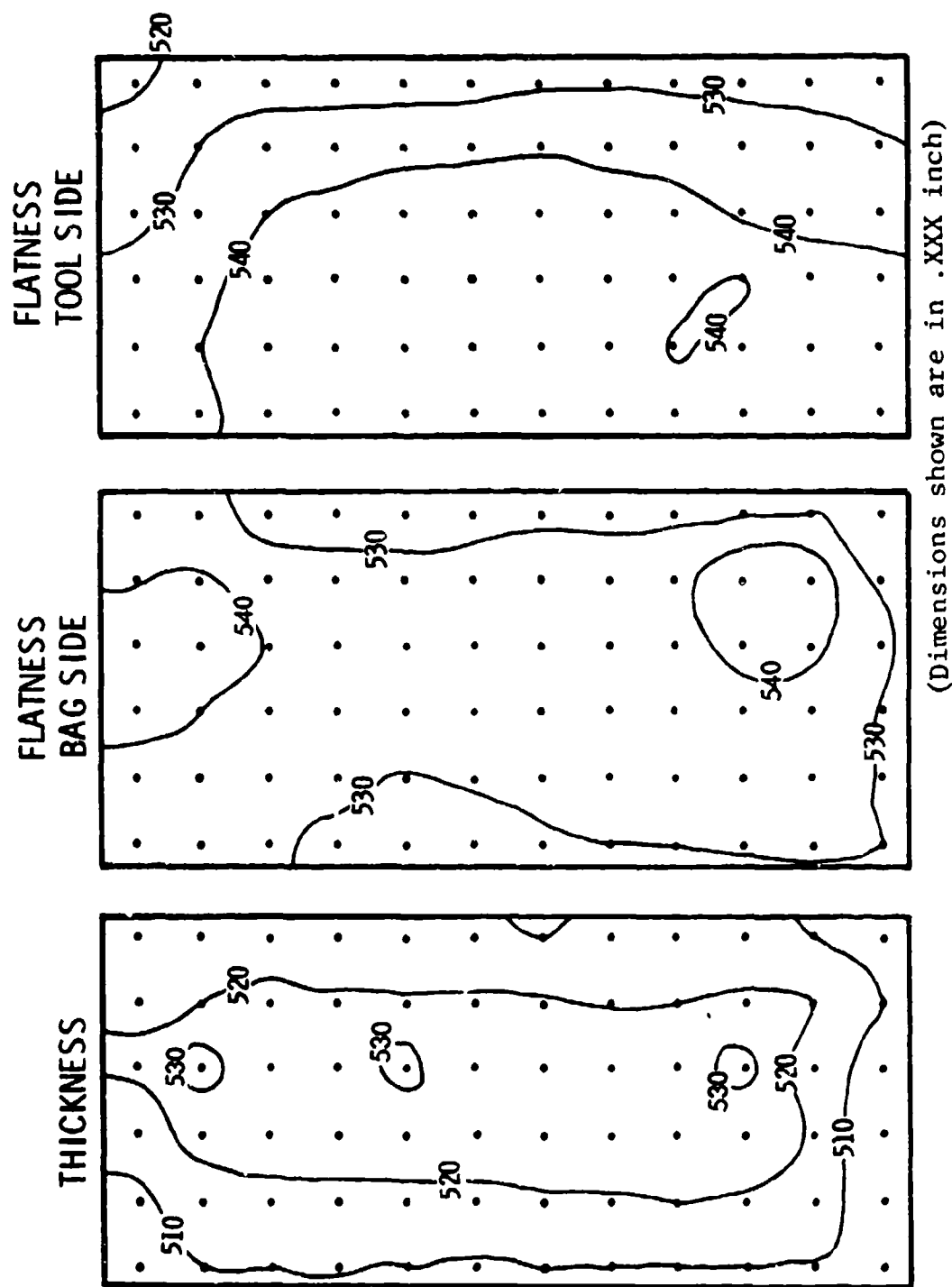


Figure 111 603FTB014 ADHESIVE BONDED PANEL

IN ORIGINAL SHEET (AS RECEIVED)
1/8" BETA C TITANIUM ALLOY SHEET

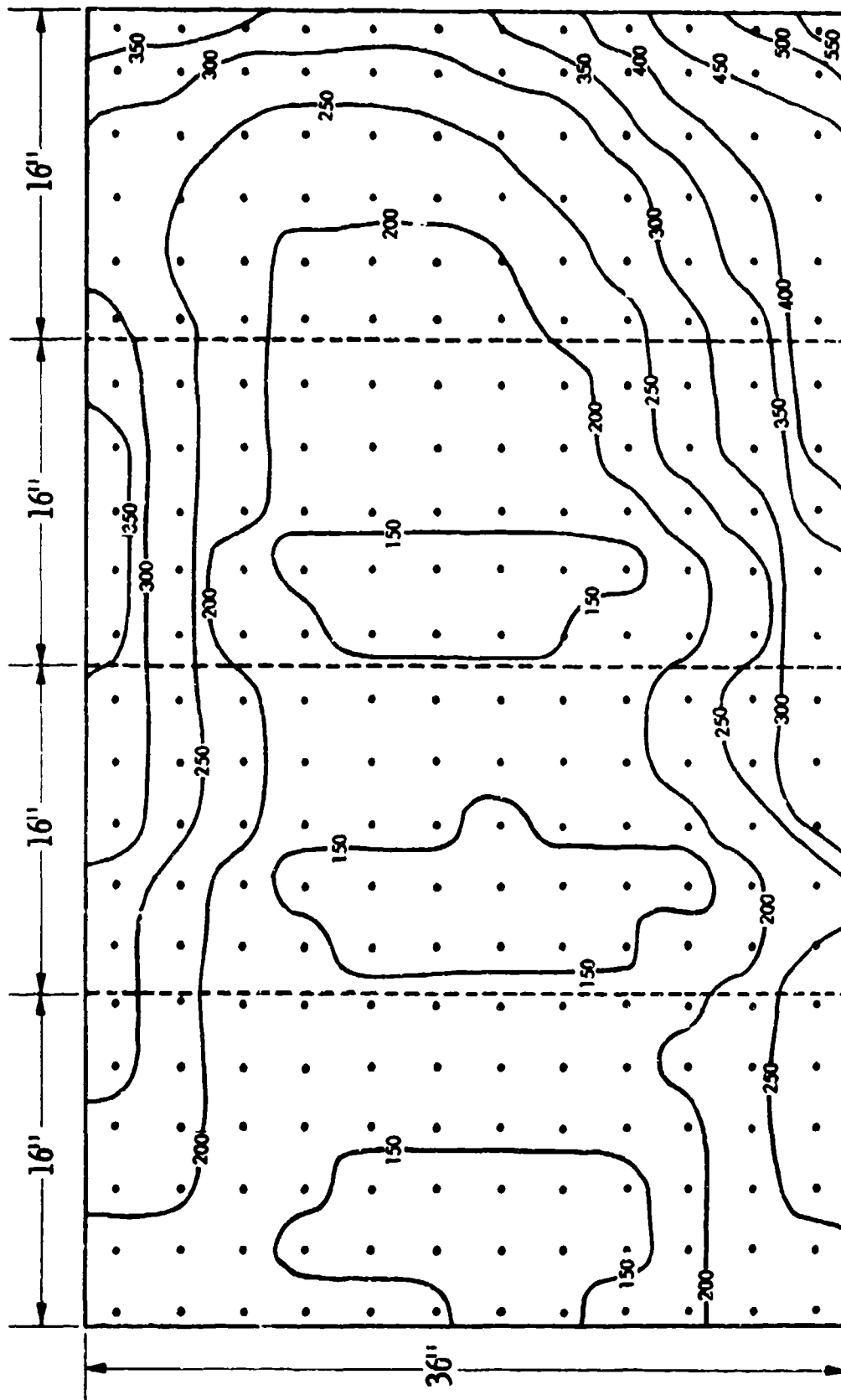
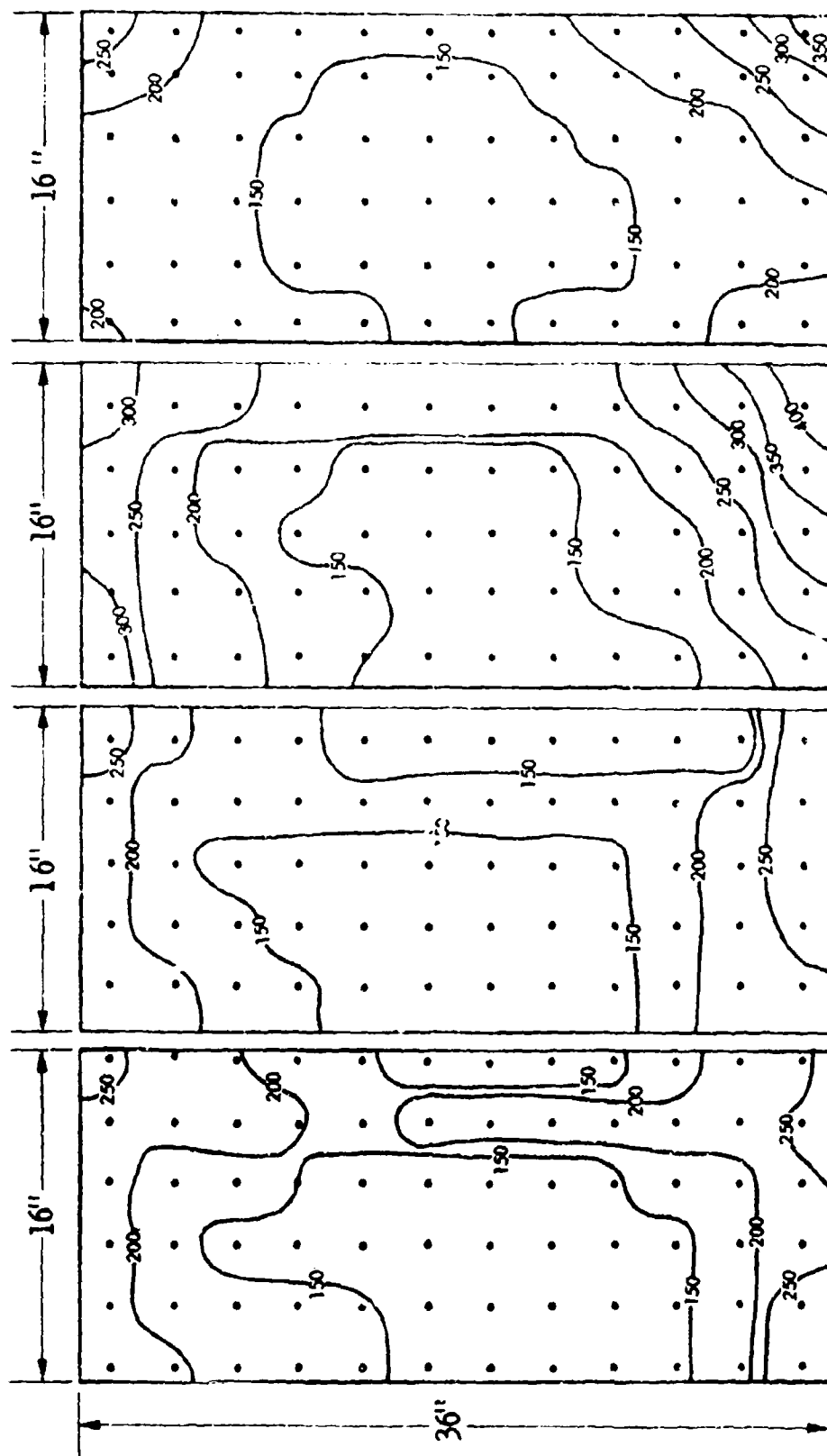


Figure 112 603FTB014 SHEET LAMINA FLATNESS

(Dimensions shown are in .XXX inch)

AFTER SHEAR OPERATION
1/8" BETA C TITANIUM ALLOY SHEET

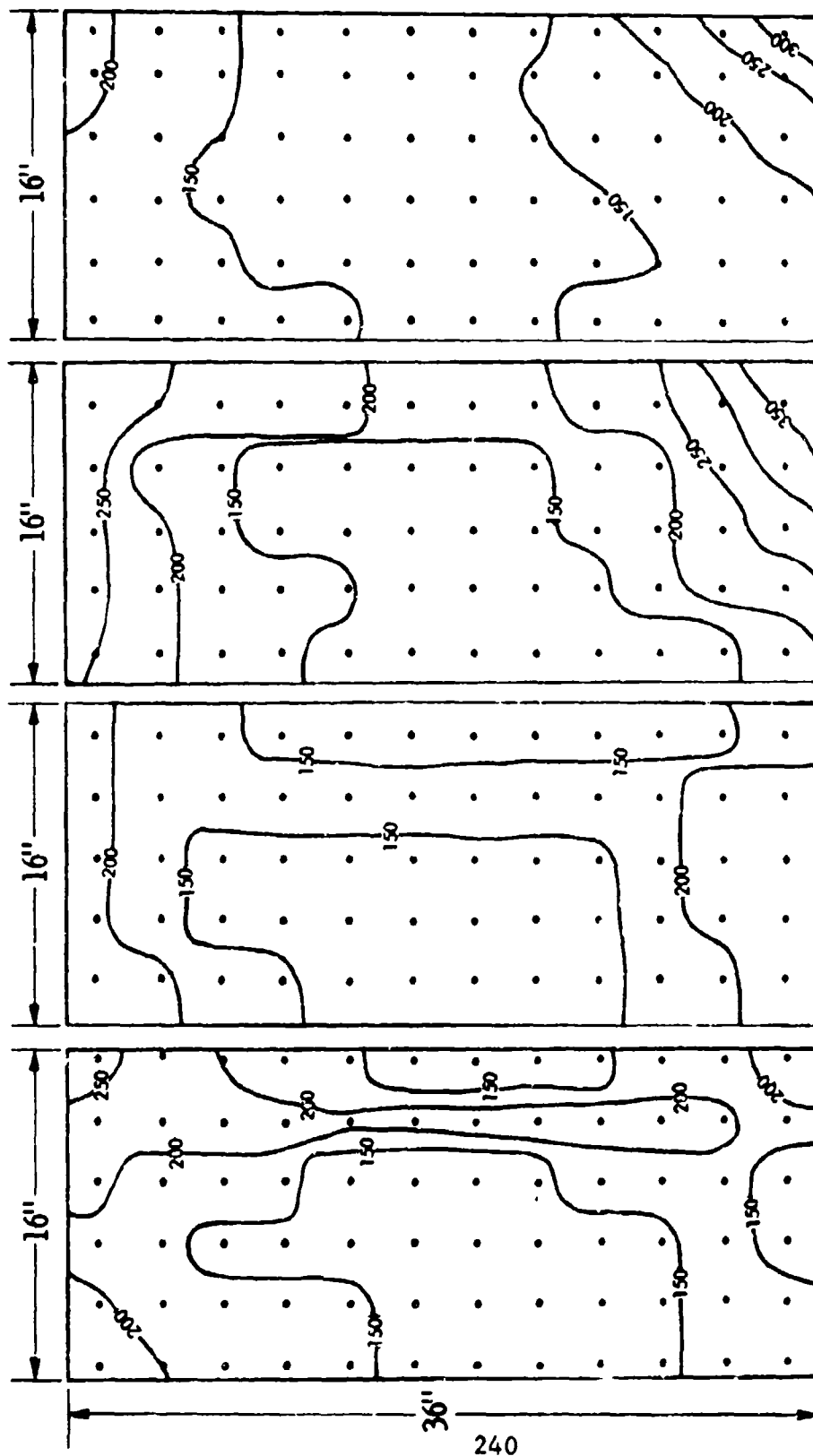


(Dimensions shown are in .XXX inch)

Figure 113 603FTB014 SHEET LAMINA FLATNESS

AFTER GRITBLAST

1/8" BETA C TITANIUM ALLOY SHEET



(Dimensions shown are in .XXX inch)

Figure 114 603FTB014 SHEET LAMINA FLATNESS

Table 32 603FTB012 ADHESIVE BONDED PANELS

S/N	-3 Configuration		-3 Configuration		
	4 Ply Doubler	2 Ply Web	5 Ply Doubler	3 Ply Web	5 Ply Web
S/N	524983	524984	524985	524986	529441
<u>Thickness</u>					
Doubler Area					
Maximum	.519	.510	.540	.542	.535
Minimum	.500	.497	.525	.525	.520
Range	.019	.013	.015	.017	.015
Web Area					
Maximum	.272	.261	.407	.424	.407
Minimum	.259	.252	.390	.389	.385
Range	.013	.009*	.017	.035**	.022
<u>Flatness (Bag Side)</u>					
Doubler Area					
Maximum	.529	.516	.546	.548	.548
Minimum	.508	.501	.529	.532	.530
Range	.021	.015	.017	.016	.018
Web Area					
Maximum	.402	.393	.485	.487	.485
Minimum	.382	.380	.469	.462	.460
Range	.020	.013	.016	.025*	.022
<u>Flatness (tool side)</u>					
Doubler Area					
Maximum	.528	.515	.546	.549	.557
Minimum	.514	.501	.533	.534	.527
Range	.014	.014	.013	.015	.030
Web Area					
Maximum	.408	.394	.470	.485	.492
Minimum	.388	.380	.460	.473	.476
Range	.020	.014	.010	.012	.022

* Web Center Not Measured.

** Panel Peeled Evaluated and Reprocessed as B/W 529441

Contour maps, showing the thickness variation and surface contour of each bonded panel, are included in Appendix, pages 292 and 293 show the thickness variation in the -3 panels; pages 294 through 296 show the thickness variation in the -1 panels. Surface contour of the -3 panels are shown on pages 297 and 298; surface contour of the -1 panels are shown on pages 299 through 301.

As previously indicated, difficulty in bonding one of the -1 configuration assemblies was encountered. The bonded panel, after cure of the adhesive, indicated thick adhesive bond lines (from measurement of the web area thickness) and NDI through transmission "C" scan indicated a large void in the web area.

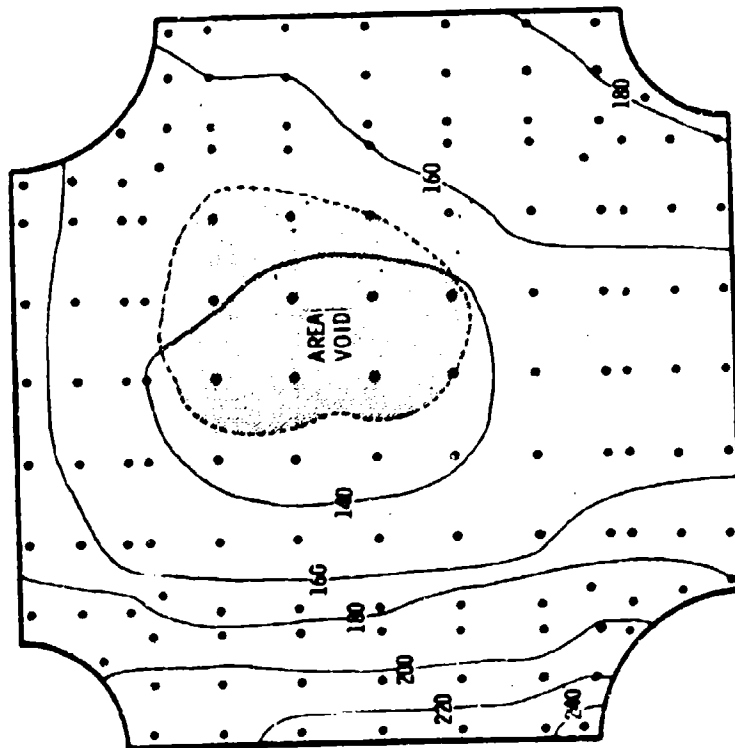
The bonded panel (S/N 524986) was disassembled and visual examination revealed a void approximately 5 inches in diameter in one adhesive bondline (shown in Figure 102) and a void approximately 3 inches in diameter in the other adhesive bondline (shown in Figure 103). The void areas were "in series" in plan view in the panel and "C" scan results appeared as if there were one continuous void present.

Analysis of the void areas showed that the adhesive filled all volumes up to a depth of .018" around the large void area and to a depth of .016" around the small void area, indicating in each case, the presence of more volumetric space than the available volume of adhesive could fill.

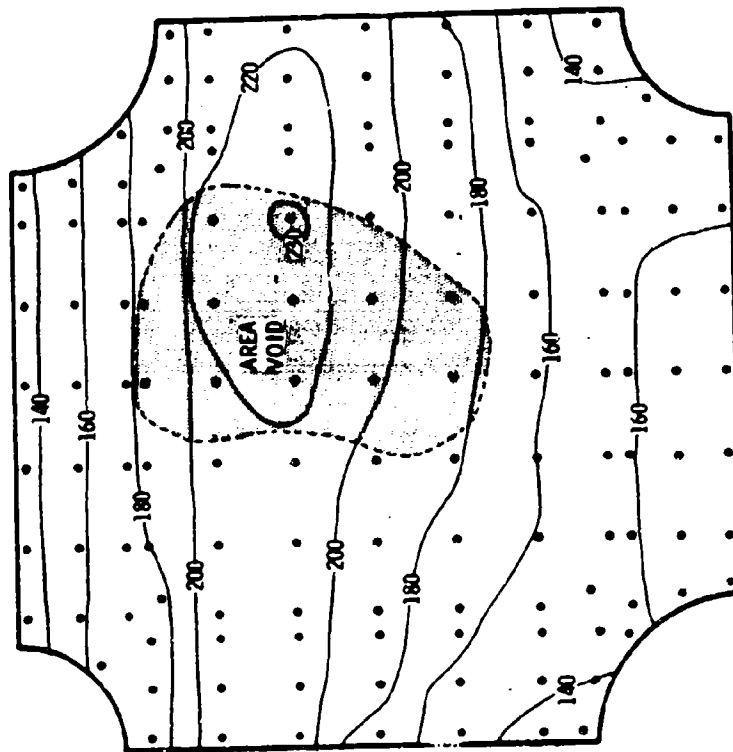
After removal of the cured adhesive from the individual details, the flatness of each detail, in the as-bonded position was measured. Contours of ply #2 and ply #3 and the location of the 5 inch void between them are shown in Figure 115 . The measurements indicate, for the 5 inch void area, a convex canned area in the top (#3) ply matched a concave canned area in the bottom (#2) ply. This caused an elipsoid shaped space, with diameter of approximately 8 inches and depth of approximately .100 inch, before pressure for cure was applied. The space was reduced to a depth of approximately .030 inch when bonding pressure of 85 psi was applied. The adhesive filled all areas having a depth of .018 inch or less.

Contours of ply #3 and ply #4 and the location of the 3" void between them are shown in Figure 116 . The measurements indicate, for the 3" void area, a narrow apex, relatively short radius (3 to 5 inches) paraboloid wave in #4 ply, which was

PLY #2 BAG SIDE UP



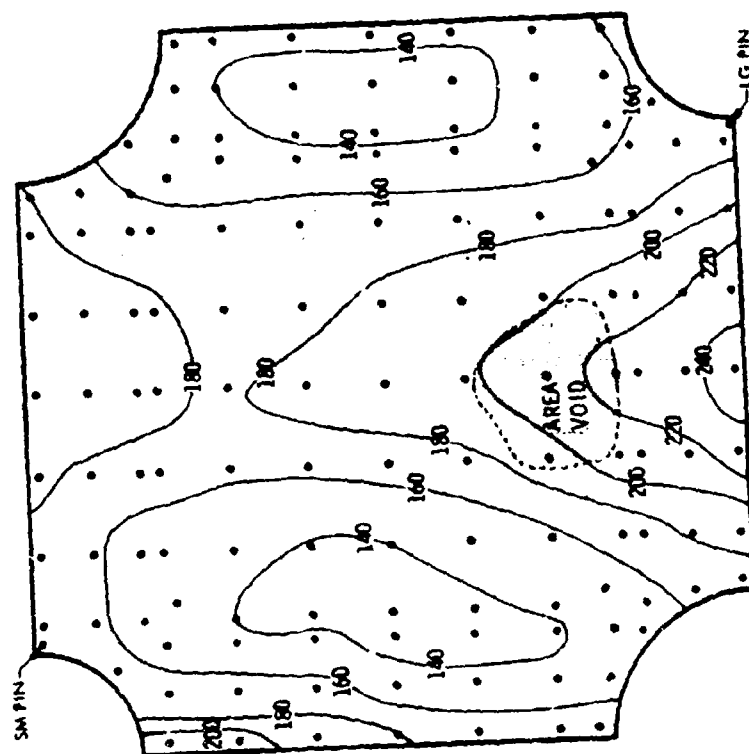
PLY #3 BAG SIDE UP



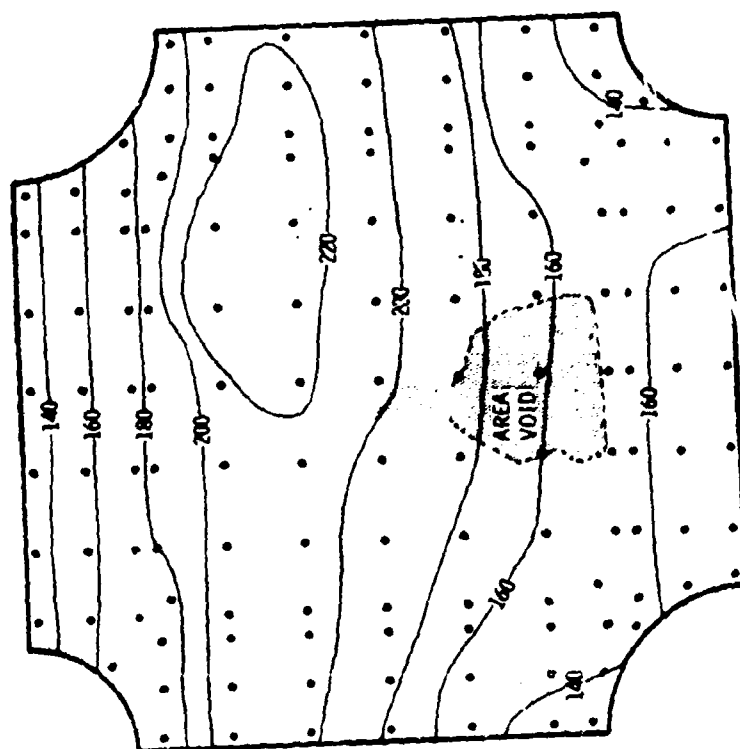
(Dimensions shown are in .XXX inch)

Figure 115 603FTB012-7 DETAIL

PLY #4 BAG SIDE UP



PLY #3 BAG SIDE UP



(Dimensions shown are in .XXX inch)

Figure 116 603FTB012-7 DETAIL

located immediately adjacent to, and slightly overlapping a concave area of #3 ply. In this case, the 85 psi pressure closed the gap between the plies to very nearly .016 as shown by the very irregular shape assumed by the void. In the case of both the 3 and 5 inch void areas, increasing the bond pressure and/or increasing the thickness of the basic adhesive film used, would totally eliminate or at least decrease the area of the voids.

After measurement of flatness, the details were reassembled and stacked (so far as configuration would allow) so as to nest convex surfaces into convex surfaces. Figure 117 shows the height of the unbonded 5 ply stack (no adhesive) as originally bonded (after peeling) and as rebonded. The rearrangement of the details resulted in reducing the height of the unbonded stacked lamina as much as .019 inch at some points to as much as .125 inch at other points. The rebond of the assembly was accomplished without difficulty and no voids were detected either by NDI "C" scan or by thickness measurements of the panel.

Measurements of the individual 18" x 18" lamina after shear and after machining to dimensional configuration indicate that the major waviness exhibited by the sheared and machined details is inherent in the large sheet from which the details are cut. Local changes due to manufacturing operations, such as removal of high or low corners and grit blast of the details may occur, but the general surface curvature of the finished detail will be the same as when cut from the sheet. Therefore, control of the sheet flatness at the mill is dictated in order to insure good quality bonded structures.

3.4.2 Laminated Brazing Process Development

3.4.2.1 Summary

All scheduled process verification and manufacturing development brazed parts are complete. Engineering test parts, including twelve 603R100-3 shear-stress panels, two 603FTB013 fastener comparison test panels, two 603FTB005-3 lower plates, two 603FTB004-13 lugs, two 603FTB050 crack arrest demonstration panels, and two 603R100-3F effect on base metal panels are complete and have been sent to the engineering test lab for test and evaluation. Five NDI test panels were also brazed and sent to the NDI test lab. for evaluation and NDI development work.

STACKED DETAILS (UNBONDED, NO ADHESIVE)

TOP PLY ELEVATION

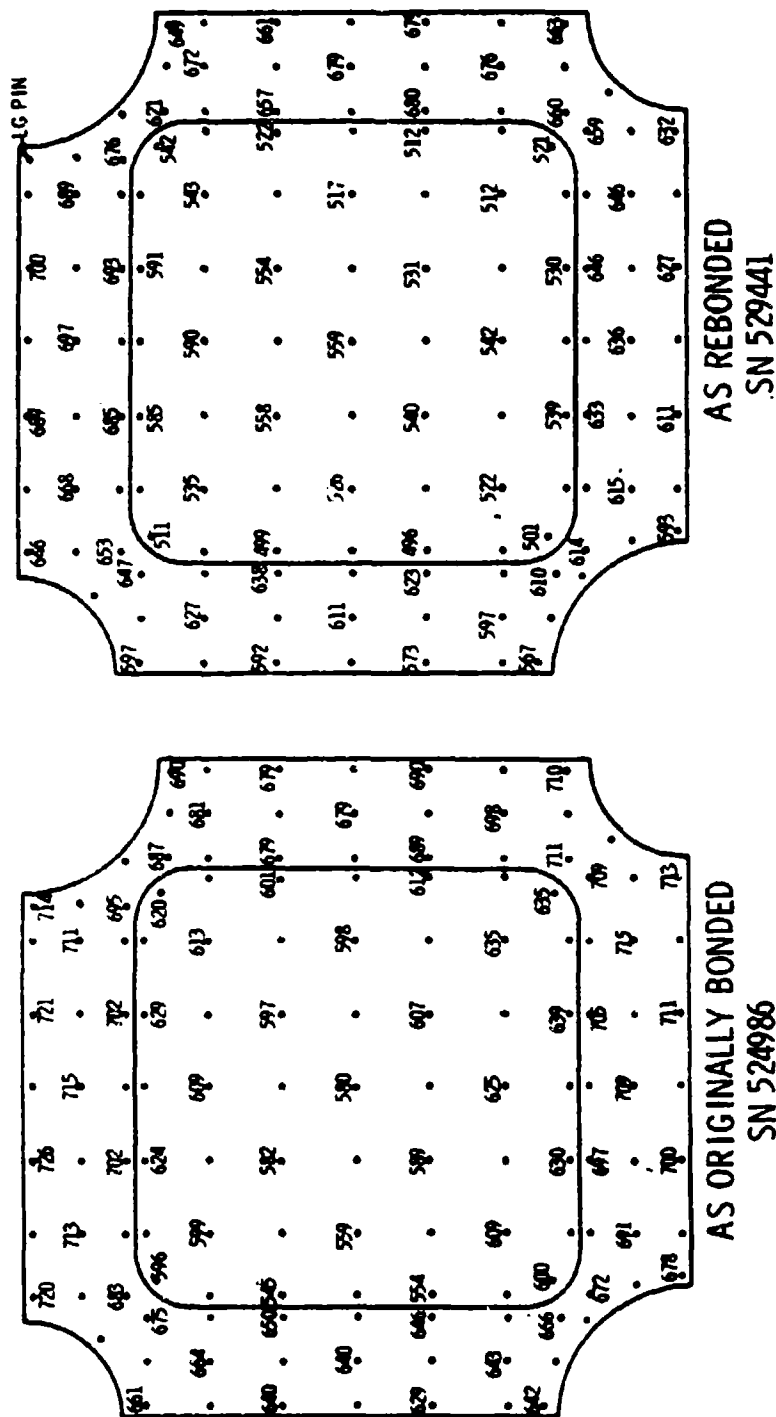


Figure 117 603FTB012-1 ASSEMBLY

Brazing parameters, tooling, manufacturing and tooling aids, detail cleaning procedures, lay-up procedures and brazing equipment were developed earlier in the program and are discussed in detail in Phase 1b Summary report AFFDL-TR-73-40, "Advanced Metallic Air Vehicle Structure Program", Volume 1, part 2.

3.4.2.2 Fabrication of Manufacturing Development Test Parts

Manufacturing development test parts brazed since the Phase 1b Summary report include one braze time evaluation test panel (slow cool), two braze pressure evaluation panels, six surface finish evaluation panels, two gap demonstration panels, two void demonstration panels, and one mismatch panel. All manufacturing development parts were single braze joint (1/2" x 15" x 24") titanium structures brazed with Ag-Al-Mn alloy. These parts are shown in Table 33 with pertinent processing variables.

The manufacturing development parts to evaluate effect of surface finish were brazed using standard procedure. Braze surfaces in separate tests were prepared using a face mill and a planer. Surface finishes evaluated were 63RMS, 125 RMS, and 250 RMS produced with a face mill and 250 RMS produced on a planer. X-ray examination showed light and scattered areas of voids, or braze line irregularities in the 63 and 125 RMS parts and moderate to heavy irregularities in the 250 RMS parts. The predominant irregularities in the rough finish parts (250 RMS) were shown as alternate light and dark areas following the machine cutter paths.

Two manufacturing development test parts were run to further evaluate the effect of brazing pressure. Brazing pressure of five and fifteen inches of mercury vacuum was used in separate tests. X-ray examination showed scattered areas of light to moderate voids in the part brazed at five inches vacuum and lighter scattered voids in the part brazed at fifteen inches mercury. The part brazed at the higher pressure had a slightly better overall appearance.

A test to determine the effect of braze alloy gap and overlap was also run in the part brazed at fifteen inches vacuum. Alloy was overlapped 1/16-inch along one side of the part and gapped 1/16 inch on the opposite side. The gap and overlap ran the entire 24-inch length of the test part. X-ray examination showed a line of heavy alloy concentration along the overlap area with adjacent light voids. A thin line void was shown

TABLE 1. SUMMARY OF TEST DATA FOR 603R100-3-31 THROUGH 603R100-3-42

Identification (Part)	Purpose	Time		Heat Up and Cool Down Time to 1000°F	Brake Pressure In. Hg. Vac.
		Min.	Max.		
603R100-3-31	Engr. Test	2	1550	130	10
603R100-3-32	Engr. Test	8	1550-1555	133	10
603R100-3-33	Engr. Test	8	1550	123	10
603R100-3-34	Engr. Shear-Stress	2	1550	114	10
603R100-3-35	Engr. Shear-Stress	2	1550	114	10
603R100-3-36	Engr. Shear-Stress	6	1550-1560	104	10
603R100-3-37	Engr. Shear-Stress	6	1550-1560	104	10
603R100-3-38	Engr. Shear-Stress	8	1550-1560	134	10
603R100-3-39	Engr. Shear-Stress	8	1550-1560	134	10
603R100-3-40	Engr. Shear-Stress	8	1550-1560	134	10
603R100-3-41	Engr. Shear-Stress	4	1550	105	10
603R100-3-42	Engr. Shear-Stress	4	1550	105	10
MD189-1	MDI Test	2	1550	100	10
MD188-1	MDI Test	2	1550	100	10
603R100-3-43	Engr. Shear-Stress	2	1550	100	10
603R100-3-44	Mfg. Development Brake Pressure	6	1550-1555	94	5
603R100-3-45	Mfg. Development Slow Cool	12	1550-1565	105	10
603R100-3-46	Mfg. Development Surface Finish	2	1550	142	10
603R100-3-47	Mfg. Development Surface Finish	2	1550	142	10

continued

Table 33 (Continued) - SUMMARY OF BRAZED PARTS WITH PERTINENT PARAMETERS

Identification (Part)	Purpose	Braze Temp. Of Time Min.	Heat Up and Cool Down Time Ambient To Braze Temp. Min.	Braze Temp to 900°F Min.	Braze Pressure In. Hg. Vac.
603R100-3-5	Mfg. Development Surface Finish	10	98	49	10
603R100-3-6	Mfg. Development Surface Finish	2	120	56	10
603R100-3-7	Mfg. Development Surface Finish	2	120	56	10
603R100-3-19	Mfg. Development Gap	4	120	49	10
603R100-3-20	Mfg. Development Gap	2	96	53	15
603R100-3-3	Mfg. Development Surface Finish	2	102	55	10
603R100-3-21	Mfg. Development Mismatch	4	104	60	10
MD3208-1	NDI Test	12	98	42	10
MD3209-1	NDI Test	12	98	42	10
603R100-3-23	Mfg. Development Braze Voids	7	100	42	10
603R100-3-24	Mfg. Development Braze Voids	7	152	44	10
603R100-3-10	Mfg. Development Braze Pressure	2	116	54	15

along the entire length of the gap; however, about 50% of the 1/16-inch gap area was filled with alloy.

The void, gap, and mismatch parts were designed with special built-in discrepancies as illustrated in the sketches in Figures 118 through 120. X-ray examination of the void part clearly shows the built-in voids and scattered, light braze line voids or irregularities throughout the part. X-ray examination of the gap part shows the shallow gap (.002" deep) as a thin dark line running the length of the part and heavier, wider lines in the area of the 0.005 and 0.020-inch deep gaps. X-rays of the mismatch part shows scattered light to very heavy voids and irregularities especially in the areas of maximum mismatch.

A test was run to determine the effect of a slow cool-down rate on the properties of a brazed part. This test was run using a normal heat-up rate but cooling was limited to a rate of 150°F per hour. This braze cycle is shown in the graph in Figure 121. For comparison purposes, a typical braze cycle is shown in the graph in Figure 122. X-ray examination of this part showed longitudinal dark areas indicating some irregularity in the braze line. The part was sent to the engineering test lab for further testing.

3.4.2.3 Fabrication of Engineering Test Parts

Engineering test parts run since the Phase Ib summary report include eleven 603R100-3 shear stress panels, one 603FTB005-3 lower plate, one 603FTB004-13 lug and one 603FTB crack arrest demonstration panel.

All manufacturing development and engineering test parts have been sent to the engineering test lab for test and evaluation. Analysis of x-ray examination presented in this section is limited to very generalized observations and is not intended to reflect opinion as to braze quality. A final correlation of data including x-ray, NDI, and engineering mechanical tests will be made before braze quality is defined.

3.4.3 Weld Development

Both Gas Tungsten Arc (GTA) and Electron Beam (EB) welding are discussed in this section. GTA welding development is being accomplished on 10 Ni steel only, as sufficient data exists for GTA welding 6Al-4V titanium. However, preliminary EB welding data is being developed for both materials.

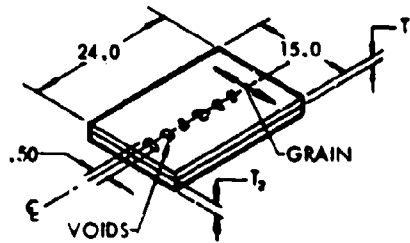
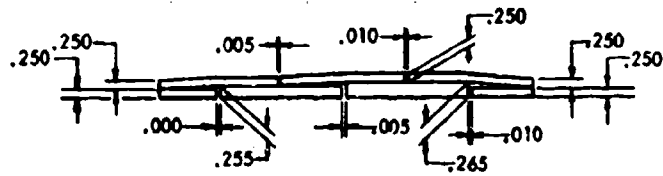


Figure 118 BRAZING TEST PANEL WITH BUILT-IN VOIDS



VIEW C-C

LOWER SURFACE SHOWN TO BE LOWER SURFACE DURING BRAZING

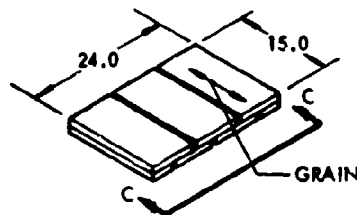
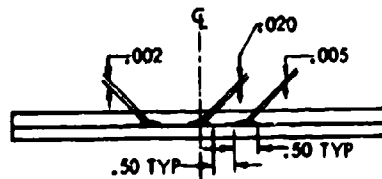


Figure 119 BRAZING (MISMATCH) TEST PANEL



VIEW B-B

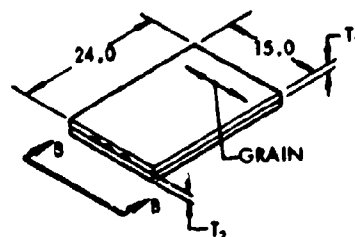
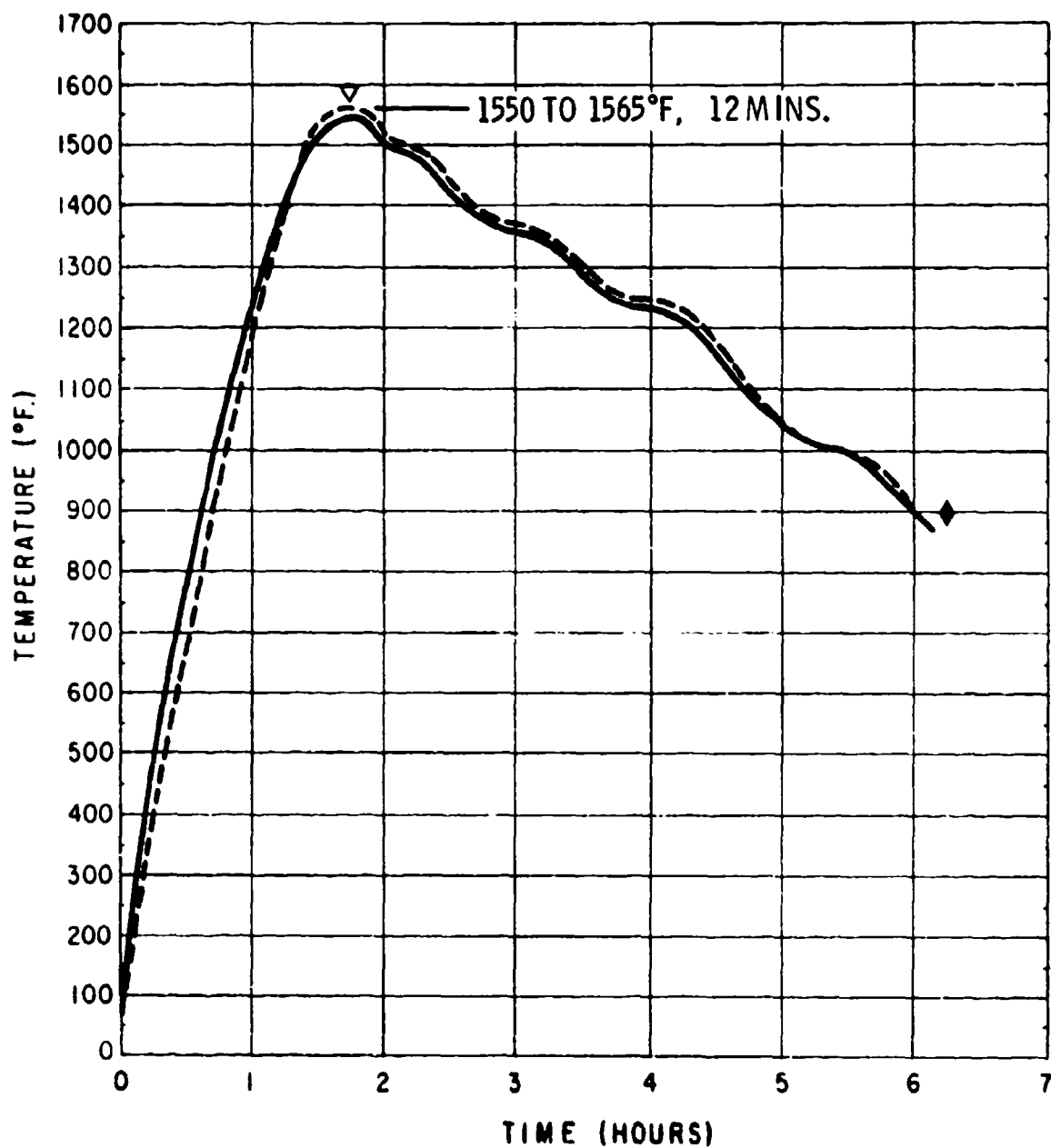


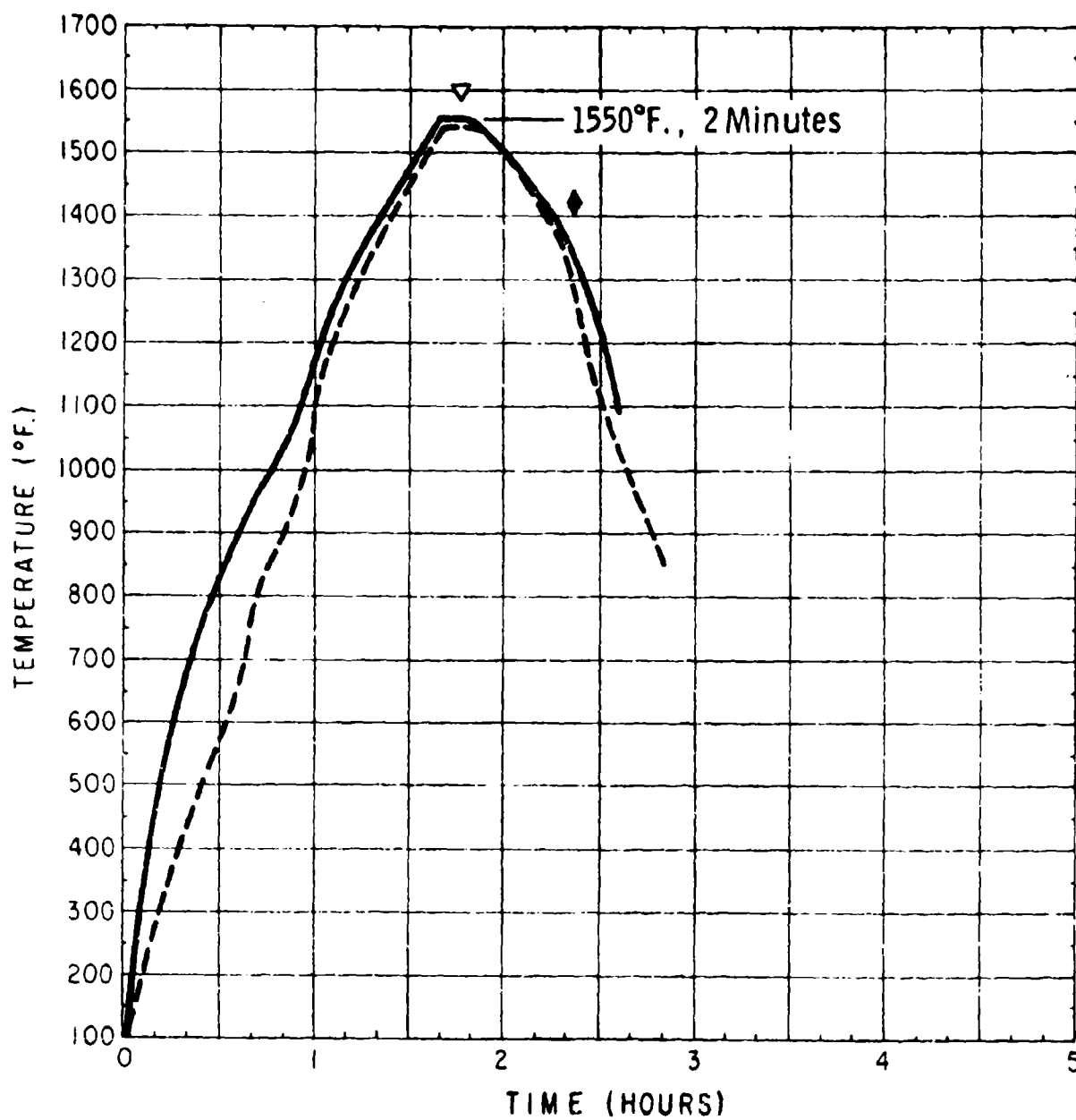
Figure 120 BRAZING (GAP) TEST PANEL



- T/C inside of braze box
- T/C on top of braze box,
covered with 0.25-in. Cerafelt
- ▽ Furnace off
- ◆ Out of furnace

Engr. No. 603 R100-3-13A
 MR&D No. (SLOW COOL) B7500-13A
 Date 3-23-73

Figure 121 CYCLE FOR BRAZE TIME (SLOW COOL) EVALUATION



- T/C inside of braze box
- T/C on top of braze box, covered with 0.25-in. Cerafelt
- ▽ Furnace off
- ◆ Out of furnace

Engr. No. TYPICAL

MR&D No. _____

Date 3-15-73

Figure 122 TYPICAL BRAZE CYCLE FOR MANUFACTURING DEVELOPMENT PARTS

3.4.3.1 GTA Welding of 10 Nickel Steel

The manufacturing engineering effort during this reporting period consisted of engineering design consultation of welded concepts, review of available material-process data and the welding and mechanical property evaluation of GTA welding of 10 Nickel steel.

The "NO BOX" box configuration was designed using 10 Ni steel which is new to the aerospace industry. The GTA process parameters were developed on 5/8 inch thick material which had been machined to 1/2 inch net thickness to remove the heavy mill scale. The test plates are shown on 603R100-2A.

The equipment used for the welding task is shown in Figure 123. This welding unit has the following features:

1. 400 Ampere 100% duty cycle output.
2. Pulsed arc capability (1-99 Hz).
3. Automatic Voltage Control.
4. Automatic wire feed (0-100 ipm).
5. Transverse cross-seam oscillation.
6. Pivoting 6 foot side beam carriage.
7. In-out ram manipulation (6 foot).
8. Powered vertical height adjustment (6 foot).

The plate weld tooling set up is shown in Figure 124. This is a steel fixture with copper top chill bars and a copper backup bar. The tooling used for this program provides the following important functions:

1. Inert gas protection of root side of weld bead.
2. Copper backup bar to control penetration of root pass.
3. Copper top chill bars to reduce heat buildup.
4. Reduces heat affected zone.

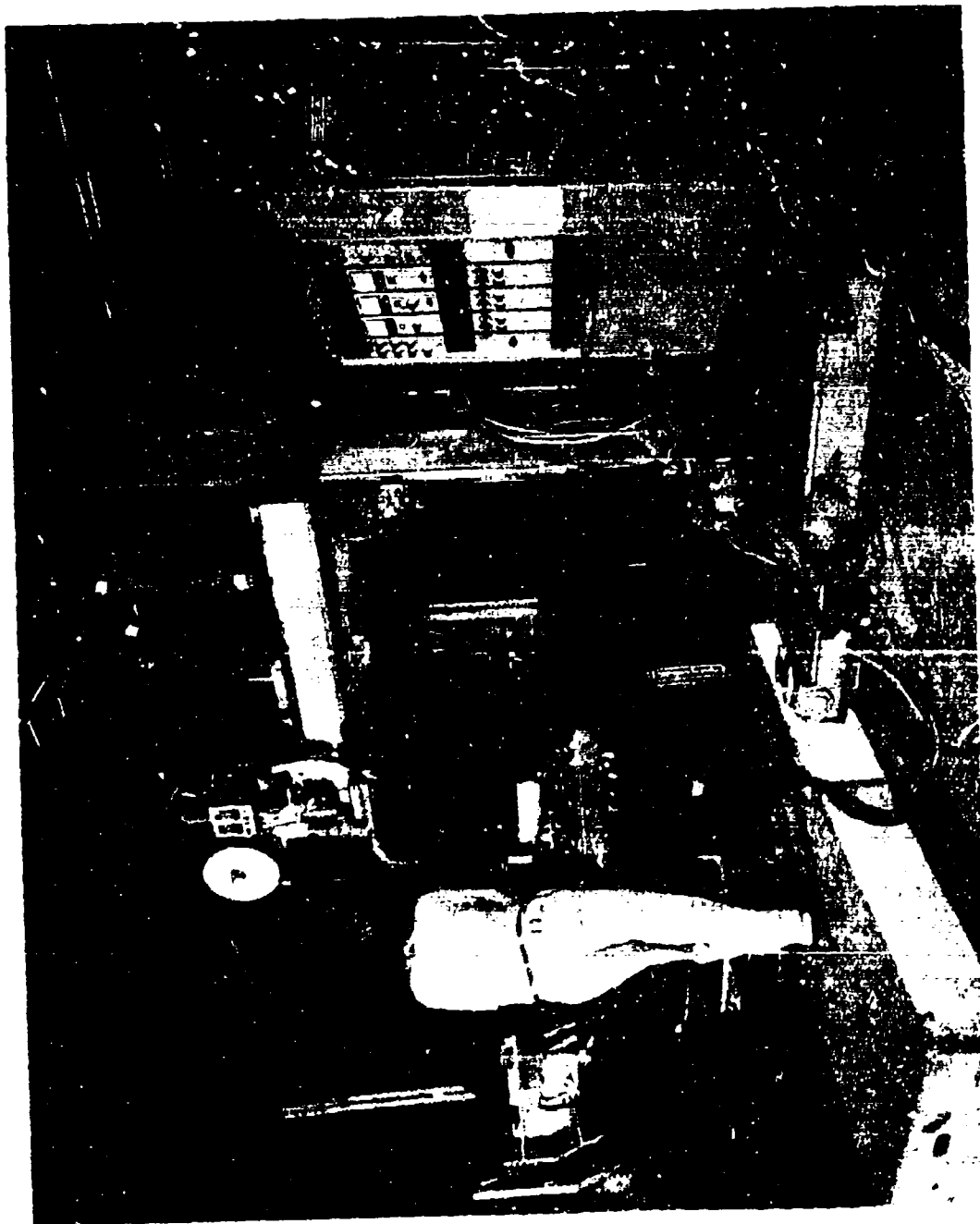


Figure 123 AUTOMATIC 400-AMP. GTA FUSION WELDER

4-1821



Figure 124 GTA PLATE WELD FIXTURE

4-52833

5. Eliminates undercut.

6. Controls warpage.

A sketch of the weld fixture is shown in Figure 125.

The weld parameters were empirically developed, as weld schedules available from other programs were not directly applicable to the test plates fabricated in this program. Attempts were made to use existing weld parameters but satisfactory root penetration could not be achieved. Recommended parameters were discarded and new weld schedules were established. These schedules were developed using the pulsed arc welding mode.

In the pulsed mode of operation, the weld current is switched between two levels of operation. These levels are independently controlled at Level 1 and Level 2. The weld time at Level 1 and Level 2 can also be independently controlled from one to 99 cycles duration, in steps of one cycle, based on 60 cycles per second. The repeated pulsation will produce an output current trace of essentially square wave form whose amplitude of current and width of pulse is adjustable. The theoretical plot of current versus time would illustrate a square wave saw toothed pattern. However, because of the equipment inductance and reactance time the plot would be somewhat modified. The actual current trace is shown in Figure 126.

The weld schedule developed for GTA welding of the 10 Nickel steel is shown in Figure 127. Beginning with the fourth welded plate, the weld process parameters were frozen and the only changes made were the number of filler passes used to compensate for various plate thicknesses. Two additional passes were used (11th and 12th passes) to attempt to age the previous weld passes. This was done to assure that, after the weld reinforcement was removed, all remaining weld metal had been aged. This reinforcement is shown in Figure 128.

Run in and run out tabs were used to assure that no arc initiation or termination points remained in the weld. The weld tab is shown in Figure 129. The run out tabs were sawed off after the weld was completed.

The test plates identified in the Engineering Drawing 603R100-20 have been welded. A total of fourteen -1 assemblies have been completed and will be used for the tension, fatigue and fatigue crack growth specimens. The two -3 fracture toughness test

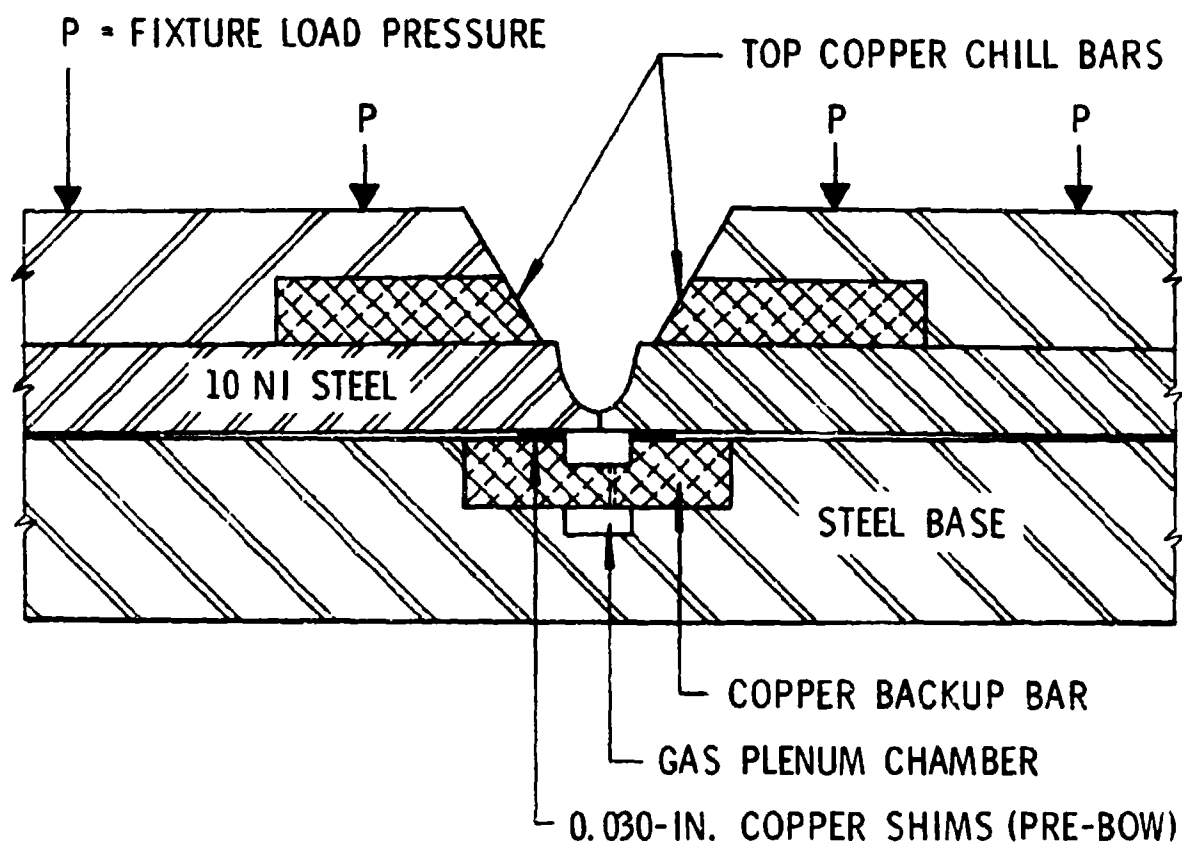


Figure 125 SECTION OF GTA WELD FIXTURE

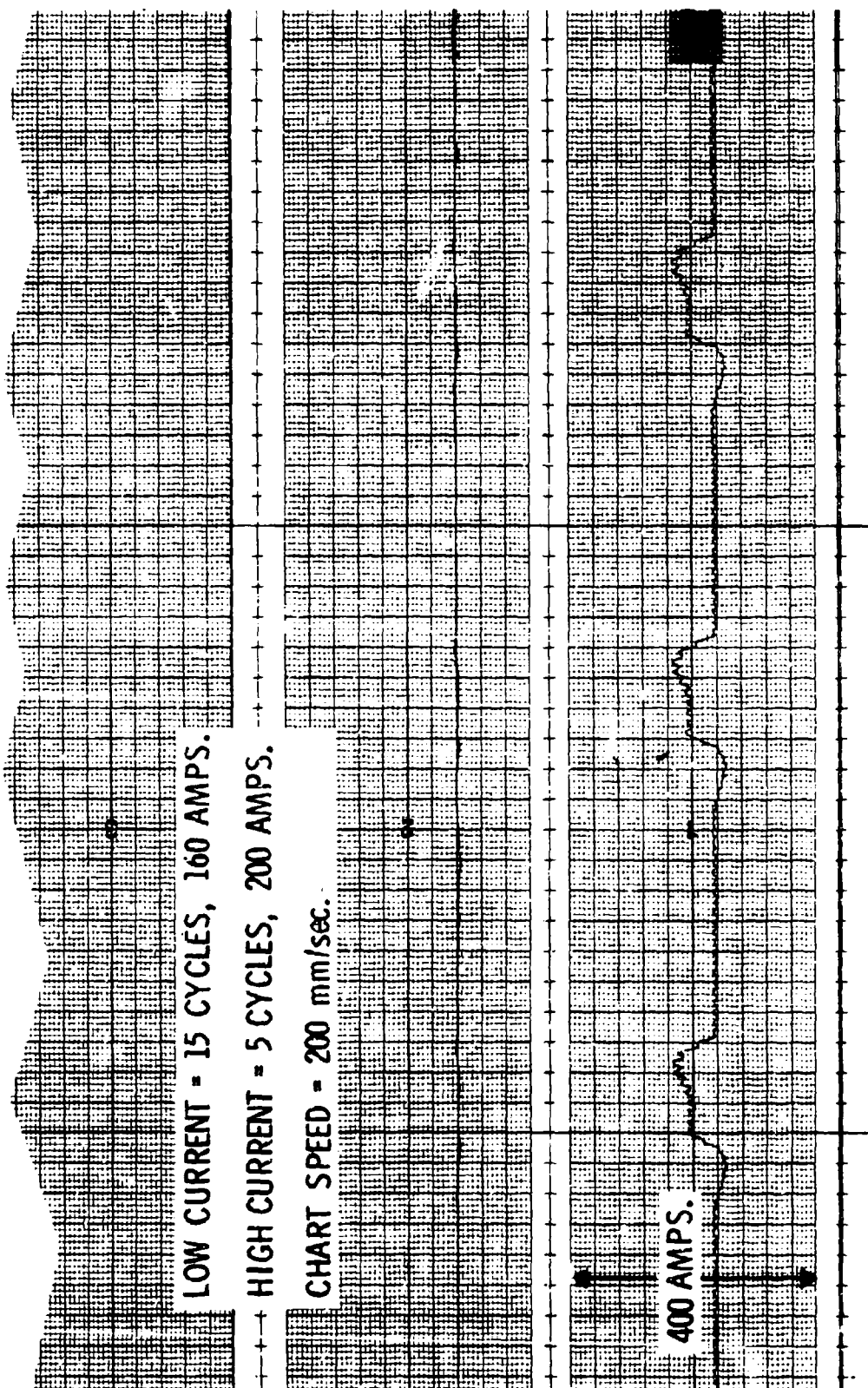


Figure 126 PULSED GTA CURRENT TRACE

WELDING SCHEDULE FOR MECHANIZED FUSION WELDING

PROGRAM Air/AVS DATE 4-4-73

MATERIAL 10 NI STEEL THICKNESS 0.500 IN. CONDITION AUST. QUENCH & AGE

EQUIPMENT NO. 36911 PART NO. 603 R 100-2

PREHEAT TEMP. RT INTERPASS TEMP. 150-180°F.

PRECLEANING MACHINED EDGE, WIRE BRUSH, MEK-WIPED

NOZZLE SIZE NO. 10 TUNGSTEN: Type 2% TH Diameter 0.125 IN.

TUNGSTEN: Extension 0.500 IN. Shape 15° ANGLE

FILLER WIRE: Type 10 NI Diameter 0.045 IN.

TORCH GAS: Type HE Flow 90 cfh; BACKUP GAS: Type HE Flow 15 cfh

Weld Pass No.	1	2	3	4	5	6	7	8	9	10	11	12
Voltage	13	13	13	13	13	13	13	13	13	13.5	13.5	13.5
Weld current (amperage)												
Level 1	225	160	160	160	160	160	160	160	160	160	160	120
Level 2	180	200	200	200	200	200	200	200	200	200	200	160
Number of cycles												
Level 1	10	15	15	15	15	15	15	15	15	15	15	15
Level 2	5	5	5	5	5	5	5	5	5	5	5	5
Wire speed (ipm)	32	32	32	32	32	32	32	32	32	32	32	16
Weld speed (ipm)	2	4	4	4	4	4	4	4	4	4	4	4

Figure 127 GTA WELDING SCHEDULE FOR 10 NICKEL STEEL



TOP SURFACE

4-52634



BOTTOM SURFACE

4-52635

Figure 128 10 NICKEL STEEL WELDED PLATE
FILLER WIRE REINFORCEMENT



Figure 129 SETUP FOR USING WELD TABS

4-52636

plates have also been welded. Each of the welded plates have been x-rayed, magnetic particle, and ultrasonically inspected.

The test plates were post weld aged at 950°F for (4) four hours and air cooled as specified by Engineering. The stability of a warped plate was observed before and after the post weld age cycle. No movement or relaxation of stresses could be detected.

The plates have been delivered to the Engineering Test Laboratory for specimen removal and testing.

The transverse weld shrinkage was measured at both the beginning and termination end of the plate. The average shrinkage was .021 and .025 inches respectively.

Various design concepts were reviewed for producibility for the NBB concept. Typical representative sections were chosen to develop the manufacturing data necessary to GTA weld the proposed NBB designs.

3.4.3.2 Electron Beam Welding Development

3.4.3.2.1 EB Welding of 6AL-4V Titanium - Phase IB Summary Report (AFFDL-TR-73-40) describes in detail the completed program of EB welding of Beta processed 6AL-4V titanium. A brief summary of this information is as follows:

EB welded joints on 5/8, 1 and 2 inch thick 6AL-4V titanium were made, inspected and sent to the Engineering Test Laboratory for mechanical property testing.

Representative areas of the various weldment designs under consideration were analyzed for producibility. Two typical structural sections were chosen for producibility demonstration. The first was a corner joint with dissimilar thickness. The second element built was a wide angle flange joint to eliminate extensive machine hog outs. Five assemblies of each design were produced. In addition to the weld development efforts, the resulting joints were provided for a NDI development program. Intentional flaws were made in the weld joints to simulate defects that could occur in production such as:

1. Arc outs

2. Lack of fusion.
3. Porosity.
4. Missed root.

Conclusions:

1. Beta processed 6AL-4V titanium can be welded by the EB process, defect free, up to 2 inch thickness.
2. Reproducibility can be assured by beam current monitoring.
3. Transverse weld shrinkage can be predicted on all EB welded titanium joints.
4. Corner welds of dissimilar thickness can be made by using run out tabs and a fitted backup block.
5. Multi-pass welds on 6AL-4V titanium can be made with up to 2 inch thickness material.
6. Use of a filler wire increases the gap allowance from $\pm .005$ " to ± 0.020 inches.
7. A machine clean up reinforcement of 0.030" on each side of the weld joint should be provided on all EB welds.

3.4.3.2.2 Electron Beam Welding of 10 Nickel Steel - Since 10 Ni steel (Hy 180) is a candidate material for building the AMAVS, several EB weldments on this steel are under consideration

Very little information is available from industry regarding EB welding of 10 Nickel. A limited program was outlined to establish "in-house" capability as well as establishing design guidelines.

Representative joint designs will be welded to establish weld parameters and to provide engineering a limited number of mechanical property test welds.

The remaining task to be accomplished is:

1. Develop weld parameters for .37, .090 and 2.10 inch thick 10 Ni. steel.
2. Weld two producibility demonstration structural "H" sections that will include the major EB welded joints now under consideration for the NBB design.

3.4.4 Machining

A basic machining evaluation has been initiated on HY 180 (10 Ni.) steel. The inconsistent machining results obtained thus far on test specimen preparation, using band sawing, face milling, profile milling, and drilling operations, has established a need for specific machining guidelines.

Machining tests are in progress to determine metal removal characteristics as related to producibility. Test are based on the use of stock cutting tools with variation in speeds and feeds for establishing producibility comparison to D6ac steel (where machining data and cost have been established).

Band sawing tests have been conducted using high speed steel (Simond, weld edge) band stock on a conventional Do-All saw. A band speed of 55 surface feet/minute (SFM) has been established as adequate for saw band life. An average sawing rate of .5 square inches/minute was achieved on one inch plate stock without the aid of coolant. The sawing rate of HY 180 steel is 50% of annealed D6ac steel.

Boring and turning tests on HY 180 steel using carbide inserts (TPG-322A), indicates that the metal removal rate is 30% greater than for heat treated D6ac (220-240 KSI). 100 SFM for roughing operations and 150 SFM for finishing cuts are adequate for HY180. Feeds of .0075 inches per revolution (I.P.R.) for roughing and .005 I.P.R. for finishing offers the best selection for initial machining operations.

Future machining tests will be conducted for pocket milling, face milling and fastener hole preparation. Special emphasis is being placed on testing of tool geometry variation that may be more efficient for cutting HY180. A machining comparison test is planned for HY180 (solution treated) versus HY180 (solution treated and aged) to determine material procurement cost advantages relative to machining cost impact of the two heat treat conditions.

3.4.5 Manufacturing Engineering Design Support

On board design studies were supported by manufacturing engineers in selecting the most efficient design concepts based on cost and reliability of the manufacturing process. Input to these studies was in the form of preliminary costing analysis of components and assemblies and subsequent ratings for the manufacturability of the designs. These inputs were utilized in the final evaluation of the three design concepts under study in Phase Ib of this program as previously discussed in AFFDL-TR-73-40.

3.4.5.1 Preliminary Cost Estimates for Basic Manufacturing Trade Studies

Cost estimates prepared at the on-board design level were made by manufacturing engineers with assists as deemed necessary from other manufacturing specialists and Material and Industrial Engineering estimators. These preliminary estimates were limited to basic fabrication and assembly costs without benefit of estimated scrap rate, quality control costs, manufacturing and tooling follow-up efforts, and other miscellaneous charges. The major items of cost which were considered are materials, manufacturing labor costs, special sub-contract fabrication charges, and tooling fabrication and material costs. These estimates do not reflect the total cost of details or components but were used for comparisons of part costs in preliminary manufacturing trade studies of proposed designs.

The following component designs for the WCTS configurations were evaluated. Cost estimates were prepared on each design for production units of 1, 6, and 200. Ratings of designs were based on production quantities of 200 ship sets.

A list of drawings, with references to other report documents or sections of this report is shown for the readers assistance in locating these drawings.

<u>Drawing No.</u>	<u>Configuration</u>	<u>Reference Location</u>
603R149	NBB	AFFDL-TR-73-40 Vol. II
603R170"B'	FSRL	AFFDL-TR-73-40 Vol. II
603R171	FSRL	AFFDL-TR-73-40 Vol. II
603R172	NBB	AFFDL-TR-73-40 Vol. II
603R173	NBB	AFFDL-TR-73-40 Vol. II
603R195	NBB	AFFDL-TR-73-40 Vol. II
603R196	NBB	AFFDL-TR-73-40 Vol. II

<u>Drawing No.</u>	<u>Configuration</u>	<u>Reference Location</u>
603R197	NBB	AFFDL-TR-73-40 Vol. II
603R198	NBB	AFFDL-TR-7 -40 Vol. II
603R214	FSRL	Section 3.1.1
603R215	FSRL	Section 3.1.1
603R228	FSRL	Section 3.1.1

3.4.5.1.1 Upper Plate Assembly FSRL Drawing No. 603R170"B"
 This drawing defined two assemblies designated as 603R170-1 and 603R170-3.

The 603R170-1 assembly was designated as a titanium assembly. The lugs, cover plates, and honeycomb panel covers were all 6-6-2 and 6-4 titanium except the aluminum honeycomb core.

The 603R170-3 assembly was designated as a titanium and aluminum assembly. All machined and bonded panels of titanium inboard of X_F 84 rib were replaced by bonded honeycomb panels of 7050 aluminum. This design showed a significant reduction in cost over 603R170-1 and eventually became the winning upper plate design for the FSRL configuration at the end of Phase Ib.

3.4.5.1.2 Closure Rib X_F 119.0 (NBB) - Three designs were evaluated as improved versions over the original preliminary design designated as Drawing No. 603R114.

Drawing No. 603R149 represented two design versions of fabrication. One is considered as a monolithic structure to be machined from 10 Ni steel plate. The other version is an adhesive bonded assembly of two machined plates bonded back-to-back at the web centerline. Studies of these two finished components indicated a slight cost increase in the bonded assembly due to bonding, tooling and factory operations not required for the monolithic part.

Drawing No. 603R197 is an electron beam (EB) welded assembly of 10 Ni steel machined after welding to finished dimensions. Accessibility to the weld joints with the EB welder head and wire feeding system presents a major problem. Estimated costs of this design is close to 603R198 design.

Drawing No. 603R198 is an EB welded assembly of 10 Ni steel plates, machined after welding. This design involves less production risk than 603R197. Cost difference should not be a major factor until welding tests are performed to determine

reliability of each design. Until tests are run 603R198 design would be preferred for manufacturing ease and cost over other mentioned candidates. The basic cost savings in this design is in reduced material requirements and machining time due to the rough configuration produced by the E.B. welding of relatively light plate stock.

3.4.5.1.3 Main Landing Gear Drag Brace Fitting Drawing No. 603R171 (NBB) - This design was evaluated against Drawing No. 603R142 which consisted of two 6Al-4V titanium machined forgings welded together. The basic component of the new design is the 603R171-7/8 aluminum fitting, machined from a proposed hand forging of 7050 aluminum alloy. A considerable cost reduction was obtained by this design.

3.4.5.1.4 Bulkhead Y_F 992 (NBB) - Two improved designs were evaluated against two existing designs, 603R047 and 603R109. The new designs were 603R173 and 603R195. The early designs were of a plate and stringer type concept of 10 Ni steel.

Drawing No. 603R173 introduced an adhesive bonded 7050 aluminum honeycomb panel 144 inches long, extending from Y_F 72.00 left to Y_F 72.00 right between the upper and lower bulkhead caps. The panel replaced the early plate stringer concept and made other improvements in the lug joints. This new design provided manufacturing break joints, bolted, at upper and lower caps, approximately at stations Y_F 48 upper and Y_F 52 lower. This design produced a significant cost reduction compared to early designs and was later altered under drawing No. 603R195 to provide for a 7050 aluminum beam under the Z_F 0.00 cap to replace the 10 Ni steel beam and farther reduce the total bulkhead assembly cost.

Drawing No. 603R195 made changes in the pivot lug attaching method and eliminated the bolted joints near stations Y_F 48 and Y_F 52 in favor of welded joints near stations Y_F 84 upper and Y_F 38.70 lower. It also used the same 7050 aluminum honeycomb panel and beam under Z_F 0.00 cap as described under Drawing No. 603R173. These changes farther reduced costs and made this design the selected one.

3.4.5.1.5 Bulkhead Y_F 932 (NBB) - Designs for this bulkhead followed and were typical to those made for Bulkhead Y_F 992. Early designs 603R046 and 603R113 were similar in concept to 603R047 and 603R109 respectively.

1
Drawing No. 603R172 used an adhesive bonded 7050 aluminum honeycomb panel to replace early design webs and stiffeners of 10 Ni steel and retained mechanical splice joints, on upper and lower caps.

Drawing No. 603R196 retained the 7050 aluminum honeycomb panel, replaced mechanical splice joints with weld joints and used a 7050 aluminum beam below Z_F 0.00 station. This final design made a significant contribution to the cost reduction position.

3.4.5.1.6 Lower Plate (FSIL) - Three candidate design concepts were studied as improvements over the lower plate assembly design established at the end of Phase Ib. The Phase Ib assembly consisted of:

603R174 Plate Assembly
603R147 Pivot Lug Assembly
603R140 Longerons Fittings

Drawing No. 603R214 deviated from the basic "removable lug" concept by incorporating an "integral lug" with the inboard assembly section and providing forward and aft longeron attach surfaces as an integral part to make a brazed laminated titanium assembly. This design eliminated the integral flanges attaching the end closure rib and the forward and aft bulkheads and provided attach angles that are Taper-Lok bolted to the brazed plate assembly. The design reduced the total number of fasteners required in the longeron area by one row. It retained the basic splice pattern at the airplane centerline.

Revision "A" to 603R214 made provisions to have identical cutouts in the upper and lower plates of the assembly, allowing left and right hand assemblies to be made with common tooling. Subsequent machine operations to the brazed assembly makes the basic assemblies into right and left hand components.

Revision "B" to 603R214 farther improved the design by reducing the forward and aft longeron attaching surfaces and in turn reducing the stock plate sizes and machining costs. Cutout sizes and shapes were likewise redesigned to improve machining costs. The upper attach angles in area of the outboard closure rib were removed and replaced with a subsequent longeron design, Drawing No. 603R238. Major improvements for manufacturing for this design was elimination of the brazed plank concept, in favor of the brazed laminated concept, due to the requirement for close tolerance machining of plank details.

Drawing No. 603R215 consists of two brazed laminates of 6Al-4V titanium assembled with Taper-Lok bolts in the area of the outboard longeron. The splice joints are male and female and the bolt pattern attaches an angle detail which locates the outboard closure rib. The inboard assembly is a three plate brazed titanium laminate with angle details, for joining forward and aft bulkheads, bolted to the laminate.

Revision "A" to Drawing No. 603R215 made provisions for adding the aft attaching surface to the brazed lug laminate and reduced the same attach area previously shown on the inboard assembly. These specific changes are questionable as to the effect on manufacturing and assembly. Some reduction in the total material requirements was obtained by the change.

The basic advantage of the 603R215 design is that it allows the use of smaller detail plates at fabrication, including brazing.

One disadvantage of the design concept is in the joint fit. Critical tolerances are necessary and problems associated with obtaining these tolerances are great, especially in the "pocketed" area of the longeron aft attaching lug.

An area of added machining and tooling costs found in the 603R215 design, as compared to the 603R214 design, is in the cutouts required in the upper and lower brazed plates inboard of the longeron. These cutouts are smaller and greater in number on each plate of the 603R215 assembly. This condition produces higher machining time due to extra inches of finishing cuts. Upper and lower cutout patterns are not common as mentioned for consideration under 603R214 evaluation. More tooling for detail fabrication and brazing operations will be required.

Analysis of advantages and disadvantages of Drawings Nos. 603R214 and 603R215 produced a requirement for a hybrid concept designated as 603X215 assembly. Without benefit of an engineering drawing, estimates were made of total manufacturing costs to produce the lower plate assembly. It would be composed of two brazed laminate assemblies as shown in Drawing No. 603R215 with the inboard assembly incorporating the advantages of the upper and lower plate cutouts as shown on Drawing No. 604R214.

Results of preliminary studies on 603R214, 603R215, and 603X215 concepts showed the 603R214 concept to be lowest in cost. The reduction in cost was due to elimination of splice joint at the longeron, ability to make right hand and left hand assemblies with the same tooling, and reduced machining of basic detail parts. The 603X215 concept was next in cost.

3.4.5.2 Configuration Rating System for Manufacturing

The basis for selecting concepts at the end of Phase Ib was the Merit Rating System as established during Phase Ia preliminary design. Details of the total system has been discussed in previous report AFFDL-TR-73-40 volume II.

The weighing factors which related to manufacturing processes and their maximum score as related to the total score are:

Manufacturing cost	18% Maximum
Technology advancement for manufacturing	9% Maximum
Manufacturability	2% Maximum

The rational for evaluating and rating design concepts is discussed as follows.

3.4.5.2.1 Manufacturing Costs - Ratings for manufacturing costs were made on the basis of 200 production units. Costs for details and assemblies were estimated for each of the three candidate configurations and accumulated for comparison of individual concept costs.

Items which made up the total cost package are:

Material - Estimates were made on requirements for raw stock sizes, plus an attrition factor. Dollar values were based on factors of stock size and projected market price for the ordering time period. Estimates for forgings and extrusions were obtained from potential vendors on basic items with others being estimated using past experience as a basis. Tooling costs for forgings and extrusions were carried under separate tooling costs and prorated over the 200 production units.

Basic Detail Fabrication - A preliminary manufacturing analysis was made of each detail part. Estimates were made for the cost of fabricating a single unit. Learning curve factors, based on

judgement and history, were applied to the single unit estimate to obtain total costs for 200 production units. The basic tooling, plus tooling as required for production rates of 5 units per month, was estimated in the preliminary manufacturing analysis and accumulated under tooling costs. The Preliminary Cost Estimate form (Figure 130) was used to itemize manufacturing costs.

Assembly and Joining - Preliminary estimates were made for fabrication of one unit and tooling as required. Total estimates followed the same procedure as described under basic detail fabrication.

Tooling - All tool manufacturing estimates accumulated from basic detail and assembly fabrication studies were carried under a separate item of cost. A factor for maintenance of tooling was added based on past history.

Rates for Costing - Estimated costs for labor hours of part fabrication and tool manufacture were based on an estimated direct hourly labor rate plus an estimated overhead rate.

Estimates of Total Cost - Individual costs of material, fabrication, and tooling for the projected 200 units were combined to obtain total cost.

3.4.5.2.2 Manufacturing Technology Advancement - A prime goal of this program has been advancements in manufacturing technology. However, these advancements could be utilized only if they enhanced the status of other disciplines such as weight, cost, reliability, etc.

An early decision was made that each of the three candidate concepts met the criteria for technology advancement. For this reason the ratings for each concept were considered equal and a full score was given each.

3.4.5.2.3 Manufacturability - Rating of concepts for this category is based on performance level and reliability of the manufacturing processes employed in the fabrication of each concept. Since manufacturing cost is rated in a separate category, no consideration was given to that item during this evaluation.

To best analyze the total value of each concept, a breakdown of manufacturing phases was utilized. These phases and their respective ratings are:

PRELIMINARY COST ESTIMATE BASIC METAL PROCESSING

PART NO. _____ NEXT ASSEMBLY _____

NAME _____ REQ. PER A/C _____

MATERIAL _____ (COST \$ _____ /LBS.) PROD. QTY. _____

MANUFACTURING PROCESS _____ METHOD NO. _____

ITEM	DETAILS OF COST	MATERIAL & O.C.	HOURS	
			FAB.	TOOLS
MATERIAL				
FORMING				
WELDING				
MACHINING				
OTHER				
TOTAL				
RECAPITULATION			AMOUNT	
MATERIAL				
FAB.				
TOOLING				

Figure 130 PRELIMINARY COST ESTIMATE FORM

Basic detail manufacturing	30% Maximum
Secondary manufacturing (joining)	30% Maximum
Sub-assembly	20% Maximum
Final assembly	20% Maximum

Total	<u>100%</u>
-------	-------------

The final rating of the three candidate designs and a break-down of ratings by manufacturing phases are shown below. The numbers are related to the maximum grade of 3.0 for manufacturability as established in the basic merit rating system.

Manufacturability Ratings

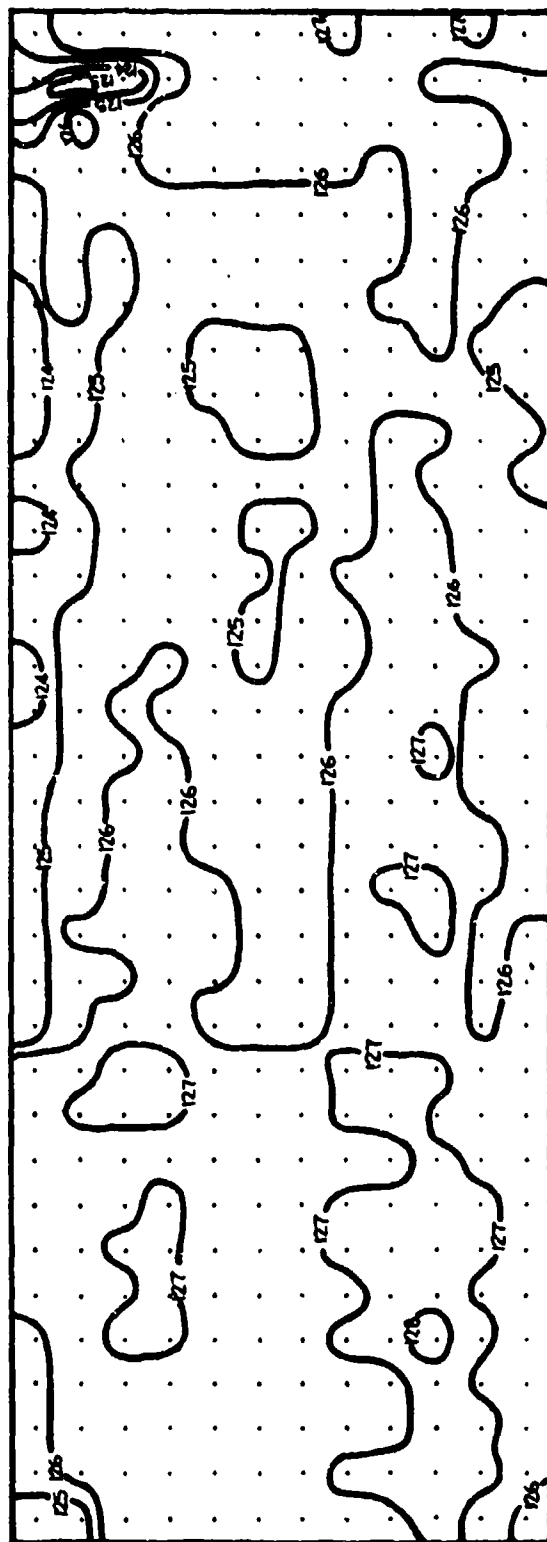
Manufacturing Phase	Configuration		
	NBB	FSIL	DTIL
Basic Mfg.	.539	.514	.557
Secondary Mfg.	.810	.687	.888
Sub-Assy.	.384	.539	.560
Final Assy.	.341	.252	.252
Total Rating	<u>2.074</u>	<u>1.992</u>	<u>2.257</u>

APPENDIX

**PHYSICAL CHARACTERISTICS OF RAW MATERIAL
AND DESIGN VERIFICATION TEST SPECIMENS**

SHEET 1-1 HT 304324-19

37" X 101"

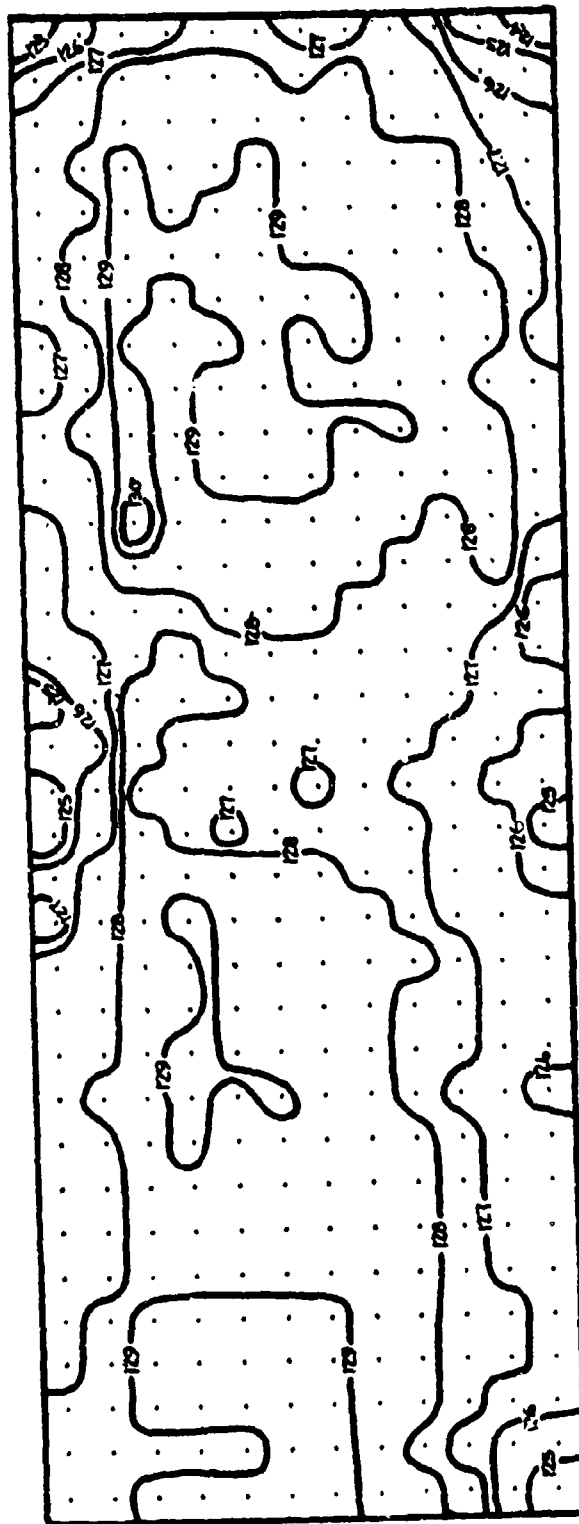


MAX	.128	RANGE	.006
MIN	.122	σ	.0020
AVG	.1257	POINTS	408

SHEET THICKNESS VARIATION BETA C TITANIUM ALLOY 1/8" SHEET (GROUND)

SHEET 1-2 HT 304324-19

37" X 99 1/2"

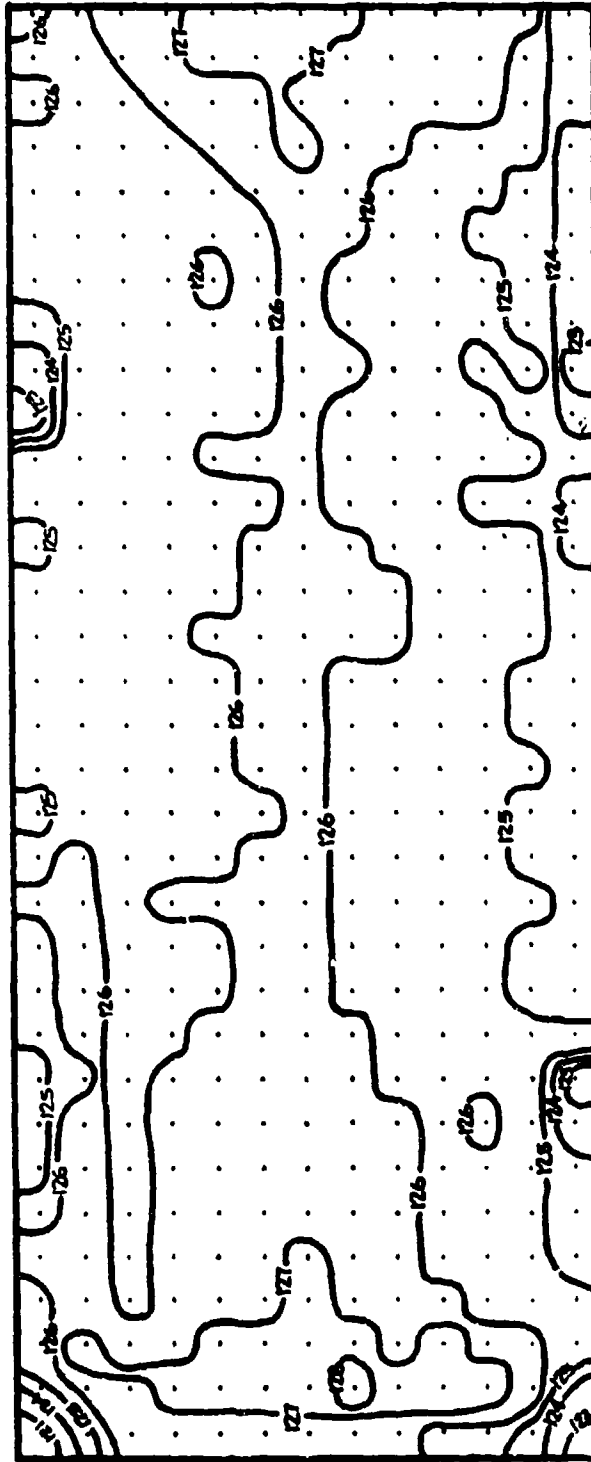


MAX	.130	RANGE	.007
MIN	.123	σ	.0006
AVG	.1273	POINTS	408

SHEET THICKNESS VARIATION BETA C TITANIUM ALLOY 1/8" SHEET (GROUND)

SHEET 1-6 HT 304324-19

39" X 97 3/4"

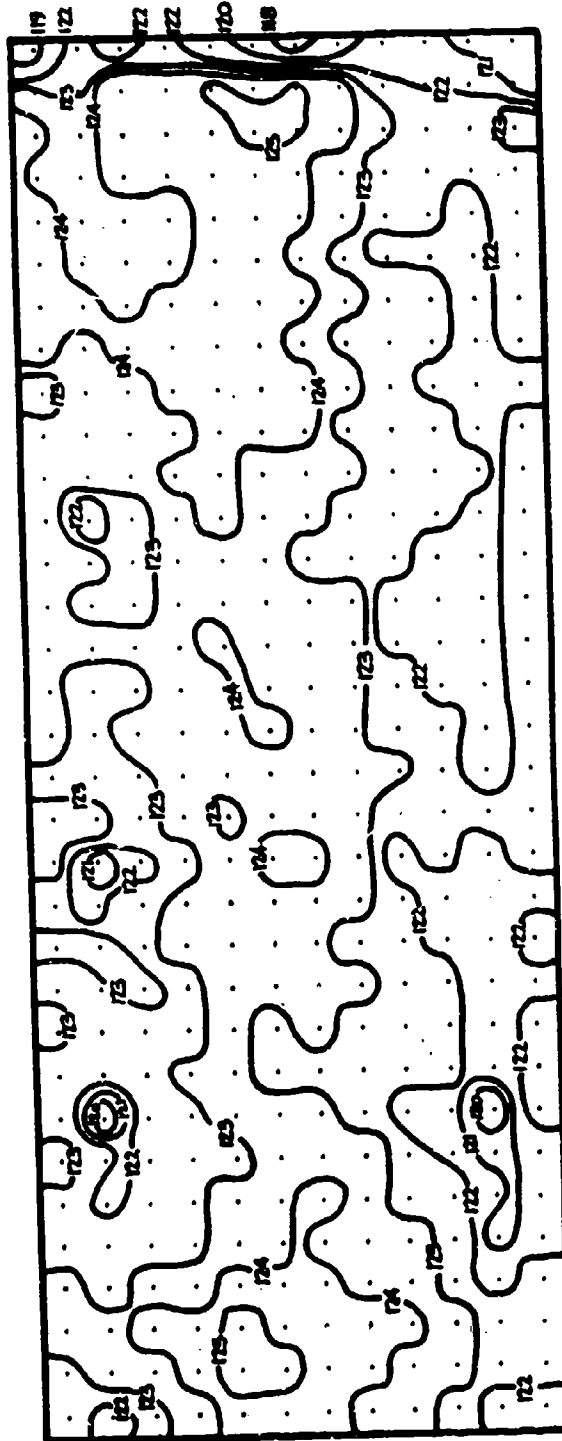


MAX	.128	RANGE	.0075
MIN	.1205	σ	.0009
AVG	.1255	POINTS	429

SHEET THICKNESS VARIATION BETA C TITANIUM ALLOY 1/8" SHEET (GROUND)

SHEET 1-7 HT 304324-19

36 3/4' X 97 1/2'

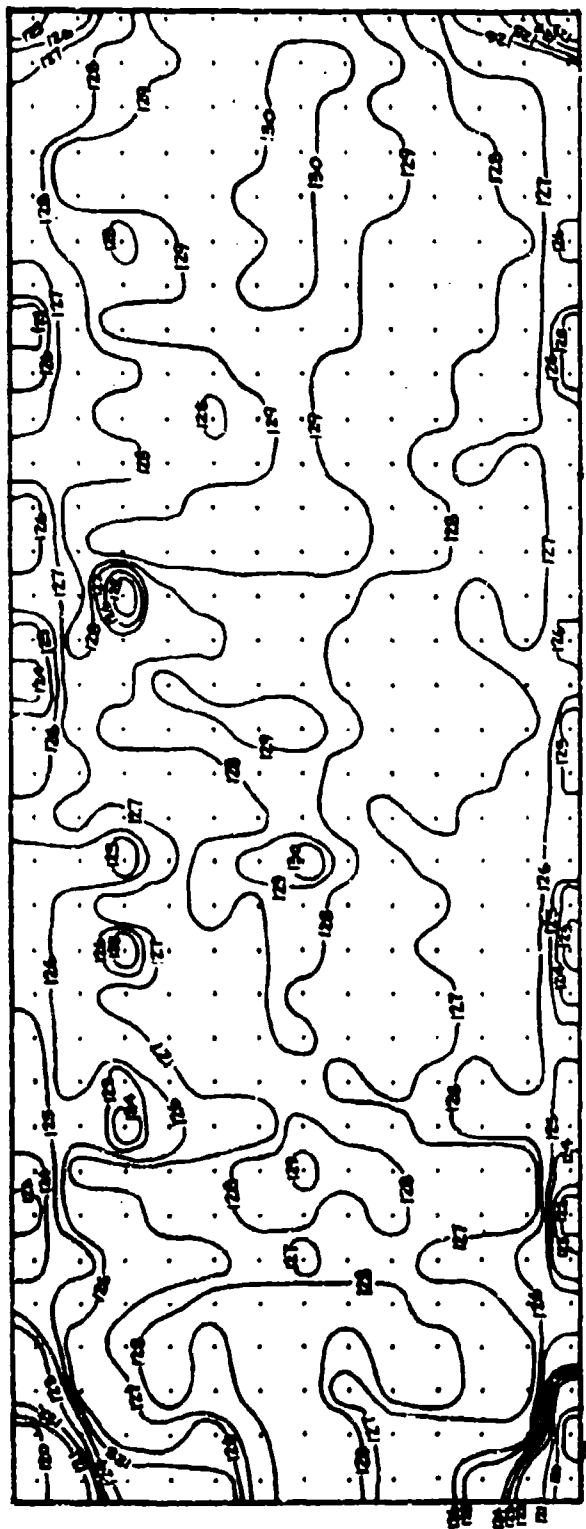


MAX	.125	RANGE	.0075
MIN	.1175	σ	.0010
AVG	.1219	POINTS	396

SHEET THICKNESS VARIATION BETA C TITANIUM ALLOY 1/8" SHEET (GROUND)

SHEET 1-8 HT 304324-19

38 3/4" X 101"



MAX	.1305	RANGE	.0125
MIN	.118	σ	.0011
AVG	.1271	POINTS	442

SHEET THICKNESS VARIATION BETA C TITANIUM ALLOY 1/8" SHEET (GROUND)

SHEET 1-3 HT 304324-25

38 3/4" X 103 1/4"

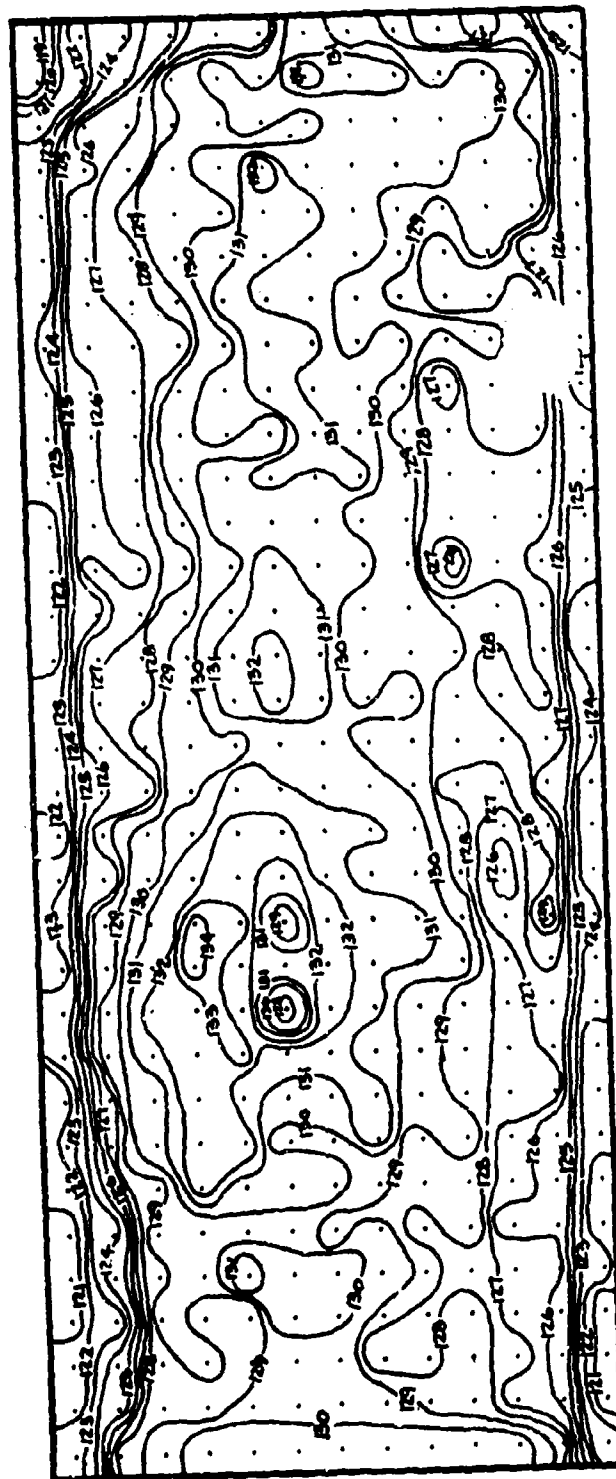


MAX	.1385	RANGE	.0170
MIN	.1215	σ	.004
AVG	.1303	POINTS	442

SHEET THICKNESS VARIATION BETA C TITANIUM ALLOY 1/8" SHEET (ROLLED AND PICKLED)

SHEET 1-4 HT 304324-25

38 3/4" X 97"



MAX	.1345	RANGE	.0165
MIN	.1180	σ	.0021
AVG	.1275	POINTS	429

SHEET THICKNESS VARIATION BETA C TITANIUM ALLOY 1/8" SHEET (ROLLED AND PICKLED)

SHEET 1-5 HT 304324-25

39" X 103 1/2"

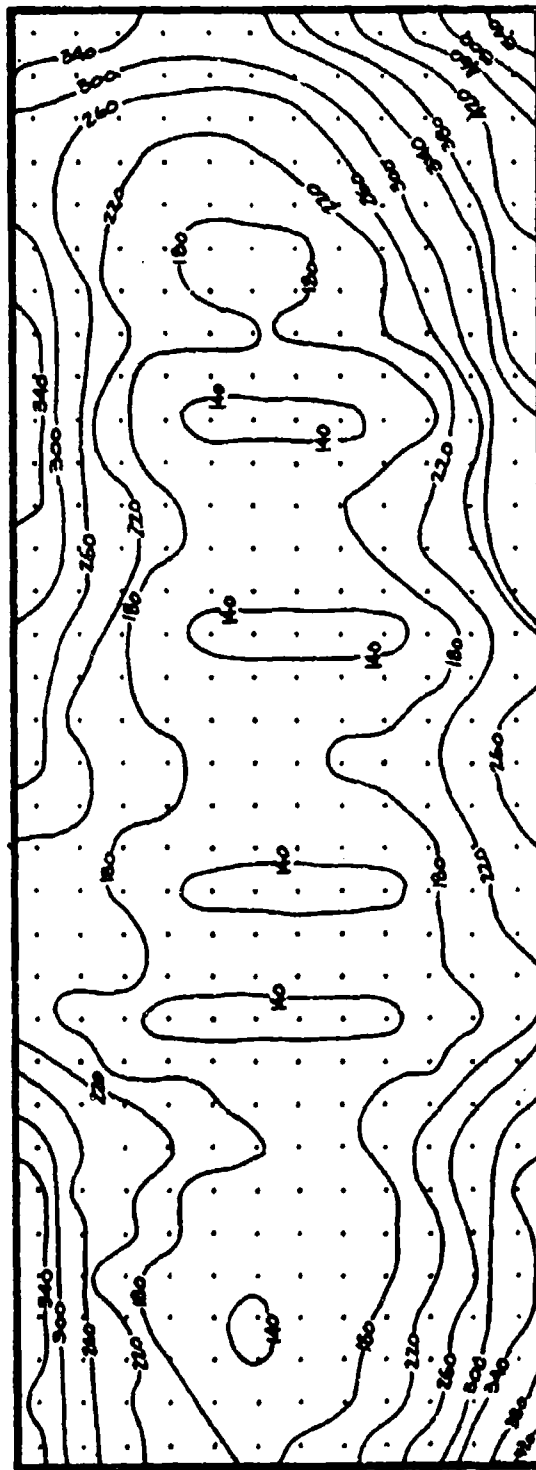


MAX	.135	RANGE	.0145
MIN	.1205	σ	.0029
AVG	.1295	POINTS	455

SHEET THICKNESS VARIATION BETA C TITANIUM ALLOY 1/8" SHEET (ROLLED AND PICKLED)

SHEET 1-1 HT 304324-19

37" X 101"

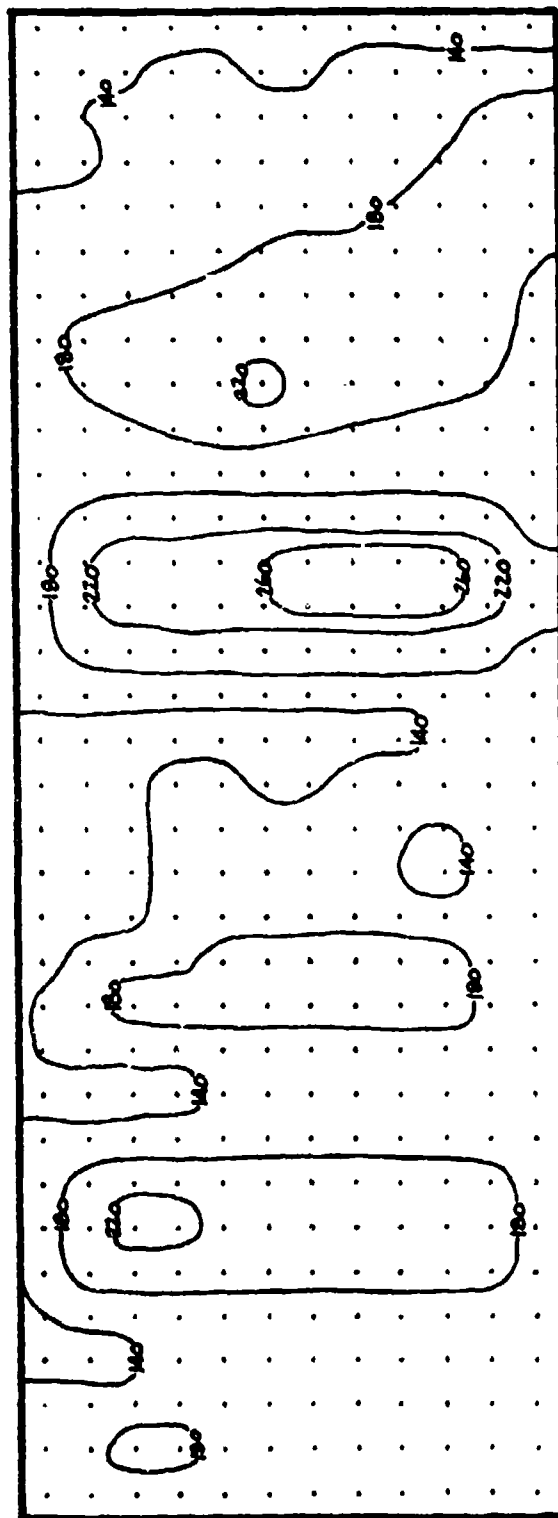


MAX	.557	RANGE	.427
MIN	.130	σ	.078
AVG	.2243	POINTS	408

SHEET FLATNESS VARIATION BETA C TITANIUM ALLOY 1/8" SHEET (GROUND)

SHEET 1-2 HT 304324-19

37' X 99 1/2'

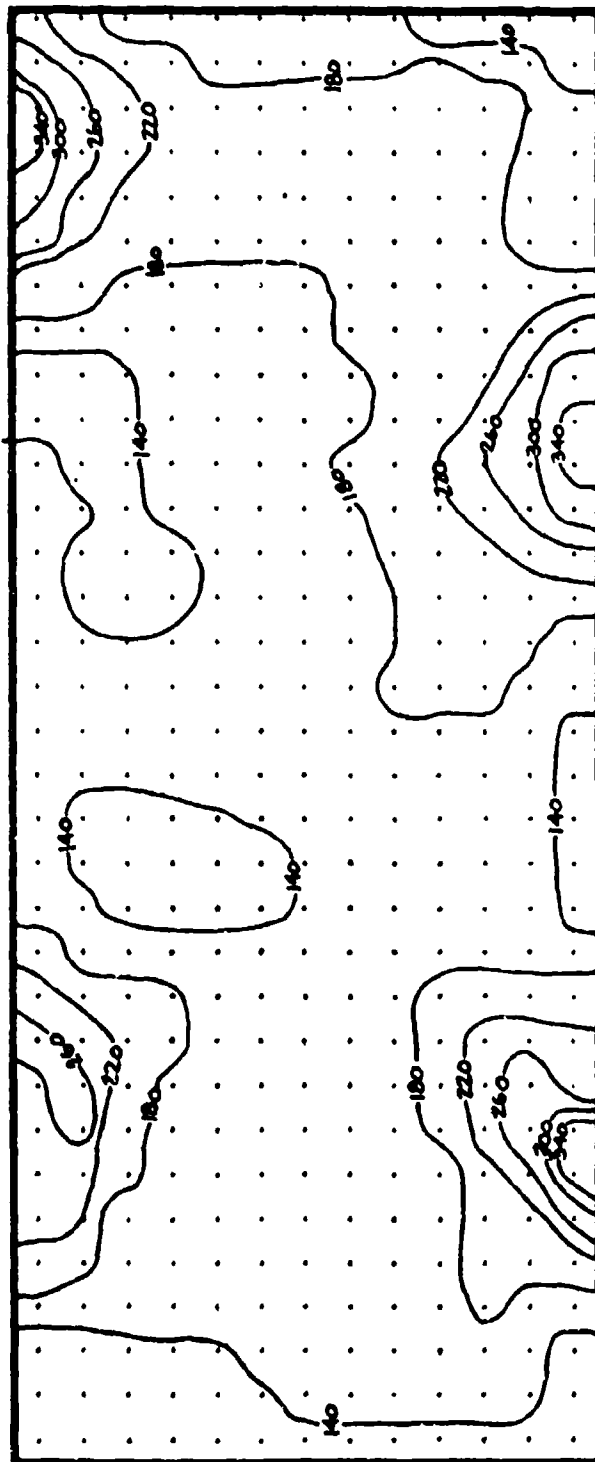


MAX	.274	RANGE	.145
MIN	.129	σ	.030
AVG	.1706	POINTS	408

SHEET FLATNESS VARIATION BETA C TITANIUM ALLOY 1/8" SHEET (GROUND)

SHEET 1-6 HT 304324-19

39" X 97 3/4"



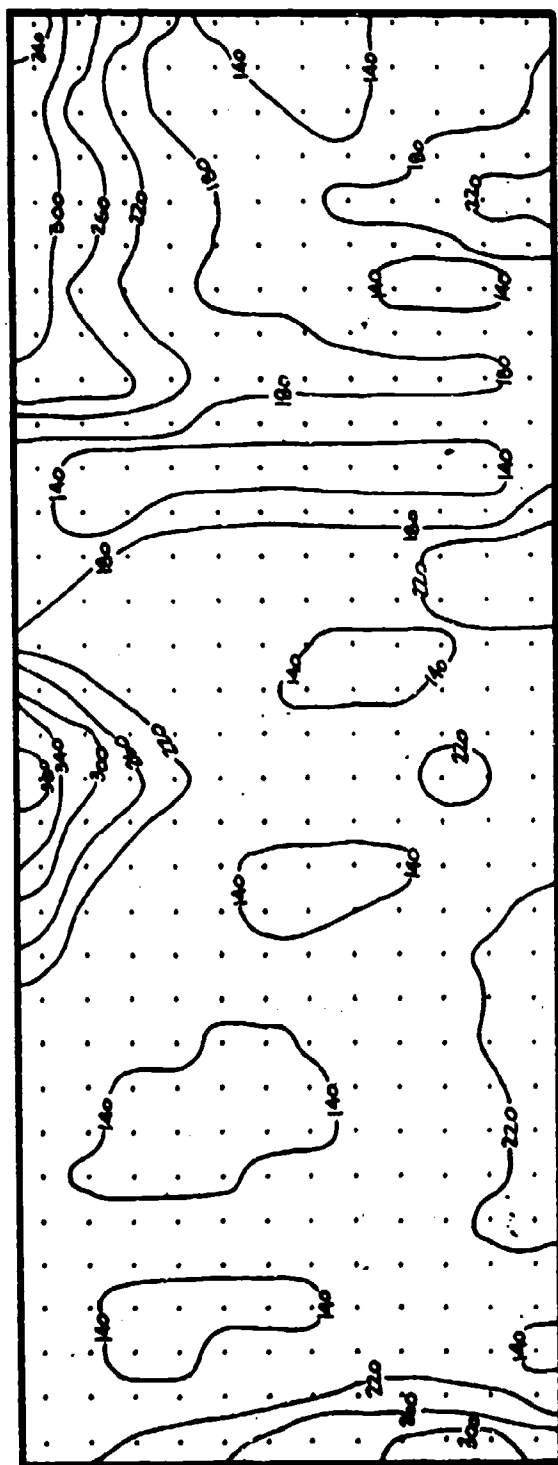
MAX	.375	RANGE	.252
MIN	.123	σ	.0451
AVG	.1782	POINTS	429

SHEET FLATNESS VARIATION BETA C TITANIUM ALLOY 1/8" SHEET (GROUND)

SHEET 1-7 HT 304324-19

36 3/4" X 97 1/2"

(MEASUREMENTS INCLUDES METAL THICKNESS)



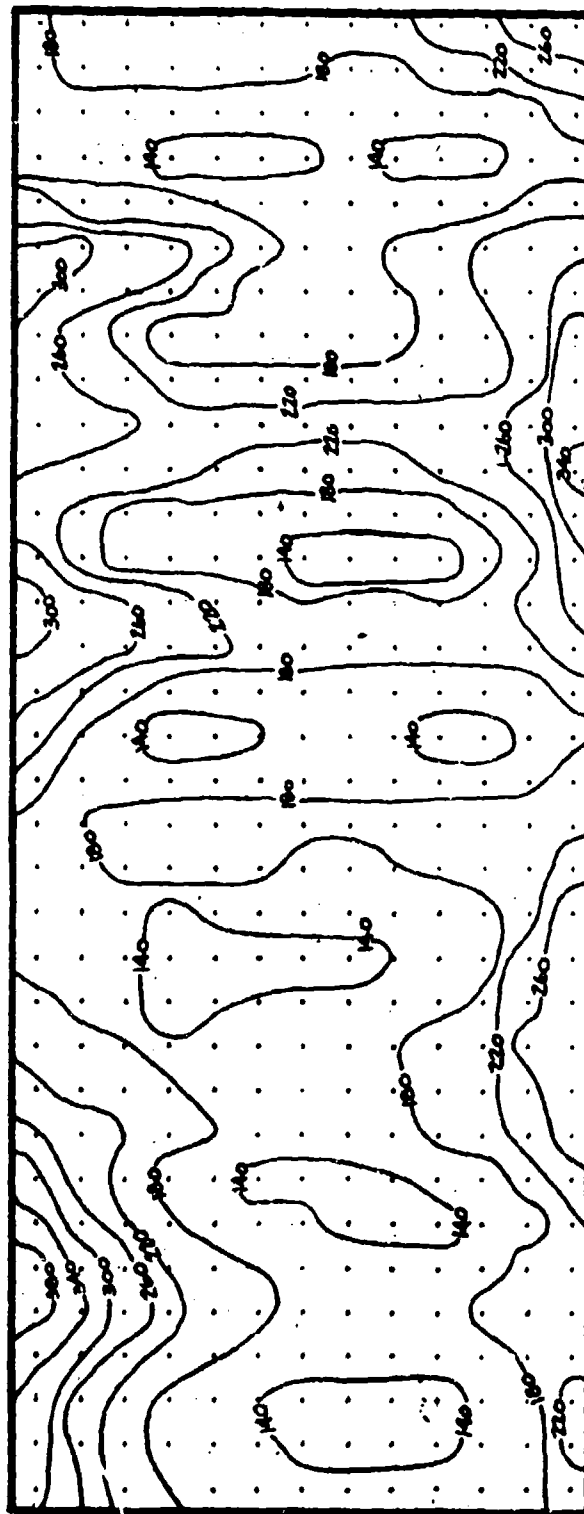
MAX	.396	RANGE	.271
MIN	.125	σ	.0486
AVG	.1862	POINTS	396

SHEET FLATNESS VARIATION BETA C TITANIUM ALLOY 1/8" SHEET (GROUND)

SHEET 1-8 HT 304324-19

38 3/4" X 101"

(MEASUREMENTS INCLUDE METAL THICKNESS)



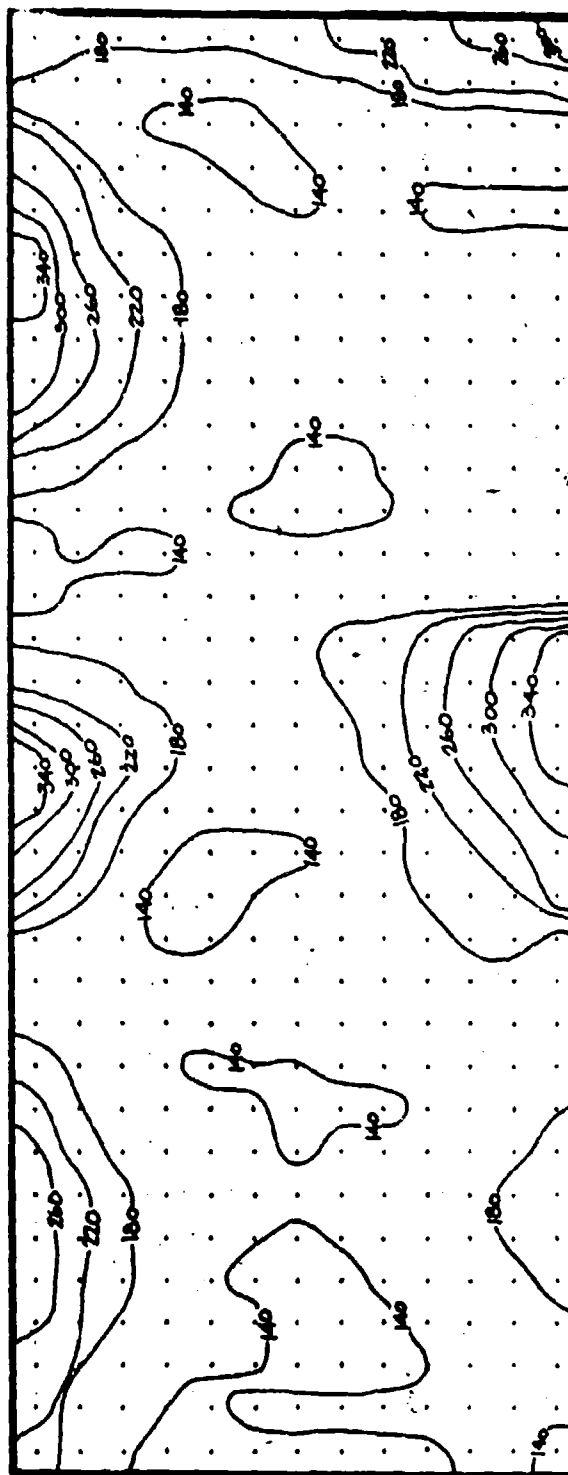
MAX	.396	RANGE	.264
MIN	.132	σ	.0160
AVG	.1948	POINTS	442

SHEET FLATNESS VARIATION BETA C TITANIUM ALLOY 1/8" SHEET (GROUND)

SHEET 1-3 HT 304324-25

38 3/4" X 103 1/4"

(MEASUREMENTS INCLUDE METAL THICKNESS)



MAX	.374	RANGE	.242
MIN	.132	σ	.046
AVG	.1764	POINTS	456

SHEET FLATNESS VARIATION BETA C TITANIUM ALLOY 1/8" SHEET (ROLLED AND PICKLED)

SHEET 1-4 HT 304324-25

38 3/4" X 97"

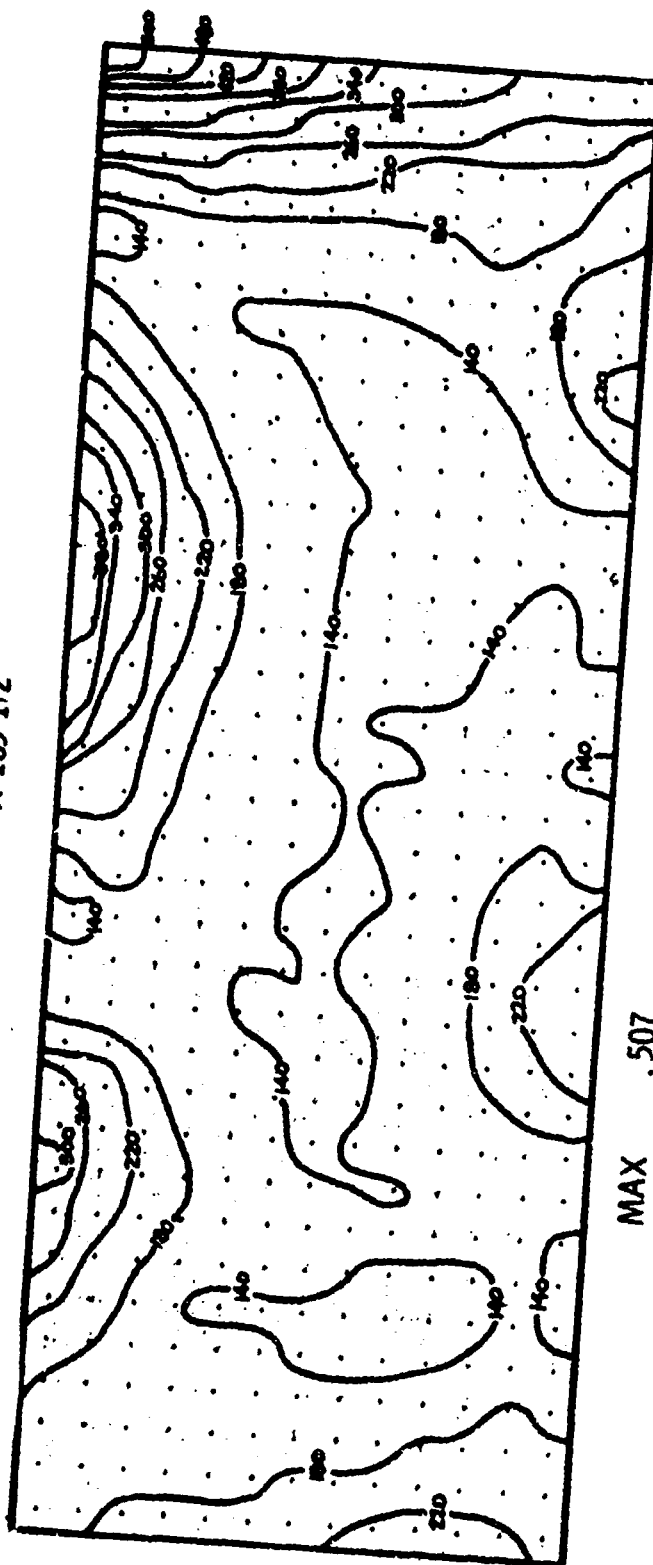


MAX	.221	RANGE	.098
MIN	.123	σ	.023
AVG	.1736	POINTS	429

SHEET FLATNESS VARIATION BETA C TITANIUM ALLOY 1/8" SHEET (ROLLED AND PICKLED)

SHEET 1-5 HT 304324-25

39" X 103 1/2"

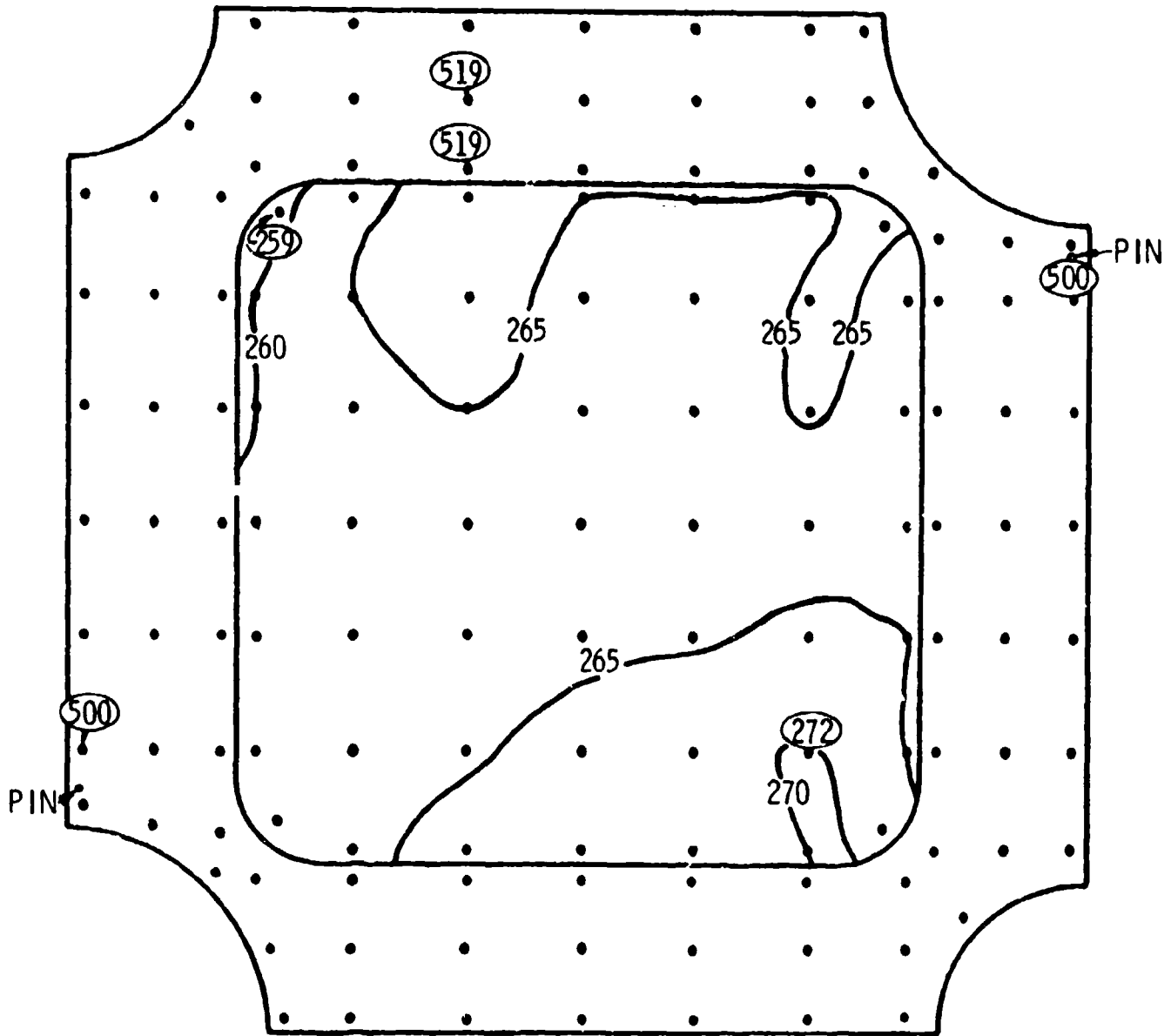


MAX .507
MIN .130
AVG .18727

RANGE .377
 σ .0590
POINTS 455

SHEET FLATNESS VARIATION BETA C TITANIUM ALLOY 1/8" SHEET (ROLLED AND PICKLED)

THICKNESS

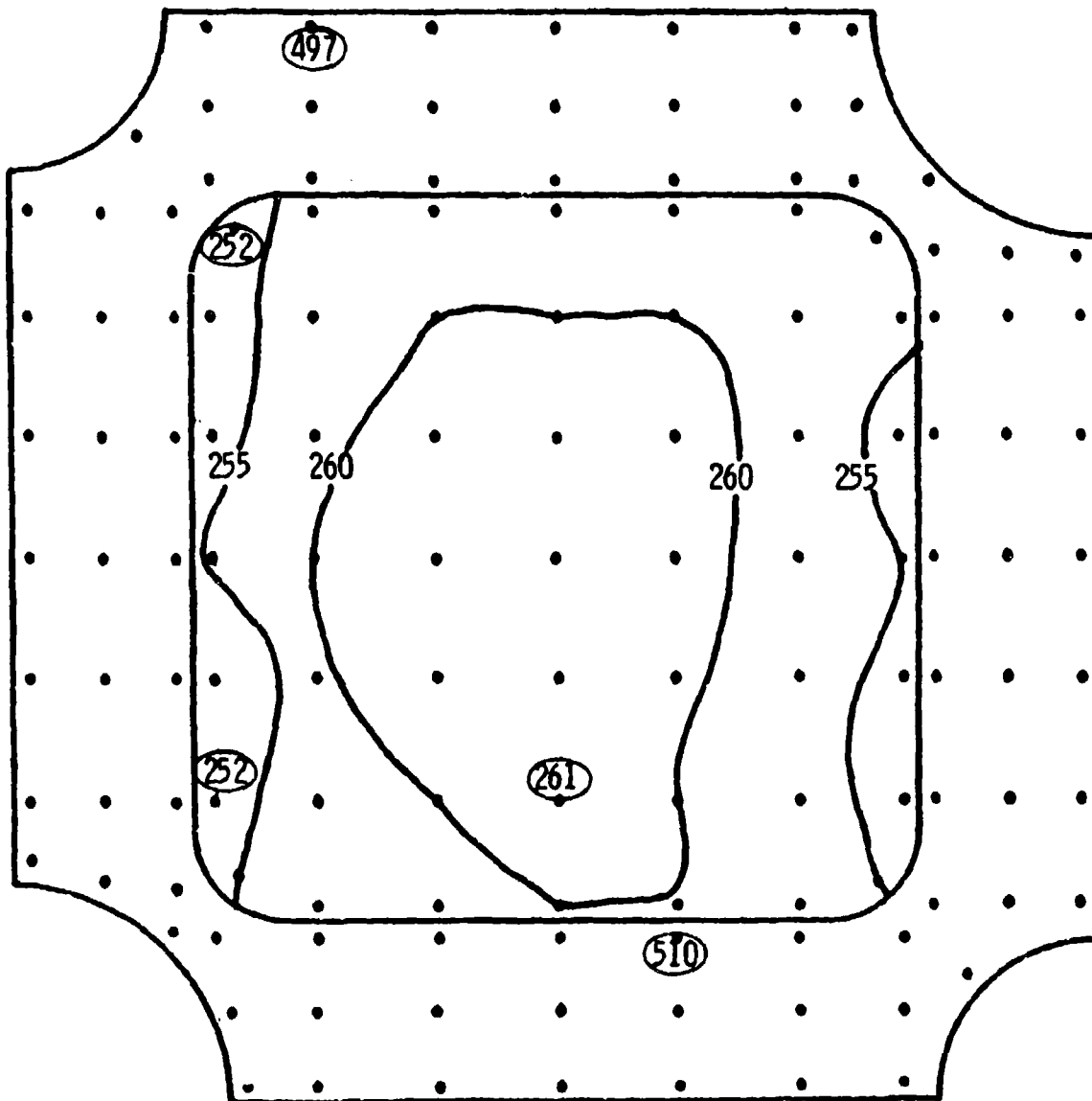


WEB	
MAX	.272
MIN	.259
RANGE	.013

DOUBLER	
MAX	.519
MIN	.500
RANGE	.019

603FTB012-3 (F524983) 18"x18"

THICKNESS

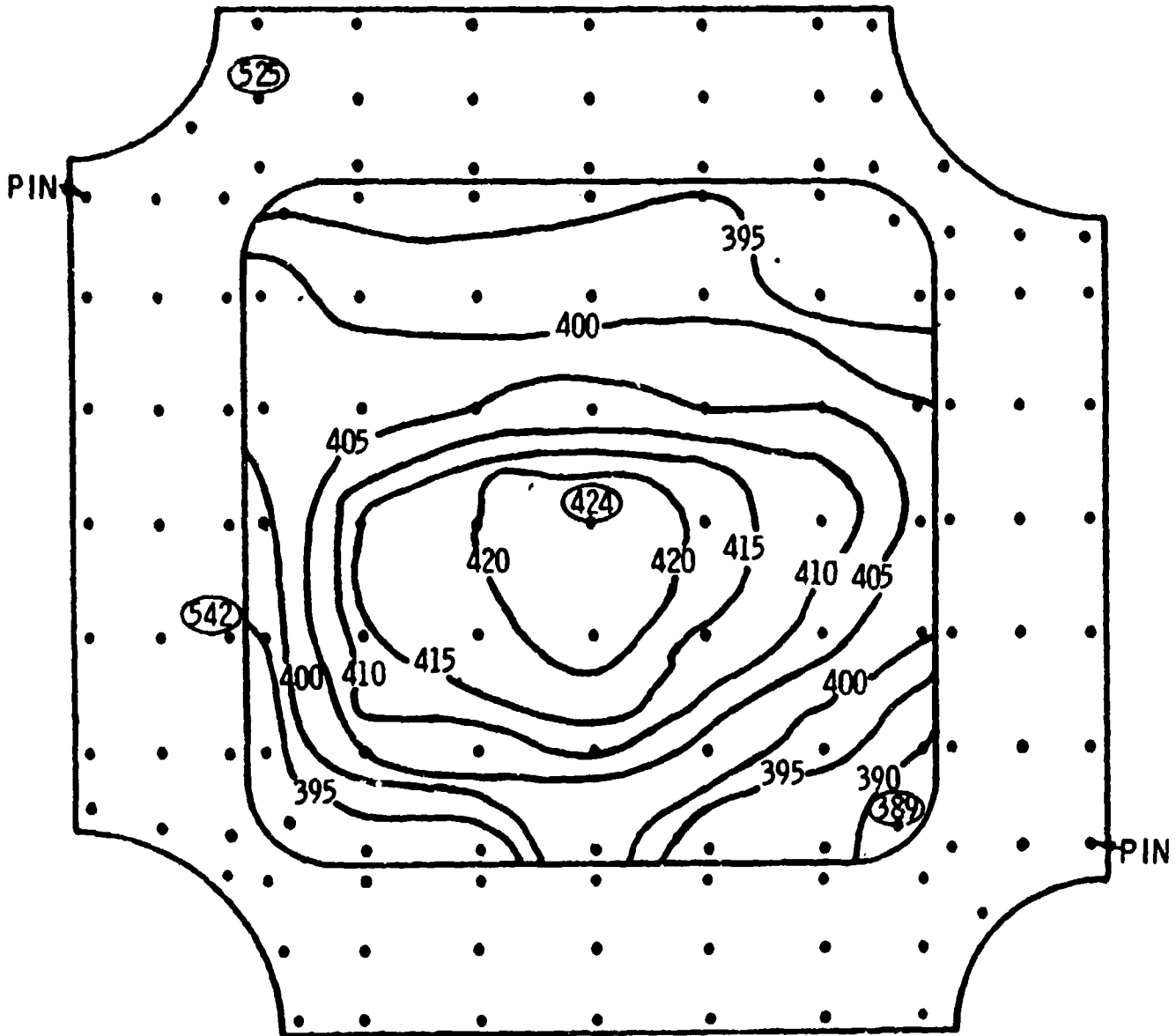


<u>WEB</u>	
MAX	.261
MIN	.252
RANGE	.009

<u>DOUBLER</u>	
MAX	.510
MIN	.497
RANGE	.013

603FTB012-3 (F524984) 18"x18"

THICKNESS

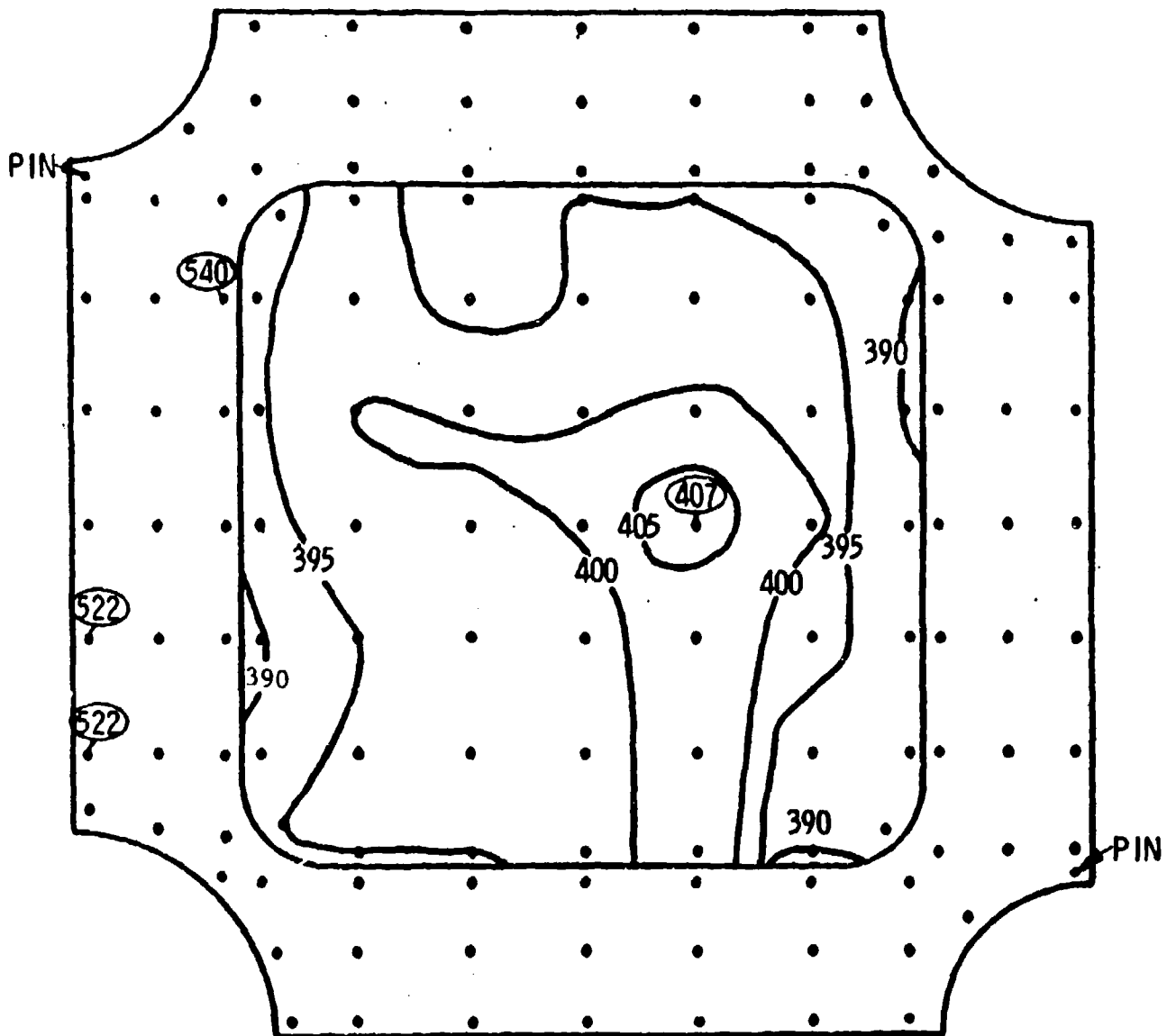


WEB	
MAX	.424
MIN	.389
RANGE	.035

DOUBLER	
MAX	.542
MIN	.525
RANGE	.017

603FTB012-1 (F524986) 18"x18"

THICKNESS

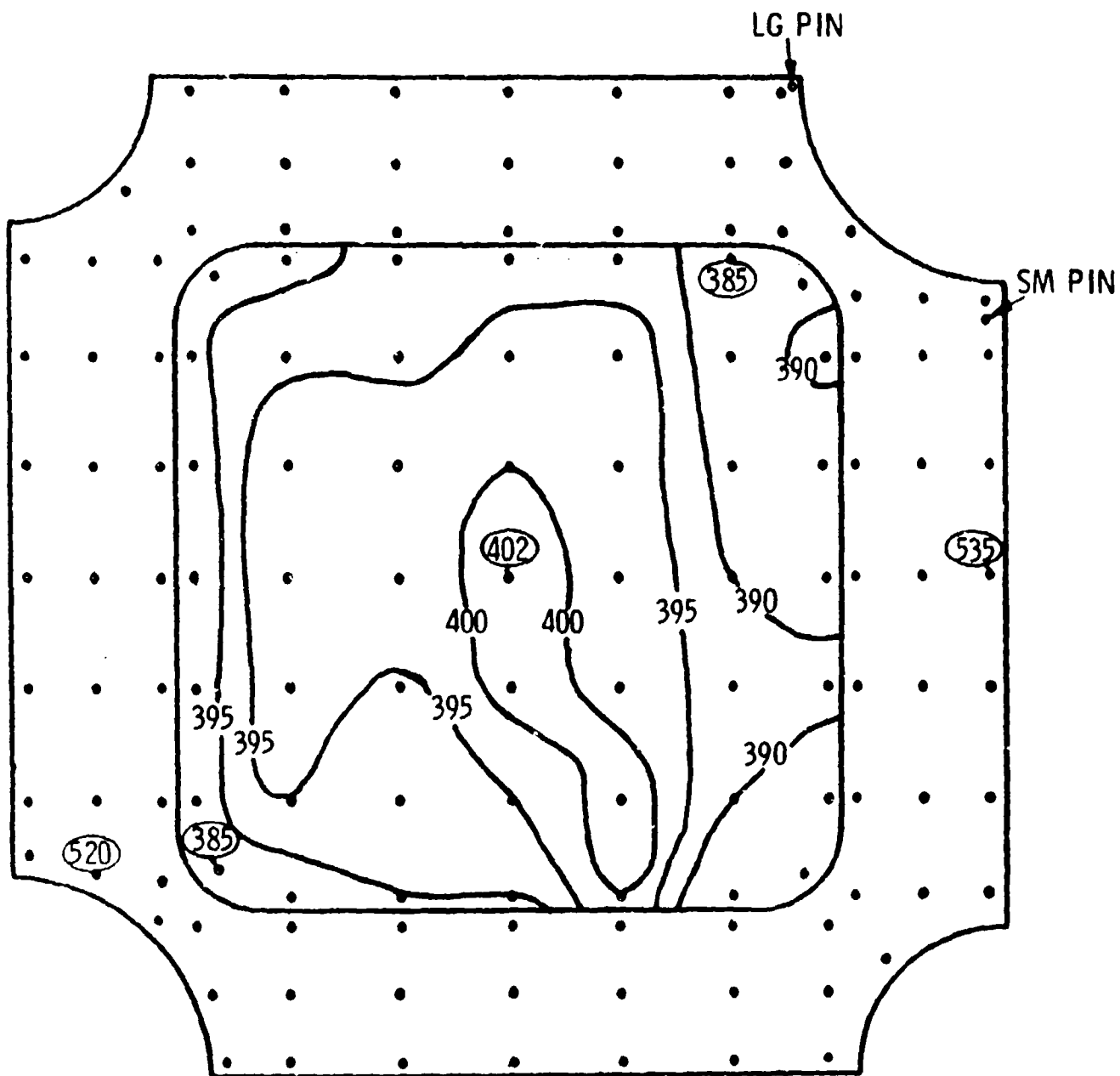


WEB	
MAX	.407
MIN	.390
RANGE	.017

DOUBLER	
MAX	.540
MIN	.522
RANGE	.018

603FTB012-1 (F524985) 18"x18"

THICKNESS



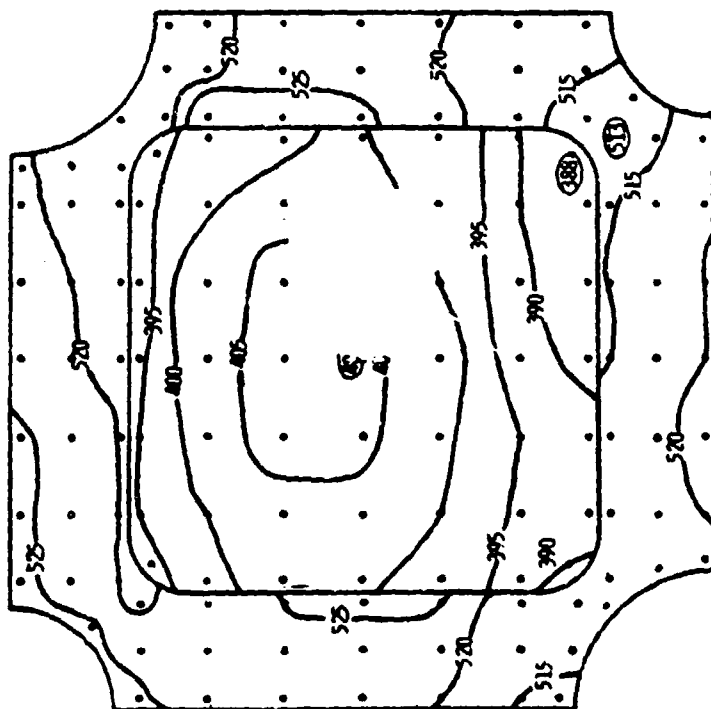
WEB	
MAX	.402
MIN	.385
RANGE	.017

DOUBLER	
MAX	.535
MIN	.520
RANGE	.015

603FTB012-1 (F529441) 18"x18"

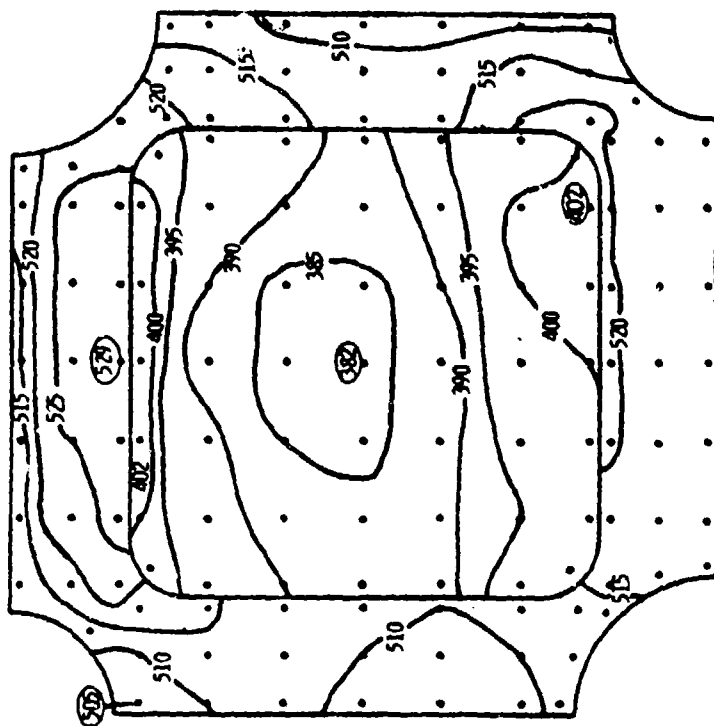
FLATNESS

TOOL SIDE



WEB	DOUBLER
MAX .408	MAX .528
MIN .388	MIN .513
RANGE .020	RANGE .015

BAG SIDE

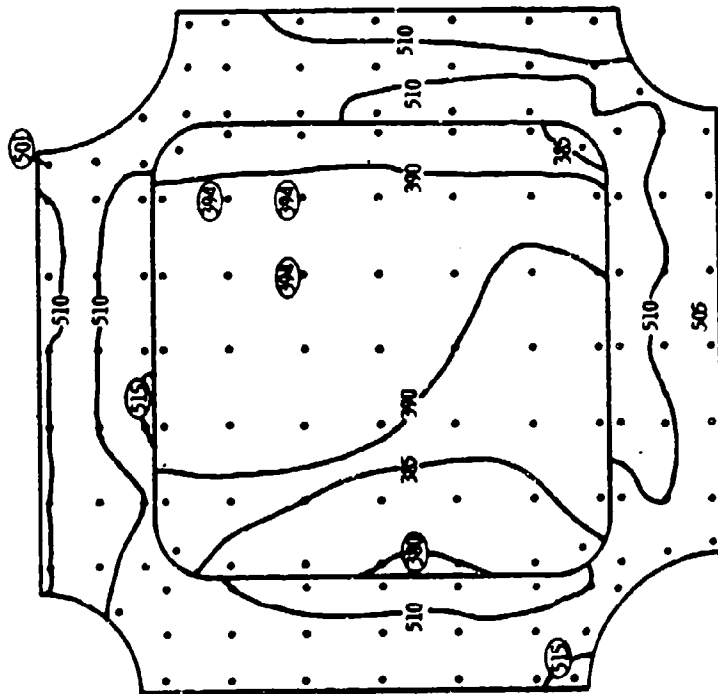


WEB	DOUBLER
MAX .402	MAX .529
MIN .382	MIN .505
RANGE .020	RANGE .024

603FTB012-3 (F524983) 18"x18"

FLATNESS

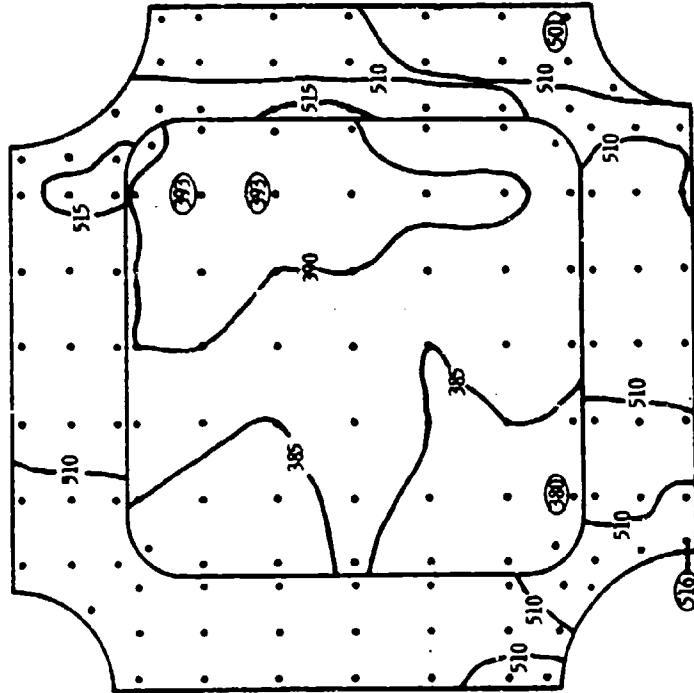
TOOL SIDE



WEB	
MAX	.394
MIN	.380
RANGE	.014

DOUBLER	
MAX	.515
MIN	.501
RANGE	.014

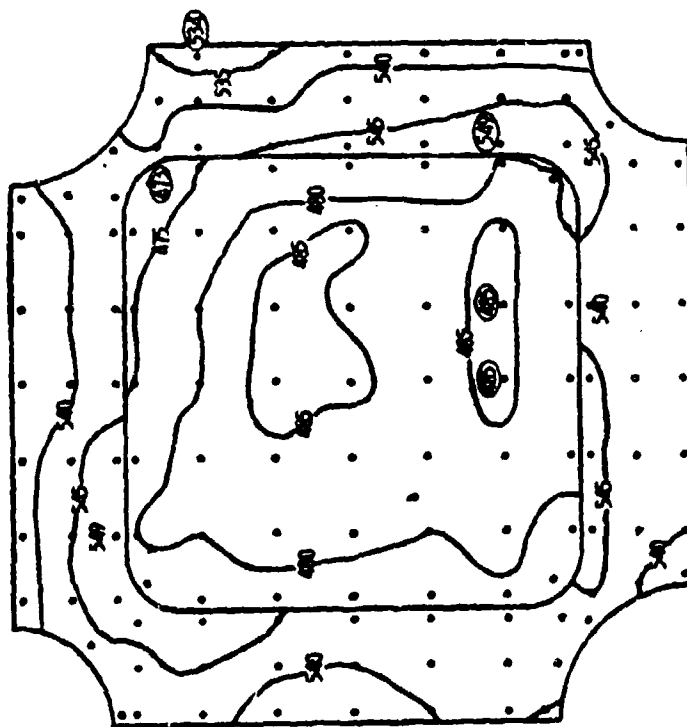
BAG SIDE



WEB	
MAX	.393
MIN	.380
RANGE	.013

DOUBLER	
MAX	.516
MIN	.501
RANGE	.015

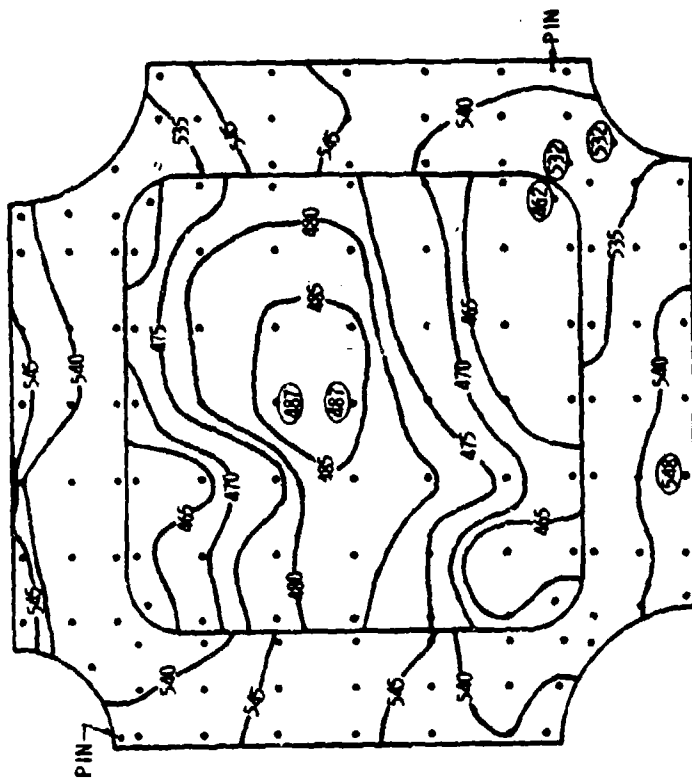
TOOL SIDE



MAX	.485
MIN	.473
RANGE	.012

DOUBLER	
MAX	.549
MIN	.534
RANGE	.015

BAG SIDE

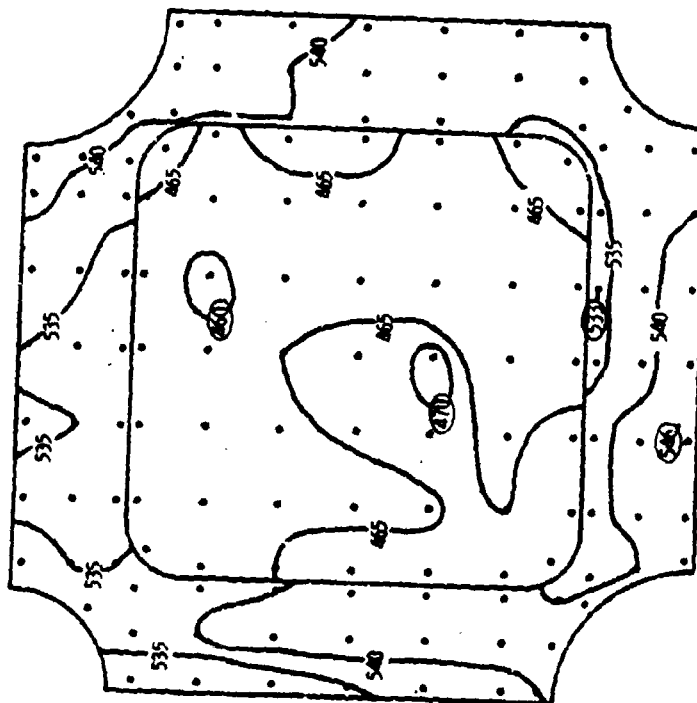


WEB
MAX . 487
MIN . 462
RANGE . 025

DOUBLER	
MAX	.548
MIN	.532
RANGE	.016

FLATNESS

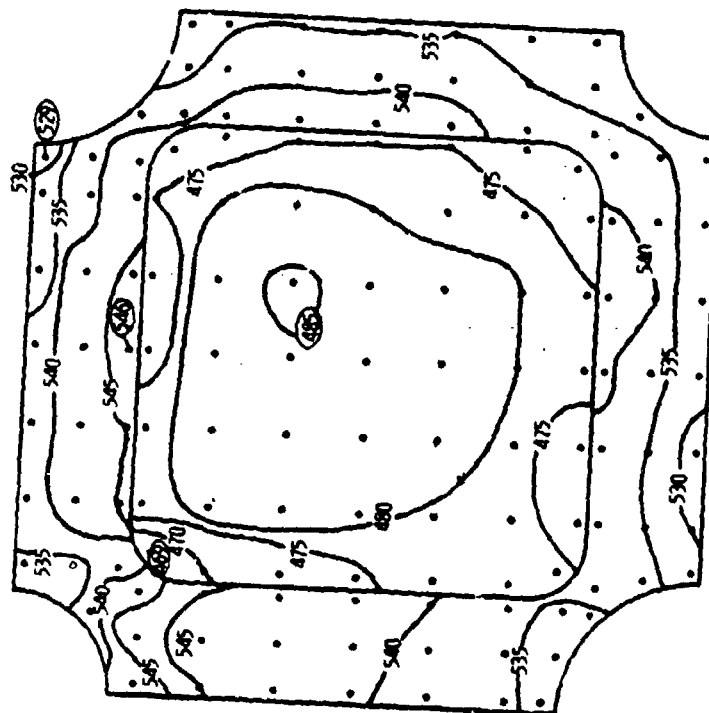
TOOL SIDE



WEB
MAX .470
MIN .460
RANGE .010

DOUBLER
MAX .546
MIN .533
RANGE .013

BAG SIDE



WEB
MAX .485
MIN .469
RANGE .016

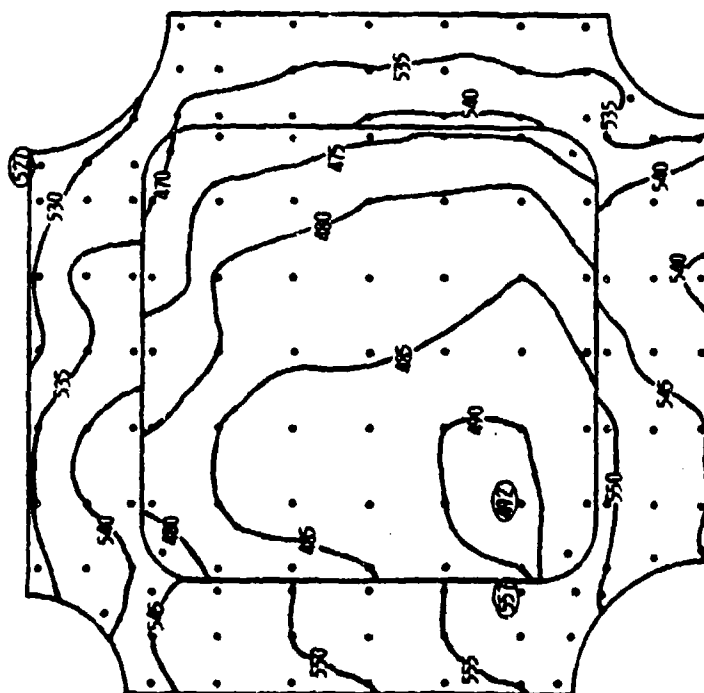
DOUBLER
MAX .546
MIN .529
RANGE .017

300

603FTB012-1 (F524985) 18"x18"

FLATNESS

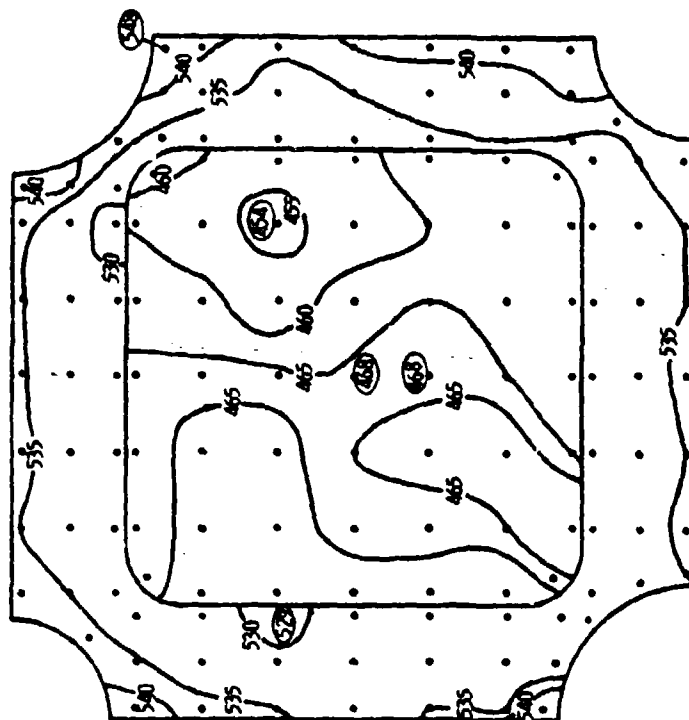
TOOL SIDE



WEB	
MAX	.492
MIN	.470
RANGE	.022

DOUBLER	
MAX	.537
MIN	.527
RANGE	.010

BAG SIDE



WEB	
MAX	.468
MIN	.454
RANGE	.014

DOUBLER	
MAX	.548
MIN	.529
RANGE	.019

REFERENCES

1. Wheeler, O. E., "Crack Propagation Under Spectrum Loading", FZM-5602, 30 June 1970.
2. Phase Ib Summary Report. AMAVS Program AFFDL-TR-73-40 Vol 1, Part 1, General Dynamics Corp., Fort Worth Division, Mar. 1973.
3. Przemieniecki, J. S., Theory of Matrix Structural Analysis, McGraw Hill, 1968.

Unclassified

Security Classification

DOCUMENT CONTROL DATA - R & D		
<small>(Security classification of title, body of abstract and indexing annotation must be entered when the overall report is classified)</small>		
1. ORIGINATING ACTIVITY (Corporate author)		2a. REPORT SECURITY CLASSIFICATION
Air Force Flight Dynamics Laboratory (FBA) Wright-Patterson Air Force Base, Ohio 45433		Unclassified
		2b. GROUP
3. REPORT TITLE		
ADVANCED METALLIC AIR VEHICLE STRUCTURE PROGRAM		
4. DESCRIPTIVE NOTES (Type of report and inclusive dates)		
Interim Technical Report (16 December 1972 thru 15 June 1973)		
5. AUTHOR(S) (First name, middle initial, last name)		
C. E. Hart, et al.		
6. REPORT DATE	7a. TOTAL NO. OF PAGES	7b. NO. OF REFS
July 1973	302	3
8a. CONTRACT OR GRANT NO.	8b. ORIGINATOR'S REPORT NUMBER(S)	
AF33615-73-C-3001	AFFDL-TR-73-77	
b. PROJECT NO.	8c. OTHER REPORT NO(S) (Any other numbers that may be assigned this report)	
486U		
c.		
d.		
10. DISTRIBUTION STATEMENT		
11. SUPPLEMENTARY NOTES		12. SPONSORING MILITARY ACTIVITY
		Air Force Flight Dynamics Laboratory Wright-Patterson AFB, Ohio 45433
13. ABSTRACT		
<p>Refinement of the three designs for a wing carrythrough structure was continued to the end of Phase Ib. On the basis of trade studies, materials and component testing and the results of NDI and manufacturing development work, two of the configurations were chosen for the detail design phase.</p> <p>Materials testing was substantially completed for the beta annealed 6Al-4V titanium and testing is underway for the Beta C titanium and 10 Ni steel. Group I component tests (those performed to verify design concepts) are virtually complete. Tests to evaluate the welding, brazing and bonding processes are also well underway.</p> <p>Design of the test fixture is proceeding with some manufacturing effort already started. Detail design and analysis of the simulated fuselage structure for the test article is also in work.</p> <p>Additional trade studies were conducted early in Phase II and several design changes were incorporated into the two wing carrythrough structure configurations as a result of these studies. A ZrO panel was added to the "No Box" Box design. The Fail Safe Removable Lug Configuration was redesignated the Fail Safe Integral Lug Configuration after an integral lower plate-lug arrangement was selected for detail design.</p>		

DD FORM 1 NOV 66 1473

303

Unclassified

Security Classification

Unclassified

Security Classification

14 KEY WORDS	LINK A		LINK B		LINK C	
	ROLE	WT	ROLE	WT	ROLE	WT
Structural Design Stress Analysis Fracture Mechanics Materials Manufacturing Technology Damage Tolerance						

Unclassified

Security Classification